

DISSERTATION

**Description of Drell-Yan pair
production in a phenomenological
parton model**

Fabian EICHSTÄDT

Justus-Liebig-Universität Gießen
Fachbereich 07 - Mathematik und Informatik, Physik, Geographie
2011

Gutachter:

Prof. Dr. Ulrich Mosel (Justus-Liebig-Universität Gießen)

Prof. Dr. Stefan Leupold (Uppsala universitet)

Dekan:

Prof. Dr. Christian Diller

Tag der Disputation:

02.12.2011

Dissertation aus dem Fachbereich 07 - Mathematik und Informatik, Physik, Geographie der Justus-Liebig-Universität Gießen

Das Schicksal mischt die Karten,
und wir spielen.

Arthur Schopenhauer

Danksagung

Zuallererst möchte ich meinem Betreuer Professor Ulrich Mosel für die Aufnahme in sein Institut, seine stetige Unterstützung und seine konzeptionellen Anregungen bei der Anfertigung dieser Arbeit danken. Ebenso dankbar bin ich dafür, daß er es mir ermöglicht hat an vielen internationalen Veranstaltungen teilzunehmen und die Ergebnisse meiner Arbeit vorzustellen.

Zu ganz besonderem Dank bin ich Professor Stefan Leupold verpflichtet: er hatte stets ein offenes Ohr und eine passende Antwort für alle meine Fragen, gleich ob technischer oder grundlegend physikalischer Natur. Seine Unterstützung während der kritischen Phasen dieser Arbeit waren für mich von unschätzbarem Wert und es war immer eine Freude mit ihm zusammen zu arbeiten, genauso wie auch alle nicht-physikalischen Zusammentreffen mit ihm. Hendrik van Hees danke ich für die vielen hilfreichen Physik-Diskussionen, speziell zur Quantenfeldtheorie, sowie Hinweise auf die passende Literatur. Ein Dank geht auch an Kai Gallmeister, speziell für die PYTHIA-Rechnungen, die in diese Arbeit mit eingeflossen sind.

Abdul Ahad Ataie und Andreas Fedoseew möchte ich für die schöne Zeit bei vielen gemeinsamen Unternehmungen während der vergangenen Jahre des Studiums und der Promotionszeit, sowie bei den Veranstaltungen der Graduiertenkollegs und des Instituts danken. Meinen Kollegen bei der Computeradministration, Oliver Buss und Janus Weil, danke ich für die sehr gute jahrelange Zusammenarbeit. Man konnte sich stets aufeinander verlassen und ich hatte viel Spaß beim gemeinsamen Erledigen der Aufgaben unter der guten Leitung von Professor Horst Lenske. Für die vielen Diskussionen und Gespräche (gleich welcher Natur) während der Pausen, die gute Arbeitatmosphäre im Institut, sowie für hilfreiche kleine und große Tips aller Art geht mein Dank an Stefan Bender, Theodoros Gaitanos, David Kalok, Murat Kaskulov, Patrick Konrad, Ivan Lappo-Danilevski, Tina Leitner, Stefanie Lourenco, Stefano Mattiello, Birger Steinmüller, Stefan Strauß und Stefan Winkelmann. Elke Jung bin ich für die Unterstützung bei der Erledigung aller Arten von Verwaltungsangelegenheiten sehr dankbar. Man konnte sich stets auf sie verlassen und sie sorgte dafür, daß man den „Rücken frei“ hatte, um sich ganz auf die Arbeit zu konzentrieren.

Meinen Eltern und meiner ganzen Familie danke ich herzlich für die konstante Unterstützung aller Art während meiner Promotionszeit. Ohne sie wäre ich nicht da, wo ich jetzt bin. Kathrin Steckbauer danke ich für ihre Toleranz und Aufmunterungen während der Höhen und Tiefen, die eine Promotion mit sich bringt. Das Zusammensein mit ihr ist mir unglaublich wichtig.

Contents

I	Preface	1
1	Introduction	3
1.1	Motivation	3
1.2	Outline	7
II	Mathematical tools	9
2	Loops and regularisation	11
2.1	The quark selfenergy	11
2.2	Regularisation schemes	12
2.2.1	Momentum cut-off	13
2.2.2	Pauli-Villars regularisation	13
2.2.3	Lattice regularisation	13
2.2.4	Analytic regularisation	14
2.3	Dimensional regularisation	14
2.3.1	Example	14
2.3.2	Extension to d dimensions	15
2.3.3	Feynman parameters	18
2.3.4	Wick rotation	22
2.3.5	d -dimensional spherical coordinates	25
2.3.6	Laurent expansion around $d = 4$ dimensions	31
3	One-loop integrals	35
3.1	The three-point function	35
3.1.1	Feynman parametrisation	36
3.1.2	Spence function (Dilogarithm)	39
3.1.3	Integral transformations	40
3.1.4	Reduction to Spence functions	45
3.2	Expansion for small mass m_3	49

III Physical background	53
4 Remarks on renormalisation	55
4.1 Basics of renormalisation	55
4.1.1 Example: renormalisation in QED	55
4.1.2 Renormalisation group equation	58
4.2 The massive quark selfenergy	59
4.3 Field strength renormalisation	61
4.3.1 The full spin- $\frac{1}{2}$ propagator	62
4.3.2 Spectral decomposition of the full propagator	63
4.4 QCD field strength renormalisation for massive quarks	70
5 Infrared divergences and soft radiation	75
5.1 Example of an infrared divergence	75
5.2 Soft gluon bremsstrahlung	78
5.2.1 Cross section	79
5.2.2 Phase space integral for soft gluons	81
5.3 Aspects of soft bremsstrahlung	85
6 Nucleon structure	87
6.1 Electron scattering	87
6.1.1 Elastic scattering on point-like targets	88
6.1.2 Elastic scattering on the nucleon	93
6.1.3 Inelastic scattering on the nucleon	96
6.2 The parton model	101
6.2.1 Bjorken scaling	101
6.2.2 Formal derivation of the parton model	104
6.2.3 General properties of parton distribution functions	113
6.2.4 Scaling violations and the DGLAP equations	115
IV Drell-Yan	121
7 The Drell-Yan process at leading order	123
7.1 Introduction - the Drell-Yan process in the parton model	123
7.2 Observables, conventions and notation	125
7.3 Partonic subprocess cross section at leading order	126
7.3.1 Cross section for virtual photon production	127
7.3.2 Connection of virtual photon and DY pair production	128
7.3.3 Current conservation	131
7.4 Kinematics	132
7.4.1 Standard collinear parton model	132

7.4.2	Naive collinear parton model	134
7.4.3	Intrinsic transverse momentum	138
7.4.4	Quark masses	144
7.5	Distributions	146
7.5.1	Transverse momentum distributions	147
7.5.2	Mass distributions	147
7.6	Results of the leading order approach	149
7.6.1	E866 - p_T spectra	149
7.6.2	E439 - M spectrum	151
7.7	Conclusion for the LO calculation	152
8	Next-to-leading order corrections to the Drell-Yan process	155
8.1	Vertex correction	155
8.1.1	Vertex function	157
8.1.2	Cross section	164
8.1.3	Soft gluon divergence	165
8.1.4	Kinematics	167
8.1.5	Current conservation	167
8.1.6	Renormalised charge	169
8.2	General kinematics of partonic NLO cross sections	171
8.3	Gluon bremsstrahlung	174
8.3.1	Cross section	174
8.3.2	Kinematics	175
8.4	Gluon Compton scattering	183
8.4.1	Cross section	183
8.4.2	Kinematics	184
8.5	Influence of quark mass distributions on DY p_T spectra	187
8.6	Collinear (mass) singularities and parton distribution functions	189
8.6.1	Collinear singularities in pQCD	189
8.6.2	Collinear singularities in our model	192
8.7	Influence of initial transverse momentum distributions on DY p_T spectra	196
V	Results and predictions	197
9	Drell-Yan in high energy proton-proton collisions - fixing parameters	199
9.1	E866 - p_T spectrum	199
9.2	E866 - M spectrum	207
10	Results and predictions for DY p_T and M spectra in proton and antiproton induced reactions	209
10.1	E772 (pd)	209

10.2	E605 (pCu)	211
10.3	E288 (pNucleus)	212
10.4	E439 (pW)	213
10.5	E537 ($\bar{p}W$)	214
10.6	Prediction for \bar{P} ANDA ($\bar{p}p$)	216
VI Conclusion		223
11 Summary and conclusion		225
11.1	Summary	225
11.2	Outlook	228
Appendices		231
A Conventions and notation		233
A.1	Units	233
A.2	Light-cone coordinates	233
A.3	Complex logarithm	234
A.4	Metric, Dirac algebra and completeness relations	234
A.5	SU(3) color algebra	236
A.6	Cross sections	236
B Feynman rules and color factors		237
B.1	Feynman rules	237
B.2	Color factors	240
C Formulas		243
C.1	Vertex function integrals	243
C.2	Dirac traces	250
D Numerics		253
D.1	Parton distribution functions	253
D.2	Numerical integration	253
D.3	Special functions	253
Bibliography		255

Part I
Preface

1

Introduction

Our current picture of the composition of the universe is dominated by the standard model of cosmology [Lid09]. It states that the universe is made up out of three different components: dark energy, a kind of uniformly distributed energy, that interacts only through gravity, and the nature of which is still undetermined. Dark matter, which also only interacts gravitationally, but, in contrast to dark energy, seems to form clusters. Only the gravitational effects of these (electromagnetically) invisible clusters actually hinted to the existence of dark matter [Zwi33] and its composition is basically still unknown. And finally baryonic matter, which interacts through all four elementary forces, and out of which all the visible objects in the universe, like galaxies, stars and planets, are built. Remarkably the WMAP experiment found, that only less than 5% of the energy of the universe is present in form of baryonic matter. Dark matter accounts for about 22% and dark energy for about 73% [JBD⁺11]. Thus, it is fair to say, that for the most part we do not know what the universe is made of. However, we do know, that the mass of the atoms which form baryonic matter is almost totally concentrated in the atomic nuclei, which consist of nucleons (protons and neutrons). Although being studied for over 80 years now, many features and details of the nucleon and its inner structure are still not really understood. This thesis is devoted to the study of the structure of the nucleon through means of the Drell-Yan process [DY70].

1.1 Motivation

In 1911 Ernest Rutherford, in analysing the results of the famous Geiger-Marsden experiment, discovered, that atoms are made up of a small and positively charged

nucleus and a diffuse and negatively charged electron cloud [Rut11]. Furthermore, when bombarding nitrogen with α -particles (helium nuclei), he found that some of the reaction products were actually hydrogen nuclei. Based on atomic mass analysis he decided, that the hydrogen nucleus must be a building block of the nucleus of all heavier elements and, therefore, named it the proton (Greek: the first). In 1932 his student James Chadwick discovered the neutron as the second particle in atomic nuclei [Cha32]. While initially thought to be elementary particles, electron-proton scattering experiments performed by Robert Hofstadter and collaborators in 1956 actually showed, that the proton has a finite diameter of about 0.8 fm [MH56]. This proof of the non-point like nature of the proton was the advent of all further nucleon structure studies. In the 1960s deep inelastic electron scattering experiments on protons hinted to the existence of point like particles inside the proton. This led Richard Feynman to propose the famous parton model of the nucleon which states, that protons, neutrons and, in fact, all hadrons are composed of point like partons [Fey69]. About the same time Murray Gell-Mann, Kazuhiko Nishijima and others tried to organise the ever growing list of hadrons found in collider experiments. They developed the quark model [GM64], which allowed to account for the quantum numbers of these hadrons by picturing them as a composition of only a few elementary states, namely the quarks. Although the quarks were initially thought to be not real particles, but merely invented as kind of a book keeping device, they were later on identified through their quantum numbers as the charged partons inside the nucleon. In this simplified picture, the proton, for example, is made up out of two up- and one down-quark(s), which carry exactly the quantum numbers of the proton. Remarkably, one found, again in electron scattering experiments, that the quarks only carry about 50% of the proton's momentum [HM84] which hinted to the presence of uncharged partons inside the proton. The advent of quantum chromodynamics (QCD) in the 1970s provided an answer as to the origin of these particles. In QCD quarks, in addition to their other quantum numbers, also carry a color charge. The interaction among these colored objects is mediated via gauge bosons, called gluons. These gluons themselves carry the color charge, but are electrically neutral. They are believed to be exactly those particles, that carry the other half of the proton's momentum.

Having found the elementary particles, out of which the nucleon appears to be constructed, one, of course, would like to study these particles further. However, QCD has a very important property, that complicates matters: confinement. In nature, color charge carrying objects (quarks and gluons) always appear to be confined inside hadrons and have been, so far, never found separately. Thus, traditional approaches to study the properties of elementary particles, like e.g. quark-quark scattering, are not applicable. Nevertheless, another property of the strong force (as described by QCD) provides a way out, namely asymptotic freedom, discovered by Gross, Wilczek and Politzer in 1973 [GW73, Pol73]. The important feature of asymptotic freedom is, that the strong coupling constant actually decreases with increasing energy or, equivalently, decreasing distance. Thus, by probing strongly interacting objects, like the

nucleon, at very high energies, the small coupling constant actually allows the application of the well known methods of perturbation theory. In this limit there exist factorisation theorems, that effectively allow to separate the soft (long distance) interactions among the partons from the hard (short distance) interactions of the partons with the experimental probes. The hard subprocesses can then be evaluated using standard perturbative QCD (pQCD) calculations, while the soft part, so far, has to be inferred from experiment. Thus, studies of the nucleon structure have been trying to determine the various distributions of the partons inside the nucleon, since these distributions contain information about the soft interactions among the partons.

Until today the prevalent tool to study the parton distributions has been deep inelastic electron-nucleon scattering (DIS) [BD65], because of the following advantages: electron beams are readily available, as are detectors for the outgoing electrons. In addition the partonic sub process (electron-quark scattering) is theoretically well under control. Employing Feynman's parton model one can fix in this way, e.g., the longitudinal parton distribution functions (PDFs), which encode the longitudinal (along the nucleon's direction of motion) momentum distributions of the quarks and gluons. In the simplest parton model these distributions are functions of the parton momentum fractions x (fraction of the parent hadron's momentum, that is carried by the parton) only. However in DIS experiments scaling violations, i.e. dependence of the PDFs on the energy of the probe, were discovered. Perturbative QCD showed that the violations originate in the interaction among the partons and proved successful in describing this phenomenon, which confirmed further QCD as the correct theory of the strong interaction. Since one can show, that the PDFs obtained in DIS and through pQCD are universal, one can make predictions for other processes and so test the validity of all the model assumptions.

One of these processes was first described by (and subsequently named after) Drell and Yan in 1970 [DY70]. They anticipated, that in hadron-hadron collisions a quark from one hadron and an antiquark from another hadron could annihilate to form a lepton pair with large invariant mass M . This DY process is more exclusive than DIS: since two partons are involved, one can actually probe products of *two* parton distributions, instead of probing just one in DIS. In addition, the detection of the transverse momentum of the produced lepton pair provides insights into the transverse distributions of the participating partons. Furthermore, one can directly probe sea-quark distributions [AMP06], i.e. distributions of virtual quarks generated by the strong interaction, and at next-to-leading order (NLO) also the distribution of gluons. One encounters, however, also additional problems, when trying to describe DY observables: the most simple scheme is the parton model description, which is a leading order (LO) approach ($O(\alpha_s^0)$). In this scheme one pictures the two hadrons moving towards each other in the hadron c.m. frame at such high momentum, that all the interactions among the partons are suppressed by relativistic time dilation. Then both hadrons basically appear as a bunch of partons, all moving in the same direction and each carrying some momentum fraction x of the hadron's momentum. However, this

simple approach does not fully describe the interesting observables: while the shape of the M spectra of the DY pair can be reproduced, the absolute height can only be accounted for by including an additional K factor. This implies that NLO corrections are relevant, since at energies available at current experiments the strong coupling α_s is still sizable. Furthermore transverse momentum (p_T) spectra are not accessible at all [G⁺95], since one assumes from the beginning, that the partons carry no transverse momentum and so, by four momentum conservation, does the DY pair.

In the literature different paths have been taken in trying to remedy these shortcomings. Since the data show Gaussian p_T spectra at not too large p_T , one often simply modifies the LO calculation by folding in a phenomenological Gaussian distribution for the parton transverse momentum [DM04], but keeping the parton model collinear kinematics in the hard subprocess. The width of the distribution then has to be fitted to data. However, since these distributions are normalised, the absolute size of the cross sections is still underestimated [DM04]. The next logical step is to include hard subprocesses up to NLO ($O(\alpha_s)$). An example for such a process is gluon bremsstrahlung, where one of the participating quarks radiates a gluon before annihilating with the antiquark. In this scenario the DY pair can recoil against the gluon and obtain a finite p_T . However, such a calculation brings about additional problems: since in pQCD the quarks are commonly treated as massless, the calculated p_T spectra are divergent for $p_T \rightarrow 0$. In fact, for massless quarks they are divergent in any fixed order of the strong coupling α_s . Note, that these divergences are of the same nature as those leading to the scaling violations of the PDFs mentioned above. It is possible to remove these divergences by an all-order resummation, however, since p_T is no longer a hard scale at $p_T \rightarrow 0$, additional non-perturbative (i.e., experimental) input is needed in these (and all other pQCD) approaches to describe the region of very small p_T [CSS85, DWS85, FQZ03].

The continued interest in this process has sparked many different experiments in the past and for the future: in antiproton-proton ($\bar{p}p$) collisions at CERN [UA292], Fermilab [A⁺88], PAX [PAX05] and in the future at PANDA (FAIR) [TLP⁺09], in proton-proton (pp) collisions at CERN [CCOR79], Fermilab [NuSea03], RHIC [BSSV00, B⁺08], J-PARC [P⁺06, G⁺07, Kum08], IHEP [A⁺05] and JINR [SSNI09], in proton-nucleus reactions at Fermilab [I⁺81, S⁺81, M⁺91, E77294] and in pion-nucleon collisions at COMPASS [COMPASS97, COMPASS96]. An overview of the experimental situation can be found in [Rei07]. PANDA, for example, will allow measurements at hadron c.m. energies of a few GeV, where non-perturbative effects are expected to become more important. Together with the shortcomings of the pQCD type approaches discussed above, this highlights the need to model these effects in a phenomenological picture, at which this thesis is aiming at.

We will present our model in a two-step process: first an LO calculation, in which we remedy some of the shortcomings of the standard parton model. In the latter one always assumes that the partons move collinearly with their parent nucleon and do not interact during the time the hard process takes place. However, this is an idealisa-

tion of the situation in real experiments and so we take the following steps to improve on this: we parametrise the soft interactions among the partons by incorporating phenomenological transverse momentum and quark mass distributions and we take into account the full kinematics in the hard LO subprocess, i.e., the usual collinear approximation is overcome. We will show, that in this approach we can reproduce the shape of the p_T spectra, but still underestimate the data by a constant K factor. This finding triggered a complete calculation of all hard subprocesses to $O(\alpha_s)$ including the full kinematics, which will be presented next. As mentioned above, such a calculation would suffer from divergent p_T spectra if the quarks were massless. However, we will show that the phenomenological quark mass distributions now effectively smear out the divergent behavior. Such mass distributions or spectral functions are a well known concept in nuclear physics, where they are applied to the strongly coupled system of nucleons in nuclei, see for example [DMDS90]. Thus, it is worthwhile to test the same concept in the nucleon, which is a strongly coupled system of quarks and gluons. As already mentioned above, the PDF scaling violations and the divergent DY p_T spectra at NLO have a common origin: they both stem from collinear (or mass) singularities in the hard subprocesses. When calculating (p_T integrated) M spectra these divergent $O(\alpha_s)$ contributions are commonly absorbed into the PDFs. Since we will consider all these processes explicitly and regulate them with our mass distributions, we will then introduce a subtraction scheme to prevent double-counting. Finally we will find, that in our model we can describe data of DY p_T and M spectra taken at different hadronic energies and in different reactions without the need for a K factor, which enables us to make predictions for DY pair production at low hadronic energies, where, for example, the PANDA experiment will measure.

1.2 Outline

This thesis is structured in the following way: in Part II we will present selected mathematical tools, that were employed in the calculations of our model. Since we will have to calculate loop diagrams, we will begin in Chapter 2 with an introduction to regularisation methods of loop integrals in quantum field theories and then focus in detail on the method of dimensional regularisation. Furthermore a detailed walk through the evaluation of a typical loop integral (the three-point function) will be given in Chapter 3.

The details of the physical background for our model are presented in Part III. First in Chapter 4 a few selected topics of renormalisation will be discussed and a calculation of the QCD field strength renormalisation for massive quarks presented, which we will need in our model later on. Since infrared divergences play an important role in this work, in Chapter 5 we will present a typical example. In addition we will calculate the cross section for DY with soft gluon bremsstrahlung, which we will put to use at a later stage to show that our model is actually free of soft gluon divergences.

In Chapter 6 a detailed introduction to the studies of the structure of an unpolarised nucleon in elastic and inelastic lepton scattering will be given. Afterwards we will introduce the parton model and describe Bjorken scaling, and then formally derive the PDFs for DIS. The general properties of the PDFs will be discussed and a motivation for the scaling violations and the resulting DGLAP equations, that govern the evolution of the PDFs with the hard scale, will be given.

Part IV contains all the main details about our phenomenological model for DY pair production. First we will present a detailed introduction to the DY process at LO in Chapter 7 and then calculate the general subprocess cross section. Since we want to study the influence of distributions of intrinsic parton transverse momentum and quark mass on DY spectra, we will then give the details of the kinematics for the different cases of the collinear parton model, the model with intrinsic transverse momentum and the model with massive quarks. Furthermore, the distributions we have chosen will be presented, followed by the results of the different LO approaches of the chapter. We will find, that none of the LO models can account for the a priori undetermined K factor, since they all still underestimate the data. We will, therefore, in Chapter 8 extend our model to include all relevant processes to $O(\alpha_s)$: first we will present the virtual processes that modify the electromagnetic quark-photon vertex and then cover in detail the issues related to the soft gluon divergences, gauge invariance and current conservation for our case of quarks with unequal masses. After that, the real processes at $O(\alpha_s)$, gluon bremsstrahlung and gluon Compton scattering, will be introduced and their cross sections and kinematics explored. Finally we will study the influence of our distributions on the DY p_T spectra and describe in detail the treatment of collinear (or mass) singularities in pQCD and in our model. In the latter part we will motivate a subtraction scheme, devised in our model to prevent double-counting of divergent contributions of the NLO processes, which in pQCD are already absorbed into the PDFs.

The results of our full model will be presented in Part V. First we will fix the phenomenological parameters of our model at data taken in proton-proton reactions at high energies in Chapter 9 and will find, that a good description of DY p_T spectra is possible in our model without an additional K factor. Using the fixed parameters we will then in Chapter 10 compare the results of our model with data from other experiments, performed at several different energies and in proton-nucleus as well as in antiproton-proton reactions. Again we will show, that we are able to reproduce well these data in our full model. Having confirmed our choice of parameters, we will finally present our predictions for low energy DY pair production in the \bar{P} ANDA kinematics.

We will close with a summary of our findings and a conclusion in Chapter 11. In the Appendix our conventions and notation, reference formulas and information about the used computer routines are collected.

Part II

Mathematical tools

2

Loops and regularisation

In quantum field theoretical calculations beyond tree level one has to cope with the complications that arise through loops. Naive loop calculations usually are not well defined due to the divergent nature of loops. However in quantum field theories, like for example QED and QCD, an efficient tool, namely renormalisation, can be used to systematically remove the divergences and thus provide well defined results. Before renormalisation can be applied the divergent expressions need to be regularised, thus making the divergences manifest. This chapter is meant as an introduction to the concept of regularisation. More details and a deeper analysis can be found for example in [Mut98, PS95], on which this chapter is based.

2.1 The quark selfenergy

A typical loop example is the first order QCD quark selfenergy, depicted in Fig. 2.1. We will keep the quark massless in this chapter for simplicity. Note that this will lead to problems later on, namely mass singularities. However the following arguments concerning the regularisation procedures are untouched by these problems and we will take care of them later on.

According to the Feynman rules of QCD, see Appendix B, the selfenergy in Feynman gauge reads:

$$-i\Sigma(p) = C_F \int \frac{d^4k}{(2\pi)^4} (ig\gamma^\mu) \frac{i(\not{p}-\not{k})}{(p-k)^2 + i\epsilon} (ig\gamma^\nu) \frac{-ig_{\mu\nu}}{k^2 + i\epsilon}. \quad (2.1)$$

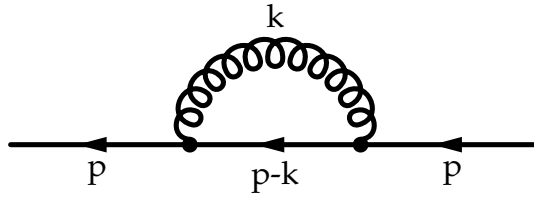


Figure 2.1: The first order QCD quark selfenergy diagram.

The color factor C_F can be calculated with the algebra of the $SU(3)$ color symmetry group, see Appendix B.2. Contracting the Lorentz indices we can rewrite the selfenergy:

$$\Sigma(p) = -ig^2 C_F \int \frac{d^4 k}{(2\pi)^4} \frac{\gamma^\mu (\not{p} - \not{k}) \gamma_\mu}{[(p-k)^2 + i\epsilon] [k^2 + i\epsilon]} . \quad (2.2)$$

Already at this point it is obvious that Σ is not well defined, since in the region of very large k the integrand appears to behave like $\frac{k}{k^4}$. A more thorough analysis, cf. Sec. 2.3, reveals that in the high momentum region of the integral one finds

$$\Sigma(p) \sim \int d^4 k \frac{1}{k^4} \rightarrow \infty , \quad (2.3)$$

and so the integral is logarithmically divergent as we integrate to higher and higher momenta. The divergence appears at the upper limit (∞) of the integral and is thus called ultraviolet (UV) divergence. Our immediate goal is now to devise a scheme in such a form that this divergence is regularised. This can actually be done by finding a convergent prescription in which as a certain limit we recover our original integral of Eq. (2.2).

2.2 Regularisation schemes

There are several different procedures known by which regularisation can be performed. Some of them have a rather intuitive motivation, but break some general physical principles, for example gauge invariance or Lorentz invariance. While other procedures retain these principles, they have different complications. In any case renormalisation has to be performed such that one recovers a theory which again obeys all these principles. To simplify this matter it is very useful to choose from the start a regularisation procedure which preserves as many of the general physical principles as possible. We will present here a selected overview of regularisation procedures, outlining their features and problems, and we treat one of the most important ones, namely dimensional regularisation, in detail in Section 2.3. A more detailed presentation of this topic can be found in [Lei75, Mut98].

2.2.1 Momentum cut-off

One of the simplest possibilities to make the divergent integral finite is to introduce an upper limit Λ for the three momentum integration, such that $|\vec{k}|^2 < \Lambda^2$. Then the divergence is controlled by the (arbitrary) parameter Λ . However in this scheme the selfenergy is not invariant under shifts of four momenta under the integral: translational invariance is broken. In addition gauge invariance is broken [JR76], which make this method unsuitable for regularising gauge theories.

2.2.2 Pauli-Villars regularisation

Another regularisation method dates back to Pauli and Villars [PV49]. The idea is to subtract from the propagator, in our case for example of the photon, another propagator of a fictitious particle with a very large mass M :

$$\frac{1}{k^2 + i\epsilon} \rightarrow \frac{1}{k^2 + i\epsilon} - \frac{1}{k^2 - M^2 + i\epsilon} = \frac{-M^2}{[k^2 + i\epsilon][k^2 - M^2 + i\epsilon]}, \quad (2.4)$$

which implies that in the limit of $M \rightarrow \infty$ our original divergent integral is recovered. The regularised integral now reads

$$\Sigma_{\text{PV}}(p) = -ig^2 C_F \int \frac{d^4k}{(2\pi)^4} \frac{\gamma^\mu (\not{p} - \not{k}) \gamma_\mu (-M^2)}{[(p-k)^2 + i\epsilon][k^2 + i\epsilon][k^2 - M^2 + i\epsilon]}. \quad (2.5)$$

For small k^2 and large M^2 the integrand in Eq. (2.5) is basically unchanged. On the other hand for very large $k^2 \gg M^2$ the integrand behaves like k^{-6} and so the integral is convergent. This is exactly what we want: The behavior of our original integral in Eq. (2.2) is recovered in the small momentum region and Σ_{PV} is finite.

This method of regularisation preserves translational and Lorentz invariance. It was also found that this method respects gauge invariance in QED and QCD (actually in all massless Yang-Mills theories), but fails in massive Yang-Mills theories: the selfenergy of the W -boson cannot be regularised in a gauge invariant way by this method [Mut98, tH71].

2.2.3 Lattice regularisation

A totally different approach to regularisation is the lattice method. The idea is to discretise space-time with a fixed distance d between lattice points. This implies that short-range correlations are suppressed in this scheme. Since short distances correspond to large momenta one effectively provides a cut-off, basically of $O(d^{-1})$, in the momentum integration. However problems are imminent: Lorentz invariance is not preserved and translational invariance is broken, since arbitrary translations will end

up outside the grid. However one can formulate the theory such that gauge invariance is manifestly preserved. While the aforementioned problems make this procedure not really satisfying for regularising a gauge theory, it allows for a non-perturbative calculation of gauge theories, especially QCD [Cre83].

2.2.4 Analytic regularisation

A precursor to Section 2.3 is the analytic continuation method [Lei75]. The idea is to change the exponent of the propagator such, that the integral converges. For this purpose one introduces a complex parameter α with $\Re(\alpha) > 1$ and rewrites the propagator:

$$\frac{1}{k^2 + i\epsilon} \rightarrow \frac{1}{(k^2 + i\epsilon)^\alpha}. \quad (2.6)$$

Then the integrand of

$$\Sigma_{\text{AC}}(p) = -ig^2 C_F \int \frac{d^4k}{(2\pi)^4} \frac{\gamma^\mu (\not{p} - \not{k}) \gamma_\mu}{[(p-k)^2 + i\epsilon] [k^2 + i\epsilon]^\alpha} \quad (2.7)$$

behaves like $k^{-2(1+\alpha)}$ for large k^2 and thus the result is finite (remember that for $\alpha = 1$ the integral is logarithmically divergent). This result is now continued analytically to $\alpha = 1$ and the original divergence shows up as a pole at $\alpha = 1$. Unfortunately the method is not gauge invariant [Mut98], however the idea of analytic continuation is also crucial for the concept of dimensional regularisation, to which we devote the entire next section.

2.3 Dimensional regularisation

The method of dimensional regularisation, first formulated by 't Hooft and Veltman in the early 1970s [tH71, tHV72], is one of the most important regularisation procedures for gauge theories today. The basic idea behind it is the following: certain types of integrals are divergent when calculated in a certain number of dimensions, while they converge for other numbers. In this section we will apply this concept on the quark selfenergy in Eq. (2.2) and work out the necessary mathematical ingredients along the way.

2.3.1 Example

Here is a simple example: Let $a > 0$ and consider the integral

$$I_2 = \int_{a < |x|} d^3x \frac{1}{|x|^3}. \quad (2.8)$$

Then using spherical coordinates we find

$$\begin{aligned}
 I_2 &= \int d\Omega \lim_{K \rightarrow \infty} \int_a^K x^2 dx \frac{1}{x^3} \\
 &= 4\pi \lim_{K \rightarrow \infty} \log \left(\frac{K}{a} \right) \rightarrow \infty,
 \end{aligned} \tag{2.9}$$

and so in three dimensions the integral is not well defined. However in two dimension the integral poses no problem:

$$\begin{aligned}
 I_1 &= \int_{a < |x|} d^2x \frac{1}{|x|^3} \\
 &= \int_0^{2\pi} d\phi \lim_{K \rightarrow \infty} \int_a^K x dx \frac{1}{x^3} \\
 &= 2\pi \lim_{K \rightarrow \infty} \left(-\frac{1}{K} + \frac{1}{a} \right) \\
 &= \frac{2\pi}{a}.
 \end{aligned} \tag{2.10}$$

In fact the integral will converge as long as the dimension $d < 3$. In dimensional regularisation one can exploit this fact: one first calculates the integral without fixing the number of dimensions d and only requiring that d is chosen such that the integral converges. Then one continues analytically d to the number of dimensions d' of the divergent integral. The divergence then shows up as poles in $d - d'$. Using our example for the quark selfenergy of Eq. (2.2) we will present this procedure in detail in the next sections.

2.3.2 Extension to d dimensions

As we have seen in Eq. (2.3) our quark selfenergy $\Sigma(p)$ is not well defined in $d = 4$ dimensions. However looking back at our example in Section 2.3.1 we anticipate that $\Sigma(p)$ is well defined if only d is small enough. To verify this we have to rewrite $\Sigma(p)$ for a general number of space-time dimensions d . At first we will restrict ourselves to integer numbers for d .

Changing the number of dimensions has several consequences. First of all momenta now have $d - 1$ instead of three space components. To evaluate the contractions of the Dirac γ -matrices in d dimensions we need a metric tensor for d dimensions and especially its contraction identity

$$g^{\mu\nu} g_{\mu\nu} = d. \tag{2.11}$$

Since we have the anticommutation relation for the Dirac matrices

$$\{\gamma^\mu, \gamma^\nu\} = 2g^{\mu\nu}, \quad (2.12)$$

the contraction identities for the Dirac matrices are modified, see Appendix A.4.2. The Dirac algebra is however otherwise unchanged. The trace relations for the Dirac matrices, see Appendix A.4.2, are in general modified in d dimensions. However in the end we are always only interested in results for $d \rightarrow 4$ and we can also stick to the trace relations in four dimensions [Mut98]:

$$\text{Tr}[\gamma^\mu \gamma^\nu] = 4g^{\mu\nu}. \quad (2.13)$$

For the integral measure we choose

$$\frac{d^d k}{(2\pi)^d}. \quad (2.14)$$

Note that this is a convention and instead of $(2\pi)^d$ we could have also chosen $(2\pi)^4$, since again in the end we are only interested in the limit $d \rightarrow 4$.

Of great importance is also the fact, that the coupling constant g is generally not dimensionless for an arbitrary number of space time dimensions d . One can deduce the dimension of g by observing, that the QCD action \mathcal{S} has to be a dimensionless quantity:

$$\dim[\mathcal{S}] = \dim\left[\int d^d x \mathcal{L}\right] = 0, \quad (2.15)$$

where \mathcal{L} is the QCD Lagrangian and $\dim[A]$ is the mass dimension of the expression A . In natural units, see Appendix A.1, the mass dimension of lengths is -1 and so

$$\dim[d^d x] = -d \Rightarrow \dim[\mathcal{L}] = d. \quad (2.16)$$

The classical QCD Lagrangian reads [Mut98]:

$$\mathcal{L} = \sum_{k=1}^{N_f} \bar{\Psi}^k (i\not{D} - m_k) \Psi^k - \frac{1}{4} F_a^{\mu\nu} F_{a\mu\nu} \quad (2.17)$$

where the sum runs over all quark flavors k and m_k are the quark masses. D^μ is the covariant derivative,

$$D^\mu = \partial^\mu - igt^a A_a^\mu, \quad (2.18)$$

and $F_a^{\mu\nu}$ the QCD field strength tensor:

$$F_a^{\mu\nu} = \partial^\mu A_a^\nu - \partial^\nu A_a^\mu + gf_{abc} A_b^\mu A_c^\nu. \quad (2.19)$$

Here A_a^μ is the gluon field, f_{abc} are the structure constants of SU(3) and t^a its generators, see also Appendix A.5. Now we immediately find for the mass dimension of the quark fields Ψ^k :

$$\dim[\bar{\Psi}^k m_k \Psi^k] = d \Rightarrow \dim[\Psi^k] = \frac{d-1}{2}. \quad (2.20)$$

Since

$$\dim[\partial^\mu] = \dim\left[\frac{\partial}{\partial x_\mu}\right] = 1, \quad (2.21)$$

we find

$$\dim[F_a^{\mu\nu} F_{a\mu\nu}] = \dim[\partial^\mu A_a^\nu \partial_\mu A_{a\nu}] = d \Rightarrow \dim[A_a^\mu] = \frac{d-2}{2}. \quad (2.22)$$

Therefore

$$\dim[\bar{\Psi}^k \not{D} \Psi^k] = \dim[\Psi^k g A_a^\mu \Psi^k] = d \Rightarrow \dim[g] = \frac{4-d}{2}, \quad (2.23)$$

and so g is only dimensionless for $d = 4$. However we can relate g to a dimensionless coupling constant g_0 if we introduce an arbitrary mass scale μ :

$$g := g_0 \cdot \mu^{\frac{4-d}{2}}. \quad (2.24)$$

The arbitrary mass scale μ can of course have no observable physical consequences. Thus, after undergoing a suitable renormalisation procedure, the observable quantities are independent of μ , cf. Sec. 4.1.

With our conventions given above the quark selfenergy of Eq. (2.2) becomes in d dimensions

$$\begin{aligned} \Sigma(p) &= -ig^2 C_F \int \frac{d^d k}{(2\pi)^d} \frac{\gamma^\mu (\not{p} - \not{k}) \gamma_\mu}{[(p-k)^2 + i\epsilon][k^2 + i\epsilon]} \\ &= -ig^2 C_F \int \frac{d^d k}{(2\pi)^d} \frac{(2-d)(\not{p} - \not{k})}{[(p-k)^2 + i\epsilon][k^2 + i\epsilon]}, \end{aligned} \quad (2.25)$$

where in the last step we have used the contraction identity

$$\gamma^\mu \gamma_\alpha \gamma_\mu = (2-d)\gamma_\alpha. \quad (2.26)$$

Note that the denominator of Eq. (2.25) is quite unpleasant: there are terms of order k^2 , k^3 and k^4 . One would like to have a denominator which is quadratic in k , since the integrals of such forms are well known. We will demonstrate in the next section how to accomplish this for the general case of integrals with propagator denominators.

2.3.3 Feynman parameters

The idea of Feynman parameters is to rewrite products of propagator denominators into sums, since by shifting the integration variable it is then easy to acquire a denominator quadratic in the shifted variable. The concept is however rather general and can also be applied in different contexts.

Consider a general expression of the form $\frac{1}{A \cdot B}$. Then we claim

$$\frac{1}{A \cdot B} = \int_0^1 dx \int_0^1 dy \frac{\delta(1-x-y)}{[xA + yB]^2}. \quad (2.27)$$

The proof goes as follows: we exploit the δ function and obtain

$$\begin{aligned} \int_0^1 dx \int_0^1 dy \frac{\delta(1-x-y)}{[xA + yB]^2} &= \int_0^1 dx \frac{1}{[xA + (1-x)B]^2} \\ &= \int_0^1 dx \frac{1}{[x(A-B) + B]^2} \\ &= \left[\frac{1}{A-B} \cdot \frac{-1}{x(A-B) + B} \right]_0^1 \\ &= \frac{-1}{(A-B) \cdot A} + \frac{1}{(A-B) \cdot B} \\ &= \frac{1}{A \cdot B}. \end{aligned} \quad (2.28)$$

Note that one can easily extend this concept with A and B raised to integer powers by repeatedly differentiating Eq. (2.27) by A and/or B . However one can find an even more general identity with an arbitrary number n of factors in the denominator, each raised to some *complex* power. The claim reads

$$\frac{1}{A_1^{\alpha_1} \cdot A_2^{\alpha_2} \cdots A_n^{\alpha_n}} = \frac{\Gamma(\sum_{i=1}^n \alpha_i)}{\prod_{i=1}^n \Gamma(\alpha_i)} \int_0^1 dx_1 \int_0^1 dx_2 \cdots \int_0^1 dx_n \frac{\prod_{i=1}^n x_i^{\alpha_i-1} \delta(1 - \sum_{i=1}^n x_i)}{[\sum_{i=1}^n x_i A_i]^{\sum_{i=1}^n \alpha_i}} \quad (2.29)$$

and we require

$$\Re(\alpha_i) > 0. \quad (2.30)$$

$\Gamma(x)$ is the Gamma function, which has many different representations, one of which is

$$\Gamma(x) = \int_0^{\infty} dz z^{x-1} \cdot \exp(-z), \quad (2.31)$$

for $x \neq -n$ with $n \in \mathcal{N}_0$. Note that Γ interpolates the factorial function, since one finds

$$x \in \mathcal{N} \Rightarrow \Gamma(x) = (x-1)! . \quad (2.32)$$

Note also that Γ has poles at all integers $n \leq 0$, which will be of relevance later on.

At this point it is worthwhile to introduce a related function, namely the Beta function, which can be written as

$$B(x, y) = \int_0^1 dz z^{x-1} (1-z)^{y-1} , \quad (2.33)$$

where we require that $\Re(x) > 0$ and $\Re(y) > 0$. Beta and Gamma function are connected via

$$B(x, y) = \frac{\Gamma(x)\Gamma(y)}{\Gamma(x+y)} . \quad (2.34)$$

Now we have all the tools we need to prove Eq. (2.29). First we consider the case of two factors in the denominator ($n = 2$):

$$\begin{aligned} I_2 &= \frac{\Gamma(\alpha_1 + \alpha_2)}{\Gamma(\alpha_1)\Gamma(\alpha_2)} \int_0^1 dx_1 \int_0^1 dx_2 \frac{x_1^{\alpha_1-1} x_2^{\alpha_2-1} \delta(1-x_1-x_2)}{[x_1 A_1 + x_2 A_2]^{(\alpha_1+\alpha_2)}} \\ &= \frac{\Gamma(\alpha_1 + \alpha_2)}{\Gamma(\alpha_1)\Gamma(\alpha_2)} \int_0^1 dx_1 \frac{x_1^{\alpha_1-1} (1-x_1)^{\alpha_2-1}}{[x_1 A_1 + (1-x_1) A_2]^{(\alpha_1+\alpha_2)}} . \end{aligned} \quad (2.35)$$

Note that the prefactor in Eq. (2.35) immediately reminds us of Eq. (2.34) and the powers in the numerator remind us of Eq. (2.33), which gives us a hint what to do: rewrite Eq. (2.35) into the representation of the Beta function Eq. (2.33), so that the integral basically cancels the prefactor. We substitute

$$y = \frac{x_1 A_1}{x_1 A_1 + (1-x_1) A_2} \quad (2.36)$$

$$\Rightarrow 1-y = \frac{(1-x_1) A_2}{x_1 A_1 + (1-x_1) A_2} \quad (2.37)$$

and so for the integral measure we find

$$\frac{dy}{dx_1} = \frac{A_1}{x_1 A_1 + (1-x_1) A_2} - \frac{x_1 A_1 (A_1 - A_2)}{[x_1 A_1 + (1-x_1) A_2]^2} = \frac{A_1 A_2}{[x_1 A_1 + (1-x_1) A_2]^2} . \quad (2.38)$$

Then

$$\begin{aligned}
 I_2 &:= \frac{\Gamma(\alpha_1 + \alpha_2)}{\Gamma(\alpha_1)\Gamma(\alpha_2)} \int_0^1 dy \frac{[x_1 A_1 + (1 - x_1) A_2]^2}{A_1 A_2} \frac{y^{\alpha_1 - 1} (1 - y)^{\alpha_2 - 1}}{A_1^{\alpha_1 - 1} B_1^{\alpha_2 - 1} [x_1 A_1 + (1 - x_1) A_2]^2} \\
 &= \frac{1}{A_1^{\alpha_1} B_1^{\alpha_2}} \frac{\Gamma(\alpha_1 + \alpha_2)}{\Gamma(\alpha_1)\Gamma(\alpha_2)} \int_0^1 dy y^{\alpha_1 - 1} (1 - y)^{\alpha_2 - 1} \\
 &= \frac{1}{A_1^{\alpha_1} B_1^{\alpha_2}} \frac{\Gamma(\alpha_1 + \alpha_2)}{\Gamma(\alpha_1)\Gamma(\alpha_2)} B(\alpha_1, \alpha_2) \\
 &= \frac{1}{A_1^{\alpha_1} B_1^{\alpha_2}}, \tag{2.39}
 \end{aligned}$$

and so Eq. (2.29) holds for $n = 2$. The proof for general n now goes by induction: if Eq. (2.29) holds for a certain n , then for $n + 1$ we find

$$\frac{1}{A_1^{\alpha_1} \cdot A_2^{\alpha_2} \cdot \dots \cdot A_n^{\alpha_n}} \cdot \frac{1}{A_{n+1}^{\alpha_{n+1}}} = \frac{\Gamma(\sum_{i=1}^n \alpha_i)}{\prod_{i=1}^n \Gamma(\alpha_i)} \int_0^1 dx_1 \dots \int_0^1 dx_n \frac{\prod_{i=1}^n x_i^{\alpha_i - 1} \delta(1 - \sum_{i=1}^n x_i)}{[\sum_{i=1}^n x_i A_i]^{\sum_{i=1}^n \alpha_i} \cdot A_{n+1}^{\alpha_{n+1}}}. \tag{2.40}$$

Now we can make use of our result for I_2 and combine the two factors in the denominator of Eq. (2.40):

$$\begin{aligned}
 C_{n+1} &:= \frac{1}{[\sum_{i=1}^n x_i A_i]^{\sum_{i=1}^n \alpha_i} \cdot A_{n+1}^{\alpha_{n+1}}} \\
 &= \frac{\Gamma(\sum_{i=1}^n \alpha_i + \alpha_{n+1})}{\Gamma(\sum_{i=1}^n \alpha_i)\Gamma(\alpha_{n+1})} \int_0^1 dx_{n+1} \int_0^1 dy \frac{x_{n+1}^{(\alpha_{n+1} - 1)} y^{(\sum_{i=1}^n \alpha_i - 1)} \delta(1 - y - x_{n+1})}{[y(\sum_{i=1}^n x_i A_i) + x_{n+1} A_{n+1}]^{\sum_{i=1}^n \alpha_i + \alpha_{n+1}}} \\
 &= \frac{\Gamma(\sum_{i=1}^{n+1} \alpha_i)}{\Gamma(\sum_{i=1}^n \alpha_i)\Gamma(\alpha_{n+1})} \int_0^1 dx_{n+1} \int_0^1 dy \frac{x_{n+1}^{(\alpha_{n+1} - 1)} y^{(\sum_{i=1}^n \alpha_i - 1)} \delta(1 - y - x_{n+1})}{[\sum_{i=1}^n (y \cdot x_i) A_i + x_{n+1} A_{n+1}]^{\sum_{i=1}^{n+1} \alpha_i}}. \tag{2.41}
 \end{aligned}$$

Now we insert C_{n+1} into Eq. (2.40):

$$\begin{aligned}
 I_{n+1} &:= \frac{1}{A_1^{\alpha_1} \cdot A_2^{\alpha_2} \cdot \dots \cdot A_{n+1}^{\alpha_{n+1}}} \\
 &= \frac{\Gamma(\sum_{i=1}^n \alpha_i)}{\prod_{i=1}^n \Gamma(\alpha_i)} \int_0^1 dx_1 \dots \int_0^1 dx_n \prod_{i=1}^n x_i^{\alpha_i - 1} \delta\left(1 - \sum_{i=1}^n x_i\right) \\
 &\quad \times \frac{\Gamma(\sum_{i=1}^{n+1} \alpha_i)}{\Gamma(\sum_{i=1}^n \alpha_i)\Gamma(\alpha_{n+1})} \int_0^1 dx_{n+1} \int_0^1 dy \frac{x_{n+1}^{(\alpha_{n+1} - 1)} y^{(\sum_{i=1}^n \alpha_i - 1)} \delta(1 - y - x_{n+1})}{[\sum_{i=1}^n (y \cdot x_i) A_i + x_{n+1} A_{n+1}]^{\sum_{i=1}^{n+1} \alpha_i}}. \tag{2.42}
 \end{aligned}$$

Substituting

$$\hat{x}_i = y \cdot x_i \Rightarrow dx_i = \frac{d\hat{x}_i}{y} \quad (2.43)$$

for $i = 1 \dots n$, we recover

$$\begin{aligned} I_{n+1} &= \frac{\Gamma(\sum_{i=1}^{n+1} \alpha_i)}{\prod_{i=1}^{n+1} \Gamma(\alpha_i)} \int_0^1 dy \int_0^1 d\hat{x}_1 \dots \int_0^1 d\hat{x}_n \frac{1}{y^n} \prod_{i=1}^n \left(\frac{\hat{x}_i}{y} \right)^{\alpha_i-1} \delta \left(1 - \sum_{i=1}^n \frac{\hat{x}_i}{y} \right) \\ &\times \int_0^1 dx_{n+1} \frac{x_{n+1}^{(\alpha_{n+1}-1)} y^{(\sum_{i=1}^n \alpha_i-1)} \delta(1-y-x_{n+1})}{[\sum_{i=1}^n \hat{x}_i A_i + x_{n+1} A_{n+1}]^{(\sum_{i=1}^{n+1} \alpha_i)}} \\ &= \frac{\Gamma(\sum_{i=1}^{n+1} \alpha_i)}{\prod_{i=1}^{n+1} \Gamma(\alpha_i)} \int_0^1 dy \int_0^1 d\hat{x}_1 \dots \int_0^1 d\hat{x}_n \prod_{i=1}^n \hat{x}_i^{\alpha_i-1} \delta \left(1 - \sum_{i=1}^n \frac{\hat{x}_i}{y} \right) \\ &\times \int_0^1 dx_{n+1} \frac{x_{n+1}^{(\alpha_{n+1}-1)} \delta(1-y-x_{n+1})}{[\sum_{i=1}^n \hat{x}_i A_i + x_{n+1} A_{n+1}]^{(\sum_{i=1}^{n+1} \alpha_i)}} \underbrace{\left(y^{-n} \cdot y^{(-\sum_{i=1}^n \alpha_i+n)} \cdot y^{(\sum_{i=1}^n \alpha_i-1)} \right)}_{y^{-1}}. \end{aligned} \quad (2.44)$$

Now we note that

$$\begin{aligned} &\int_0^1 dy \int_0^1 d\hat{x}_n \int_0^1 dx_{n+1} \frac{\delta \left(1 - \sum_{i=1}^n \frac{\hat{x}_i}{y} \right) \delta(1-y-x_{n+1})}{y} \\ &= \int_0^1 dy \int_0^1 d\hat{x}_n \int_0^1 dx_{n+1} \frac{\delta(y - \sum_{i=1}^n \hat{x}_i) \cdot y \cdot \delta(1-y-x_{n+1})}{y} \\ &= \int_0^1 d\hat{x}_n \int_0^1 dx_{n+1} \delta \left(1 - x_{n+1} - \sum_{i=1}^n \hat{x}_i \right). \end{aligned} \quad (2.45)$$

Finally we can again replace everywhere \hat{x}_i with x_i and thus

$$I_{n+1} = \frac{\Gamma(\sum_{i=1}^{n+1} \alpha_i)}{\prod_{i=1}^{n+1} \Gamma(\alpha_i)} \int_0^1 dx_1 \dots \int_0^1 dx_{n+1} \frac{\prod_{i=1}^{n+1} x_i^{\alpha_i-1} \delta \left(1 - \sum_{i=1}^{n+1} x_i \right)}{[\sum_{i=1}^{n+1} x_i A_i]^{(\sum_{i=1}^{n+1} \alpha_i)}}. \quad (2.46)$$

This concludes our proof of Eq. (2.29).

After this short detour, we are now ready to rewrite the quark selfenergy in Eq. (2.25) into a more pleasant form. Using Eq. (2.28) we combine the propagators:

$$\begin{aligned}\Sigma(p) &= -ig^2 C_F \int_0^1 dx \int \frac{d^d k}{(2\pi)^d} \frac{(2-d)(\not{p}-\not{k})}{[x((p-k)^2 + i\epsilon) + (1-x)(k^2 + i\epsilon)]^2} \\ &= -ig^2 C_F \int_0^1 dx \int \frac{d^d k}{(2\pi)^d} \frac{(2-d)(\not{p}-\not{k})}{[k^2 - 2xp \cdot k + xp^2 + i\epsilon]^2}.\end{aligned}\quad (2.47)$$

Now one can complete the square in the denominator,

$$\Sigma(p) = -ig^2 C_F \int_0^1 dx \int \frac{d^d k}{(2\pi)^d} \frac{(2-d)(\not{p}-\not{k})}{[(k-xp)^2 - x^2 p^2 + xp^2 + i\epsilon]^2} \quad (2.48)$$

and shift the momentum integration

$$k \rightarrow l = k - xp \Rightarrow d^4 k \rightarrow d^4 l. \quad (2.49)$$

Then

$$\begin{aligned}\Sigma(p) &= -ig^2 C_F \int_0^1 dx \int \frac{d^d l}{(2\pi)^d} \frac{(2-d)(\not{p}-\not{l}-x\not{p})}{[l^2 + x(1-x)p^2 + i\epsilon]^2} \\ &= -ig^2 C_F \int_0^1 dx \int \frac{d^d l}{(2\pi)^d} \frac{(2-d)((1-x)\not{p}-\not{l})}{[l^2 + x(1-x)p^2 + i\epsilon]^2}.\end{aligned}\quad (2.50)$$

2.3.4 Wick rotation

We now have to tackle the momentum integral in

$$\Sigma(p) = -ig^2 C_F \int_0^1 dx \int \frac{d^d l}{(2\pi)^d} \frac{(2-d)((1-x)\not{p}-\not{l})}{[l^2 - \Delta + i\epsilon]^2}, \quad (2.51)$$

with $\Delta = -x(1-x)p^2$.

Before we start calculating we note that

$$\int d^d l \frac{l^\mu}{[l^2 - \Delta + i\epsilon]^2} = 0. \quad (2.52)$$

This follows directly from symmetry considerations: the numerator is antisymmetric in the momentum component l^μ while the denominator is symmetric. Thus the integral over dl^μ vanishes. The same argumentation can immediately be generalised to all integrals of the type of Eq. (2.52) with an *odd* power of l in the numerator:

$$\int d^d l \frac{\prod_{i=1}^{2n+1} l^{\mu_i}}{[l^2 - \Delta + i\epsilon]^k} = 0 \quad (2.53)$$

with $n \in \mathcal{N}_0$ and $k \in \mathcal{N}$. Then one also finds

$$\int d^d l \frac{l^\mu l^\nu}{[l^2 - \Delta + i\epsilon]^k} = 0 \text{ for } \mu \neq \nu \quad (2.54)$$

and so only for $\mu = \nu$ the last integral does not vanish. Thus, since there are no Dirac matrices involved, Lorentz covariance of the integral requires that it must be proportional to the metric tensor $g^{\mu\nu}$:

$$\int d^d l \frac{l^\mu l^\nu}{[l^2 - \Delta + i\epsilon]^k} = \int d^d l \frac{f(l^2) g^{\mu\nu}}{[l^2 - \Delta + i\epsilon]^k}. \quad (2.55)$$

$f(l^2)$ is readily found by contracting both sides of Eq. (2.55) with $g_{\mu\nu}$:

$$\begin{aligned} g_{\mu\nu} l^\mu l^\nu &= f(l^2) g^{\mu\nu} g_{\mu\nu} \\ \Rightarrow f(l^2) &= \frac{l^2}{d} \end{aligned} \quad (2.56)$$

and so

$$\int d^d l \frac{l^\mu l^\nu}{[l^2 - \Delta + i\epsilon]^k} = \int d^d l \frac{\frac{1}{d} l^2 g^{\mu\nu}}{[l^2 - \Delta + i\epsilon]^k}. \quad (2.57)$$

Similar identities to Eq. (2.57) hold for other combinations with even numbers of components of l in the numerator [PS95].

Now back to the quark selfenergy: Eq. (2.52) tells us, that we can drop the term $\mathcal{I} = \gamma_\mu l^\mu$ in Eq. (2.51). So there remains

$$\Sigma(p) = -ig^2 C_F \int_0^1 dx \int \frac{d^d l}{(2\pi)^d} \frac{(2-d)((1-x)\not{p})}{[l^2 - \Delta + i\epsilon]^2}. \quad (2.58)$$

Note that the last integral is defined in d -dimensional Minkowski space. One could now carry out the l^0 integration via a contour integral in the complex l^0 plane. It is

thus useful to study the pole structure of the integrand in Eq. (2.58). For $\Delta > 0$ we find:

$$\begin{aligned}
 l^2 - \Delta + i\epsilon &= (l^0)^2 - (\vec{l})^2 - \Delta + i\epsilon \stackrel{!}{=} 0 \\
 \Rightarrow l^0 &= \pm \sqrt{(\vec{l})^2 + \Delta - i\epsilon} \\
 &= \pm \sqrt{(\vec{l})^2 + \Delta} \mp \frac{i\epsilon}{2\sqrt{(\vec{l})^2 + \Delta}} + O(\epsilon^2) \\
 &\approx \pm \sqrt{(\vec{l})^2 + \Delta} \mp i\epsilon'.
 \end{aligned} \tag{2.59}$$

The integrand has poles in the upper left and in the lower right quadrant of the complex l^0 plane, see Fig. 2.2. Since for large $|l^0|$ the integrand behaves like $|l^0|^{-2}$, we can close the integration contour either in the upper or lower half plane, while the infinite half-circle does not contribute to the integral in either case. Thus the l^0 integration is determined by the poles inside the integration contour and we could now apply the residue theorem. Then only a $(d-1)$ -dimensional integral over the spatial components in Euclidean space would remain. However there is a more elegant method, namely the Wick rotation.

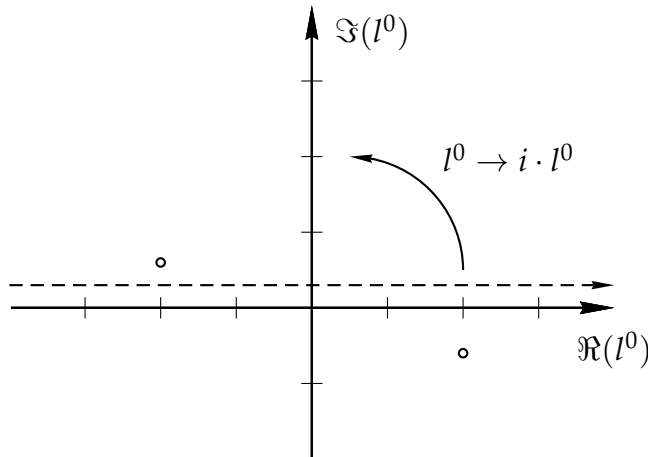


Figure 2.2: Position of the poles in the complex l^0 plane. The dashed line indicates the contour of the integration. By rotating this contour 90 degrees counter clockwise the dashed line does *not* cross a pole and so the result of the integration is unchanged.

We note that by rotating the path of the l^0 integration in the complex plane by 90 degrees counter clockwise, the contour does *not* cross any pole:

$$l^0 \rightarrow i \cdot l^0_{\text{E}}, \tag{2.60}$$

where E stands for Euclidean. The residue theorem now states that the value of the integration is unchanged by this procedure. We find

$$dl^0 \rightarrow i \cdot dl_E^0, \quad (2.61)$$

$$l^2 = (l^0)^2 - (\vec{l})^2 \rightarrow -(l^0)^2 - (\vec{l})^2 = -l_E^2 \quad (2.62)$$

and the integral of Eq. (2.58) becomes

$$\begin{aligned} \Sigma(p) &= -ig^2 C_F \int_0^1 dx \int \frac{i \cdot d^d l_E (2-d) ((1-x)p)}{(2\pi)^d [-l_E^2 - \Delta + i\epsilon]^2} \\ &= g^2 C_F \int_0^1 dx \frac{(2-d) ((1-x)p)}{(2\pi)^d} \int \frac{d^d l_E}{[l_E^2 + \Delta - i\epsilon]^2}. \end{aligned} \quad (2.63)$$

Now we have to solve a d -dimensional integral in Euclidean space and we note that the integrand only depends on the absolute value of l_E , which makes the use of spherical coordinates a good choice.

2.3.5 d -dimensional spherical coordinates

To calculate the second integral in Eq. (2.63), we here consider the general solution for integrals of the type:

$$I = \int \frac{d^d x \cdot (x^2)^{\frac{n}{2}}}{[x^2 + \Delta - i\epsilon]^k}, \quad (2.64)$$

with $n + d < 2k$. We introduce d -dimensional spherical coordinates and note that for $\Delta > 0$, i.e. $p^2 < 0$, the integrand has no poles and we can drop the $i\epsilon$ term. Therefore we will keep p space-like in the following calculations and later on continue analytically the result to time-like p , keeping in mind that Δ has a tiny negative imaginary part.

It is instructive to study the construction of spherical coordinates in the common two and three dimensions and then to expand the scheme to d dimensions. In all dimensions we understand the absolute value of the coordinate vector to be defined as $r = |\vec{x}|$.

In two dimensions spherical (polar) coordinates are defined via

$$\begin{aligned} x_1 &= r \sin(\theta_1), \\ x_2 &= r \cos(\theta_1), \end{aligned} \quad (2.65)$$

with $0 < \theta_1 < 2\pi$. For three dimensions one finds:

$$\begin{aligned} x_1 &= r \sin(\theta_1) \sin(\theta_2), \\ x_2 &= r \cos(\theta_1) \sin(\theta_2), \\ x_3 &= r \cos(\theta_2), \end{aligned} \quad (2.66)$$

with $0 < \theta_1 < 2\pi$ and $0 < \theta_2 < \pi$. We now continue along this path and define

$$\begin{aligned} x_1 &= r \sin(\theta_1) \sin(\theta_2) \dots \sin(\theta_{d-1}) , \\ x_2 &= r \cos(\theta_1) \sin(\theta_2) \dots \sin(\theta_{d-1}) , \\ &\vdots \\ x_{d-1} &= r \cos(\theta_{d-2}) \sin(\theta_{d-1}) , \\ x_d &= r \cos(\theta_{d-1}) , \end{aligned} \tag{2.67}$$

with $0 < \theta_1 < 2\pi$ and $0 < \theta_i < \pi$ for $i = 2 \dots (d-1)$. To transform the integral measure in Eq. (2.64),

$$d^d x = |D_d| \cdot dr \cdot \prod_{i=1}^{d-1} d\theta_i , \tag{2.68}$$

we calculate the determinant of the Jacobian

$$D_d = \det \left[\frac{\partial(x_1, \dots, x_d)}{\partial(r, \theta_1, \dots, \theta_{d-1})} \right] = \det \begin{pmatrix} \frac{\partial x_1}{\partial r} & \dots & \frac{\partial x_d}{\partial r} \\ \frac{\partial x_1}{\partial \theta_1} & \dots & \frac{\partial x_d}{\partial \theta_1} \\ \vdots & & \vdots \\ \frac{\partial x_1}{\partial \theta_{d-1}} & \dots & \frac{\partial x_d}{\partial \theta_{d-1}} \end{pmatrix} . \tag{2.69}$$

For D_d we claim:

$$D_d = (-1)^{d-1} r^{d-1} \prod_{i=1}^{d-1} \sin^{i-1}(\theta_i) . \tag{2.70}$$

The proof is not difficult and goes by induction. For $d = 2$ one finds

$$\begin{aligned} D_2 &= \det \begin{pmatrix} \frac{\partial x_1}{\partial r} & \frac{\partial x_2}{\partial r} \\ \frac{\partial x_1}{\partial \theta_1} & \frac{\partial x_2}{\partial \theta_1} \end{pmatrix} \\ &= \det \begin{pmatrix} \sin(\theta_1) & \cos(\theta_1) \\ r \cos(\theta_1) & -r \sin(\theta_1) \end{pmatrix} \\ &= -r , \end{aligned} \tag{2.71}$$

which confirms Eq. (2.70) for $d = 2$. If the claim holds for $d - 1$ ($d \geq 3$), we find for d :

$$D_d = \det \begin{pmatrix} \frac{\partial x_1}{\partial r} & \dots & \frac{\partial x_{d-1}}{\partial r} & \frac{\partial x_d}{\partial r} \\ \frac{\partial x_1}{\partial \theta_1} & \dots & \frac{\partial x_{d-1}}{\partial \theta_1} & 0 \\ \vdots & & \vdots & \vdots \\ \frac{\partial x_1}{\partial \theta_{d-2}} & \dots & \frac{\partial x_{d-1}}{\partial \theta_{d-2}} & 0 \\ \frac{\partial x_1}{\partial \theta_{d-1}} & \dots & \frac{\partial x_{d-1}}{\partial \theta_{d-1}} & \frac{\partial x_d}{\partial \theta_{d-1}} \end{pmatrix} , \tag{2.72}$$

where the zeros in the last column are a consequence of x_d being a function of r and θ_{d-1} only. A Laplace expansion along the last column yields:

$$\begin{aligned}
 D_d &= (-1)^{d+1} \cdot \frac{\partial x_d}{\partial r} \cdot \det \begin{pmatrix} \frac{\partial x_1}{\partial \theta_1} & \cdots & \frac{\partial x_{d-1}}{\partial \theta_1} \\ \vdots & & \vdots \\ \frac{\partial x_1}{\partial \theta_{d-1}} & \cdots & \frac{\partial x_{d-1}}{\partial \theta_{d-1}} \end{pmatrix} \\
 &+ (-1)^{2d} \cdot \frac{\partial x_d}{\partial \theta_{d-1}} \cdot \det \begin{pmatrix} \frac{\partial x_1}{\partial r} & \cdots & \frac{\partial x_{d-1}}{\partial r} \\ \frac{\partial x_1}{\partial \theta_1} & \cdots & \frac{\partial x_{d-1}}{\partial \theta_1} \\ \vdots & & \vdots \\ \frac{\partial x_1}{\partial \theta_{d-2}} & \cdots & \frac{\partial x_{d-1}}{\partial \theta_{d-2}} \end{pmatrix}. \tag{2.73}
 \end{aligned}$$

According to Eq. (2.67) one finds for $i = 1 \dots (d-1)$:

$$\frac{\partial x_i}{\partial \theta_{d-1}} = \frac{\cos(\theta_{d-1})}{\sin(\theta_{d-1})} x_i = \frac{r \cos(\theta_{d-1})}{\sin(\theta_{d-1})} \frac{\partial x_i}{\partial r}, \tag{2.74}$$

and so

$$\begin{aligned}
 \det \begin{pmatrix} \frac{\partial x_1}{\partial \theta_1} & \cdots & \frac{\partial x_{d-1}}{\partial \theta_1} \\ \vdots & & \vdots \\ \frac{\partial x_1}{\partial \theta_{d-1}} & \cdots & \frac{\partial x_{d-1}}{\partial \theta_{d-1}} \end{pmatrix} &= \frac{r \cos(\theta_{d-1})}{\sin(\theta_{d-1})} \cdot \det \begin{pmatrix} \frac{\partial x_1}{\partial \theta_1} & \cdots & \frac{\partial x_{d-1}}{\partial \theta_1} \\ \vdots & & \vdots \\ \frac{\partial x_1}{\partial \theta_{d-2}} & \cdots & \frac{\partial x_{d-1}}{\partial \theta_{d-2}} \\ \frac{\partial x_1}{\partial r} & \cdots & \frac{\partial x_{d-1}}{\partial r} \end{pmatrix} \\
 &= (-1)^{d-2} \cdot \frac{r \cos(\theta_{d-1})}{\sin(\theta_{d-1})} \cdot \det \begin{pmatrix} \frac{\partial x_1}{\partial r} & \cdots & \frac{\partial x_{d-1}}{\partial r} \\ \frac{\partial x_1}{\partial \theta_1} & \cdots & \frac{\partial x_{d-1}}{\partial \theta_1} \\ \vdots & & \vdots \\ \frac{\partial x_1}{\partial \theta_{d-2}} & \cdots & \frac{\partial x_{d-1}}{\partial \theta_{d-2}} \end{pmatrix}, \tag{2.75}
 \end{aligned}$$

where in the last step we have exploited that determinants change their sign under exchange of two neighboring lines. Note that the d -dimensional coordinates $x_1 \dots x_{d-1}$ are related to the $(d-1)$ -dimensional coordinates $\hat{x}_1 \dots \hat{x}_{d-1}$ via $x_i = \sin(\theta_{d-1}) \cdot \hat{x}_i$, cf. Eq. (2.67). Since multiplication of one line of a matrix with a factor a changes also the determinant by a factor a we find

$$\begin{aligned}
 \det \begin{pmatrix} \frac{\partial x_1}{\partial r} & \cdots & \frac{\partial x_{d-1}}{\partial r} \\ \frac{\partial x_1}{\partial \theta_1} & \cdots & \frac{\partial x_{d-1}}{\partial \theta_1} \\ \vdots & & \vdots \\ \frac{\partial x_1}{\partial \theta_{d-2}} & \cdots & \frac{\partial x_{d-1}}{\partial \theta_{d-2}} \end{pmatrix} &= \sin^{d-1}(\theta_{d-1}) \cdot \det \begin{pmatrix} \frac{\partial \hat{x}_1}{\partial r} & \cdots & \frac{\partial \hat{x}_{d-1}}{\partial r} \\ \frac{\partial \hat{x}_1}{\partial \theta_1} & \cdots & \frac{\partial \hat{x}_{d-1}}{\partial \theta_1} \\ \vdots & & \vdots \\ \frac{\partial \hat{x}_1}{\partial \theta_{d-2}} & \cdots & \frac{\partial \hat{x}_{d-1}}{\partial \theta_{d-2}} \end{pmatrix} \\
 &= \sin^{d-1}(\theta_{d-1}) \cdot D_{d-1} \tag{2.76}
 \end{aligned}$$

Therefore,

$$D_d = \left[(-1)^{d+1} \cdot \frac{\partial x_d}{\partial r} \cdot (-1)^{d-2} \cdot r \cos(\theta_{d-1}) \sin^{d-2}(\theta_{d-1}) \right. \\ \left. + (-1)^{2d} \cdot \frac{\partial x_d}{\partial \theta_{d-1}} \cdot \sin^{d-1}(\theta_{d-1}) \right] \cdot D_{d-1} \quad (2.77)$$

$$= (-1)^{2d} \cdot \sin^{d-2}(\theta_{d-1}) \cdot \left[-r \cos^2(\theta_{d-1}) - r \sin^2(\theta_{d-1}) \right] \cdot D_{d-1} \\ = -r \cdot \sin^{d-2}(\theta_{d-1}) \cdot D_{d-1} \\ = -r \cdot \sin^{d-2}(\theta_{d-1}) \cdot (-1)^{d-2} r^{d-2} \prod_{i=1}^{d-2} \sin^{i-1}(\theta_i) \\ = (-1)^{d-1} r^{d-1} \prod_{i=1}^{d-1} \sin^{i-1}(\theta_i). \quad (2.78)$$

This concludes our proof of Eq. (2.70).

Since $|r| = r$, $\sin^0(\theta_1) = 1$ and $0 \leq \sin(\theta_i) \leq 1$ for $i = 2 \dots (d-1)$, the integral measure of Eq. (2.68) becomes:

$$d^d x = r^{d-1} \prod_{i=1}^{d-1} \sin^{i-1}(\theta_i) \cdot dr \prod_{i=1}^{d-1} d\theta_i = r^{d-1} dr d\Omega_d. \quad (2.79)$$

Thus, we can rewrite Eq. (2.64):

$$I = \int \frac{d^d x (x^2)^{\frac{n}{2}}}{[x^2 + \Delta]^k} = \int d\Omega_d \int_0^\infty dr \frac{r^{n+d-1}}{[r^2 + \Delta]^k}. \quad (2.80)$$

As mentioned above the integrand in Eq. (2.80) is independent of all angles and we can evaluate the integration over the surface $d\Omega_d$ separately. Now, instead of integrating over all $(d-1)$ angles, we will apply a more elegant method [PS95], which uses the well known result for the Gaussian integral:

$$\int_{-\infty}^{\infty} dx \exp(-x^2) = \sqrt{\pi}. \quad (2.81)$$

Then

$$\begin{aligned}
 (\sqrt{\pi})^d &= \left(\int_{-\infty}^{\infty} dx \exp(-x^2) \right)^d \\
 &= \int_{-\infty}^{\infty} \prod_{i=1}^d dx_i \exp(-x_i^2) \\
 &= \int d^d y \exp(-y^2) \\
 &= \int d\Omega_d \int_0^{\infty} dy y^{d-1} \exp(-y^2) \\
 &= \int d\Omega_d \int_0^{\infty} \frac{1}{2} dy^2 (y^2)^{\frac{d-2}{2}} \exp(-y^2) \\
 &= \int d\Omega_d \frac{1}{2} \Gamma\left(\frac{d}{2}\right), \tag{2.82}
 \end{aligned}$$

where in the last step the definition of the Gamma function was exploited, cf. Eq. (2.31). Now one finds for the surface integral:

$$S_d := \int d\Omega_d = \frac{2(\sqrt{\pi})^d}{\Gamma\left(\frac{d}{2}\right)}, \tag{2.83}$$

which is nothing but the surface area of the d -dimensional unit sphere. We note the special and well known cases:

$$d = 2 \Rightarrow S_2 = 2\pi, \tag{2.84}$$

$$d = 3 \Rightarrow S_3 = 4\pi, \tag{2.85}$$

where the following properties of the Gamma function were employed:

$$\Gamma\left(\frac{1}{2}\right) = \sqrt{\pi}, \tag{2.86}$$

$$\Gamma(x+1) = x \cdot \Gamma(x). \tag{2.87}$$

Eq. (2.80) now becomes:

$$I = \frac{2(\sqrt{\pi})^d}{\Gamma\left(\frac{d}{2}\right)} \int_0^{\infty} dr \frac{r^{n+d-1}}{[r^2 + \Delta]^k}. \tag{2.88}$$

Note that the Beta function can be written as ($\Re(x) > 0, \Re(y) > 0$)

$$B(x, y) = \int_0^{\infty} dt \frac{t^{x-1}}{(1+t)^{x+y}}, \quad (2.89)$$

which hints at how to rewrite Eq. (2.88):

$$\begin{aligned} I &= \frac{2(\sqrt{\pi})^d}{\Gamma\left(\frac{d}{2}\right)} \int_0^{\infty} r dr \frac{r^{n+d-2}}{\Delta^k \left[\frac{r^2}{\Delta} + 1\right]^k} \\ &= \frac{2(\sqrt{\pi})^d}{\Gamma\left(\frac{d}{2}\right)} \Delta^{\left(\frac{n+d}{2}-k\right)} \int_0^{\infty} \frac{1}{2} d\left(\frac{r^2}{\Delta}\right) \frac{\left(\frac{r^2}{\Delta}\right)^{\frac{n+d-2}{2}}}{\left[\frac{r^2}{\Delta} + 1\right]^k} \\ &= \frac{(\sqrt{\pi})^d}{\Gamma\left(\frac{d}{2}\right)} \Delta^{\left(\frac{n+d}{2}-k\right)} B\left(\frac{n+d}{2}, k - \frac{n+d}{2}\right) \\ &= \frac{(\sqrt{\pi})^d}{\Gamma\left(\frac{d}{2}\right)} \Delta^{\left(\frac{n+d}{2}-k\right)} \frac{\Gamma\left(\frac{n+d}{2}\right) \Gamma\left(k - \frac{n+d}{2}\right)}{\Gamma(k)}. \end{aligned} \quad (2.90)$$

Eq. (2.90) is a general result for the type of momentum integrals that occur in loop calculations. We remember that in general Δ has a tiny negative imaginary part.

Finally we are in a position to proceed with the evaluation of the quark selfenergy

in Eq. (2.63):

$$\begin{aligned}
 \Sigma(p) &= g^2 C_F \int_0^1 dx \frac{(2-d) \not{x} ((1-x) \not{p})}{(2\pi)^d} \cdot \frac{(\sqrt{\pi})^d}{\Gamma\left(\frac{d}{2}\right)} \Delta^{\left(\frac{d}{2}-2\right)} \frac{\Gamma\left(\frac{d}{2}\right) \Gamma\left(2-\frac{d}{2}\right)}{\Gamma(2)} \\
 &= g^2 C_F \int_0^1 dx \frac{(2-d) \not{x} ((1-x) \not{p})}{(4\pi)^{\frac{d}{2}}} \cdot \Delta^{\left(\frac{d-4}{2}\right)} \cdot \Gamma\left(\frac{4-d}{2}\right) \\
 &= g^2 C_F \frac{(2-d) \not{p}}{(4\pi)^{\frac{d}{2}}} \Gamma\left(\frac{4-d}{2}\right) \int_0^1 dx (1-x) \left(-x(1-x)p^2\right)^{\left(\frac{d-4}{2}\right)} \\
 &= g^2 C_F \frac{(2-d) \not{p}}{(4\pi)^{\frac{d}{2}}} \Gamma\left(\frac{4-d}{2}\right) (-p^2)^{\left(\frac{d-4}{2}\right)} \int_0^1 dx x^{\left(\frac{d-4}{2}\right)} (1-x)^{\left(\frac{d-2}{2}\right)} \\
 &= g^2 C_F \frac{(2-d) \not{p}}{(4\pi)^{\frac{d}{2}}} \Gamma\left(\frac{4-d}{2}\right) (-p^2)^{\left(\frac{d-4}{2}\right)} \cdot B\left(\frac{d-2}{2}, \frac{d}{2}\right) \\
 &= g^2 C_F \frac{(2-d) \not{p}}{(4\pi)^{\frac{d}{2}}} \Gamma\left(\frac{4-d}{2}\right) (-p^2)^{\left(\frac{d-4}{2}\right)} \cdot \frac{\Gamma\left(\frac{d-2}{2}\right) \Gamma\left(\frac{d}{2}\right)}{\Gamma(d-1)}, \tag{2.91}
 \end{aligned}$$

where again the definition of the Beta function, Eq. (2.33), was used.

2.3.6 Laurent expansion around $d = 4$ dimensions

Eq. (2.91) is the expression for the quark selfenergy in d space-time dimensions. However we are interested in the case $d = 4$ and now have to carefully extract the behavior of $\Sigma(p)$ around this value of d (remember that our aim is to make the divergence of the selfenergy at $d = 4$ manifest). For this purpose it is common and useful to introduce a new variable,

$$\epsilon = \frac{4-d}{2}, \tag{2.92}$$

since we expect the divergence to show up as poles in ϵ . Also considering Eq. (2.24) one has to replace the coupling constant g and finds:

$$\begin{aligned}
 \Sigma(p) &= g_0^2 \cdot (\mu^2)^\epsilon C_F \frac{(2\epsilon-2) \not{p}}{(4\pi)^{(2-\epsilon)}} \Gamma(\epsilon) (-p^2)^{(-\epsilon)} \cdot \frac{\Gamma(1-\epsilon) \Gamma(2-\epsilon)}{\Gamma(3-2\epsilon)} \\
 &= g_0^2 C_F \frac{\not{p}}{(4\pi)^2} \left(\frac{4\pi\mu^2}{-p^2}\right)^\epsilon \cdot \Gamma(\epsilon) \frac{(2\epsilon-2) \Gamma(1-\epsilon) \Gamma(2-\epsilon)}{\Gamma(3-2\epsilon)}. \tag{2.93}
 \end{aligned}$$

We are interested in the limit $\epsilon \rightarrow 0$ and thus have to expand $\Sigma(p)$ in ϵ to $O(\epsilon^0) = O(1)$. The expansion of the Gamma function near $\epsilon = 0$ reads [PS95]:

$$\Gamma(\epsilon) = \frac{1}{\epsilon} - \gamma + O(\epsilon), \quad (2.94)$$

where γ is the Euler-Mascheroni constant. Note that all other expressions in Eq. (2.93) are convergent for $\epsilon \rightarrow 0$. Since $\Gamma(\epsilon)$ diverges like $\frac{1}{\epsilon}$, it is thus sufficient to expand these expressions to $O(\epsilon)$. With $\Gamma(x+1) = x\Gamma(x)$ we recover

$$\Gamma(1-\epsilon) = -\epsilon\Gamma(-\epsilon) = -\epsilon \left(-\frac{1}{\epsilon} - \gamma + O(\epsilon) \right) = 1 + \gamma\epsilon + O(\epsilon^2) \quad (2.95)$$

and so

$$\begin{aligned} \frac{(2\epsilon-2)\Gamma(1-\epsilon)\Gamma(2-\epsilon)}{\Gamma(3-2\epsilon)} &= \frac{(2\epsilon-2)\Gamma(1-\epsilon)(1-\epsilon)\Gamma(1-\epsilon)}{(2-2\epsilon)(1-2\epsilon)\Gamma(1-2\epsilon)} \\ &= \frac{(-1)(1-\epsilon)(1+\gamma\epsilon+O(\epsilon^2))^2}{(1-2\epsilon)(1+2\gamma\epsilon+O(\epsilon^2))} \\ &= \frac{(-1)(1-\epsilon)(1+2\gamma\epsilon+O(\epsilon^2))}{(1+2\gamma\epsilon-2\epsilon+O(\epsilon^2))} \\ &= (-1)(1-\epsilon)(1+2\gamma\epsilon+O(\epsilon^2))(1-2\gamma\epsilon+2\epsilon+O(\epsilon^2)) \\ &= (-1)(1-\epsilon)(1+2\epsilon+O(\epsilon^2)) \\ &= (-1)(1+\epsilon+O(\epsilon^2)) \end{aligned} \quad (2.96)$$

In addition we find:

$$\left(\frac{4\pi\mu^2}{-p^2} \right)^\epsilon = \exp \left(\epsilon \ln \frac{4\pi\mu^2}{-p^2} \right) = 1 + \epsilon \ln \frac{4\pi\mu^2}{-p^2} + O(\epsilon^2). \quad (2.97)$$

Collecting the pieces, Eq. (2.93) becomes:

$$\Sigma(p) = g_0^2 C_F \frac{\not{p}}{(4\pi)^2} \left(1 + \epsilon \ln \frac{4\pi\mu^2}{-p^2} \right) \left(\frac{1}{\epsilon} - \gamma \right) (-1)(1+\epsilon) + O(\epsilon). \quad (2.98)$$

Now we drop all terms that vanish for $\epsilon \rightarrow 0$ and obtain the final result for the regularised one loop quark selfenergy:

$$\Sigma(p) = -\frac{g_0^2}{(4\pi)^2} C_F \not{p} \left(\frac{1}{\epsilon} - \gamma + 1 + \ln \frac{4\pi\mu^2}{-p^2} \right). \quad (2.99)$$

For space-like p the logarithm in Eq. (2.99) is unambiguous, however at $p^2 > 0$ our logarithm has a branch cut, cf. Appendix A.3. We remember that $\Delta = -x(1-x)p^2$

has a tiny negative imaginary part and since $0 < x < 1$, so does $-p^2$. Thus for time-like p one has to replace in the logarithm $-p^2 \rightarrow -p^2 - i\epsilon'$.

Note that the selfenergy has become a function of the arbitrary mass scale μ , which we introduced to keep the coupling constant dimensionless. Any physical observable calculated from $\Sigma(p)$ must be independent of μ , which has to be achieved through renormalisation, cf. Sec. 4.1.

3

One-loop integrals

This chapter is devoted to the methods of calculating one-loop integrals in quantum field theoretical contexts. We will illustrate these methods with the help of a common example, which will prove to be useful in Sec. 8.1. There we will have to calculate certain loop corrections for DY pair production. These calculations are straightforward, but lengthy, and therefore we already give their derivation in this chapter. The mathematics presented here are based on the excellent paper by 't Hooft and Veltman [tHV79], to which we refer for more details.

3.1 The three-point function

A typical example for a one-loop process is the three-point function with three particles in the loop. Fig. 3.1 shows such a process with scalar particles. While in standard calculations the particles are fermions and bosons, the additional complications introduced, for example by the Dirac algebra, do not interfere with the methods of calculation presented here. Therefore the result we will obtain, will be generally useful.

Note that for our purposes we restrict ourselves to the case where the masses of the internal and external particles are identical:

$$\begin{aligned} p_1^2 &= m_1^2, \\ p_2^2 &= m_2^2, \end{aligned} \tag{3.1}$$

and to the particle with momentum k we assign a mass m_3 . Then the amplitude of

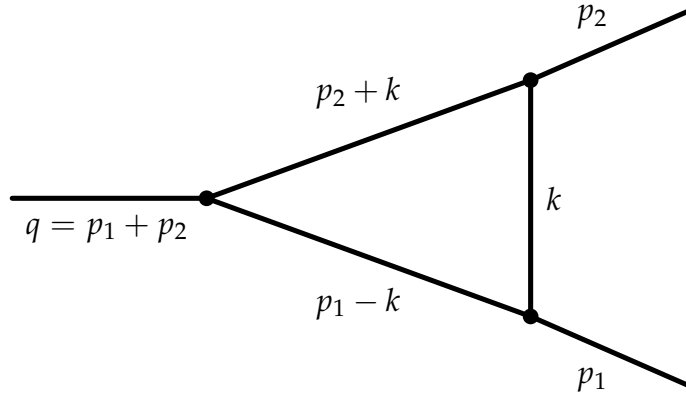


Figure 3.1: Loop process with three scalar particles in the loop.

the process in Fig. 3.1 is proportional to the loop integral

$$I = \int d^d k \frac{1}{(p_1 - k)^2 - m_1^2 + i\epsilon} \cdot \frac{1}{(p_2 + k)^2 - m_2^2 + i\epsilon} \cdot \frac{1}{k^2 - m_3^2 + i\epsilon} . \quad (3.2)$$

3.1.1 Feynman parametrisation

Now we can make use of the results of Chapter 2. First we introduce Feynman parameters to combine the propagators:

$$\begin{aligned} I &= \int_0^1 dx dy dz \delta(x + y + z - 1) \int d^d k \\ &\quad \times \frac{2}{[x((p_1 - k)^2 - m_1^2 + i\epsilon) + y((p_2 + k)^2 - m_2^2 + i\epsilon) + z(k^2 - m_3^2 + i\epsilon)]^3} \\ &= \int_0^1 dx dy dz \delta(x + y + z - 1) \int d^d k \frac{2}{K^3} . \end{aligned} \quad (3.3)$$

The next step is to rewrite K so we can shift the variable of the momentum integral:

$$\begin{aligned} K &= -2xp_1 \cdot k + 2yp_2 \cdot k + (x + y + z)(k^2 + i\epsilon) - zm_3^2 \\ &= [k + (-xp_1 + yp_2)]^2 - (-xp_1 + yp_2)^2 - zm_3^2 + i\epsilon \\ &= l^2 - (x^2 m_1^2 - 2xy p_1 \cdot p_2 + y^2 m_2^2) - zm_3^2 + i\epsilon \\ &= l^2 - [m_1^2 x(x + y) + m_2^2 y(x + y) - xy q^2 + (1 - x - y)m_3^2 - i\epsilon] \\ &= l^2 - \Delta , \end{aligned} \quad (3.4)$$

where we have used the onshell relations (3.1), $x + y + z = 1$ and $q^2 = (p_1 + p_2)^2$. Since $d^d k = d^d l$, the momentum integral is now solved by first Wick rotating the zeroth component of l and then integrating in d -dimensional spherical coordinates:

$$\begin{aligned}
 I_2 &= \int d^d l \frac{1}{[l^2 - \Delta]^3} \\
 l^0 \rightarrow il_E^0 &= -i \int d^d l_E \frac{1}{[l_E^2 + \Delta]^3} \\
 &= -i \int d\Omega_d \cdot \int d|l_E| |l_E|^{d-1} \frac{1}{[|l_E|^2 + \Delta]^3} \\
 \text{Eq. (2.83)} &= -i \frac{2\sqrt{\pi}^d}{\Gamma\left(\frac{d}{2}\right)} \cdot \int d|l_E| |l_E|^{d-1} \frac{1}{[|l_E|^2 + \Delta]^3} \\
 \text{Eqs. (2.88- 2.90)} &= -i \frac{\sqrt{\pi}^d}{\Gamma\left(\frac{d}{2}\right)} \cdot \Delta^{\left(\frac{d}{2}-3\right)} \cdot \frac{\Gamma\left(\frac{d}{2}\right) \Gamma\left(3 - \frac{d}{2}\right)}{\Gamma(3)}. \tag{3.5}
 \end{aligned}$$

The last result is convergent for $d = 4$ and so one finds:

$$I_2 = -\frac{i\pi^2}{2} \cdot \frac{1}{\Delta}. \tag{3.6}$$

We define

$$\begin{aligned}
 I_3 &:= \frac{I}{-i\pi^2} = \int_0^1 dx dy dz \delta(x + y + z - 1) \Delta^{-1} \\
 &= \int_0^1 dx \int_0^{1-x} dy \left[m_1^2 x(x+y) + m_2^2 y(x+y) - xyq^2 + (1-x-y)m_3^2 - i\epsilon \right]^{-1}. \tag{3.7}
 \end{aligned}$$

The structure of the integrand is simplified by the following substitution, which removes the term proportional to y in the denominator:

$$a = x + y, \tag{3.8}$$

$$b = x - y, \tag{3.9}$$

$$\Rightarrow dx dy = \frac{1}{2} da db, \tag{3.10}$$

which implies

$$x = \frac{a+b}{2}, \quad (3.11)$$

$$y = \frac{a-b}{2}, \quad (3.12)$$

$$xy = \frac{a^2 - b^2}{4}. \quad (3.13)$$

Then Eq. (3.7) becomes

$$I_3 = \frac{1}{2} \int_0^1 da \int_{-a}^a db \left[m_1^2 a \frac{a+b}{2} + m_2^2 a \frac{a-b}{2} - \frac{a^2 - b^2}{4} q^2 + (1-a)m_3^2 - i\epsilon \right]^{-1}. \quad (3.14)$$

Once more we substitute

$$b' = \frac{b+a}{2} \Leftrightarrow b = 2b' - a \quad (3.15)$$

$$\Rightarrow db = 2db', \quad (3.16)$$

and obtain

$$\begin{aligned} I_3 &= \int_0^1 da \int_0^a db' \left[m_1^2 ab' + m_2^2 (a-b')a - \frac{a^2 - 4b'^2 + 4b'a - a^2}{4} q^2 + (1-a)m_3^2 - i\epsilon \right]^{-1} \\ &= \int_0^1 da \int_0^a db' \left[a^2 m_2^2 + b'^2 q^2 + ab' (m_1^2 - m_2^2 - q^2) + a(-m_3^2) + m_3^2 - i\epsilon \right]^{-1} \\ &= \int_0^1 dx \int_0^x dy \left[k_1 x^2 + k_2 y^2 + k_3 xy + k_4 x + k_5 \right]^{-1}. \end{aligned} \quad (3.17)$$

Note that all coefficients in Eq. (3.17) are real numbers, with the exception of k_5 :

$$k_1 = m_2^2, \quad (3.18)$$

$$k_2 = q^2, \quad (3.19)$$

$$k_3 = m_1^2 - m_2^2 - q^2 \Rightarrow m_1^2 = k_1 + k_2 + k_3, \quad (3.20)$$

$$k_4 = -m_3^2, \quad (3.21)$$

$$k_5 = m_3^2 - i\epsilon. \quad (3.22)$$

The idea how to solve Eq. (3.17) is the following: substitute for y such, that the denominator becomes linear in x . Then by interchanging the order of integrations, one can easily integrate over x . The remaining integral is not analytically solvable but connected to the Dilogarithm or Spence function, the properties of which are well known, see Sec. 3.1.2.

3.1.2 Spence function (Dilogarithm)

As shown in [tHV79] all integrals to one-loop order can be written in terms of Spence functions, which we shortly introduce in this section. Note that if the particles in the loop are massless these Spence functions usually reduce to logarithms and constants.

The Spence function or Dilogarithm for complex argument x is defined by [Lew81]:

$$\begin{aligned} \text{Sp}(x) &= - \int_0^x dz \frac{\ln(1-z)}{z} \\ &= - \int_0^1 dt \frac{\ln(1-xt)}{t} . \end{aligned} \quad (3.23)$$

Note that there exist deviating definitions for the Spence function, see for example [AS64]. In this work we will stick to the definition in Eq. (3.23). In our definition of the complex logarithm, cf. Appendix A.3, it has a branch cut along the negative real axis and so the Spence function has a branch cut along the positive real axis for $x \geq 1$. Important properties are:

$$\text{Sp}(x) = -\text{Sp}(1-x) + \frac{\pi^2}{6} - \ln(x) \ln(1-x) , \quad (3.24)$$

$$\text{Sp}(x) = -\text{Sp}\left(\frac{1}{x}\right) - \frac{\pi^2}{6} - \frac{1}{2} \ln^2(-x) , \quad (3.25)$$

which imply

$$\text{Sp}(0) = 0 , \quad (3.26)$$

$$\text{Sp}(1) = \frac{\pi^2}{6} . \quad (3.27)$$

The Spence function can be approximated by truncating the following series expansion:

$$\text{Sp}(x) = \sum_{n=0}^{\infty} B_n \frac{[-\ln(1-x)]^{n+1}}{(n+1)!} , \quad (3.28)$$

where B_n are the Bernoulli numbers, with

$$B_0 = 1 , B_1 = -\frac{1}{2} , B_2 = \frac{1}{6} , \dots . \quad (3.29)$$

3.1.3 Integral transformations

As already pointed out in Sec. 3.1.1, we now have to transform the integral in Eq. (3.17). Substituting

$$y' = y - \alpha x \quad (3.30)$$

$$\Rightarrow dy' = dy, \quad (3.31)$$

one finds

$$\begin{aligned} I_3 &= \int_0^1 dx \int_{-\alpha x}^{(1-\alpha)x} dy' \left[k_1 x^2 + k_2 (y'^2 + 2y'\alpha x + \alpha^2 x^2) + k_3 x (y' + \alpha x) + k_4 x + k_5 \right]^{-1} \\ &= \int_0^1 dx \int_{-\alpha x}^{(1-\alpha)x} dy' \left[(k_1 + k_2 \alpha^2 + k_3 \alpha) x^2 + k_2 y'^2 + (2k_2 \alpha + k_3) x y' + k_4 x + k_5 \right]^{-1}. \end{aligned} \quad (3.32)$$

Now we can choose α such that the coefficient of x^2 vanishes:

$$\begin{aligned} k_1 + k_2 \alpha^2 + k_3 \alpha &\stackrel{!}{=} 0 \\ \Rightarrow \alpha_{\pm} &= -\frac{k_3}{2k_2} \pm \sqrt{\frac{k_3^2}{4k_2^2} - \frac{k_1}{k_2}}. \end{aligned} \quad (3.33)$$

Note that α_{\pm} are real numbers, since the argument of the square root in Eq. (3.33) is positive. The proof goes as follows:

$$\begin{aligned} A &= \frac{k_3^2}{4k_2^2} - \frac{k_1}{k_2} \\ &= \frac{(m_1^2 - m_2^2 - q^2)^2}{4q^4} - \frac{m_2^2}{q^2} \\ &= \frac{(m_1^2 - m_2^2)^2 + q^4 - 2m_1^2 q^2 + 2m_2^2 q^2 - 4m_2^2 q^2}{4q^4} \\ &= \frac{(m_1^2 - m_2^2)^2 + q^2(q^2 - 2m_1^2 - 2m_2^2)}{4q^4}. \end{aligned} \quad (3.34)$$

To find the minimum of the numerator we differentiate by q^2 and note that $q^2 = (p_1 + p_2)^2 \geq (m_1 + m_2)^2$:

$$\begin{aligned} \frac{\partial(4q^4 A)}{\partial q^2} &= (q^2 - 2m_1^2 - 2m_2^2) + q^2 \\ &= 2(q^2 - m_1^2 - m_2^2) \\ &\geq 4m_1 m_2 \\ &> 0. \end{aligned} \quad (3.35)$$

The derivative is always positive and thus the numerator of A has its minimum at the minimum of q^2 :

$$\begin{aligned}
 4q^4 A &\geq (m_1^2 - m_2^2)^2 + (m_1 + m_2)^2((m_1 + m_2)^2 - 2m_1^2 - 2m_2^2) \\
 &= (m_1 + m_2)^2(m_1 - m_2)^2 + (m_1 + m_2)^2(-1)(m_1 - m_2)^2 \\
 &= 0 \\
 \Rightarrow A &\geq 0.
 \end{aligned} \tag{3.36}$$

$\alpha_{\pm} \in \mathcal{R}$ is proven and from now on we choose $\alpha = \alpha_+$. Eq. (3.32) then becomes:

$$\begin{aligned}
 I_3 &= \int_0^1 dx \int_{-\alpha_+ x}^{(1-\alpha_+)x} dy' \left[k_2 y'^2 + \underbrace{(2k_2 \alpha_+ + k_3)}_{h_1} x y' + k_4 x + k_5 \right]^{-1} \\
 &= \int_0^1 dx \int_{-\alpha_+ x}^{(1-\alpha_+)x} dy' \left[x(k_4 + h_1 y') + k_2 y'^2 + k_5 \right]^{-1}.
 \end{aligned} \tag{3.37}$$

We have achieved our goal and the denominator of the integrand has become linear in x . The next step is to change the order of integrations, so we can integrate over x first. Since α_+ is real, one can easily rewrite the integral:

$$\int_0^1 dx \int_{-\alpha_+ x}^{(1-\alpha_+)x} dy' = \int_0^1 dx \int_0^{(1-\alpha_+)x} dy' - \int_0^1 dx \int_0^{-\alpha_+ x} dy' \tag{3.38}$$

Note that if α_+ were complex, one would have to check the integrand for singularities inside the triangle $(0, (1 - \alpha_+)x, -\alpha_+ x)$ in the complex y' plane, since they would spoil the transformation in Eq. (3.38). The order of integration can now be changed by realising that for $a > 0$:

$$\begin{aligned}
 \int_0^1 dx \int_0^{ax} dy &= \int dx \int dy \Theta(ax - y) \Theta(y) \Theta(x) \Theta(1 - x) \\
 &= \int dx \int dy \Theta(x - \frac{y}{a}) \Theta(y) \Theta(x) \Theta(1 - x) \\
 &= \int dx \int dy \Theta(x - \frac{y}{a}) \Theta(y) \Theta(1 - x) \\
 &= \int dx \int dy \Theta(x - \frac{y}{a}) \Theta(y) \Theta(a - y) \Theta(1 - x) \\
 &= \int_0^a dy \int_{\frac{y}{a}}^1 dx.
 \end{aligned} \tag{3.39}$$

A similar equation holds for $a < 0$. Then Eq. (3.38) becomes

$$\int_0^1 dx \int_0^{(1-\alpha_+)x} dy' - \int_0^1 dx \int_0^{-\alpha_+x} dy' = \int_0^{1-\alpha_+} dy' \int_{\frac{y'}{1-\alpha_+}}^1 dx - \int_0^{-\alpha_+} dy' \int_{\frac{y'}{-\alpha_+}}^1 dx. \quad (3.40)$$

Finally the x integration can be performed:

$$\begin{aligned} I_3 &= \int_0^{1-\alpha_+} dy' \int_{\frac{y'}{1-\alpha_+}}^1 dx \left[x(k_4 + h_1 y') + k_2 y'^2 + k_5 \right]^{-1} \\ &\quad - \int_0^{-\alpha_+} dy' \int_{\frac{y'}{-\alpha_+}}^1 dx \left[x(k_4 + h_1 y') + k_2 y'^2 + k_5 \right]^{-1} \\ &= \int_0^{1-\alpha_+} dy' \frac{1}{k_4 + h_1 y'} \ln \left(\frac{k_4 + h_1 y' + k_2 y'^2 + k_5}{\frac{y'}{1-\alpha_+} (k_4 + h_1 y') + k_2 y'^2 + k_5} \right) \\ &\quad - \int_0^{-\alpha_+} dy' \frac{1}{k_4 + h_1 y'} \ln \left(\frac{k_4 + h_1 y' + k_2 y'^2 + k_5}{\frac{y'}{-\alpha_+} (k_4 + h_1 y') + k_2 y'^2 + k_5} \right) \\ &= \int_{-\alpha_+}^{1-\alpha_+} dy' \frac{1}{k_4 + h_1 y'} \ln \left(k_4 + h_1 y' + k_2 y'^2 + k_5 \right) \\ &\quad - \int_0^{1-\alpha_+} dy' \frac{1}{k_4 + h_1 y'} \ln \left(\frac{y'}{1-\alpha_+} (k_4 + h_1 y') + k_2 y'^2 + k_5 \right) \\ &\quad + \int_0^{-\alpha_+} dy' \frac{1}{k_4 + h_1 y'} \ln \left(\frac{y'}{-\alpha_+} (k_4 + h_1 y') + k_2 y'^2 + k_5 \right). \end{aligned} \quad (3.41)$$

The arguments of the logarithms in the last equation are quadratic in y' . If we can factorise them, we will obtain logarithms with arguments linear in y' . Then the integrand will already bear a great resemblance to the definition of the Spence function

in Eq. (3.23). However before we proceed with the factorisation, we add 0 in the form:

$$\begin{aligned}
 0 = & - \int_{-\alpha_+}^{1-\alpha_+} dy' \frac{1}{k_4 + h_1 y'} \ln(k_2 y_0^2 + k_5) \\
 & + \int_0^{1-\alpha_+} dy' \frac{1}{k_4 + h_1 y'} \ln(k_2 y_0^2 + k_5) \\
 & - \int_0^{-\alpha_+} dy' \frac{1}{k_4 + h_1 y'} \ln(k_2 y_0^2 + k_5) , \tag{3.42}
 \end{aligned}$$

where y_0 is the root of the prefactor:

$$y_0 = -\frac{k_4}{h_1} . \tag{3.43}$$

The reason for this will become clear immediately:

$$\begin{aligned}
 I_3 = & \int_{-\alpha_+}^{1-\alpha_+} dy' \frac{1}{k_4 + h_1 y'} \left[\ln(k_4 + h_1 y' + k_2 y'^2 + k_5) - \ln(k_2 y_0^2 + k_5) \right] \\
 & - \int_0^{1-\alpha_+} dy' \frac{1}{k_4 + h_1 y'} \left[\ln\left(\frac{y'}{1-\alpha_+}(k_4 + h_1 y') + k_2 y'^2 + k_5\right) - \ln(k_2 y_0^2 + k_5) \right] \\
 & + \int_0^{-\alpha_+} dy' \frac{1}{k_4 + h_1 y'} \left[\ln\left(\frac{y'}{-\alpha_+}(k_4 + h_1 y') + k_2 y'^2 + k_5\right) - \ln(k_2 y_0^2 + k_5) \right] . \tag{3.44}
 \end{aligned}$$

We have achieved a convenient form for I_3 : the residue at the pole $y' = y_0$ vanishes and so later on we can choose the most convenient integration contour to solve the integrals. Since all three integrals in I_3 are essentially of the same type except for the integration boundaries, we substitute to get three very similar integrals:

$$\begin{aligned}
 1. \quad & y = y' + \alpha_+ \Rightarrow dy' = dy , \\
 & y_1 = y_0 + \alpha_+ \Rightarrow y_0 = y_1 - \alpha_+ , \tag{3.45}
 \end{aligned}$$

$$\begin{aligned}
 2. \quad & y = \frac{y'}{1-\alpha_+} \Rightarrow dy' = (1-\alpha_+)dy , \\
 & y_2 = \frac{y_0}{1-\alpha_+} \Rightarrow y_0 = (1-\alpha_+)y_2 , \tag{3.46}
 \end{aligned}$$

$$\begin{aligned}
 3. \quad & y = \frac{y'}{-\alpha_+} \Rightarrow dy' = -\alpha_+ dy , \\
 & y_3 = \frac{y_0}{-\alpha_+} \Rightarrow y_0 = -\alpha_+ y_3 , \tag{3.47}
 \end{aligned}$$

for the first, second and third integral of I_3 , respectively. Eq. (3.44) becomes:

$$\begin{aligned}
 I_3 = & \int_0^1 dy \frac{1}{k_4 + h_1 y - h_1 \alpha_+} \left[\ln \left(k_4 + h_1(y - \alpha_+) + k_2(y - \alpha_+)^2 + k_5 \right) \right. \\
 & \left. - \ln \left(k_2(y_1 - \alpha_+)^2 + k_5 \right) \right] \\
 & - \int_0^1 dy \frac{1 - \alpha_+}{k_4 + h_1 y(1 - \alpha_+)} \left[\ln \left(y(k_4 + h_1 y(1 - \alpha_+)) + k_2 y^2(1 - \alpha_+)^2 + k_5 \right) \right. \\
 & \left. - \ln \left(k_2 y_2^2(1 - \alpha_+)^2 + k_5 \right) \right] \\
 & + \int_0^1 dy \frac{-\alpha_+}{k_4 - h_1 y \alpha_+} \left[\ln \left(y(k_4 - h_1 y \alpha_+) + k_2 y^2 \alpha_+^2 + k_5 \right) \right. \\
 & \left. - \ln \left(k_2 y_3^2 \alpha_+^2 + k_5 \right) \right] . \tag{3.48}
 \end{aligned}$$

Using the defining equation for α_+ ,

$$k_1 + k_2 \alpha_+^2 + k_3 \alpha_+ = 0 \tag{3.49}$$

and

$$h_1 \alpha_+ = 2\alpha_+^2 k_2 + k_3 \alpha_+ = -k_1 + k_2 \alpha_+^2 \tag{3.50}$$

one can rewrite the logarithms and so I_3 reads:

$$\begin{aligned}
 I_3 = & \frac{1}{h_1} \int_0^1 dy \frac{1}{y - y_1} \left[\ln \left(k_2 y^2 + k_3 y + k_1 + k_4 + k_5 \right) - \ln \left(k_2 y_1^2 + k_3 y_1 + k_1 + k_4 + k_5 \right) \right] \\
 & - \frac{1}{h_1} \int_0^1 dy \frac{1}{y - y_2} \left[\ln \left((k_1 + k_2 + k_3) y^2 + k_4 y + k_5 \right) \right. \\
 & \left. - \ln \left((k_1 + k_2 + k_3) y_2^2 + k_4 y_2 + k_5 \right) \right] \\
 & + \frac{1}{h_1} \int_0^1 dy \frac{1}{y - y_3} \left[\ln \left(k_1 y^2 + k_4 y + k_5 \right) - \ln \left(k_1 y_3^2 + k_4 y_3 + k_5 \right) \right] . \tag{3.51}
 \end{aligned}$$

We have rewritten I_3 in terms of three integrals,

$$I_3 = \frac{1}{h_1} (J_1 - J_2 + J_3) , \quad (3.52)$$

which are of exactly the same type:

$$S = \int_0^1 dx \frac{1}{x - x_0} \left[\ln(ax^2 + bx + c) - \ln(ax_0^2 + bx_0 + c) \right] . \quad (3.53)$$

Now all left to do is to solve Eq. (3.53).

3.1.4 Reduction to Spence functions

In this section we will show that the integral in Eq. (3.53) can be entirely rewritten in terms of Spence functions, which were introduced in Sec. 3.1.2. To do this we have to factorise the arguments of the logarithms. Since the factorisation involves manipulation of the complex logarithm, which has a branch cut along the negative real axis, it is worthwhile to realise the following relations:

$$\ln(ab) = \ln(a) + \ln(b) , \text{ if } \text{sgn}(\Im(a)) \neq \text{sgn}(\Im(b)) , \quad (3.54)$$

$$\ln\left(\frac{a}{b}\right) = \ln(a) - \ln(b) , \text{ if } \text{sgn}(\Im(a)) = \text{sgn}(\Im(b)) . \quad (3.55)$$

The proof goes as follows: let $a = |a| \exp(i\phi_a)$ with $0 \leq \phi_a \leq \pi$ and let $b = |b| \exp(i\phi_b)$ with $-\pi \leq \phi_b \leq 0$. Then obviously:

$$\Im(a) = |a| \cdot \sin(\phi_a) \geq 0 , \quad (3.56)$$

$$\Im(b) = |b| \cdot \sin(\phi_b) \leq 0 , \quad (3.57)$$

$$\Im(ab) = |a| \cdot |b| \cdot \sin(\phi_a + \phi_b) . \quad (3.58)$$

Since $-\pi \leq \phi_a + \phi_b \leq \pi$, one finds that $\ln(a)$, $\ln(b)$ and $\ln(ab)$ are all on the same branch and the branch cut is never crossed. Therefore no additional terms of $\pm 2\pi i$ appear in Eq. (3.54). The proof for $\ln\left(\frac{a}{b}\right)$ is analogous with $b \rightarrow b^{-1} = |b|^{-1} \exp(-i\phi_b)$.

Note that $y_1, y_2, y_3, k_1, k_2, k_3, k_4 \in \mathcal{R}$ and $k_5 \in \mathcal{C}$. Therefore we also have $x_0, a, b \in \mathcal{R}$ and the only complex number in S is c . Then one finds:

$$ax^2 + bx + c \stackrel{!}{=} 0 \quad (3.59)$$

$$\Rightarrow x_{\pm} = \underbrace{-\frac{b}{2a}}_{\in \mathcal{R}} \pm \underbrace{\sqrt{\frac{b^2}{4a^2} - \frac{c}{a}}}_{\in \mathcal{C}} \quad (3.60)$$

$$\Rightarrow \Im(x_+) = -\Im(x_-) \quad (3.61)$$

$$\Rightarrow \ln(ax^2 + bx + c) = \ln[a(x - x_+)(x - x_-)] = \ln(a) + \ln(x - x_+) + \ln(x - x_-) . \quad (3.62)$$

Eq. (3.53) now becomes:

$$S = \int_0^1 dx \frac{1}{x - x_0} [\ln(x - x_+) - \ln(x_0 - x_+) + \ln(x - x_-) - \ln(x_0 - x_-)] . \quad (3.63)$$

Once again we have to solve two similar integrals and thus we define:

$$S_2 = \int_0^1 dx \frac{1}{x - x_0} [\ln(x - x_1) - \ln(x_0 - x_1)] . \quad (3.64)$$

To rewrite S_2 in terms of Spence functions we substitute $x' = x - x_1$:

$$S_2 = \int_{-x_1}^{1-x_1} dx' \frac{1}{x' + x_1 - x_0} [\ln(x') - \ln(x_0 - x_1)] . \quad (3.65)$$

Note that the residue at the pole $x' = x_0 - x_1$ vanishes and that $\mathfrak{S}(-x_1) = \mathfrak{S}(1 - x_1)$ and so along the triangle $(0, -x_1, 1 - x_1)$ the logarithms do not cross a branch cut. Therefore one can change the integration contour:

$$\begin{aligned} S_2 &= \int_0^{1-x_1} dx' \frac{1}{x' + x_1 - x_0} [\ln(x') - \ln(x_0 - x_1)] \\ &\quad - \int_0^{-x_1} dx' \frac{1}{x' + x_1 - x_0} [\ln(x') - \ln(x_0 - x_1)] . \end{aligned} \quad (3.66)$$

The integration boundaries in the definition of the Spence function (3.23) are 0 and 1 and thus we substitute $z = (1 - x_1)^{-1}x'$ in the first integral in Eq. (3.66) and $z = (-x_1)^{-1}x'$ in the second:

$$\begin{aligned} S_2 &= \int_0^1 dz \frac{1 - x_1}{(1 - x_1)z + x_1 - x_0} [\ln(z(1 - x_1)) - \ln(x_0 - x_1)] \\ &\quad - \int_0^1 dz \frac{-x_1}{-x_1z + x_1 - x_0} [\ln(-x_1z) - \ln(x_0 - x_1)] \\ &= \int_0^1 dz \frac{\partial}{\partial z} (\ln((1 - x_1)z + x_1 - x_0)) [\ln(z(1 - x_1)) - \ln(x_0 - x_1)] \\ &\quad - \int_0^1 dz \frac{\partial}{\partial z} (\ln(-x_1z + x_1 - x_0)) [\ln(-x_1z) - \ln(x_0 - x_1)] . \end{aligned} \quad (3.67)$$

Since

$$\frac{\partial}{\partial z} \ln(x_1 - x_0) = 0 \quad (3.68)$$

and

$$\text{sgn}(\Im(x_1(1-z))) = \text{sgn}(\Im(x_1)) = \text{sgn}(\Im(x_1 - x_0)) , \quad (3.69)$$

we can add 0 without having any logarithm crossing a branch cut:

$$\begin{aligned} S_2 &= \int_0^1 dz \frac{\partial}{\partial z} \left(\ln \left(\frac{(1-x_1)z + x_1 - x_0}{x_1 - x_0} \right) \right) [\ln(z(1-x_1)) - \ln(x_0 - x_1)] \\ &\quad - \int_0^1 dz \frac{\partial}{\partial z} \left(\ln \left(\frac{-x_1z + x_1 - x_0}{x_1 - x_0} \right) \right) [\ln(-x_1z) - \ln(x_0 - x_1)] . \end{aligned} \quad (3.70)$$

Integrating by parts yields:

$$\begin{aligned} S_2 &= \ln \left(\frac{1-x_0}{x_1-x_0} \right) [\ln(1-x_1) - \ln(x_0-x_1)] - \int_0^1 dz \frac{1}{z} \ln \left(\frac{(1-x_1)z}{x_1-x_0} + 1 \right) \\ &\quad - \ln \left(\frac{-x_0}{x_1-x_0} \right) [\ln(-x_1) - \ln(x_0-x_1)] + \int_0^1 dz \frac{1}{z} \ln \left(\frac{-x_1z}{x_1-x_0} + 1 \right) \\ &= \ln \left(\frac{1-x_0}{x_1-x_0} \right) [\ln(1-x_1) - \ln(x_0-x_1)] + \text{Sp} \left(\frac{x_1-1}{x_1-x_0} \right) \\ &\quad - \ln \left(\frac{-x_0}{x_1-x_0} \right) [\ln(-x_1) - \ln(x_0-x_1)] - \text{Sp} \left(\frac{x_1}{x_1-x_0} \right) . \end{aligned} \quad (3.71)$$

With

$$\Im(1-x_1) = \Im(-x_1) = \Im(x_0-x_1) \quad (3.72)$$

we can combine the logarithms, since again no branch cut is crossed:

$$\begin{aligned} S_2 &= \ln \left(\frac{1-x_0}{x_1-x_0} \right) \ln \left(\frac{1-x_1}{x_0-x_1} \right) + \text{Sp} \left(\frac{x_1-1}{x_1-x_0} \right) \\ &\quad - \ln \left(\frac{-x_0}{x_1-x_0} \right) \ln \left(\frac{-x_1}{x_0-x_1} \right) - \text{Sp} \left(\frac{x_1}{x_1-x_0} \right) . \end{aligned} \quad (3.73)$$

Finally the Spence functions can be rewritten with the help of Eq. (3.24):

$$\begin{aligned}
 S_2 &= \ln \left(\frac{1-x_0}{x_1-x_0} \right) \ln \left(\frac{1-x_1}{x_0-x_1} \right) - \text{Sp} \left(1 - \frac{x_1-1}{x_1-x_0} \right) + \frac{\pi^2}{6} \\
 &\quad - \ln \left(\frac{x_1-1}{x_1-x_0} \right) \ln \left(1 - \frac{x_1-1}{x_1-x_0} \right) \\
 &\quad - \ln \left(\frac{-x_0}{x_1-x_0} \right) \ln \left(\frac{-x_1}{x_0-x_1} \right) + \text{Sp} \left(1 - \frac{x_1}{x_1-x_0} \right) - \frac{\pi^2}{6} \\
 &\quad + \ln \left(\frac{x_1}{x_1-x_0} \right) \ln \left(1 - \frac{x_1}{x_1-x_0} \right) \\
 &= \text{Sp} \left(\frac{x_0}{x_0-x_1} \right) - \text{Sp} \left(\frac{x_0-1}{x_0-x_1} \right) .
 \end{aligned} \tag{3.74}$$

Then S of Eqs. (3.53,3.63) reads:

$$S = \text{Sp} \left(\frac{x_0}{x_0-x_+} \right) - \text{Sp} \left(\frac{x_0-1}{x_0-x_+} \right) + \text{Sp} \left(\frac{x_0}{x_0-x_-} \right) - \text{Sp} \left(\frac{x_0-1}{x_0-x_-} \right) . \tag{3.75}$$

The last equation is the solution for each of the three integrals J_1, J_2, J_3 in Eq. (3.52) and, thus, the integral I in Eq. (3.2) is solved:

$$I = -i\pi^2 \frac{1}{2k_2\alpha_+ + k_3} [J_1 - J_2 + J_3] . \tag{3.76}$$

The auxiliary functions are:

$$J_1 = \text{Sp} \left(\frac{y_1}{y_1-a_+} \right) - \text{Sp} \left(\frac{y_1-1}{y_1-a_+} \right) + \text{Sp} \left(\frac{y_1}{y_1-a_-} \right) - \text{Sp} \left(\frac{y_1-1}{y_1-a_-} \right) , \tag{3.77}$$

with

$$y_1 = \alpha_+ - \frac{k_4}{2k_2\alpha_+ + k_3} , \tag{3.78}$$

$$a_{\pm} = -\frac{k_3}{2k_2} \pm \sqrt{\frac{k_3^2}{4k_2^2} - \frac{k_1}{k_2} + i\epsilon} . \tag{3.79}$$

$$J_2 = \text{Sp} \left(\frac{y_2}{y_2-b_+} \right) - \text{Sp} \left(\frac{y_2-1}{y_2-b_+} \right) + \text{Sp} \left(\frac{y_2}{y_2-b_-} \right) - \text{Sp} \left(\frac{y_2-1}{y_2-b_-} \right) , \tag{3.80}$$

with

$$y_2 = -\frac{k_4}{2k_2\alpha_+ + k_3} \frac{1}{1-\alpha_+} , \tag{3.81}$$

$$b_{\pm} = -\frac{k_4}{2(k_1+k_2+k_3)} \pm \sqrt{\frac{k_4^2}{4(k_1+k_2+k_3)^2} + \frac{k_4}{k_1+k_2+k_3} + \frac{i\epsilon}{k_1+k_2+k_3}} . \tag{3.82}$$

$$J_3 = \text{Sp} \left(\frac{y_3}{y_3 - c_+} \right) - \text{Sp} \left(\frac{y_3 - 1}{y_3 - c_+} \right) + \text{Sp} \left(\frac{y_3}{y_3 - c_-} \right) - \text{Sp} \left(\frac{y_3 - 1}{y_3 - c_-} \right), \quad (3.83)$$

with

$$y_3 = \frac{k_4}{2k_2\alpha_+ + k_3\alpha_+}, \quad (3.84)$$

$$c_{\pm} = -\frac{k_4}{2k_1} \pm \sqrt{\frac{k_4^2}{4k_1^2} + \frac{k_4}{k_1} + \frac{i\epsilon}{k_1}}. \quad (3.85)$$

Finally we have everywhere

$$\alpha_+ = -\frac{k_3}{2k_2} \pm \sqrt{\frac{k_3^2}{4k_2^2} - \frac{k_1}{k_2}}. \quad (3.86)$$

3.2 Expansion for small mass m_3

In Sec. 8.1 we will calculate the QCD one-loop correction to the electromagnetic vertex for DY pair production. There we will identify the exchange particle with momentum k in Fig. 3.1 with a gluon to which we assign a (fictitious) gluon mass λ to regularise infrared divergences. However in the end we will only be interested in the *real part* of terms that do not vanish for $\lambda \rightarrow 0$, i.e. only in constants and in divergent terms in $\frac{1}{\lambda}$. The expansion is lengthy, and therefore we present it already at this point.

We will treat the three integrals J_1, J_2, J_3 separately for simplicity. For J_1 one finds:

$$a = k_2, \quad (3.87)$$

$$b = k_3, \quad (3.88)$$

$$c = k_1 + k_4 + k_5, \quad (3.89)$$

$$y_1 = -\frac{k_4}{h_1} + \alpha_+, \quad (3.90)$$

$$\begin{aligned} \Rightarrow a_{\pm} &= -\frac{k_3}{2k_2} \pm \sqrt{\frac{k_3^2}{4k_2^2} - \frac{k_1}{k_2} + i\epsilon} \\ \epsilon \ll 1 &\approx \alpha_{\pm} \pm i\epsilon. \end{aligned} \quad (3.91)$$

Then

$$\begin{aligned} \Re(J_1) &= \Re \left[\text{Sp} \left(\frac{y_1}{y_1 - a_+} \right) - \text{Sp} \left(\frac{y_1 - 1}{y_1 - a_+} \right) + \text{Sp} \left(\frac{y_1}{y_1 - a_-} \right) - \text{Sp} \left(\frac{y_1 - 1}{y_1 - a_-} \right) \right] \\ &= \Re \left[\text{Sp} \left(\frac{-k_4 + h_1\alpha_+}{-k_4 - h_1i\epsilon} \right) - \text{Sp} \left(\frac{-k_4 + h_1(\alpha_+ - 1)}{-k_4 - h_1i\epsilon} \right) \right. \\ &\quad \left. + \text{Sp} \left(\frac{-k_4 + h_1\alpha_+}{-k_4 + h_1(\alpha_+ - \alpha_-) + h_1i\epsilon} \right) - \text{Sp} \left(\frac{-k_4 + h_1(\alpha_+ - 1)}{-k_4 + h_1(\alpha_+ - \alpha_-) + h_1i\epsilon} \right) \right]. \end{aligned} \quad (3.92)$$

3 One-loop integrals

In the limit $-k_4 = m_3^2 \rightarrow 0$ this reads (note that we can drop the $i\epsilon$ terms, since the real part is not sensitive to the branch cuts):

$$\begin{aligned} \Re(J_1) &= \Re \left[\text{Sp} \left(\frac{h_1 \alpha_+}{-k_4} \right) - \text{Sp} \left(\frac{h_1(\alpha_+ - 1)}{-k_4} \right) + \text{Sp} \left(\frac{\alpha_+}{\alpha_+ - \alpha_-} \right) - \text{Sp} \left(\frac{\alpha_+ - 1}{\alpha_+ - \alpha_-} \right) \right] \\ \text{Eqs. (3.25-3.27)} &= \Re \left[\text{Sp} \left(\frac{\alpha_+}{\alpha_+ - \alpha_-} \right) - \text{Sp} \left(\frac{\alpha_+ - 1}{\alpha_+ - \alpha_-} \right) \right. \\ &\quad \left. + \frac{1}{2} \ln^2 \left(\frac{k_4}{h_1(\alpha_+ - 1)} \right) - \frac{1}{2} \ln^2 \left(\frac{k_4}{h_1 \alpha_+} \right) \right]. \end{aligned} \quad (3.93)$$

For J_2 the variables read:

$$a = k_1 + k_2 + k_3, \quad (3.94)$$

$$b = k_4, \quad (3.95)$$

$$c = k_5, \quad (3.96)$$

$$y_2 = -\frac{k_4}{h_1} \frac{1}{1 - \alpha_+} \quad (3.97)$$

$$\begin{aligned} \Rightarrow b_{\pm} &= -\frac{k_4}{2(k_1 + k_2 + k_3)} \pm \sqrt{\frac{k_4^2}{4(k_1 + k_2 + k_3)^2} + \frac{k_4}{k_1 + k_2 + k_3} + \frac{i\epsilon}{k_1 + k_2 + k_3}} \\ k_4 \rightarrow 0 &\approx \pm \sqrt{\frac{k_4}{k_1 + k_2 + k_3}} \pm i\epsilon', \end{aligned} \quad (3.98)$$

and in the limit $k_4 \rightarrow 0$ we note that

$$y_2 - b_{\pm} \rightarrow b_{\mp} \quad (3.99)$$

$$\Rightarrow \frac{y_2}{y_2 - b_{\pm}} \rightarrow 0, \quad (3.100)$$

$$y_2 - 1 \rightarrow -1. \quad (3.101)$$

The real part of J_2 can then be written as:

$$\begin{aligned}
 \Re(J_2) &= \Re \left[\text{Sp} \left(\frac{y_2}{y_2 - b_+} \right) - \text{Sp} \left(\frac{y_2 - 1}{y_2 - b_+} \right) + \text{Sp} \left(\frac{y_2}{y_2 - b_-} \right) - \text{Sp} \left(\frac{y_2 - 1}{y_2 - b_-} \right) \right] \\
 &= \Re \left[-\text{Sp} \left(\frac{-1}{b_-} \right) - \text{Sp} \left(\frac{-1}{b_+} \right) \right] \\
 \text{Eqs. (3.25-3.27)} \quad &= \Re \left[\frac{\pi^2}{6} + \frac{1}{2} \ln^2(b_-) + \frac{\pi^2}{6} + \frac{1}{2} \ln^2(b_+) \right] \\
 &= \Re \left[\frac{\pi^2}{3} + \frac{1}{2} \ln^2 \left(\sqrt{\frac{k_4}{k_1 + k_2 + k_3}} \right) + \frac{1}{2} \ln^2 \left(-\sqrt{\frac{k_4}{k_1 + k_2 + k_3}} \right) \right] \\
 &= \Re \left[\frac{\pi^2}{3} + \frac{1}{2} \ln^2 \left(\sqrt{\frac{k_4}{k_1 + k_2 + k_3}} \right) - \frac{1}{2} \pi^2 + \frac{1}{2} \ln^2 \left(\sqrt{\frac{k_4}{k_1 + k_2 + k_3}} \right) \right] \\
 &= \Re \left[-\frac{\pi^2}{6} + \left(\frac{1}{2} + \ln \left(\frac{k_4}{k_1 + k_2 + k_3} \right) \right)^2 \right] \\
 &= \Re \left[-\frac{\pi^2}{6} + \frac{1}{4} + \ln \left(\frac{k_4}{k_1 + k_2 + k_3} \right) + \ln^2 \left(\frac{k_4}{k_1 + k_2 + k_3} \right) \right]. \tag{3.102}
 \end{aligned}$$

For J_3 the variables read:

$$a = k_1, \tag{3.103}$$

$$b = k_4, \tag{3.104}$$

$$c = k_5, \tag{3.105}$$

$$y_3 = -\frac{k_4}{h_1} \frac{1}{(-\alpha_+)}, \tag{3.106}$$

$$\begin{aligned}
 \Rightarrow c_{\pm} &= -\frac{k_4}{2k_1} \pm \sqrt{\frac{k_4^2}{4k_1^2} + \frac{k_4}{k_1} + \frac{i\epsilon}{k_1}} \\
 k_4 \rightarrow 0 &\approx \pm \sqrt{\frac{k_4}{k_1}} \pm i\epsilon', \tag{3.107}
 \end{aligned}$$

and in the limit $k_4 \rightarrow 0$ we note that

$$y_3 - c_{\pm} \rightarrow c_{\mp} \tag{3.108}$$

$$\Rightarrow \frac{y_3}{y_3 - c_{\pm}} \rightarrow 0, \tag{3.109}$$

$$y_3 - 1 \rightarrow -1. \tag{3.110}$$

This is completely analogous to J_2 and so we can read off the result for J_3 of Eq.

(3.102):

$$\Re(J_3) = \Re \left[-\frac{\pi^2}{6} + \frac{1}{4} + \ln \left(\frac{k_4}{k_1} \right) + \ln^2 \left(\frac{k_4}{k_1} \right) \right]. \quad (3.111)$$

Then the real part of I_3 , Eq. (3.52), becomes:

$$\begin{aligned} \Re(h_1 \cdot I_3) &= \Re(J_1 - J_2 + J_3) \\ &= \Re \left[\text{Sp} \left(\frac{\alpha_+}{\alpha_+ - \alpha_-} \right) - \text{Sp} \left(\frac{\alpha_+ - 1}{\alpha_+ - \alpha_-} \right) \right. \\ &\quad + \frac{1}{2} \ln^2 \left(\frac{k_4}{h_1(\alpha_+ - 1)} \right) - \frac{1}{2} \ln^2 \left(\frac{k_4}{h_1 \alpha_+} \right) \\ &\quad - \ln \left(\frac{k_4}{k_1 + k_2 + k_3} \right) - \ln^2 \left(\frac{k_4}{k_1 + k_2 + k_3} \right) \\ &\quad \left. + \ln \left(\frac{k_4}{k_1} \right) + \ln^2 \left(\frac{k_4}{k_1} \right) \right] \\ &= \Re \left[\text{Sp} \left(\frac{\alpha_+}{\alpha_+ - \alpha_-} \right) - \text{Sp} \left(\frac{\alpha_+ - 1}{\alpha_+ - \alpha_-} \right) \right. \\ &\quad + \frac{1}{2} \ln^2(\alpha_+ - 1) - \frac{1}{2} \ln^2(\alpha_+) + \ln \left(\frac{k_4}{h_1} \right) \ln \left(\frac{\alpha_+}{\alpha_+ - 1} \right) \\ &\quad \left. + \ln \left(\frac{k_1 + k_2 + k_3}{k_1} \right) - \ln^2 \left(\frac{h_1 k_4}{h_1(k_1 + k_2 + k_3)} \right) + \ln^2 \left(\frac{h_1 k_4}{h_1 k_1} \right) \right] \\ &= \Re \left[\text{Sp} \left(\frac{\alpha_+}{\alpha_+ - \alpha_-} \right) - \text{Sp} \left(\frac{\alpha_+ - 1}{\alpha_+ - \alpha_-} \right) \right. \\ &\quad + \frac{1}{2} \ln^2(\alpha_+ - 1) - \frac{1}{2} \ln^2(\alpha_+) + \ln \left(\frac{k_4}{h_1} \right) \ln \left(\frac{\alpha_+}{\alpha_+ - 1} \right) \\ &\quad + \ln \left(\frac{k_1 + k_2 + k_3}{k_1} \right) - \ln^2 \left(\frac{h_1}{k_1 + k_2 + k_3} \right) \\ &\quad \left. + \ln^2 \left(\frac{h_1}{k_1} \right) + \ln \left(\frac{k_4}{h_1} \right) \ln \left(\frac{k_1 + k_2 + k_3}{k_1} \right) \right]. \quad (3.112) \end{aligned}$$

We will need this result in Sec. 8.1 and Appendix C.1 to calculate the one loop vertex correction to DY pair production.

Part III

Physical background

4

Remarks on renormalisation

In this chapter we will touch briefly on the basics and a few selected topics of renormalisation, which are relevant for the model presented in this thesis. These remarks are by no means complete and only serve the purpose to provide some very introductory insights. A much more detailed introduction to renormalisation is given for example in [PS95, Mut98, Col84], which provide the basis for this chapter.

4.1 Basics of renormalisation

In Part II we have studied regularisation procedures for the UV divergent loop processes, which one encounters in quantum field theoretical calculations, for example in QED and in QCD. However, regularisation is just a mathematical tool, which enables us to handle the infinite contributions arising from the loops. The physically important procedure is called renormalisation. Renormalisation schemes provide means to systematically and consistently remove the UV divergences from the calculated physical quantities, such that only predictions of finite observables remain. We will illustrate this procedure in the following on the example of QED.

4.1.1 Example: renormalisation in QED

The Lagrangian of QED reads:

$$\mathcal{L} = -\frac{1}{4}(F_{\mu\nu})_0(F^{\mu\nu})_0 + \bar{\Psi}_0 (i\not{\partial} - m_0) \Psi_0 - e_0 \bar{\Psi}_0 \gamma_\mu \Psi_0 A_0^\mu, \quad (4.1)$$

where $(F^{\mu\nu})_0 = \partial^\mu A_0^\nu - \partial^\nu A_0^\mu$. Note the index 0 on the fields Ψ and A and on the electron mass m and charge e , which we will explain in a minute. Suppose one would

like to measure one of these quantities, for example the charge. The Lagrangian in Eq. (4.1) tells us, that obviously the charge e_0 is associated with the electron-photon vertex. Thus, a simple (but too naive) idea to measure the charge e_0 is a scattering experiment (e.g. $e^-e^+ \rightarrow e^-e^+$), where the exchanged photon interacts with the electron (or positron), see the left diagram in Fig. 4.1. However, we cannot switch off the interactions among the particles while we perform the measurement, and so what one actually measures is the coherent sum of all the processes in Fig. 4.1. Thus, the bare

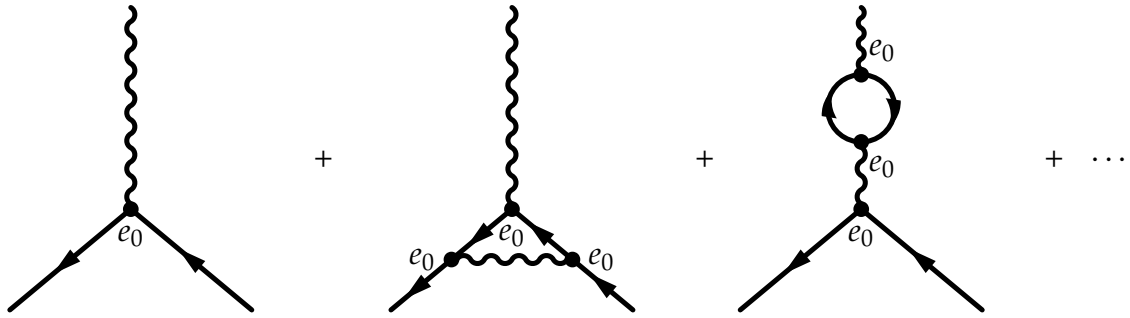


Figure 4.1: The bare electromagnetic vertex and its loop corrections.

charge e_0 is not an observable quantity, since it somehow hides behind all the higher-order corrections. The same holds for the other quantities in the Lagrangian, which is why they all carry the index 0 to mark them as bare (unmeasurable) quantities. In fact, instead of measuring e_0 , one measures

$$e_0 \left(1 + e_0^2 A_1(q^2) + e_0^4 A_2(q^2) + \dots \right) . \quad (4.2)$$

When trying to calculate the loop corrections, which give rise to the coefficient functions $A_i(q^2)$, one encounters the UV divergences mentioned above. So not only is e.g. the bare charge not directly measurable, but it also receives infinite corrections from higher-order processes. While at first glance the situation looks awkward, there is actually an elegant way to resolve it: neither the bare quantities nor the infinite loop corrections are actually physical observables. Thus, there is nothing wrong with absorbing both into new *renormalised* quantities. The renormalised charge then reads:

$$e_r = e_0 \left(1 + e_0^2 A_1(q^2) + e_0^4 A_2(q^2) + \dots \right) . \quad (4.3)$$

Note, that while the bare charge is a (non-measurable) constant, the renormalised charge e_r is a function of the hard scale q^2 at which the experiment probes the charge. This property has very important consequences and gives rise to the renormalisation

group equation, cf. Sec. 4.1.2. The virtue of renormalisation is now the following: if one calculates the amplitude M of any specific process (e.g. $e^-e^+ \rightarrow e^-e^+$) to a certain loop-order in terms of the *bare* quantities e_0, m_0, \dots and neglects the processes that modify the external legs (field strength), one encounters the infinities associated with the UV divergences. However, a special class of theories, called renormalisable theories, has a distinct feature: if one performs the same calculation of M in terms of the *renormalised* quantities e_r, m_r, \dots all the UV divergences exactly cancel and only finite quantities remain, since the field strength renormalisation factors are automatically taken into account. QED and QCD are important examples for renormalisable theories and the proof of renormalisation actually paved the way for their success in describing the electromagnetic and the strong interaction.

A systematic approach to remove the divergences is the introduction of counterterms in the Lagrangian. The idea is to split the Lagrangian into two parts: one unperturbed part, which only depends on the renormalised quantities and fields, and a counterterm part, which contains all the infinities. In the QED case the Lagrangian then becomes [PS95]:

$$\begin{aligned} \mathcal{L} = & -\frac{1}{4}(F_{\mu\nu})_r(F^{\mu\nu})_r + \bar{\Psi}_r(i\not{\partial} - m_r)\Psi_r - e_r\bar{\Psi}_r\gamma_\mu\Psi_r A_r^\mu \\ & -\frac{1}{4}\delta_3(F_{\mu\nu})_r(F^{\mu\nu})_r + \bar{\Psi}_r(i\delta_2\not{\partial} - \delta_m)\Psi_r - e_r\delta_1\bar{\Psi}_r\gamma_\mu\Psi_r A_r^\mu. \end{aligned} \quad (4.4)$$

Note, that we have just rewritten the original Lagrangian in Eq. (4.1). The renormalisation parameters $\delta_1, \delta_2, \delta_3$ and δ_m are connected to the bare quantities and fields as, for example, one finds $\bar{\Psi}_r(\delta_m + m_r)\Psi_r = \bar{\Psi}_0 m_0 \Psi_0$. Obviously the splitting into unperturbed part (e.g. m_r) and counterterms (e.g. δ_m) is not unique and in fact arbitrary and, therefore, one has to choose a certain renormalisation scheme to fix the renormalisation parameters. A common choice for QED is to choose the physical (pole) mass m and the physical charge e (at $q^2 = 0!$) of the electron for the renormalised values m_r and e_r . In this case the first line of Eq. (4.4) is just the standard QED Lagrangian with bare quantities and fields replaced by their renormalised versions. The second line containing the counterterms gives rise to additional Feynman rules, which automatically take care of the cancellation of all the UV divergences in the theory. This kind of calculational scheme is called renormalised perturbation theory and it can be understood as a useful bookkeeping device when dealing with the UV divergences. Remember, however, that the Lagrangian in Eq. (4.4) was just a rewrite of the original Lagrangian in Eq. (4.1). Therefore, it is evident that renormalised perturbation theory must be completely equivalent to bare perturbation theory, which is based on Eq. (4.1), i.e. to calculating the relevant processes with the bare quantities, taking into account all the propagator, vertex and external leg corrections. The latter, though, can become very tedious in multi-loop calculations, which is why for these cases renormalised perturbation theory is advantageous.

Note, that in the chosen case of $m_r = m$ and $e_r = e$ the renormalisation parameters can also be expressed in terms of field strength and charge renormalisation in the

following way:

$$\delta_2 = Z_2 - 1 , \quad (4.5)$$

which implies

$$\Psi_0 = \sqrt{Z_2} \Psi_r , \quad (4.6)$$

where Z_2 is called the field strength renormalisation of the electron field. We will explore the significance of this quantity in more detail in Sec. 4.3. Similarly with

$$\delta_3 = Z_3 - 1 , \quad (4.7)$$

$$\delta_1 = Z_1 - 1 , \quad (4.8)$$

$$\delta_m = Z_2 m_0 - m \quad (4.9)$$

one finds

$$A_0^\mu = \sqrt{Z_3} A_r^\mu , \quad (4.10)$$

$$e_0 Z_2 \sqrt{Z_3} = e Z_1 . \quad (4.11)$$

Here Z_3 is the field strength renormalisation of the photon field. In QED the charge renormalisation Z_1 is actually not an independent quantity, since the Ward-Takahashi identities show, that $Z_1 = Z_2$ [PS95].

4.1.2 Renormalisation group equation

In Sec. 4.1.1 we discussed, that to fix the renormalised charge, and, in fact, all renormalisation parameters, one has to choose a certain renormalisation scheme. This includes fixing the hard scale q^2 , which we found e.g. in Eq. (4.3), at a certain value μ^2 , which is called the renormalisation scale. Once again the choice of this scale is completely arbitrary and, thus, any observables calculated in the renormalised perturbation theory must not depend on it. This basically acknowledges, that the renormalised perturbation theory must give the same answers as the bare perturbation theory, which, just like nature, does not know anything about a renormalisation scale. Thus, the derivative with respect to μ of any amplitude M calculated in the renormalised scheme must vanish. For the case of QED we found $Z_1 = Z_2$, so M can only depend on three independent renormalisation parameters (e.g. e , Z_1 and Z_3) and one finds:

$$\mu \frac{d}{d\mu} M(e, Z_1, Z_3) = \left[\mu \frac{\partial}{\partial \mu} + \mu \frac{\partial e}{\partial \mu} \frac{\partial}{\partial e} + \mu \frac{\partial Z_1}{\partial \mu} \frac{\partial}{\partial Z_1} + \mu \frac{\partial Z_3}{\partial \mu} \frac{\partial}{\partial Z_3} \right] M(e, Z_1, Z_3) = 0 . \quad (4.12)$$

This equation shows, that any infinitesimal change of the scale $\mu \rightarrow \mu + \delta\mu$ is exactly compensated by infinitesimal changes of the renormalisation parameters. The coefficient of the derivative with respect to e is an important mathematical object, called the β -function (of QED):

$$\beta(e) = \mu \frac{\partial e}{\partial \mu}. \quad (4.13)$$

It describes the change of the renormalised charge (coupling) with the scale μ at which the charge is probed. This scale-dependence of the electric coupling constant is called the running of the coupling. Note, that in contrast the bare coupling e_0 is really a constant. The β -function of QED to one-loop order reads [PS95].

$$\beta(e) = +\frac{e^3}{12\pi^2}. \quad (4.14)$$

Note the sign of $\beta(e)$, which is positive. This indicates that the charge increases with increasing scale (or energy) μ . In this picture e reaches its minimum value at $\mu = 0$, where it is measured to be $e(\mu = 0) \approx \sqrt{\frac{4\pi}{137}}$ (in natural units). However, one has to be careful when extrapolating to very large energies, since as soon as e becomes $O(1)$ the concept of perturbation theory breaks down and the derivation of $\beta(e)$ becomes invalid.

In QCD the situation is completely different. The β -function of the strong renormalised coupling constant g reads [PS95]

$$\beta(g) = -\left(11 - \frac{2n_f}{3}\right) \frac{g^3}{16\pi^2}, \quad (4.15)$$

where n_f is the number of quark flavors. For $n_f = 6$, as in the standard model of particle physics, the sign of $\beta(g)$ is negative! This implies, that with increasing energy the coupling strength decreases and eventually perturbation theory becomes applicable. This very important physical phenomenon is called *asymptotic freedom* and it was discovered by Wilczek, Gross and Politzer [GW73, Pol73]. Unfortunately, asymptotic freedom also implies that at small (soft) energy scales the strong coupling becomes really strong, i.e. $O(1)$ and, thus, perturbative methods alone are no longer applicable. This is why the soft interactions among the quarks and gluons in the nucleon are so hard to access theoretically. Therefore, non-perturbative phenomenological approaches to this problem might help to improve the theoretical situation. This thesis is exactly aiming at producing such an approach.

4.2 The massive quark selfenergy

In Chapter 2 we calculated the massless quark selfenergy to one-loop order in QCD, cf. Fig. 2.1. We want to repeat this calculation here for massive quarks and for gluons

with a (fictitious) finite mass. This calculation will serve as input for Sec. 4.4, where we will determine the field strength renormalisation constant for the massive quark case. This constant will then enter into our model in Sec. 8.1. To regularise anticipated infrared divergences, a finite gluon mass is assumed. It is clear that any physical observable must not depend on this fictitious mass and in Sec. 8.1.3 we will show why this is indeed not the case.

Introducing a quark mass m and a gluon mass λ the quark selfenergy to one-loop order reads:

$$\Sigma(p) = -ig^2 C_F \int \frac{d^d k}{(2\pi)^d} \frac{\gamma^\mu (\not{p} - \not{k} + m) \gamma_\mu}{[(p-k)^2 - m^2 + i\epsilon] [k^2 - \lambda^2 + i\epsilon]} . \quad (4.16)$$

Again we can draw on our results of Sec. 2.3. Introducing a Feynman parameter the selfenergy becomes:

$$\Sigma(p) = -ig^2 C_F \int \frac{d^d k}{(2\pi)^d} \int_0^1 dx \frac{\gamma^\mu (\not{p} - \not{k} + m) \gamma_\mu}{[(1-x)((p-k)^2 - m^2 + i\epsilon) + x(k^2 - \lambda^2 + i\epsilon)]^2} . \quad (4.17)$$

Shifting the momentum integration,

$$l = k - (1-x)p , \quad (4.18)$$

one finds:

$$\Sigma(p) = -ig^2 C_F \int \frac{d^d l}{(2\pi)^d} \int_0^1 dx \frac{\gamma^\mu (x\not{p} - \not{l} + m) \gamma_\mu}{[l^2 - \Delta(x)]^2} , \quad (4.19)$$

with

$$\Delta(x) = -x(1-x)p^2 + (1-x)m^2 + x\lambda^2 - i\epsilon . \quad (4.20)$$

The Dirac structure in the numerator can be simplified by noting, that the term proportional to l vanishes due to symmetry considerations, and by contracting the γ matrices:

$$\Sigma(p) = -ig^2 C_F \int_0^1 dx ((2-d)x\not{p} + dm) \int \frac{d^d l}{(2\pi)^d} \frac{1}{[l^2 - \Delta(x)]^2} . \quad (4.21)$$

The momentum integral is solved by a Wick rotation and an integration over d -dimensional spherical coordinates, cf. Eq. (2.90):

$$\Sigma(p) = -ig_0^2 \cdot (\mu^2)^\epsilon C_F \int_0^1 dx ((2-d)x\not{p} + dm) \frac{i}{(4\pi)^{\frac{d}{2}}} \Gamma\left(2 - \frac{d}{2}\right) \Delta^{2-\frac{d}{2}}(x) , \quad (4.22)$$

where we have replaced the coupling constant g by a dimensionless coupling g_0 and a mass scale μ , cf. Sec. 2.3.2. With $\epsilon' = \frac{4-d}{2}$ and expanding around $\epsilon' = 0$ the selfenergy now reads:

$$\Sigma(p) = \frac{g_0^2}{(4\pi)^2} C_F \int_0^1 dx \left((2\epsilon' - 2)x\not{p} + (4 - 2\epsilon')m \right) \left[\frac{1}{\epsilon'} - \gamma + \ln \left(\frac{4\pi\mu^2}{\Delta(x)} \right) \right]. \quad (4.23)$$

Finally, dropping all terms that vanish for $\epsilon' \rightarrow 0$, one obtains:

$$\begin{aligned} \Sigma(p) = \frac{g_0^2}{(4\pi)^2} C_F \left[\not{p} - 2m + (-\not{p} + 4m) \left(\frac{1}{\epsilon'} - \gamma + \ln(4\pi\mu^2) \right) \right. \\ \left. + \int_0^1 dx 2(x\not{p} - 2m) \ln(\Delta(x)) \right]. \end{aligned} \quad (4.24)$$

The evaluation of the last integral in Eq. (4.24) is straightforward, however for our purposes we postpone this calculation to Sec. 4.4.

4.3 Field strength renormalisation

In this section we introduce the concept of field strength renormalisation. To motivate this concept, we recall that the propagator of a scalar particle in a free field theory has the following form in momentum space [PS95]:

$$D(p, m_0) = \frac{i}{p^2 - m_0^2 + i\epsilon} = \int d^4x \exp(ipx) \langle 0 | T \phi(x) \phi(0) | 0 \rangle, \quad (4.25)$$

which is the Fourier transform of the time-ordered two-point function. The analytic structure of $D(p, m_0)$ can be read off immediately:

$$D(p, m_0) = \frac{i}{\left(p_0 - \sqrt{\vec{p}^2 + m_0^2} + i\epsilon \right) \left(p_0 + \sqrt{\vec{p}^2 + m_0^2} - i\epsilon \right)}. \quad (4.26)$$

The free propagator has two isolated poles in the complex p_0 plane and thus it describes the propagation of a pure one-particle state with mass m_0 , which is the (bare) mass from the associated Lagrangian. Note that while for spin- $\frac{1}{2}$ fields the propagator has additionally a Dirac structure, it still retains the analytic properties of the scalar propagator concerning the pole structure.

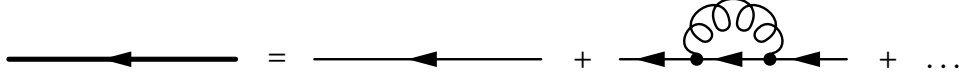


Figure 4.2: The full propagator as a sum of the free propagator and an infinite series of selfenergy insertions.

4.3.1 The full spin- $\frac{1}{2}$ propagator

In an interacting field theory the picture changes: due to self-interactions the propagator acquires a more complicated analytic structure, which we will explore in the following. In Fig. 4.2 we illustrate the concept of the full propagator for an interacting theory with spin- $\frac{1}{2}$ particles: by ordering diagrams by the number of selfenergy insertions Σ , one finds, that the full propagator is represented by an infinite series of diagrams.

In formulas, the full (interacting) propagator D_I can thus be written as [PS95]:

$$\begin{aligned}
 D_I(p) &= \frac{i(\not{p} + m_0)}{p^2 - m_0^2 + i\epsilon} + \frac{i(\not{p} + m_0)}{p^2 - m_0^2 + i\epsilon} [-i\Sigma(p)] \frac{i(\not{p} + m_0)}{p^2 - m_0^2 + i\epsilon} + \dots \\
 &= \sum_{n=0}^{\infty} \frac{i(\not{p} + m_0)}{p^2 - m_0^2 + i\epsilon} \left[\frac{\Sigma(p) \cdot (\not{p} + m_0)}{p^2 - m_0^2 + i\epsilon} \right]^n.
 \end{aligned} \tag{4.27}$$

Exploiting the known limit of the geometric series, Eq. (4.27) becomes:

$$\begin{aligned}
 D_I(p) &= \frac{i(\not{p} + m_0)}{p^2 - m_0^2 + i\epsilon} \left[1 - \frac{\Sigma(p) \cdot (\not{p} + m_0)}{p^2 - m_0^2 + i\epsilon} \right]^{-1} \\
 &= \frac{i}{\not{p} - m_0 - \Sigma(p)},
 \end{aligned} \tag{4.28}$$

where we have dropped the $i\epsilon$ term in the last step. Note how the analytic structure of the propagator has changed from the free case: the pole mass m_0 has been shifted to a value m , where m is the solution of

$$[\not{p} - m_0 - \Sigma(p)]_{\not{p}=m} = 0. \tag{4.29}$$

Close to the pole $\not{p} = m$ one can expand Eq. (4.29) and finds [PS95]:

$$[\not{p} - m_0 - \Sigma(p)] = 0 + (\not{p} - m) \left[1 - \left. \frac{\partial \Sigma(p)}{\partial \not{p}} \right|_{\not{p}=m} \right] + O((\not{p} - m)^2). \quad (4.30)$$

Ignoring all terms of $O((\not{p} - m)^2)$ and higher, the full propagator becomes:

$$\begin{aligned} D_I(p) &\simeq \frac{i}{\not{p} - m} \cdot \left[1 - \left. \frac{\partial \Sigma(p)}{\partial \not{p}} \right|_{\not{p}=m} \right]^{-1} \\ &= \frac{iZ_2}{\not{p} - m} \\ &= \frac{iZ_2(\not{p} + m)}{p^2 - m^2}. \end{aligned} \quad (4.31)$$

The last result is very similar to the first term in Eq. (4.27): close to the pole the full propagator looks like the propagator of a free particle with mass m , weighted by the factor

$$Z_2 = \left[1 - \left. \frac{\partial \Sigma(p)}{\partial \not{p}} \right|_{\not{p}=m} \right]^{-1}. \quad (4.32)$$

This factor is known as the field strength renormalisation factor and it is common to name it Z_2 .

4.3.2 Spectral decomposition of the full propagator

We will now explore the physical meaning of Z_2 , as well as of the higher order contributions in Eq. (4.30) (for simplicity we will use a scalar field theory for that purpose). To do this, one has to investigate the time ordered two point function for the interacting theory, which is, just as in the free case, the Fourier transform of the momentum space propagator:

$$\int \frac{d^4 p}{(2\pi)^4} \exp(-ip(x-y)) \cdot D_I(p) = \langle V | T \phi(x) \phi(y) | V \rangle, \quad (4.33)$$

where $|V\rangle$ is the vacuum (ground state) of the interacting theory. To simplify matters, we will investigate the structure of the free propagator first and then generalise the result for an interacting theory.

A very simple case of a free (non-interacting) field is the free Klein-Gordon field. The excitations of this field are scalars (spin-0 particles) and in the following we briefly summarise important properties [PS95]. The Lagrangian reads:

$$\mathcal{L} = \frac{1}{2} (\partial_\mu \phi) (\partial^\mu \phi) + \frac{1}{2} m_0^2 \phi^2, \quad (4.34)$$

from which the equation of motion follows directly:

$$(\partial_\mu \partial^\mu + m_0^2)\phi = 0. \quad (4.35)$$

Generalising the concept of the description of the harmonic oscillator in terms of ladder operators, one finds for the time-independent field operator (with $\phi = \phi^\dagger$):

$$\phi(\vec{x}) = \int \frac{d^3p}{(2\pi)^3} \frac{1}{\sqrt{2E_p}} (a_p + a_{-p}^\dagger) \exp(i\vec{p}\vec{x}), \quad (4.36)$$

where $E_p = \sqrt{\vec{p}^2 + m_0^2}$ is the energy of a particle with momentum \vec{p} and the creation and annihilation operators obey a commutation relation:

$$[a_p, a_{p'}^\dagger] = (2\pi)^3 \delta^{(3)}(\vec{p} - \vec{p}'). \quad (4.37)$$

The Hamiltonian can be written as:

$$\mathcal{H} = \int \frac{d^3p}{(2\pi)^3} E_p \frac{1}{2} (a_p^\dagger a_p + a_p a_p^\dagger) \quad (4.38)$$

and the momentum operator is given by:

$$\vec{P} = \int \frac{d^3p}{(2\pi)^3} \vec{p} a_p^\dagger a_p. \quad (4.39)$$

For the commutator of \mathcal{H} and \vec{P} one finds:

$$[\mathcal{H}, \vec{P}] = \int \frac{d^3p}{(2\pi)^3} \frac{E_p}{2} \frac{d^3q}{(2\pi)^3} \vec{q} [a_p^\dagger a_p + a_p a_p^\dagger, a_q^\dagger a_q]. \quad (4.40)$$

With the help of Eq. (4.37) one can evaluate the commutator in Eq. (4.40):

$$\begin{aligned} [a_p^\dagger a_p + a_p a_p^\dagger, a_q^\dagger a_q] &= (2\pi)^3 \delta^{(3)}(\vec{p} - \vec{q}) (a_p^\dagger a_q - a_q^\dagger a_p) \\ &= (2\pi)^3 \delta^{(3)}(\vec{p} - \vec{q}) (a_p^\dagger a_p - a_p^\dagger a_p) \\ &= 0. \end{aligned} \quad (4.41)$$

Inserting this result into Eq. (4.40) gives:

$$[\mathcal{H}, \vec{P}] = \int \frac{d^3p}{(2\pi)^3} \frac{E_p}{2} \vec{p} (a_p^\dagger a_p - a_p^\dagger a_p) = 0. \quad (4.42)$$

Since \mathcal{H} and \vec{P} commute they have a common set of eigenstates. These eigenstates can be easily constructed, in total analogy to the harmonic oscillator, by successively

applying creation operators on the ground state of the theory. We denote the ground state for this free theory by $|0\rangle$ and note that, as usual:

$$a_p|0\rangle = 0. \quad (4.43)$$

A one-particle state with momentum \vec{p} is given by:

$$|p\rangle = \sqrt{2E_p} a_p^\dagger |0\rangle, \quad (4.44)$$

where the normalisation factor $\sqrt{2E_p}$ ensures, that the scalar product of one-particle states is invariant under Lorentz transformations:

$$\langle q|p\rangle = \langle 0|a_q \sqrt{4E_q E_p} a_p^\dagger |0\rangle = (2\pi)^3 2E_p \delta^{(3)}(\vec{p} - \vec{q}), \quad (4.45)$$

where in the last step we have used the commutator relation (4.37) and the normalisation $\langle 0|0\rangle = 1$. Lorentz invariance of $\langle q|p\rangle$ follows directly from the Lorentz invariance of

$$\frac{d^3 p}{2E_p} \equiv d^4 p \delta^{(4)}(p^2 - m_0^2) \Theta(p_0). \quad (4.46)$$

Many-particle states are of a different nature than one-particle states: their energy is not fixed for a fixed total momentum \vec{p} , but depends on the momenta of the particles of the state. For example, for a two-particle state the energy is given by:

$$E = \sqrt{\vec{p}_1^2 + m_0^2} + \sqrt{\vec{p}_2^2 + m_0^2}, \quad (4.47)$$

where \vec{p}_1 and $\vec{p}_2 = \vec{p} - \vec{p}_1$ are the momenta of the two particles. However, we can also express E in terms of the total momentum \vec{p} and the invariant mass of the state M :

$$E = \sqrt{\vec{p}^2 + M^2}. \quad (4.48)$$

For a given invariant mass M the lowest energy of the state is realised for $\vec{p} = 0$:

$$E = M = 2\sqrt{\vec{p}_1^2 + m_0^2} \geq 2m_0. \quad (4.49)$$

Since \vec{p}_1 is not fixed, the energy spectrum of two-particle states is continuous. Obviously, the same statement holds for all states with $n > 1$ particles. Thus, we can characterise all states by their number of particles n , their total momentum \vec{p} and the specific combination n_λ of the momenta of each of the n particles:

$$|n_{\lambda,p}\rangle. \quad (4.50)$$

We assume the states $|n_{\lambda,p}\rangle$ to be orthonormalised and so the completeness relation for the full Hilbert space of states can then be written as:

$$\mathbb{1} = |0\rangle\langle 0| + \sum_{n=1}^{\infty} \sum_{n_{\lambda}} \int \frac{d^3p}{(2\pi)^3} \frac{1}{2E_p(m_{\lambda})} |n_{\lambda,p}\rangle\langle n_{\lambda,p}|. \quad (4.51)$$

Later on we will also need the completeness relation for the pure one-particle states ($n = 1, m_{\lambda} = m_0$):

$$\mathbb{1}_{1 \text{ part.}} = \int \frac{d^3p}{(2\pi)^3} \frac{1}{2E_p(m_0)} |1_{0,p}\rangle\langle 1_{0,p}|. \quad (4.52)$$

Before we study the structure of the two-point function in detail, we note, that in the Heisenberg picture one finds for the four momentum operator $P = (\mathcal{H}, \vec{P})$ and for an operator O :

$$[P^{\mu}, O] = -i\partial^{\mu}O, \quad (4.53)$$

from which immediately follows [PS95]:

$$\phi(x) = \exp(iPx)\phi(0)\exp(-iPx), \quad (4.54)$$

where $\phi(x) = \phi(t, \vec{x})$ is the time-dependent field operator. Especially the time evolution of $\phi(\vec{x})$ as given in Eq. (4.36) reads:

$$\phi(\vec{x}, t) = \exp(i\mathcal{H}t) \cdot \phi(\vec{x}) \cdot \exp(-i\mathcal{H}t). \quad (4.55)$$

The series expansion of the exponential reads:

$$\exp(i\mathcal{H}t) = \sum_{n=0}^{\infty} \frac{(i\mathcal{H}t)^n}{n!}, \quad (4.56)$$

and so to interchange the first exponential and $\phi(\vec{x})$ in Eq. (4.55), one needs these commutators:

$$[\mathcal{H}, a_p] = -a_p E_p \quad (4.57)$$

$$[\mathcal{H}, a_p^{\dagger}] = a_p^{\dagger} E_p. \quad (4.58)$$

Then the time-dependent field operator becomes:

$$\begin{aligned} \phi(x) &= \int \frac{d^3p}{(2\pi)^3} \frac{1}{\sqrt{2E_p}} \exp(i\mathcal{H}t) \left(a_p \exp(i\vec{p}\vec{x}) + a_p^{\dagger} \exp(-i\vec{p}\vec{x}) \right) \exp(-i\mathcal{H}t) \\ &= \int \frac{d^3p}{(2\pi)^3} \frac{1}{\sqrt{2E_p}} \left(a_p \exp(-iE_p t) \exp(i\vec{p}\vec{x}) + a_p^{\dagger} \exp(iE_p t) \exp(-i\vec{p}\vec{x}) \right) \\ &= \int \frac{d^3p}{(2\pi)^3} \frac{1}{\sqrt{2E_p}} \left(a_p \exp(-ipx) + a_p^{\dagger} \exp(ipx) \right). \end{aligned} \quad (4.59)$$

Finally we are ready to investigate the time-ordered two point function of the free Klein-Gordon field: first we insert a complete set of states, cf. Eq. (4.51). Then for $x^0 > y^0$ one finds:

$$\begin{aligned} \langle 0|\phi(x)\phi(y)|0\rangle &= \langle 0|\phi(x)|0\rangle\langle 0|\phi(y)|0\rangle \\ &+ \sum_{n=1}^{\infty} \sum_{n_\lambda} \int \frac{d^3p}{(2\pi)^3} \frac{1}{2E_p(m_\lambda)} \langle 0|\phi(x)|n_{\lambda,p}\rangle \langle n_{\lambda,p}|\phi(y)|0\rangle . \end{aligned} \quad (4.60)$$

The first term vanishes, since the annihilation and creation operators in $\phi(x)$ act on the vacuum state to the right and to the left, respectively, giving 0. The matrix element for all the particle states can be simplified with the help of Eq. (4.54):

$$\begin{aligned} \langle 0|\phi(x)|n_{\lambda,p}\rangle &= \langle 0|\exp(iPx)\phi(0)\exp(-iPx)|n_{\lambda,p}\rangle \\ &= \langle 0|\phi(0)|n_{\lambda,p}\rangle \exp(-ipx) , \end{aligned} \quad (4.61)$$

where in the last step we have used, that the vacuum has total momentum $\vec{p} = \vec{0}$. The momentum dependence of the matrix element has been factorised out into the exponential, which can be seen in the following way [PS95]: we define a Lorentz transformation Λ_p , which performs a boost from \vec{p} to $\vec{0}$. Then we twice insert the identity $\mathbb{1} = \Lambda_p^{-1}\Lambda_p$:

$$\langle 0|\Lambda_p^{-1}\Lambda_p\phi(0)\Lambda_p^{-1}\Lambda_p|n_{\lambda,p}\rangle = \langle 0|\phi(0)|n_{\lambda,0}\rangle , \quad (4.62)$$

where the Lorentz invariance of the vacuum and of $\phi(0)$ have entered. Inserting Eqs. (4.61,4.62) into Eq. (4.60), the two point function is thus given by:

$$\langle 0|\phi(x)\phi(y)|0\rangle = \sum_{n=1}^{\infty} \sum_{n_\lambda} |\langle 0|\phi(0)|n_{\lambda,0}\rangle|^2 \int \frac{d^3p}{(2\pi)^3} \frac{1}{2E_p(m_\lambda)} \exp(-ip(x-y)) . \quad (4.63)$$

For $y^0 > x^0$ the result (4.63) is identical with x and y interchanged. Therefore, the time-ordered two point function reads:

$$\begin{aligned} \langle 0|\mathbb{T}\phi(x)\phi(y)|0\rangle &= \sum_{n=1}^{\infty} \sum_{n_\lambda} |\langle 0|\phi(0)|n_{\lambda,0}\rangle|^2 \int \frac{d^3p}{(2\pi)^3} \frac{1}{2E_p(m_\lambda)} \\ &\times \left[\exp(-ip(x-y))|_{x^0>y^0} + \exp(-ip(y-x))|_{y^0>x^0} \right] . \end{aligned} \quad (4.64)$$

The momentum integral is nothing but the Fourier transform of the Feynman (time-ordered) propagator of a particle with mass m_λ :

$$\langle 0|\mathbb{T}\phi(x)\phi(y)|0\rangle = \sum_{n=1}^{\infty} \sum_{n_\lambda} |\langle 0|\phi(0)|n_{\lambda,0}\rangle|^2 \int \frac{d^4p}{(2\pi)^4} \frac{i \exp(-ip(x-y))}{p^2 - m_\lambda^2 + i\epsilon} . \quad (4.65)$$

All left to do is to calculate the matrix element in the last equation, which is straightforward for the free Klein-Gordon field (note that for the one-particles states we have $|p\rangle = |1_{0,p}\rangle$):

$$\begin{aligned}\langle 0|\phi(0)|n_{\lambda,0}\rangle &= \int \frac{d^3p}{(2\pi)^3} \frac{1}{\sqrt{2E_p}} \langle 0| (a_p + a_p^\dagger) |n_{\lambda,0}\rangle \\ &= \int \frac{d^3p}{(2\pi)^3} \frac{1}{2E_p} \langle 1_{0,p}|n_{\lambda,0}\rangle .\end{aligned}\quad (4.66)$$

Remember that many-particle states $|n_{\lambda,0}\rangle$ are created by successively applying creation operators on the vacuum:

$$|n_{\lambda,0}\rangle \sim \prod_{i=1}^n a_{p_i}^\dagger |0\rangle , \quad (4.67)$$

with $\sum_{i=1}^n \vec{p}_i = 0$. Thus, the matrix element in Eq. (4.66) can be evaluated with the help of the commutator (4.37):

$$\begin{aligned}\langle 1_{0,p}|n_{\lambda,0}\rangle &\sim \langle 0|a_p \prod_{i=1}^n a_{p_i}^\dagger |0\rangle \\ &= \langle 0| (a_{p_1}^\dagger a_p + (2\pi)^3 \delta^{(3)}(\vec{p} - \vec{p}')) \prod_{i=2}^n a_{p_i}^\dagger |0\rangle \\ &= 0 + \langle 0| \prod_{i=2}^n a_{p_i}^\dagger |0\rangle (2\pi)^3 \delta^{(3)}(\vec{p} - \vec{p}') \\ &= \delta_{n1} (2\pi)^3 \delta^{(3)}(\vec{p} - \vec{p}') ,\end{aligned}\quad (4.68)$$

and so obviously the matrix element vanishes for $n > 1$, since any creation operator acting on the vacuum to the left gives zero. Thus, we find:

$$\begin{aligned}\langle 0|\phi(0)|n_{\lambda,0}\rangle &= \int \frac{d^3p}{(2\pi)^3} \frac{1}{2E_p} \langle 1_{0,p}|1_{0,0}\rangle \\ &= \int \frac{d^3p}{(2\pi)^3} \frac{1}{2E_p} 2E_p (2\pi)^3 \delta^{(3)}(\vec{p}) \delta_{n1} \\ &= \delta_{n1} ,\end{aligned}\quad (4.69)$$

and so:

$$\begin{aligned}\langle 0|T\phi(x)\phi(y)|0\rangle &= \sum_{n=1}^{\infty} \sum_{n_\lambda} |\langle 0|\phi(0)|n_{\lambda,0}\rangle|^2 \int \frac{d^4p}{(2\pi)^4} \frac{i \exp(-ip(x-y))}{p^2 - m_\lambda^2 + i\epsilon} \\ &= \int \frac{d^4p}{(2\pi)^4} \frac{i \exp(-ip(x-y))}{p^2 - m_0^2 + i\epsilon} .\end{aligned}\quad (4.70)$$

In a free field theory the time-ordered two-point function is just the Fourier transform of the momentum space propagator of a particle with mass m_0 , i.e. it describes the propagation of an exact one-particle state, since the matrix element in Eq. (4.68) vanishes for all particle numbers $n \neq 1$.

Finally we will consider the case of an interacting theory, building on the statements above. First one has to find the full Hamiltonian:

$$\mathcal{H}_F = \mathcal{H}_{\text{free}} + \mathcal{H}_{\text{int}}, \quad (4.71)$$

which commutes with the momentum operator \vec{P}_F for the interacting theory. This again implies, that they have a common basis of eigenstates, which are characterised by particle number n , momentum state n_λ and total momentum \vec{p} . The completeness relation for the full Hilbert space then reads ($|V\rangle$ is the vacuum of the interacting theory):

$$\mathbb{1} = |V\rangle\langle V| + \sum_{n=1}^{\infty} \sum_{n_\lambda} \int \frac{d^3p}{(2\pi)^3} \frac{1}{2E_p(m_\lambda)} |n_{\lambda,p}\rangle\langle n_{\lambda,p}|. \quad (4.72)$$

Here m_λ is again the invariant mass of the n -particle momentum state n_λ . For $n = 1$ one finds $m_\lambda = m$, which is the physical mass of an exact one-particle state and which for an interacting theory in general differs from the bare mass m_0 in the Lagrangian. The lower bound of m_λ might be somewhat below $n \cdot m$, since in an interacting theory bound states of $n > 1$ particles may form. Employing the same formalism as above for the free theory, one finds for the time-ordered two-point function:

$$\begin{aligned} & \langle V | T \phi(x) \phi(y) | V \rangle \\ &= \text{const.} + \sum_{n=1}^{\infty} \sum_{n_\lambda} |\langle V | \phi(0) | n_{\lambda,0} \rangle|^2 \int \frac{d^4p}{(2\pi)^4} \frac{i \exp(-ip(x-y))}{p^2 - m_\lambda^2 + i\epsilon} \\ &= \text{const.} + |\langle V | \phi(0) | 1_{0,0} \rangle|^2 \int \frac{d^4p}{(2\pi)^4} \frac{i \exp(-ip(x-y))}{p^2 - m^2 + i\epsilon} \\ & \quad + \sum_{n=2}^{\infty} \sum_{n_\lambda} |\langle V | \phi(0) | n_{\lambda,0} \rangle|^2 \int \frac{d^4p}{(2\pi)^4} \frac{i \exp(-ip(x-y))}{p^2 - m_\lambda^2 + i\epsilon}, \end{aligned} \quad (4.73)$$

where $|1_{0,0}\rangle$ is a one-particle state with mass m and momentum $\vec{p} = 0$. The constant term usually vanishes (as in the free case above) [PS95] and so the first contributing term in this expansion by particle numbers is just the one-particle state. Then the propagator in the interacting theory (the Fourier transform of the time-ordered two-point function) takes the form:

$$\tilde{D}_I(p) = \frac{i |\langle V | \phi(0) | 1_{0,0} \rangle|^2}{p^2 - m^2 + i\epsilon} + \text{mult.-particle contributions}. \quad (4.74)$$

Close to the pole $p^2 = m^2$ the propagator looks like a propagator for a free particle with mass m , multiplied by the factor $Z_2 = |\langle V|\phi(0)|1_{0,0}\rangle|^2$. Thus, the interpretation of Z_2 for the interacting theory has become clear. It is the probability to create from the vacuum an exact one-particle state. In contrast to the free theory this probability is in general no longer 1, but one finds $0 \leq Z_2 < 1$ [BD65].

This result for Z_2 can be generalised to spin- $\frac{1}{2}$ fields [PS95] and so returning to Eq. (4.31) we can write for the full spin- $\frac{1}{2}$ propagator:

$$D_I(p) = \frac{iZ_2(\not{p} + m)}{p^2 - m^2 + i\epsilon} + \text{mult.-particle contributions}$$

close to the positive-energy pole $\approx \sum_s \frac{i(\sqrt{Z_2}\bar{u}_s(p))(\sqrt{Z_2}u_s(p))}{p^2 - m^2 + i\epsilon},$ (4.75)

where we have used the completeness relation for the Dirac spinors, see Appendix A.4.3. Finally, Eq. (4.75) implies how to modify the Feynman rules for the interacting theory: for every external fermion assign an additional factor $\sqrt{Z_2}$.

4.4 QCD field strength renormalisation for massive quarks

In Sec. 8.1 we will need the field strength renormalisation factor Z_2 calculated to first order in the QCD coupling $\alpha_s = \frac{g_0^2}{4\pi}$ and we will calculate this quantity already at this point. Starting from Eq. (4.32) an expansion in α_s yields:

$$Z_2 = \left[1 - \left. \frac{\partial \Sigma(p)}{\partial \not{p}} \right|_{p=m} \right]^{-1}$$

$$= 1 + \left. \frac{\partial \Sigma(p)}{\partial \not{p}} \right|_{p=m} + O(\alpha_s^2). \quad (4.76)$$

Inserting the expression for the quark selfenergy derived in Eq. (4.24) one finds:

$$\left. \frac{\partial \Sigma(p)}{\partial \not{p}} \right|_{p=m} = \frac{\alpha_s}{4\pi} C_F \left[1 - \frac{1}{\epsilon'} + \gamma - \ln(4\pi\mu^2) \right.$$

$$\left. + \int_0^1 dx \left(2x \ln(\Delta)|_{p=m} + 2(x-2)m \left. \frac{\partial \ln(\Delta)}{\partial \not{p}} \right|_{p=m} \right) \right], \quad (4.77)$$

with

$$\Delta = -x(1-x)p^2 + (1-x)m^2 + x\lambda^2 - i\epsilon. \quad (4.78)$$

Using $p^2 = (\not{p})^2$ the integral becomes:

$$\begin{aligned}
 I &= \int_0^1 dx \left(2x \ln(\Delta)|_{\not{p}=m} + 2(x-2)m \frac{\partial \ln(\Delta)}{\partial \not{p}} \Big|_{\not{p}=m} \right) \\
 &= \int_0^1 dx 2x \ln \left((1-x)^2 m^2 + x\lambda^2 - i\epsilon \right) + \int_0^1 dx 4m^2 \frac{x(1-x)(2-x)}{(1-x)^2 m^2 + x\lambda^2 - i\epsilon}. \quad (4.79)
 \end{aligned}$$

We note that:

$$\frac{\partial}{\partial x} \ln \left((1-x)^2 m^2 + x\lambda^2 - i\epsilon \right) = \frac{-2(1-x)m^2}{(1-x)^2 m^2 + x\lambda^2 - i\epsilon} + \frac{\lambda^2}{(1-x)^2 m^2 + x\lambda^2 - i\epsilon}, \quad (4.80)$$

and so we can rewrite the second integral:

$$\begin{aligned}
 I_2 &= \int_0^1 dx 4m^2 \frac{x(1-x)(2-x)}{(1-x)^2 m^2 + x\lambda^2 - i\epsilon} \\
 &= \int_0^1 dx 2x(2-x) \left[-\frac{\partial}{\partial x} \ln \left((1-x)^2 m^2 + x\lambda^2 - i\epsilon \right) + \frac{\lambda^2}{(1-x)^2 m^2 + x\lambda^2 - i\epsilon} \right]. \quad (4.81)
 \end{aligned}$$

Integration by parts yields:

$$\begin{aligned}
 I_2 &= -2 \ln(\lambda^2 - i\epsilon) + \int_0^1 dx 4(1-x) \ln \left((1-x)^2 m^2 + x\lambda^2 - i\epsilon \right) \\
 &\quad + \int_0^1 dx 2 \frac{\lambda^2}{(1-x)^2 m^2 + x\lambda^2 - i\epsilon}. \quad (4.82)
 \end{aligned}$$

Then:

$$\begin{aligned}
 I &= -2 \ln(\lambda^2 - i\epsilon) + \int_0^1 dx 4 \ln \left((1-x)^2 m^2 + x\lambda^2 - i\epsilon \right) \\
 &\quad - \int_0^1 dx 2x \ln \left((1-x)^2 m^2 + x\lambda^2 - i\epsilon \right) + \int_0^1 dx 2 \frac{\lambda^2}{(1-x)^2 m^2 + x\lambda^2 - i\epsilon}. \quad (4.83)
 \end{aligned}$$

Substituting $y = 1 - x$ we find:

$$\begin{aligned}
 I &= -2 \ln(\lambda^2 - i\epsilon) + \int_0^1 dy 2 \ln(y^2 m^2 + (1-y)\lambda^2 - i\epsilon) \\
 &\quad + \int_0^1 dy 2y \ln(y^2 m^2 + (1-y)\lambda^2 - i\epsilon) + \int_0^1 dy 2 \frac{\lambda^2}{y^2 m^2 + (1-y)\lambda^2 - i\epsilon}. \quad (4.84)
 \end{aligned}$$

The fictitious gluon mass λ was introduced to regularise possible infrared divergences in the integrals. However all three remaining integrals are actually convergent for $\lambda = 0$, which we will show in the following. We begin with:

$$I_3 = \int_0^1 dy 2 \ln(y^2 m^2 + (1-y)\lambda^2 - i\epsilon). \quad (4.85)$$

For $\lambda = 0$ the argument of the logarithm is always positive and we can drop the $i\epsilon$ term:

$$\begin{aligned}
 I_3 &= \int_0^1 dy 2 \ln(y^2 m^2) \\
 &= 2 \ln(m^2) + 4 \int_0^1 dy \ln(y) \\
 &= 2 \ln(m^2) - 4. \quad (4.86)
 \end{aligned}$$

For the second integral one finds analogously:

$$\begin{aligned}
 I_4 &= \int_0^1 dy 2y \ln(y^2 m^2 + (1-y)\lambda^2 - i\epsilon) \\
 \xrightarrow{\lambda \rightarrow 0} &= \int_0^1 dy 2y \ln(y^2 m^2) \\
 &= \ln(m^2) + \int_0^1 dy 4y \ln(y) \\
 &= \ln(m^2) - 1. \quad (4.87)
 \end{aligned}$$

The integrand of the third integral vanishes for $\lambda \rightarrow 0$, except for the null set consisting of $y = 0$, where the integrand approaches one. Thus:

$$I_5 = \int_0^1 dy 2 \frac{\lambda^2}{y^2 m^2 + (1-y)\lambda^2 - i\epsilon}$$

$$\lambda \rightarrow 0 = \int_0^1 dy 0 = 0. \quad (4.88)$$

Summing up the results, we find:

$$I = -2 \ln(\lambda^2 - i\epsilon) + 3 \ln(m^2) - 5. \quad (4.89)$$

Since $\lambda^2 > 0$ one can drop the $i\epsilon$ term and so the field strength renormalisation factor to $O(\alpha_s)$ reads:

$$Z_2 = 1 + \left. \frac{\partial \Sigma(p)}{\partial \not{p}} \right|_{\not{p}=m} = 1 + \frac{\alpha_s}{4\pi} C_F \left[-4 - \frac{1}{\epsilon'} + \gamma - \ln\left(\frac{4\pi\mu^2}{m^2}\right) - 2 \ln\left(\frac{\lambda^2}{m^2}\right) \right]. \quad (4.90)$$

Note again the appearance of the fictitious gluon mass λ , which was introduced to regularise the infrared divergences. Any physical observables calculated with the help of Z_2 must be independent of this mass and we will show in Sec. 8.1.3 why this is indeed the case.

5

Infrared divergences and soft radiation

In theories with massless states loop integrals usually suffer from infrared divergences, as was seen in Chapter 3 and 4. However, such divergences can also arise from other processes, namely those involving the radiation of soft (close to vanishing energy) particles. In this chapter we will explore an example for such a process and then calculate the divergent contribution of soft gluon bremsstrahlung for massive quarks. In Sec. 8.1.3 we will then see, that this divergent contribution exactly cancels against the soft loop divergences, which is an explicit proof of the Kinoshita-Poggio-Quinn [KU76, Kin62, PQ76] and Kinoshita-Lee-Nauenberg [Kin62, LN64] theorems for our special case.

5.1 Example of an infrared divergence

To provide a simple example, we consider the process depicted in Fig. 5.1: two scalar particles with momenta p_1 and p_2 and identical mass m scatter into two different scalar particles, one with momentum q and mass M^2 (zigzag line) and one with momentum k and mass λ (dashed line). The exchange particle we assume also as scalar and having mass m . We will now calculate the cross section for this process and then study the massless limits $\lambda \rightarrow 0$ and $m \rightarrow 0$.

Since the scattering can occur through any of the two diagrams, we have to add their amplitudes coherently and, omitting constants, we find:

$$M = M_1 + M_2 = \frac{1}{(p_2 - k)^2 - m^2} + \frac{1}{(p_1 - k)^2 - m^2}, \quad (5.1)$$

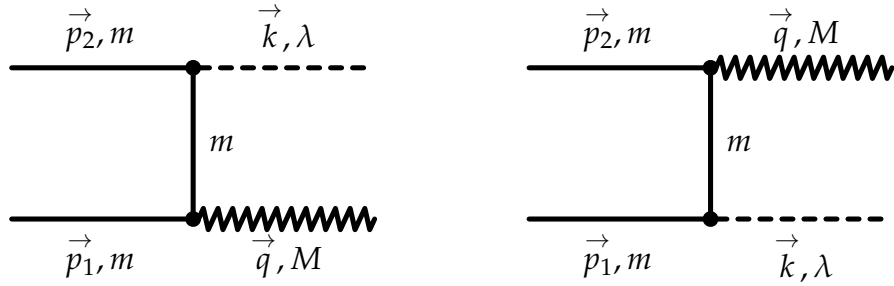


Figure 5.1: Scattering of two scalar particles into two different scalar particles.

and the relevant part of the cross section reads:

$$d\sigma \sim \delta^{(4)}(p_1 + p_2 - q - k) |M|^2 \frac{d^3q}{2E_q} \frac{d^3k}{2E_k}. \quad (5.2)$$

One can now rewrite the q integration into a four momentum integral times a δ -function:

$$\begin{aligned} d\sigma &\sim \delta^{(4)}(p_1 + p_2 - q - k) \delta(q^2 - M^2) |M|^2 d^4q \frac{d^3k}{2E_k} \\ &= \delta\left((p_1 + p_2 - k)^2 - M^2\right) |M|^2 \frac{d^3k}{2E_k}. \end{aligned}$$

In the center-of-mass (c.m.) frame, with the initial particles moving along the z -axis, the four-momenta of the particles become:

$$p_1 = \left(\frac{\sqrt{s}}{2}, 0, 0, \sqrt{\frac{s}{4} - m^2} \right), \quad (5.3)$$

$$p_2 = \left(\frac{\sqrt{s}}{2}, 0, 0, -\sqrt{\frac{s}{4} - m^2} \right), \quad (5.4)$$

$$k = \left(E_k, \vec{k} \right), \quad (5.5)$$

$$q = \left(\sqrt{s} - E_k, -\vec{k} \right), \quad (5.6)$$

with $E_k = \sqrt{|\vec{k}|^2 + \lambda^2}$. Then:

$$\begin{aligned} (p_1 + p_2 - k)^2 - M^2 &= s - M^2 + \lambda^2 - 2\sqrt{s}E_k \stackrel{!}{=} 0 \\ \Rightarrow E_k &= \frac{s - M^2 + \lambda^2}{2\sqrt{s}} \\ \Rightarrow \delta\left((p_1 + p_2 - k)^2 - M^2\right) &= \frac{\delta\left(\frac{s - M^2 + \lambda^2}{2\sqrt{s}} - E_k\right)}{2\sqrt{s}}, \end{aligned} \quad (5.7)$$

and so one can replace the δ -function in the cross section (note that $dE_k = \frac{|\vec{k}|}{E_k} d|\vec{k}|$):

$$d\sigma \sim \frac{\delta\left(\frac{s-M^2+\lambda^2}{2\sqrt{s}} - E_k\right)}{2\sqrt{s}} |M|^2 \frac{|\vec{k}| dE_k d\Omega_k}{2}. \quad (5.8)$$

The propagator denominators in Eq. (5.1) become:

$$(p_1 - k)^2 - m^2 = \lambda^2 - 2p_1 \cdot k = \lambda^2 + \left(-\sqrt{s}E_k + \sqrt{s-4m^2}|\vec{k}| \cos\theta_k\right), \quad (5.9)$$

$$\begin{aligned} (p_2 - k)^2 - m^2 &= \lambda^2 - 2p_2 \cdot k = \lambda^2 + \left(-\sqrt{s}E_k + \sqrt{s-4m^2}|\vec{k}| \cos(\pi - \theta_k)\right) \\ &= \lambda^2 + \left(-\sqrt{s}E_k - \sqrt{s-4m^2}|\vec{k}| \cos\theta_k\right), \end{aligned} \quad (5.10)$$

and, thus, the squared matrix element reads:

$$\begin{aligned} |M|^2 &= \left| \frac{1}{(p_2 - k)^2 - m^2} + \frac{1}{(p_1 - k)^2 - m^2} \right|^2 \\ &= \left| \frac{2\lambda^2 - 2\sqrt{s}E_k}{\lambda^4 + (sE_k^2 - (s-4m^2)|\vec{k}|^2 \cos^2\theta_k) - 2\lambda^2\sqrt{s}E_k} \right|^2 \\ &= \left| \frac{2\lambda^2 - 2\sqrt{s}E_k}{\lambda^4 + s\lambda^2 + s|\vec{k}|^2(1 - \cos^2\theta_k) + 4m^2|\vec{k}|^2 \cos^2\theta_k - 2\lambda^2\sqrt{s}E_k} \right|^2. \end{aligned} \quad (5.11)$$

Inserting Eq. (5.11) into the cross section formula (5.8) and carrying out the E_k integration yields:

$$d\sigma \sim \left| \frac{\lambda^2 - s + M^2}{\lambda^4 + s\lambda^2 + s|\vec{k}|^2(1 - \cos^2\theta_k) + 4m^2|\vec{k}|^2 \cos^2\theta_k - 2\lambda^2\sqrt{s}E_k} \right|^2 \frac{|\vec{k}| d\Omega_k}{4\sqrt{s}}, \quad (5.12)$$

with:

$$|\vec{k}|^2 = E_k^2 - \lambda^2 = \left(\frac{s-M^2+\lambda^2}{2\sqrt{s}}\right)^2 - \lambda^2. \quad (5.13)$$

As long as λ and m are finite this cross section is well defined. However for $\lambda \rightarrow 0$ it shows a *soft* divergence:

$$\begin{aligned} \lim_{\lambda \rightarrow 0} d\sigma &\sim \left| \frac{-s + M^2}{s \left(\frac{s-M^2}{2\sqrt{s}}\right)^2 (1 - \cos^2\theta_k) + 4m^2 \left(\frac{s-M^2}{2\sqrt{s}}\right)^2 \cos^2\theta_k} \right|^2 \frac{s - M^2}{2\sqrt{s}} \frac{d\Omega_k}{4\sqrt{s}} \\ &\sim \left| \frac{4s}{s(1 - \cos^2\theta_k) + 4m^2 \cos^2\theta_k} \right|^2 \frac{d\Omega_k}{8s(s - M^2)}. \end{aligned} \quad (5.14)$$

If we lower the c.m. energy down to $\sqrt{s} \simeq M$, the cross section becomes infinite, which is unphysical. The divergence is called soft, since $|\vec{k}| \sim s - M^2$, and thus close to the threshold, the energy of the particle with momentum k becomes arbitrarily small. However, the cross section even bears another type of divergence, namely a collinear divergence, as one can see by letting in addition $m \rightarrow 0$:

$$\lim_{\lambda, m \rightarrow 0} \sigma \sim \int_{-1}^1 d \cos \theta_k \frac{1}{(1 - \cos^2 \theta_k)^2} \rightarrow \infty, \quad (5.15)$$

which is clearly a divergent quantity. The divergence occurs for $\cos \theta_k = 1$, i.e. for $\theta_k = 0$, which implies that the particle with momentum k is emitted collinearly. Thus, this kind of divergence is called *collinear*. In physical terms this divergence can be understood by acknowledging that collinearly emitted particles continue to interact and cannot be assumed to be asymptotic states. Therefore, in the collinear regime the scattering cannot be described by the two simple diagrams in Fig. 5.1, but one would have to take into account all the interaction processes among the collinear particles.

In this section we have explored two types of infrared divergences, namely soft and collinear ones. As we have seen, soft divergences can be regularised by assigning a finite (fictitious) mass to the emitted particle. This is exactly analogous to regularising infrared divergences occurring in loop calculations, cf. for example Sec. 4.4. As already mentioned, physical observables must not depend on this fictitious mass and we will see that this is indeed the case. Note that the collinear divergences obviously only occur when both the emitted and the exchanged particle are treated as massless. Thus, collinear divergences are absent in any calculation with massive exchange particles.

5.2 Soft gluon bremsstrahlung

In Sec. 8.3 we will calculate the cross section for gluon bremsstrahlung in DY pair production. Since the gluon is massless, this cross section also suffers from a divergence originating in the emission of soft gluons. Therefore, we will introduce in Sec. 8.3 a fictitious gluon mass to regulate this divergence, just as we did for the loop process in Sec. 3.2. To proof that the cancellation of these soft divergences still holds in our scheme, we will calculate the cross section for $q\bar{q} \rightarrow \gamma^*g$ (which is closely related to DY pair production, see Sec. 7.3.2) in the soft gluon limit and isolate the divergent piece. This piece we then can compare to the divergent part of the loop correction in Sec. 8.1.3 and there we will see that they exactly cancel.

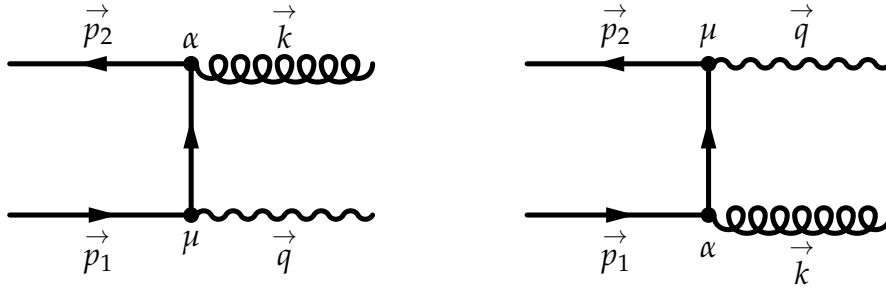


Figure 5.2: Quark-antiquark annihilation into a virtual photon with gluon emission.

5.2.1 Cross section

The relevant processes are depicted in Fig. 5.2. We employ the following conventions for the masses of the particles:

$$p_1^2 = m_1^2, \quad (5.16)$$

$$p_2^2 = m_2^2, \quad (5.17)$$

$$q^2 = M^2, \quad (5.18)$$

$$k^2 = \lambda^2, \quad (5.19)$$

and we keep the mass of the quark fixed at the quark-gluon vertex. Thus, in the left diagram the exchange quark has mass m_2 and in the right diagram mass m_1 . Note, that we break current conservation at the quark-photon vertex, since there the quark mass changes. However, this is of no consequence to the argumentation in this section and in DY pair production this problem is overcome, see Sec. 7.3.3. α and μ represent the Dirac indices at the vertices. Using the Feynman rules of Appendix B one finds for the sum of the amplitudes:

$$\begin{aligned} M &= egt^a \cdot \bar{v}_s(p_2) \left[\gamma^\alpha \frac{-\not{p}_2 + \not{k} + m_2}{(p_2 - k)^2 - m_2^2} \gamma^\mu + \gamma^\mu \frac{\not{p}_1 - \not{k} + m_1}{(p_1 - k)^2 - m_1^2} \gamma^\alpha \right] u_{s'}(p_1) \cdot \epsilon_\mu^*(q) \epsilon_\alpha^*(k) \\ &= egt^a \cdot \bar{v}_s(p_2) S^{\alpha\mu} u_{s'}(p_1) \cdot \epsilon_\mu^*(q) \epsilon_\alpha^*(k), \end{aligned} \quad (5.20)$$

where t^a are the SU(3) color matrices, cf. Appendix A.5. Averaging over initial and summing over final states, one recovers:

$$\begin{aligned} |\overline{M}|^2 &= \frac{1}{4} \sum_{s,s'} \sum_{\text{polaris.}} e^2 g^2 C_F \cdot \bar{v}_s(p_2) S^{\alpha\mu} u_{s'}(p_1) \bar{u}_{s'}(p_1) S^{\nu\beta} v_s(p_2) \cdot \epsilon_\mu^*(q) \epsilon_\alpha^*(k) \epsilon_\nu(q) \epsilon_\beta(k) \\ &= C_F \frac{e^2 g^2}{4} \text{Tr} \left[(\not{p}_2 - m_2) S^{\alpha\mu} (\not{p}_1 + m_1) S^{\nu\beta} \right] \cdot g_{\mu\nu} g_{\alpha\beta}, \end{aligned} \quad (5.21)$$

where the calculation of the color factor C_F is given in Appendix B.2. The cross section for $q\bar{q} \rightarrow \gamma^*g$ then reads:

$$d\sigma = \frac{(2\pi)^4 \delta^{(4)}(p_1 + p_2 - k - q)}{4\sqrt{(p_1 \cdot p_2)^2 - m_1^2 m_2^2}} |\overline{M}|^2 \frac{d^3q}{(2\pi)^3 2E_q} \frac{d^3k}{(2\pi)^3 2E_k}. \quad (5.22)$$

We are performing calculations in the soft gluon limit (cf. introduction of Sec. 5.2) and we define this limit by choosing an energy scale ω , which is much smaller than the energies and momenta of the participating quarks. Then we require for the energy E_k and the momentum \vec{k} of the gluon:

$$E_k \leq \omega, \quad (5.23)$$

$$|\vec{k}| \leq \omega, \quad (5.24)$$

and so we can neglect k in the following places:

$$\delta^{(4)}(p_1 + p_2 - k - q) \rightarrow \delta^{(4)}(p_1 + p_2 - q), \quad (5.25)$$

and

$$\begin{aligned} & (\not{p}_2 - m_2) S^{\alpha\mu} (\not{p}_1 + m_1) \\ &= (\not{p}_2 - m_2) \left[\gamma^\alpha \frac{-\not{p}_2 + \not{k} + m_2}{(p_2 - k)^2 - m_2^2} \gamma^\mu + \gamma^\mu \frac{\not{p}_1 - \not{k} + m_1}{(p_1 - k)^2 - m_1^2} \gamma^\alpha \right] (\not{p}_1 + m_1) \\ &\rightarrow (\not{p}_2 - m_2) \left[\gamma^\alpha \frac{-\not{p}_2 + m_2}{-2p_2 \cdot k} \gamma^\mu + \gamma^\mu \frac{\not{p}_1 + m_1}{-2p_1 \cdot k} \gamma^\alpha \right] (\not{p}_1 + m_1). \end{aligned} \quad (5.26)$$

Now we note that:

$$\begin{aligned} (\not{p}_2 - m_2) \gamma^\alpha (\not{p}_2 - m_2) &= (2p_2^\alpha - \gamma^\alpha (\not{p}_2 + m_2)) (-\not{p}_2 + m_2) \\ &= 2p_2^\alpha (-\not{p}_2 + m_2). \end{aligned} \quad (5.27)$$

An analogous relation holds for $(\not{p}_1 + m_1) \gamma^\alpha (\not{p}_1 + m_1)$. Then:

$$(\not{p}_2 - m_2) S^{\alpha\mu} (\not{p}_1 + m_1) \rightarrow (\not{p}_2 - m_2) \gamma^\mu (\not{p}_1 + m_1) \left[\frac{p_2^\alpha}{p_2 \cdot k} - \frac{p_1^\alpha}{p_1 \cdot k} \right] \quad (5.28)$$

and:

$$(\not{p}_1 + m_1) S^{\nu\beta} (\not{p}_2 - m_2) \rightarrow (\not{p}_1 + m_1) \gamma^\nu (\not{p}_2 - m_2) \left[\frac{p_2^\beta}{p_2 \cdot k} - \frac{p_1^\beta}{p_1 \cdot k} \right]. \quad (5.29)$$

Therefore the squared matrix element becomes:

$$\begin{aligned}
 |\overline{M}|^2 &\rightarrow C_F \frac{e^2 g^2}{4} \text{Tr} [(\not{p}_2 - m_2) \gamma^\mu (\not{p}_1 + m_1) \gamma^\nu] \cdot \left[\frac{p_2^\alpha}{p_2 \cdot k} - \frac{p_1^\alpha}{p_1 \cdot k} \right] \left[\frac{p_2^\beta}{p_2 \cdot k} - \frac{p_1^\beta}{p_1 \cdot k} \right] \cdot g_{\mu\nu} g_{\alpha\beta} \\
 &= C_F \frac{e^2 g^2}{4} \text{Tr} [(\not{p}_2 - m_2) \gamma^\mu (\not{p}_1 + m_1) \gamma^\nu] \cdot \left[\frac{p_2^\alpha}{p_2 \cdot k} - \frac{p_1^\alpha}{p_1 \cdot k} \right]^2 \cdot g_{\mu\nu} , \tag{5.30}
 \end{aligned}$$

where the square of the expression in brackets indicates contraction over the Lorentz index α . Inserting Eqs. (5.25) and (5.30) into the cross section formula (5.22) one finds:

$$\begin{aligned}
 d\sigma &= \frac{(2\pi)^4 \delta^{(4)}(p_1 + p_2 - q)}{4 \sqrt{(p_1 \cdot p_2)^2 - m_1^2 m_2^2}} C_F \frac{e^2 g^2}{4} \text{Tr} [(\not{p}_2 - m_2) \gamma^\mu (\not{p}_1 + m_1) \gamma^\nu] \\
 &\quad \cdot \left[\frac{p_2^\alpha}{p_2 \cdot k} - \frac{p_1^\alpha}{p_1 \cdot k} \right]^2 \cdot g_{\mu\nu} \frac{d^3 q}{(2\pi)^3 2E_q} \frac{d^3 k}{(2\pi)^3 2E_k} \\
 &= \frac{(2\pi)^4 \delta^{(4)}(p_1 + p_2 - q)}{4 \sqrt{(p_1 \cdot p_2)^2 - m_1^2 m_2^2}} \frac{e^2}{4} \text{Tr} [(\not{p}_2 - m_2) \gamma^\mu (\not{p}_1 + m_1) \gamma^\nu] \cdot (-g_{\mu\nu}) \frac{d^3 q}{(2\pi)^3 2E_q} \\
 &\quad \cdot C_F (-g^2) \left[\frac{p_2^\alpha}{p_2 \cdot k} - \frac{p_1^\alpha}{p_1 \cdot k} \right]^2 \frac{d^3 k}{(2\pi)^3 2E_k} . \tag{5.31}
 \end{aligned}$$

We have effectively separated the phase space of the virtual photon and the gluon and so all left to do, is to solve the following integral:

$$\begin{aligned}
 I &= \int_{|\vec{k}| \leq \omega} \frac{d^3 k}{E_k} \left[\frac{p_2^\alpha}{p_2 \cdot k} - \frac{p_1^\alpha}{p_1 \cdot k} \right]^2 \\
 &= \int_{|\vec{k}| \leq \omega} \frac{d^3 k}{E_k} \left[\frac{m_1^2}{(p_1 \cdot k)^2} + \frac{m_2^2}{(p_2 \cdot k)^2} + \frac{m_1^2 + m_2^2 - q^2}{(p_1 \cdot k)(p_2 \cdot k)} \right] , \tag{5.32}
 \end{aligned}$$

where we have used, that in the soft gluon limit $(p_1 + p_2)^2 \rightarrow q^2$.

The first part of Eq. (5.31) is just the Born cross section for the process $q\bar{q} \rightarrow \gamma^*$ and so the cross section for soft gluon emission becomes:

$$d\sigma = d\sigma_{q\bar{q} \rightarrow \gamma^*} \cdot C_F \frac{\alpha_s}{4\pi^2} (-I) . \tag{5.33}$$

5.2.2 Phase space integral for soft gluons

The idea how to solve the integral I in Eq. (5.32) is the following [tHV72]: in the last term shift one of the momenta by a parameter α (cf. Sec. 3.1.3) and then introduce a

Feynman parameter to combine the two factors in the denominator. Then all three integrands will be of the same type and thus all we have to do is to find their solution once:

$$\frac{1}{(p_1 \cdot k)(p_2 \cdot k)} = \frac{\alpha}{(p \cdot k)(q \cdot k)}, \quad (5.34)$$

with $p = \alpha p_1$ and $q = p_2$. We will see in a minute which value to choose for α . First we introduce Feynman parameters to combine the two denominators:

$$\begin{aligned} \frac{1}{(p \cdot k)(q \cdot k)} &= \int_0^1 dx [xp \cdot k + (1-x)q \cdot k]^{-2} \\ &= \int_0^1 dx [(xp + (1-x)q) \cdot k]^{-2} \\ &= \int_0^1 dx [\hat{k} \cdot k]^{-2}. \end{aligned} \quad (5.35)$$

Now all three terms in Eq. (5.32) are of the same form and we have to solve the following integral, where we use $p^2 = (p^0)^2 - |\vec{p}|^2 = m^2$:

$$\begin{aligned} I_2 &= \int_{|\vec{k}| \leq \omega} \frac{d^3k}{E_k} \frac{1}{(p \cdot k)^2} \\ &= \int_0^\omega |\vec{k}|^2 d|\vec{k}| \int_{-1}^1 d \cos \theta \int_0^{2\pi} d\varphi \frac{1}{\sqrt{|\vec{k}|^2 + \lambda^2}} \frac{1}{\left(p^0 \sqrt{|\vec{k}|^2 + \lambda^2} - |\vec{p}| |\vec{k}| \cos \theta \right)^2} \\ &= 2\pi \int_0^\omega |\vec{k}|^2 d|\vec{k}| \int_{-1}^1 dx \frac{1}{\sqrt{|\vec{k}|^2 + \lambda^2}} \frac{1}{\left(p^0 \sqrt{|\vec{k}|^2 + \lambda^2} - |\vec{p}| |\vec{k}| x \right)^2} \\ &= 2\pi \int_0^\omega |\vec{k}|^2 d|\vec{k}| \frac{1}{\sqrt{|\vec{k}|^2 + \lambda^2}} \frac{1}{|\vec{p}| |\vec{k}|} \left[\frac{1}{p^0 \sqrt{|\vec{k}|^2 + \lambda^2} - |\vec{p}| |\vec{k}| x} \right]_{-1}^1 \\ &= 4\pi \int_0^\omega |\vec{k}|^2 d|\vec{k}| \frac{1}{\sqrt{|\vec{k}|^2 + \lambda^2}} \frac{1}{(p^0)^2 (|\vec{k}|^2 + \lambda^2) - |\vec{p}|^2 |\vec{k}|^2} \\ &= 4\pi \int_0^\omega |\vec{k}|^2 d|\vec{k}| \frac{1}{\sqrt{|\vec{k}|^2 + \lambda^2}} \frac{1}{m^2 |\vec{k}|^2 + (p^0)^2 \lambda^2}. \end{aligned} \quad (5.36)$$

Euler substitution of the first kind gives:

$$u = \sqrt{|\vec{k}|^2 + \lambda^2} + |\vec{k}| \Rightarrow |\vec{k}| = \frac{u^2 - \lambda^2}{2u}, \quad (5.37)$$

$$\frac{d|\vec{k}|}{du} = 1 - \frac{u^2 - \lambda^2}{2u^2} = \frac{u^2 + \lambda^2}{2u^2}, \quad (5.38)$$

and so the integral becomes:

$$\begin{aligned} I_2 &= 4\pi \int_{\lambda}^{\sqrt{\omega^2 + \lambda^2} + \omega} du \frac{u^2 + \lambda^2}{2u^2} \frac{\left(\frac{u^2 - \lambda^2}{2u}\right)^2}{\left(u - \frac{u^2 - \lambda^2}{2u}\right) \left(\left(\frac{u^2 - \lambda^2}{2u}\right)^2 m^2 + \lambda^2 (p^0)^2\right)} \\ &= 4\pi \int_{\lambda}^{\sqrt{\omega^2 + \lambda^2} + \omega} du \frac{(u^2 - \lambda^2)^2}{u \left((u^2 - \lambda^2)^2 m^2 + 4u^2 \lambda^2 (p^0)^2\right)}. \end{aligned} \quad (5.39)$$

Partial fraction decomposition yields:

$$I_2 = 4\pi \int_{\lambda}^{\sqrt{\omega^2 + \lambda^2} + \omega} du \frac{1}{um^2} - 4\pi \int_{\lambda}^{\sqrt{\omega^2 + \lambda^2} + \omega} du \frac{4\lambda^2 \frac{(p^0)^2}{m^2} u}{u^4 m^2 + u^2 (2(p^0)^2 - m^2) 2\lambda^2 + \lambda^4 m^2}. \quad (5.40)$$

The integrand of the second integral in the last equation at most diverges like $\frac{1}{u^3}$ near $u = 0$, thus:

$$\begin{aligned} \lim_{\lambda \rightarrow 0} \int_{\lambda}^{\dots} du \frac{\lambda^2}{u^3} &= \lim_{\lambda \rightarrow 0} \left[\frac{-\lambda^2}{2u^2} \right]_{\lambda}^{\dots} \\ &= \left[\dots + \frac{1}{2} \right] \\ &= \text{const.}, \end{aligned} \quad (5.41)$$

and so the second integral is not divergent for $\lambda \rightarrow 0$. Since we are only interested in the divergent piece, we retain only the first integral of Eq. (5.40):

$$\begin{aligned} I_2^{\text{div}} &= 4\pi \int_{\lambda}^{\sqrt{\omega^2 + \lambda^2} + \omega} du \frac{1}{um^2} \\ &= \frac{4\pi}{m^2} \log \left(\frac{\sqrt{\omega^2 + \lambda^2} + \omega}{\lambda} \right) \\ &\xrightarrow{\lambda \ll \omega} \frac{4\pi}{m^2} \log \left(\frac{2\omega}{\lambda} \right). \end{aligned} \quad (5.42)$$

We have finally found the divergent part of the integral in Eq. (5.32):

$$I^{\text{div}} = 8\pi \log\left(\frac{2\omega}{\lambda}\right) + 4\pi(m_1^2 + m_2^2 - q^2) \int_0^1 dx \frac{\alpha}{\hat{k}^2} \log\left(\frac{2\omega}{\lambda}\right). \quad (5.43)$$

Only one integral remains:

$$\int_0^1 dx \frac{\alpha}{\hat{k}^2} = \int_0^1 dx \frac{\alpha}{[x(p-q) + q]^2} = \int_0^1 dx \frac{\alpha}{x^2(p-q)^2 + 2x(p-q)q + q^2}. \quad (5.44)$$

One can make use of the parameter α , so that the coefficient $(p-q)^2$ of x^2 vanishes, which simplifies the x -integration:

$$(p-q)^2 \stackrel{!}{=} 0 \Rightarrow \alpha^2 p_1^2 - 2\alpha p_1 p_2 + p_2^2 \stackrel{!}{=} 0. \quad (5.45)$$

In the soft gluon limit $(p_1 + p_2)^2 = q^2$ and so we find for α :

$$\alpha^2 m_1^2 + \alpha(m_1^2 + m_2^2 - q^2) + m_2^2 \stackrel{!}{=} 0 \quad (5.46)$$

$$\Rightarrow \alpha_{\pm} = -\frac{m_1^2 + m_2^2 - q^2}{2m_1^2} \pm \sqrt{\left(\frac{m_1^2 + m_2^2 - q^2}{2m_1^2}\right)^2 - \frac{m_2^2}{m_1^2}}. \quad (5.47)$$

We are free to choose among the solutions and in the following we will use:

$$\alpha := \alpha_+ = -\frac{m_1^2 + m_2^2 - q^2}{2m_1^2} + \sqrt{\left(\frac{m_1^2 + m_2^2 - q^2}{2m_1^2}\right)^2 - \frac{m_2^2}{m_1^2}}. \quad (5.48)$$

Also note that:

$$2p \cdot q = p^2 + q^2 - (p-q)^2 = p^2 + q^2 \Rightarrow 2(p-q) \cdot q = p^2 - q^2. \quad (5.49)$$

Thus, Eq. (5.44) becomes:

$$\begin{aligned} \int_0^1 dx \frac{\alpha}{\hat{k}^2} &= \int_0^1 dx \frac{\alpha}{2x(p-q)q + q^2} \\ &= \frac{\alpha}{2(p-q) \cdot q} \log\left(\frac{q^2 + 2(p-q)q}{q^2}\right) \\ &= \frac{\alpha}{p^2 - q^2} \log\left(\frac{p^2}{q^2}\right) \\ &= \frac{\alpha}{\alpha^2 m_1^2 - m_2^2} \log\left(\frac{\alpha^2 m_1^2}{m_2^2}\right), \end{aligned} \quad (5.50)$$

and so the divergent part of I finally becomes:

$$\begin{aligned} I^{\text{div}} &= 8\pi \log\left(\frac{2\omega}{\lambda}\right) + 4\pi \frac{\alpha(m_1^2 + m_2^2 - q^2)}{\alpha^2 m_1^2 - m_2^2} \log\left(\frac{\alpha^2 m_1^2}{m_2^2}\right) \log\left(\frac{2\omega}{\lambda}\right) \\ &= 2\pi \log\left(\frac{4\omega^2}{\lambda^2}\right) \left[2 + \frac{\alpha(m_1^2 + m_2^2 - q^2)}{\alpha^2 m_1^2 - m_2^2} \log\left(\frac{\alpha^2 m_1^2}{m_2^2}\right) \right]. \end{aligned} \quad (5.51)$$

Inserting the last equation into Eq. (5.33) finally yields the divergent part of the soft gluon emission cross section:

$$d\sigma^{\text{div}} = d\sigma_{q\bar{q} \rightarrow \gamma^*} \cdot C_F \frac{\alpha_s}{2\pi} \log\left(\frac{4\omega^2}{\lambda^2}\right) \left[-2 - \frac{\alpha(m_1^2 + m_2^2 - q^2)}{\alpha^2 m_1^2 - m_2^2} \log\left(\frac{\alpha^2 m_1^2}{m_2^2}\right) \right]. \quad (5.52)$$

5.3 Aspects of soft bremsstrahlung

As already mentioned above, the soft gluon divergence of the last equation exactly cancels against a similar divergence arising in virtual (loop) processes at the same order of α_s , cf. Sec. 8.1.3. This cancellation is no mathematical coincidence, but a physical necessity, as we will lay out in the following: consider an experiment, set up to measure the total cross section of exclusive bremsstrahlung, like for example $e^+e^- \rightarrow \mu^+\mu^-\gamma$, where a real photon is emitted and detected. Since the photon is massless, the results of the current chapter tell us, that the cross section should actually be infinite (soft divergence). However, measurements always find a finite cross section for such a process. The reason lies in the experimental setup itself: every real detector, for e.g. photons, has a lower sensitivity bound below which it will not detect the photon anymore. In other words, all photons with energy smaller than the energy resolution ω of the detector pass by unnoticed. All these events look like non-bremsstrahlung $e^+e^- \rightarrow \mu^+\mu^-$ processes to the experimenters. Thus, one actually measures not the total bremsstrahlung cross section, but the cross section for bremsstrahlung with photon energy $E_\gamma \geq \omega$. However, in Sec. 5.1 above we found, that the divergent (soft) part of the cross section emerges for $E_\gamma \rightarrow 0$ and so the resolution ω of the detector itself actually regularises the cross section. Thus, any prediction made by theory has to take into account the regularising resolution parameter ω .

The situation is rather different, if one considers the total cross section of an inclusive process, like $e^+e^- \rightarrow \mu^+\mu^-X$, where the particle(s) X is(are) *not* detected. While the measured cross sections are of course still finite, in theory one encounters soft divergences as shown above, for example when X is a real photon. One can regularise these divergences in any scheme of choice, for example by introducing a photon mass. However in contrast to the exclusive measurement, no regularising parameter is provided by the experiment, since the photon is not detected. Therefore,

it becomes immediately clear, that a prediction made in any consistent regularisation scheme cannot depend on a regularising parameter like a (fictitious) photon mass. The theorems by Kinoshita-Poggio-Quinn [Kin62, KU76, PQ76, Ste76] and Kinoshita-Lee-Nauenberg [Kin62, LN64] actually prove, that in perturbation theory in QED and QCD this cancellation of soft divergences in inclusive processes is fulfilled in all orders of the respective coupling constant.

6

Nucleon structure

This chapter is devoted to the details of studying the structure of the nucleon. The standard tool to experimentally access the structure of charged particles is electron scattering and we will first derive the formalism for elastic and inelastic electron-nucleon scattering. Since in inelastic scattering the partonic nature of the nucleon is revealed through Bjorken scaling, we will then study its partonic content and introduce the parton distributions functions (PDFs). Finally we will look into the properties of the PDFs and the origin of Bjorken scaling violations, which lead to the DGLAP equations, that describe the evolution of the PDFs with the hard scale. The ideas of this chapter have been drawn from [PS95, HM84, ESW96, Jaf85], to which we refer for more details.

6.1 Electron scattering

QED is the quantum theory which describes the electromagnetic interaction among charged particles and it is the best understood theory of all quantum theories. One reason for this is that the electromagnetic coupling constant α is rather small in the energy ranges accessible by experiments, which allows the application of perturbation theory. For the same reason the scattering of electrons (or in general charged leptons) is an ideal tool to probe charged objects, since the leptonic part of the interaction is well under control. In this section we will first develop the formalism for electron-muon scattering (i.e. scattering off point-like targets) and then generalise the concept to scattering off protons.

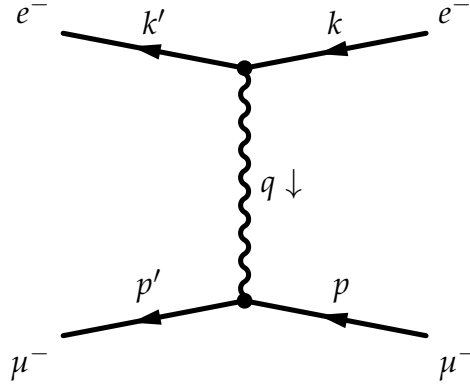


Figure 6.1: $e^- \mu^- \rightarrow e^- \mu^-$ scattering to lowest order in QED.

6.1.1 Elastic scattering on point-like targets

In Fig. 6.1 we show the process under consideration here, namely elastic electron-muon scattering to first order in QED (i.e. one-photon exchange approximation). Using the Feynman rules of Appendix B, one finds for the amplitude of this process:

$$\begin{aligned}
 iM &= \bar{u}_s(k')(-ie\gamma^\mu)u_s(k) \cdot \frac{-ig^{\mu\nu}}{q^2} \cdot \bar{u}_{s'}(p')(-ie\gamma^\nu)u_{s'}(p) \\
 \Rightarrow M &= \frac{e^2}{q^2} \bar{u}_s(k')\gamma^\mu u_s(k) \bar{u}_{s'}(p')\gamma_\mu u_{s'}(p) \\
 &= \frac{e^2}{q^2} j_{e^-}^\mu(k, k') j_{\mu^-}^\mu(p, p'), \tag{6.1}
 \end{aligned}$$

where we have introduced the leptonic currents of the electron $j_{e^-}^\mu$ and the muon $j_{\mu^-}^\mu$. Squaring the amplitude, averaging over initial and summing over final spins we obtain:

$$\begin{aligned}
 |\bar{M}|^2 &= \frac{e^4}{q^4} \cdot \left(\frac{1}{2} \sum_{s,t} \bar{u}_s(k')\gamma^\mu u_t(k) \bar{u}_t(k)\gamma^\nu u_s(k') \right) \cdot \left(\frac{1}{2} \sum_{s',t'} \bar{u}_{s'}(p')\gamma_\mu u_{t'}(p) \bar{u}_{t'}(p)\gamma_\nu u_{s'}(p') \right) \\
 &= \frac{e^4}{q^4} \cdot L_{e^-}^{\mu\nu} \cdot L_{\mu^-}^{\mu\nu}. \tag{6.2}
 \end{aligned}$$

The leptonic tensor $L_{e^-}^{\mu\nu}$ of the electron can be evaluated using the completeness relations of Appendix A.4.3 and the trace relations of Appendix A.4.2:

$$\begin{aligned}
 L_{e^-}^{\mu\nu} &= \frac{1}{2} \sum_{s,t} \bar{u}_s(k') \gamma^\mu u_t(k) \bar{u}_t(k) \gamma^\nu u_s(k') \\
 &= \frac{1}{2} \text{TR} [(k' + m) \gamma^\mu (k + m) \gamma^\nu] \\
 &= 2 \left[k'^\mu k^\nu + k'^\nu k^\mu + g^{\mu\nu} (m^2 - k' \cdot k) \right] \\
 &= 2 \left[k'^\mu k^\nu + k'^\nu k^\mu + g^{\mu\nu} (m^2 - k' \cdot k) \right] , \tag{6.3}
 \end{aligned}$$

where m is the electron mass. Completely analogous one finds for the muon tensor:

$$L_{\mu^-}^{\mu\nu} = 2 \left[p'_\mu p_\nu + p'_\nu p_\mu + g_{\mu\nu} (M^2 - p' \cdot p) \right] , \tag{6.4}$$

with the muon mass M . Note that the electron and the muon current are conserved, i.e. $q_\mu j_{e^-}^\mu = q_\mu j_{\mu^-}^\mu = 0$, where $q = k - k' = p' - p$. Thus, one also finds

$$q_\mu L_{e^-}^{\mu\nu} = q_\nu L_{e^-}^{\mu\nu} = q_\mu L_{\mu^-}^{\mu\nu} = q_\nu L_{\mu^-}^{\mu\nu} = 0 . \tag{6.5}$$

We can now contract both leptonic tensors and obtain:

$$\begin{aligned}
 L_{e^-}^{\mu\nu} \cdot L_{\mu^-}^{\mu\nu} &= 4 \left[2 (p' \cdot k') (p \cdot k) + 2 (p' \cdot k) (p \cdot k') \right. \\
 &\quad \left. - 2 (p' \cdot p) m^2 - 2 (k' \cdot k) M^2 - 4 m^2 M^2 \right] . \tag{6.6}
 \end{aligned}$$

Finally we are ready to calculate the cross section for elastic electron-muon scattering. For $2 \rightarrow 2$ scattering, as in our case, the cross section reads, cf. Appendix A.6:

$$d\sigma = \frac{(2\pi)^4 \delta^{(4)}(p + k - p' - k')}{4 \sqrt{(p \cdot k)^2 - m^2 M^2}} |\bar{M}|^2 \frac{d^3 p'}{(2\pi)^3 2p'_0} \frac{d^3 k'}{(2\pi)^3 2E'} . \tag{6.7}$$

In the laboratory (lab.) frame, where we assume the muon to be at rest, the four-momenta of the particles become:

$$k = (E, \vec{k}) , \tag{6.8}$$

$$k' = (E', \vec{k}') , \tag{6.9}$$

$$q = (v, \vec{q}) = (E - E', \vec{k} - \vec{k}') , \tag{6.10}$$

$$p = (M, \vec{0}) . \tag{6.11}$$

For large beam energies E we can neglect the mass of the electron and thus find $|\vec{k}| = E$ and $|\vec{k}'| = E'$. The cross section in the lab. frame therefore becomes:

$$\begin{aligned} d\sigma_{\text{lab}} &= \frac{e^4}{(2\pi)^2 4EMq^4} L_{e^-}^{\mu\nu} \cdot L_{\mu\nu}^{\mu^-} \delta^{(4)}(p+k-p'-k') \delta\left((p')^2\right) \Theta(p'_0) d^4p' \frac{d^3k'}{2E'} \\ &= \frac{\alpha^2}{EMq^4} L_{e^-}^{\mu\nu} \cdot L_{\mu\nu}^{\mu^-} \delta\left((p+k-k')^2 - M^2\right) \frac{d^3k'}{2E'} , \end{aligned} \quad (6.12)$$

where we have introduced the electromagnetic coupling constant $\alpha = \frac{e^2}{4\pi}$. We define the scattering angle between incoming and outgoing electron as θ , which results in:

$$\begin{aligned} q^2 &= (k-k')^2 = -2k \cdot k' = -2EE' + 2EE' \cos \theta \\ &= -4EE' \sin^2 \frac{\theta}{2} . \end{aligned} \quad (6.13)$$

Note that $p \cdot q$ is not an independent variable:

$$\begin{aligned} M^2 &= (p')^2 = (p+q)^2 = M^2 + 2p \cdot q + q^2 \\ \Rightarrow q^2 &= -2p \cdot q = -2Mv . \end{aligned} \quad (6.14)$$

The last relation is a typical feature of elastic scattering and a similar relation will play an important role in the inelastic case in Sec. 6.1.3. The energy of the outgoing electron is fixed by the δ -function in Eq. (6.12):

$$(p+k-k')^2 - M^2 \stackrel{!}{=} 0 \quad (6.15)$$

$$\Rightarrow 2M(E-E') - 4EE' \sin^2 \frac{\theta}{2} = 0 \quad (6.16)$$

$$\begin{aligned} \Rightarrow E' &= \frac{2ME}{2M + 4E \sin^2 \frac{\theta}{2}} \\ &= \frac{E}{1 + 2\frac{E}{M} \sin^2 \frac{\theta}{2}} . \end{aligned} \quad (6.17)$$

Note that the energy of the scattered particle changes since we are considering elastic scattering in the lab frame. This is due to the recoil of the target with mass M . For very heavy targets (i.e. $M \rightarrow \infty$) initial and final energy of the light scattered particle become equal, cf. Eq. (6.17). In any case in elastic scattering the final energy is fixed by the mass of the target, the initial energy and the scattering angle.

With all these considerations the contraction of the leptonic tensors can be rewritten

in terms of the initial and final energy of the electron and the scattering angle:

$$\begin{aligned}
 L_{e^-}^{\mu\nu} \cdot L_{\mu\nu}^{\mu^-} &= 4 \left[2 (k' \cdot (p + k - k')) (p \cdot k) + 2 (k' \cdot p) (k \cdot (k + p - p')) - 2 (k' \cdot k) M^2 \right] \\
 &= 4 \left[(-q^2 + 2E'M) EM + (q^2 + 2EM) E'M + q^2 M^2 \right] \\
 &= 4 \left[4M^2 EE' - Mq^2 v + q^2 M^2 \right] \\
 &= 16M^2 EE' \left[1 + \frac{v}{M} \sin^2 \frac{\theta}{2} - \sin^2 \frac{\theta}{2} \right] \\
 &= 16M^2 EE' \left[\cos^2 \frac{\theta}{2} - \frac{q^2}{2M^2} \sin^2 \frac{\theta}{2} \right]. \tag{6.18}
 \end{aligned}$$

Inserting the last equation into the cross section formula (6.12) yields:

$$d\sigma_{\text{lab}} = \frac{\alpha^2 8M}{q^4} \left[\cos^2 \frac{\theta}{2} - \frac{q^2}{2M^2} \sin^2 \frac{\theta}{2} \right] \delta \left(2M(E - E') - 4EE' \sin^2 \frac{\theta}{2} \right) (E')^2 dE' d\Omega. \tag{6.19}$$

The δ -function in the last equation can be used to perform the E' integration:

$$\begin{aligned}
 \delta \left(2M(E - E') - 4EE' \sin^2 \frac{\theta}{2} \right) dE' &= \delta \left(E' - \frac{E}{1 + 2\frac{E}{M} \sin^2 \frac{\theta}{2}} \right) \left| 2M + 4E \sin^2 \frac{\theta}{2} \right|^{-1} dE' \\
 &= \delta \left(E' - \frac{E}{1 + 2\frac{E}{M} \sin^2 \frac{\theta}{2}} \right) \frac{E'}{2ME} dE', \tag{6.20}
 \end{aligned}$$

and so finally one finds for the cross section:

$$\begin{aligned}
 \frac{d\sigma_{\text{lab}}}{d\Omega} &= \frac{4\alpha^2 (E')^3}{q^4 E} \left[\cos^2 \frac{\theta}{2} - \frac{q^2}{2M^2} \sin^2 \frac{\theta}{2} \right] \\
 &= \frac{\alpha^2}{4E^2 \sin^4 \frac{\theta}{2}} \frac{E'}{E} \left[\cos^2 \frac{\theta}{2} - \frac{q^2}{2M^2} \sin^2 \frac{\theta}{2} \right]. \tag{6.21}
 \end{aligned}$$

A closer look at Eq. (6.21) reveals the nature of the different contributions. The first term is just the cross section for Rutherford scattering:

$$\left. \frac{d\sigma_{\text{lab}}}{d\Omega} \right|_{\text{Ruth.}} = \frac{\alpha^2}{4E^2 \sin^4 \frac{\theta}{2}}. \tag{6.22}$$

It describes the scattering of a light, spinless and point-like charge on a very massive, spinless and static point-like charge and it shows the characteristic $\sin^{-4} \frac{\theta}{2}$ behavior. The second term takes into account the recoil of the target, as already mentioned above. The expression in brackets has two parts and to find their origin we consider

the case of scattering on a *spinless* muon. What changes is, that the muonic current is now simply given by [HM84]:

$$j_{\mu}^{\mu^{-}} = (p + p')_{\mu} . \quad (6.23)$$

The leptonic tensor of the muon then reads:

$$L_{\mu\nu}^{\mu^{-}} = (p + p')_{\mu}(p + p')_{\nu} , \quad (6.24)$$

and so the contraction of the two leptonic tensors for a *spinless* muon becomes (we again neglect the electron mass):

$$\begin{aligned} L_{e^{-}}^{\mu\nu} \cdot L_{\mu\nu}^{\mu^{-}} &= 2 [k'^{\mu}k^{\nu} + k'^{\nu}k^{\mu} + g^{\mu\nu}(-k' \cdot k)] (p + p')_{\mu}(p + p')_{\nu} \\ &= 2 \left[2(k' \cdot (p + p'))(k \cdot (p + p')) + (p + p')^2(-k \cdot k')^2 \right] \\ &= 2 \left[2(k' \cdot (2p + k - k'))(k \cdot (2p + k - k')) + (2p + k - k')^2(-k \cdot k') \right] \\ &= 2 \left[2 \left(2ME' - \frac{q^2}{2} \right) \left(2ME + \frac{q^2}{2} \right) + (4M^2 + 4M\nu + q^2) \frac{q^2}{2} \right] \\ 2M\nu &= 2M(E - E') = -q^2 \\ &= 2 \left[8M^2EE' + 2M^2q^2 \right] \\ &= 16M^2EE' \left[1 - \sin^2 \frac{\theta}{2} \right] \\ &= 16M^2EE' \cos^2 \frac{\theta}{2} . \end{aligned} \quad (6.25)$$

The resulting cross section is (Mott scattering):

$$\left. \frac{d\sigma_{\text{lab}}}{d\Omega} \right|_{\text{Mott}} = \frac{\alpha^2}{4E^2} \frac{E'}{\sin^4 \frac{\theta}{2}} \cos^2 \frac{\theta}{2} . \quad (6.26)$$

Comparing Eq. (6.26) with Eq. (6.21) we find, that the $\cos^2 \frac{\theta}{2}$ term must be due to the interaction of the electron with the charge of the muon, since in the former equation the muon is treated as spinless. Note that this term vanishes for backward scattering (i.e. $\theta = \pi$), which is a consequence of the helicity conservation of the vector interaction among particles at very high energies [HM84]: clearly an electron scattered at an angle of 180° would have to experience a helicity flip and thus the cross section for this process vanishes. Since the difference between Eqs. (6.26) and (6.21) is the spin of the muon, the remaining term proportional to $\sin^2 \frac{\theta}{2}$ has to originate in the interaction of the electron's spin with the muon's magnetic moment (i.e. its spin).

Obviously the structure of the target is encoded in the angular distribution given by the term in brackets in Eq. (6.21). Thus, by scattering off electrons of targets of interest and measuring the angular distribution of the outgoing electrons, information about the targets internal structure can be obtained. Specifically, any deviation from the form of Eq. (6.21) hints to a non-point-like structure.

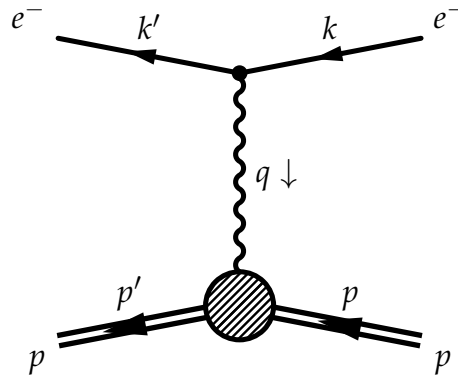


Figure 6.2: $e^- p \rightarrow e^- p$ scattering to lowest order in QED.

6.1.2 Elastic scattering on the nucleon

We are now in a position to investigate elastic electron-proton scattering for which the leading order process is shown in Fig. 6.2. The structure of the amplitude for this process is very similar to the corresponding amplitude of electron-muon scattering, cf. Eq. (6.1). The major difference is that the interaction of the virtual photon with the proton is no longer a pure vector interaction (γ^ν), but, in our ignorance of the proton's structure, we have to assume a more general form:

$$\begin{aligned}
 iM &= \bar{u}_{t'}(k')(-ie\gamma^\mu)u_t(k) \cdot \frac{-ig_{\mu\nu}}{q^2} \cdot \bar{u}_{s'}(p')(-ie\Gamma^\nu)u_s(p) \\
 \Rightarrow M &= \frac{e^2}{q^2} \bar{u}_{t'}(k')\gamma^\mu u_t(k) \bar{u}_{s'}(p')\Gamma_\mu u_s(p) \\
 &= \frac{e^2}{q^2} j^\mu(k, k') J_\mu(p, p') ,
 \end{aligned} \tag{6.27}$$

where we have introduced the hadronic current J_μ . Since Γ_μ transforms like a four-vector, Lorentz invariance demands that the most general form must be constructed out of γ_μ , γ^5 and the incoming and outgoing momenta p_μ and p'_μ . However the electromagnetic interaction conserves parity and so γ^5 cannot be involved. Employing the Dirac equation, cf. Appendix A.4.3, one finds, that the most general ansatz reads:

$$\Gamma_\mu = A\gamma_\mu + B(p' + p)_\mu + C(p' - p)_\mu , \tag{6.28}$$

where we have introduced combinations of the momenta p, p' for convenience and where A, B and C are Lorentz scalars. They depend on the Lorentz invariant quantities $p^2 = M_p^2$, $p'^2 = M_p^2$ and $p \cdot p' = M_p^2 - \frac{1}{2}q^2$. Thus, A, B and C depend only on q^2 . Finally we can exploit the conservation of the hadronic current, which demands

(remember: $q = p' - p$):

$$q^\mu J_\mu(p, p') \stackrel{!}{=} 0 \quad (6.29)$$

$$\Rightarrow \bar{u}_{s'}(p') \left(A \not{q} + B(p^2 - (p')^2) + Cq^2 \right) u_{s'}(p) = 0 \quad (6.30)$$

$$\Rightarrow \bar{u}_{s'}(p') \left(Cq^2 \right) u_{s'}(p) = 0 \quad (6.31)$$

$$\Rightarrow C = 0, \quad (6.32)$$

where we have exploited $p^2 = (p')^2 = M_p^2$ and the Dirac equation:

$$\bar{u}_{s'}(p') \not{p}' = \bar{u}_{s'}(p') M_p \quad (6.33)$$

$$\not{p} u_{s'}(p) = M_p u_{s'}(p). \quad (6.34)$$

Thus, we are left with only two terms:

$$\Gamma_\mu = A\gamma_\mu + B(p' + p)_\mu. \quad (6.35)$$

The $(p' + p)_\mu$ term actually contains a vector and a tensor interaction and it is convention to decouple these two by applying the Gordon identity, which reads for fermions with mass m [HM84]:

$$\bar{u}(p') \gamma_\mu u(p) = \bar{u}(p') \left[\frac{(p' + p)_\mu}{2m} + i \frac{\sigma_{\mu\nu} q^\nu}{2m} \right] u(p), \quad (6.36)$$

with the Dirac sigma symbol $\sigma_{\mu\nu} = \frac{i}{2} [\gamma_\mu, \gamma_\nu]$. Thus, we can replace $(p' + p)_\mu$ in Eq. (6.35):

$$\Gamma_\mu = F_1(q^2) \gamma_\mu + F_2(q^2) i \frac{\sigma_{\mu\nu} q^\nu}{2M_p}. \quad (6.37)$$

The form factors F_1 and F_2 are functions of the Lorentz invariants, which can be constructed out of p and p' or, equivalently, p and q and there are only two independent combinations, namely $p^2 = M_p^2$ and q^2 . For the case of elastic scattering, which we are considering here, $p \cdot q$ is not an independent quantity, cf. Eq. (6.14).

We have finally found the form of the hadronic current:

$$J_\mu(p, p') = \bar{u}_{s'}(p') \left[F_1(q^2) \gamma_\mu + F_2(q^2) i \frac{\sigma_{\mu\nu} q^\nu}{2M_p} \right] u_{s'}(p). \quad (6.38)$$

Therefore, the squared amplitude, averaged over initial and summed over final spin states becomes:

$$\begin{aligned} |\bar{M}|^2 &= \frac{e^4}{q^4} \cdot \left(\frac{1}{2} \sum_{t,t'} \bar{u}_{t'}(k') \gamma^\mu u_t(k) \bar{u}_t(k) \gamma^\nu u_{t'}(k') \right) \cdot \left(\frac{1}{2} \sum_{s,s'} \bar{u}_{s'}(p') \Gamma_\mu u_s(p) \bar{u}_s(p) \Gamma_\nu u_{s'}(p') \right) \\ &= \frac{e^4}{q^4} \cdot L^{\mu\nu} \cdot H_{\mu\nu}. \end{aligned} \quad (6.39)$$

The leptonic tensor $L^{\mu\nu}$ was already calculated in Eq. (6.3). For the hadronic tensor $H_{\mu\nu}$ one finds:

$$\begin{aligned} H_{\mu\nu} &= \frac{1}{2} \sum_{s'} \bar{u}_{s'}(p') \Gamma_\mu u_{s'}(p) \bar{u}_{s'}(p) \Gamma_\nu u_{s'}(p') \\ &= \frac{1}{2} \text{TR} [(\not{p}' + M_p) \Gamma_\mu (\not{p} + M_p) \Gamma_\nu] . \end{aligned} \quad (6.40)$$

Again neglecting the electron mass, the contraction of $L^{\mu\nu}$ and $H_{\mu\nu}$ in the lab. frame takes a form very similar to Eq. (6.18):

$$\begin{aligned} &L^{\mu\nu} \cdot H_{\mu\nu} \\ &= 16M_p^2 EE' \left[\left(F_1^2(q^2) - \frac{q^2}{4M_p^2} F_2^2(q^2) \right) \cos^2 \frac{\theta}{2} - \frac{q^2}{2M_p^2} \left(F_1(q^2) + F_2(q^2) \right)^2 \sin^2 \frac{\theta}{2} \right] . \end{aligned} \quad (6.41)$$

Thus, the cross section for elastic electron-proton scattering becomes, cf. Eq. (6.21):

$$\begin{aligned} \frac{d\sigma_{\text{lab}}}{d\Omega} &= \frac{\alpha^2}{4E^2 \sin^4 \frac{\theta}{2}} \frac{E'}{E} \\ &\times \left[\left(F_1^2(q^2) - \frac{q^2}{4M_p^2} F_2^2(q^2) \right) \cos^2 \frac{\theta}{2} - \frac{q^2}{2M_p^2} \left(F_1(q^2) + F_2(q^2) \right)^2 \sin^2 \frac{\theta}{2} \right] . \end{aligned} \quad (6.42)$$

The last equation is the Rosenbluth formula. For $q^2 \rightarrow 0$ the photon wavelength becomes very large and thus, one expects that the structure of the proton is no longer really resolved and it starts to look like a point-like particle with charge e and magnetic moment μ_p . This implies that the form factors should behave like:

$$F_1(q^2 = 0) = 1 \quad (6.43)$$

$$F_2(q^2 = 0) = \mu_p - 1 . \quad (6.44)$$

Experimentally one finds $\mu_p \approx 2.79$ [Group10]. F_1 and F_2 are also known as Dirac form factors. It is common to introduce combinations of F_1 and F_2 , which are known as electric and magnetic (Sachs) form factors:

$$G_E = F_1 + \frac{q^2}{4M_p^2} F_2 \quad (6.45)$$

$$G_M = F_1 + F_2 . \quad (6.46)$$

Note, that in the limit $|\vec{q}|^2 \ll M_p^2$ these form factors can be interpreted as the Fourier transforms of the electric charge and magnetic moment distribution of the proton

[HM84]. In terms of G_E and G_M the cross section takes the form:

$$\frac{d\sigma_{\text{lab}}}{d\Omega} = \frac{\alpha^2}{4E^2 \sin^4 \frac{\theta}{2}} \frac{E'}{E} \left[\frac{G_E^2 + \tau G_M^2}{1 + \tau} \cos^2 \frac{\theta}{2} - 2\tau G_M^2 \sin^2 \frac{\theta}{2} \right], \quad (6.47)$$

with $\tau = \frac{-q^2}{4M_p^2}$. Thus, by measuring the angular distribution of the scattered electrons at fixed q^2 , information about the proton's electric and magnetic structure can be obtained. Many experiments performed in this way have indicated, that the electric form factor takes a dipole form [HM84]:

$$G_E(q^2) = \left(1 - \frac{q^2}{0.71 \text{ GeV}^2} \right)^{-2}. \quad (6.48)$$

In addition, experiments which rely on the Rosenbluth formula for data analysis, including latest high precision measurements [Q⁺05], have determined a constant ratio for the electric and magnetic form factor for $-q^2 \leq 6 \text{ GeV}^2$:

$$\left. \frac{\mu_p G_E(q^2)}{G_M(q^2)} \right|_{\text{Rosenb.}} \approx 1. \quad (6.49)$$

However, recent experiments, relying on the polarisation transfer technique for measuring this ratio, show a systematic decrease of this ratio with $-q^2$ [P⁺05], which is inconsistent with the measurements employing the Rosenbluth analysis. The resolution of this discrepancy seems to be the (apparently) too simple assumption, that the electron almost exclusively interacts with the proton via one-photon exchange. Theoretical approaches incorporating two-photon exchange contributions appear to be able to describe the discrepancy [BMT05, ABC⁺05, AMT07].

Comparing the result (6.47) with the cross section for elastic scattering on the muon (6.21) one finds, that if the proton were point-like, G_E and G_M would have to be constant. However, Eq. (6.48) shows that this is not the case and so the proton must have some inner structure. A very useful tool to investigate this structure is inelastic electron scattering, which we will present in the next section.

6.1.3 Inelastic scattering on the nucleon

With increasing $Q^2 = -q^2$ the probability for elastic electron-proton scattering decreases significantly, since the elastic form factors behave like dipoles, cf. Eq. (6.48), and the proton will most likely break up into fragments. Such a process, where the initial state proton is destroyed and many fragments form the hadronic final state, is called inelastic scattering and it is depicted in Fig. 6.3. Unlike the case of elastic scattering, it is much more difficult to find the hadronic current, since the final state can be comprised of all kinds of particles and not just a single proton state. However,

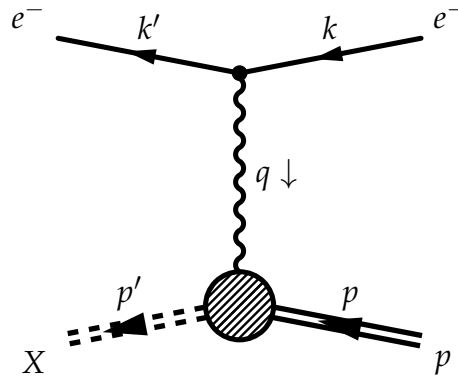


Figure 6.3: $e^- p \rightarrow e^- X$ inelastic scattering to lowest order in QED.

if one is only interested in the inclusive reaction it is possible to access this process on the cross section level. For an n -particle final state the differential cross section reads, cf. Appendix A.6:

$$d\sigma = \frac{(2\pi)^4 \delta^{(4)}(p + k - k' - \sum_{i=1}^n p'_i)}{4\sqrt{(p \cdot k)^2 - m^2 M_p^2}} |\bar{M}|^2 \frac{d^3 k'}{(2\pi)^3 2E'} \prod_{i=1}^n \left(\frac{d^3 p'_i}{(2\pi)^3 2(p'_i)_0} \right). \quad (6.50)$$

As we want to describe an inclusive cross section, we have to take into account all possible final states X_n , which we can achieve by summing over all these states:

$$d\sigma_{ep \rightarrow eX} = \sum_{X_n} \frac{(2\pi)^4 \delta^{(4)}(p + k - k' - \sum_{i=1}^n p'_i)}{4\sqrt{(p \cdot k)^2 - m^2 M_p^2}} |\bar{M}_{X_n}|^2 \frac{d^3 k'}{(2\pi)^3 2E'} \prod_{i=1}^n \left(\frac{d^3 p'_i}{(2\pi)^3 2(p'_i)_0} \right). \quad (6.51)$$

We may not know the exact form of the squared amplitude $|\bar{M}_{X_n}|^2$, but, drawing on the results for elastic scattering, we know that it can be decomposed into a leptonic and a hadronic part:

$$|\bar{M}_{X_n}|^2 = \frac{e^4}{q^4} 4\pi M_p L^{\mu\nu} \cdot X_{\mu\nu}, \quad (6.52)$$

with the leptonic tensor $L^{\mu\nu}$, cf. Eq. (6.3). The factor $4\pi M_p$ is just convention. Inserting this ansatz into the cross section formula (6.51), one finds, that the cross section

completely factorises:

$$\begin{aligned}
 d\sigma_{ep \rightarrow eX} &= \frac{1}{4\sqrt{(p \cdot k)^2 - m^2 M_p^2}} \frac{e^4}{q^4} 4\pi M_p L^{\mu\nu} \frac{d^3 k'}{(2\pi)^3 2E'} \\
 &\quad \times \sum_{X_n} \frac{(2\pi)^4 \delta^{(4)}(p + q - \sum_{i=1}^n p'_i)}{4\pi M_p} X_{\mu\nu} \prod_{i=1}^n \left(\frac{d^3 p'_i}{(2\pi)^3 2(p'_i)_0} \right) \\
 &= \frac{1}{4\sqrt{(p \cdot k)^2 - m^2 M_p^2}} \frac{e^4}{q^4} 4\pi M_p L^{\mu\nu} \frac{d^3 k'}{(2\pi)^3 2E'} \cdot W_{\mu\nu} . \tag{6.53}
 \end{aligned}$$

Once again we have to invoke general principles to constrain the otherwise unknown hadronic part $W_{\mu\nu}$, which depends only on the external momenta p and q : since in the squared and spin averaged/summed amplitude no γ matrices remain, Lorentz invariance demands that $W_{\mu\nu}$ must be constructed out of all possible combinations of the metric tensor $g_{\mu\nu}$, the Levi-Civita tensor $\epsilon^{\alpha\beta\gamma\mu}$ and the momenta p and q . Since parity is conserved by the electromagnetic force, no parity violating terms $\epsilon^{\alpha\beta\gamma\mu} p_\alpha q_\beta$ can appear and we make the following ansatz:

$$W_{\mu\nu} = A g_{\mu\nu} + B p_\mu p_\nu + C q_\mu q_\nu + D(p_\mu q_\nu + q_\mu p_\nu) + E(p_\mu q_\nu - q_\mu p_\nu) . \tag{6.54}$$

Current conservation at the hadronic vertex demands:

$$q^\mu X_{\mu\nu} = q^\nu X_{\mu\nu} = 0 \Rightarrow q^\mu W_{\mu\nu} = q^\nu W_{\mu\nu} = 0 , \tag{6.55}$$

from which follows:

$$E = 0 , \tag{6.56}$$

$$(A + Cq^2 + Dp \cdot q)q_\nu + (Bp \cdot q + Dq^2)p_\nu = 0 , \tag{6.57}$$

which can only be fulfilled for all p_ν and q_ν , if their coefficients vanish:

$$D = -\frac{p \cdot q}{q^2} B \tag{6.58}$$

$$C = -\frac{1}{q^2} A - \frac{p \cdot q}{q^2} D = -\frac{1}{q^2} A + \left(\frac{p \cdot q}{q^2} \right)^2 B . \tag{6.59}$$

Therefore, the hadronic part contains only two unknown functions:

$$\begin{aligned}
 W_{\mu\nu} &= A \left(g_{\mu\nu} - \frac{q_\mu q_\nu}{q^2} \right) + B \left(p_\mu p_\nu + \left(\frac{p \cdot q}{q^2} \right)^2 q_\mu q_\nu - \frac{p \cdot q}{q^2} (p_\mu q_\nu + q_\mu p_\nu) \right) \\
 &= W_1 \left(-g_{\mu\nu} + \frac{q_\mu q_\nu}{q^2} \right) + W_2 \frac{1}{M_p^2} \left(p_\mu - \frac{p \cdot q}{q^2} q_\mu \right) \left(p_\nu - \frac{p \cdot q}{q^2} q_\nu \right) , \tag{6.60}
 \end{aligned}$$

where we have introduced the standard inelastic structure functions W_1 and W_2 . Since they must be Lorentz scalars, they can only be functions of the invariants, which can be constructed out of p and q . For a final hadronic state with invariant mass $(p + q)^2 = W^2$ these invariants are q^2 , $p^2 = M_p^2$ and:

$$p \cdot q = \frac{W^2 - q^2 - M_p^2}{2}. \quad (6.61)$$

Thus, except for the constant p^2 , there are two independent dynamical variables involved. Instead of W^2 , however, it will prove to be useful to introduce Bjorken- x :

$$x = \frac{-q^2}{2p \cdot q} = \frac{Q^2}{2p \cdot q}. \quad (6.62)$$

Note that in the kinematics of electron scattering q^2 is always negative, cf. Eq. (6.13), and one usually introduces the positive variable $Q^2 = -q^2$. In the lab. frame the Bjorken variable takes a simple form:

$$x = \frac{Q^2}{2M_p \nu}, \quad (6.63)$$

with $\nu = E - E'$, as above. Comparing Eqs. (6.14) and (6.63), one finds in the limit of elastic scattering: $x = 1$. Therefore, Bjorken- x can be understood as a measure for the inelasticity of the process. It is important to note at this point, that elastic scattering can be described by only *one* dynamical variable (e.g. Q^2), while inelastic scattering always involves *two* independent variables (e.g. Q^2 and x).

Now that we have found the general form of the hadronic part $W_{\mu\nu}$, we can finally calculate its contraction with the leptonic tensor. For this purpose it is useful to rewrite the leptonic tensor in terms of $q = k - k'$ and $q' = k + k'$:

$$L^{\mu\nu} = q'^{\mu} q'^{\nu} - q^{\mu} q^{\nu} + g^{\mu\nu} q^2. \quad (6.64)$$

The term $q^{\mu} q^{\nu}$ does not contribute due to current conservation and so in the lab. frame the contraction reads (again we treat the electrons as massless):

$$\begin{aligned} L^{\mu\nu} W_{\mu\nu} &= W_1 (-(q')^2 - 3q^2) + W_2 \frac{1}{M_p^2} \left\{ (p \cdot q')^2 + q^2 \left(M_p^2 - \frac{p \cdot q}{q^2} \right) \right\} \\ &= W_1 4k \cdot k' + W_2 \frac{1}{M_p^2} \left\{ [p \cdot (k + k')]^2 - [p \cdot (k - k')]^2 - 2(k \cdot k') M_p^2 \right\} \\ &= W_1 4k \cdot k' + W_2 \frac{1}{M_p^2} \left\{ 4(p \cdot k)(p \cdot k') - 2(k \cdot k') M_p^2 \right\} \\ &= 4EE' \left[2W_1 \sin^2 \frac{\theta}{2} + W_2 \left(1 - \sin^2 \frac{\theta}{2} \right) \right] \\ &= 4EE' \left[W_2 \cos^2 \frac{\theta}{2} + 2W_1 \sin^2 \frac{\theta}{2} \right]. \end{aligned} \quad (6.65)$$

Finally, the cross section (6.53) becomes:

$$\begin{aligned}
\left. \frac{d\sigma_{ep \rightarrow eX}}{d\Omega dE'} \right|_{\text{lab}} &= \frac{1}{4M_p E} \frac{e^4}{(2\pi)^3 q^4} \frac{4\pi M_p E'^2}{2E'} L^{\mu\nu} \cdot W_{\mu\nu} \\
&= \frac{\alpha^2 E'}{q^4 E} L^{\mu\nu} \cdot W_{\mu\nu} \\
&= \frac{\alpha^2}{16E^2 E'^2 \sin^4 \frac{\theta}{2}} \frac{E'}{E} L^{\mu\nu} \cdot W_{\mu\nu} \\
&= \frac{\alpha^2}{4E^2 \sin^4 \frac{\theta}{2}} \left[W_2(x, Q^2) \cos^2 \frac{\theta}{2} + 2W_1(x, Q^2) \sin^2 \frac{\theta}{2} \right], \quad (6.66)
\end{aligned}$$

where we have made the dependence of the structure functions on x and Q^2 explicit. By measuring the angular and the energy distribution of the scattered electrons one can now determine the inelastic structure functions W_1 and W_2 . Note that the structure functions have dimension (energy) $^{-1}$ and it is common to introduce the dimensionless combinations $F_1 = M_p W_1$ and $F_2 = \nu W_2$ instead. In Fig. 6.4 we show

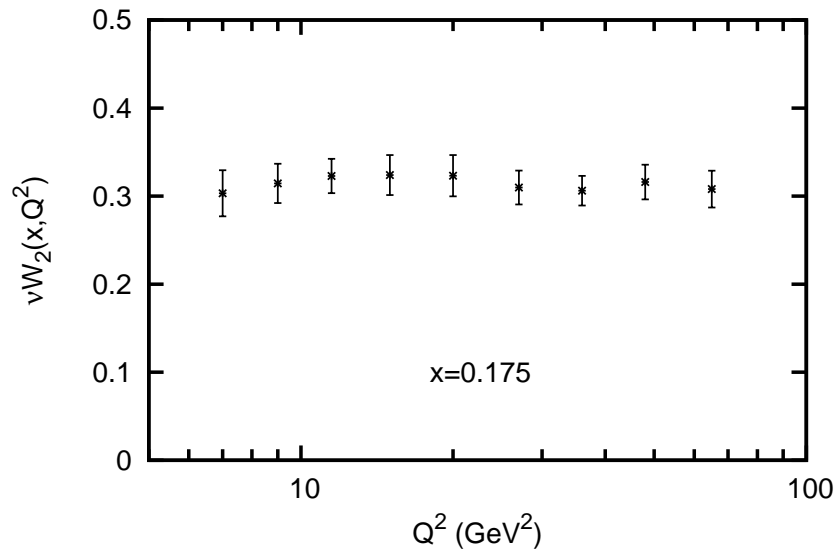


Figure 6.4: Inelastic structure function $F_2 = \nu W_2$ as a function of Q^2 at fixed x measured in $\mu p \rightarrow \mu X$. Data are from the European Muon Collaboration [Collaboration85].

the experimentally obtained F_2 at fixed $x = 0.175$ over a wide range of Q^2 . The measurement was done by the European Muon Collaboration in $\mu p \rightarrow \mu X$ reactions [Collaboration85]. It was an important discovery, that within the error bars the structure function appears to be constant with Q^2 . This behavior (dependence on only one

dimensionless variable, namely x) is called Bjorken scaling and is a hint, that actually an elastic scattering process is taking place. This points to the composite nature of the proton, since this is the kind of behavior one would expect for an interaction with point-like particles inside the proton. In the next section these particles, called partons by Bjorken, will reveal themselves to be the quarks, the interaction among which is governed by QCD.

6.2 The parton model

In the last section we determined that inelastic electron-proton scattering strongly indicates the presence of point-like particles inside the proton. This observation led to the advent of the parton model, which we will introduce in this section. First we will make the connection between the inelastic structure functions and the partons and then derive the parton distribution functions (PDFs) and explore some of their properties. Since Bjorken scaling is actually violated by the interaction among the partons, we will investigate the origin of the scaling violations in more detail. Finally we will introduce the DGLAP evolution equations, which provide means to take into account the scaling violations in the PDFs.

6.2.1 Bjorken scaling

We will now investigate the consequences for the inelastic structure functions $F_1 = M_p W_2$ and $F_2 = \nu W_1$, if we assume the partons to be point-like spin- $\frac{1}{2}$ particles. For this purpose we recall the relevant cross sections. For elastic electron-muon scattering we found:

$$\frac{d\sigma_{e\mu \rightarrow e\mu}}{d\Omega} = \frac{\alpha^2}{4E^2 \sin^4 \frac{\theta}{2}} \frac{E'}{E} \left[\cos^2 \frac{\theta}{2} - \frac{q^2}{2M^2} \sin^2 \frac{\theta}{2} \right], \quad (6.67)$$

and for inelastic electron-proton scattering:

$$\left. \frac{d\sigma_{ep \rightarrow eX}}{d\Omega dE'} \right|_{\text{lab}} = \frac{\alpha^2}{4E^2 \sin^4 \frac{\theta}{2}} \left[W_2(x, Q^2) \cos^2 \frac{\theta}{2} + 2W_1(x, Q^2) \sin^2 \frac{\theta}{2} \right]. \quad (6.68)$$

If the virtual photon actually interacts with only one spin- $\frac{1}{2}$ particle (a quark) inside the proton, the inelastic cross section (6.68) should become the elastic cross section

(6.67), except for the differing charge of the quark. Note that (cf. Eq. (6.20)):

$$\begin{aligned}
 \int dE' \delta\left(\nu - \frac{Q^2}{2m}\right) &= \int dE' \delta\left(E - E' - \frac{2}{m}EE' \sin^2 \frac{\theta}{2}\right) \\
 &= \int dE' \delta\left(E - E'\left(1 + \frac{2}{m}E \sin^2 \frac{\theta}{2}\right)\right) \\
 &= \frac{E'}{E} .
 \end{aligned} \tag{6.69}$$

And so the demand on the structure functions is (the hat indicates the partonic nature of the structure functions):

$$\hat{W}_2 \rightarrow \delta\left(\nu - \frac{Q^2}{2m}\right) , \tag{6.70}$$

$$2\hat{W}_1 \rightarrow \frac{Q^2}{2m^2} \delta\left(\nu - \frac{Q^2}{2m}\right) , \tag{6.71}$$

where m is the mass of the quark. This implies:

$$\nu \hat{W}_2 \rightarrow \delta\left(1 - \frac{Q^2}{2mv}\right) , \tag{6.72}$$

$$2m\hat{W}_1 \rightarrow \frac{Q^2}{2mv} \delta\left(1 - \frac{Q^2}{2mv}\right) , \tag{6.73}$$

and one explicitly sees, that both structure functions only depend on the dimensionless variable $\frac{Q^2}{2mv}$. Nonetheless, Eqs. (6.72) and (6.73) cannot be the final answer, since we cannot tell on which one of the proton's constituents the scattering took place. If we, however, assume that the scattering occurs exclusively on one of the partons, we can obtain the full structure functions (and so the entire cross section) by incoherently summing up the individual partonic scattering cross sections. This assumption is also known as the plane wave impulse approximation, especially in nuclear physics. It relies on the premise, that while the hard scattering process takes place, the partons do not interact among themselves and can thus be treated as quasi-free.

If the partons are quasi-free we can picture the proton as a bunch of partons moving along, each of which is carrying a fraction ζ of the proton's four momentum. Then the relation between the partonic (indicated by a hat) and the proton's four momentum is simply:

$$\hat{p} = \zeta p , \tag{6.74}$$

from which immediately follows:

$$\begin{aligned}
 m^2 &= (\hat{p})^2 = \zeta^2 p^2 = \zeta^2 M_p^2 \\
 \Rightarrow m &= \zeta M_p .
 \end{aligned} \tag{6.75}$$

This implies that the structure functions become:

$$\nu\hat{W}_2 \rightarrow \delta\left(1 - \frac{Q^2}{2\xi M_p \nu}\right) = \delta\left(1 - \frac{x}{\xi}\right), \quad (6.76)$$

$$2m\hat{W}_1 \rightarrow \frac{Q^2}{2\xi M_p \nu} \delta\left(1 - \frac{Q^2}{2\xi M_p \nu}\right) = \frac{x}{\xi} \delta\left(1 - \frac{x}{\xi}\right), \quad (6.77)$$

and so by virtue of the δ -functions the virtual photon can only interact with a parton carrying exactly the right momentum fraction $x = \frac{Q^2}{2M_p \nu}$! For each type of parton i one can now define the probability to find such a parton carrying the momentum fraction ξ by $f_i(\xi)$. These probability distributions are known as parton distributions functions (PDFs) and we will study their general properties in section 6.2.3.

Now we are ready to sum up all the individual partonic contributions. The sum runs over all parton types i and over all possible momentum fractions ξ weighted by the probability to actually find a parton with momentum fraction ξ :

$$\begin{aligned} F_2(x) &:= \nu W_2 = \sum_i \int d\xi e_i^2 f_i(\xi) \nu \hat{W}_2 \\ &= \sum_i \int d\xi e_i^2 f_i(\xi) \delta\left(1 - \frac{x}{\xi}\right) \\ &= \sum_i e_i^2 x f_i(x), \end{aligned} \quad (6.78)$$

$$\begin{aligned} F_1(x) &:= M_p W_1 = \sum_i \int d\xi e_i^2 f_i(\xi) M_p \hat{W}_1 \\ &= \sum_i \int d\xi e_i^2 f_i(\xi) \frac{M_p x}{2m \xi} \delta\left(1 - \frac{x}{\xi}\right) \\ &= \sum_i \int d\xi e_i^2 f_i(\xi) \frac{x}{2\xi^2} \delta\left(1 - \frac{x}{\xi}\right) \\ &= \frac{1}{2} \sum_i e_i^2 f_i(x), \end{aligned} \quad (6.79)$$

where we have taken into account the possible different electric charges $e_i e$ of the different parton types and where we have adopted the standard convention for the structure functions F_1 and F_2 . A very important consequence is the Callan-Gross relation:

$$2xF_1(x) = F_2(x). \quad (6.80)$$

Even in total ignorance of the PDFs this relation provides a prediction testable by experiment and it turns out, that it is well supported by the data. Furthermore it shows that the partons have to carry spin $\frac{1}{2}$, since for spin-0 particles F_1 would vanish, cf. Eq. (6.26).

6.2.2 Formal derivation of the parton model

To justify the ad-hoc introduction of the PDFs in the last subsection, we here will present a more rigorous derivation of the parton model which follows the ideas presented in [Jaf85]. The basic course of things will be the following: one rewrites the hadronic tensor $W_{\mu\nu}$ in terms of hadronic currents. The major assumption then is, that one can replace those with the currents of free quarks. After some current algebra and consequently exploiting the Bjorken limit ($Q^2, \nu \rightarrow \infty, \frac{Q^2}{\nu} = \text{const.}$) one finds that the hadronic tensor is basically given by a sum of quark matrix elements that can be identified with the PDFs.

We start out by rewriting the hadronic tensor of Eq. (6.53) in terms of the hadronic currents:

$$W_{\mu\nu} = \frac{1}{4\pi M_p} \sum_X (2\pi)^4 \delta^{(4)}(p + q - p_X) \langle p | J_\mu(0) | X \rangle \langle X | J_\nu(0) | p \rangle, \quad (6.81)$$

with the proton state $|p\rangle$, where the sum over X runs over all final states and where we have chosen the interaction to take place at $x = 0$ in space-time. The four-dimensional δ -function can also be represented by a Fourier integral and thus:

$$W_{\mu\nu} = \frac{1}{4\pi M_p} \sum_X \int d^4\xi \exp(i(p + q - p_X)\xi) \langle p | J_\mu(0) | X \rangle \langle X | J_\nu(0) | p \rangle. \quad (6.82)$$

We shift the current J_μ to the space-time point ξ with the help of the momentum operator P :

$$\begin{aligned} \langle p | \exp(ip\xi) J_\mu(0) \exp(-ip_x\xi) | X \rangle &= \langle p | \exp(iP\xi) J_\mu(0) \exp(-iP\xi) | X \rangle \\ &= \langle p | J_\mu(\xi) | X \rangle. \end{aligned} \quad (6.83)$$

Since the final states form a complete set, we can exploit the identity $\sum_X |X\rangle\langle X| = 1$ and find:

$$W_{\mu\nu} = \frac{1}{4\pi M_p} \int d^4\xi \exp(iq\xi) \langle p | J_\mu(\xi) J_\nu(0) | p \rangle. \quad (6.84)$$

Note the following relation:

$$\begin{aligned} &\int d^4\xi \exp(iq\xi) \langle p | J_\nu(0) J_\mu(\xi) | p \rangle \\ &= \sum_X \int d^4\xi \exp(iq\xi) \langle p | J_\nu(0) | X \rangle \langle X | J_\mu(\xi) | p \rangle \\ &= \sum_X \int d^4\xi \exp(i(p_x + q - p)\xi) \langle p | J_\nu(0) | X \rangle \langle X | J_\mu(0) | p \rangle \\ &= \sum_X (2\pi)^4 \delta^{(4)}(p_x + q - p) \langle p | J_\nu(0) | X \rangle \langle X | J_\mu(0) | p \rangle. \end{aligned} \quad (6.85)$$

We will work in the proton rest frame, where one finds that the δ -function in the last equation vanishes: in this frame the energy of the virtual photon is positive ($q^0 = \nu > 0$) and the energy of the proton target is just its rest mass ($p^0 = M_p$). Since the electromagnetic interaction conserves the baryon number B , the final state X must also have $B = 1$ like the proton. As the proton is the lightest baryon, the energy of the final state has to be at least equal to the proton's rest mass ($p_X^0 \geq M_p$). Also in deep inelastic scattering one finds $q^2 = \nu^2 - (\vec{q})^2 < 0$ and so there is always a momentum transfer to the target. Then the energy of the final state actually obeys $p_X^0 \geq \sqrt{M_p^2 + (\vec{q})^2} > M_p = p^0$. Thus, the δ -function in Eq. (6.85) requires $q^0 = p^0 - p_X^0 < 0$, which is obviously not fulfilled in the proton rest frame. Therefore, we can simply replace the current product in Eq. (6.84) by a commutator, since the term we have subtracted vanishes:

$$W_{\mu\nu} = \frac{1}{4\pi M_p} \int d^4\xi \exp(iq\xi) \langle p | [J_\mu(\xi), J_\nu(0)] | p \rangle . \quad (6.86)$$

The major assumption of QCD now is, that the virtual photon actually interacts with the quarks and, thus, we can replace hadronic currents by quark currents. In addition in the parton model one assumes the quarks to be quasi-free:

$$J_\mu(\xi) = e_q \bar{\Psi}(\xi) \gamma_\mu \Psi(\xi) , \quad (6.87)$$

$$J_\nu(0) = e_q \bar{\Psi}(0) \gamma_\nu \Psi(0) , \quad (6.88)$$

$$(6.89)$$

where the photon interacts with the fractional quark charge e_q . Using the following commutator and anticommutator relations we can rewrite the current commutator:

$$\begin{aligned} [AB, C] &= A [B, C] - [C, A] B \\ [A, BC] &= \{A, B\} C - B \{A, C\} . \end{aligned} \quad (6.90)$$

The current commutator then becomes (the sum runs over all quark flavors i):

$$\begin{aligned} [J_\mu(\xi), J_\nu(0)] &= \sum_i e_i^2 [\bar{\psi}_i(\xi) \gamma_\mu \psi_i(\xi), \bar{\psi}_i(0) \gamma_\nu \psi_i(0)] \\ &= \sum_i e_i^2 (\bar{\psi}_i(\xi) \gamma_\mu [\psi_i(\xi), \bar{\psi}_i(0) \gamma_\nu \psi_i(0)] \\ &\quad - [\bar{\psi}_i(0) \gamma_\nu \psi_i(0), \bar{\psi}_i(\xi)] \gamma_\mu \psi_i(\xi)) \\ &= \sum_i e_i^2 (\bar{\psi}_i(\xi) \gamma_\mu \{ \psi_i(\xi), \bar{\psi}_i(0) \} \gamma_\nu \psi_i(0) \\ &\quad - \bar{\psi}_i(0) \gamma_\nu \{ \bar{\psi}_i(\xi), \psi_i(0) \} \gamma_\mu \psi_i(\xi)) , \end{aligned} \quad (6.91)$$

where we have exploited, that:

$$\{ \psi_i(\xi), \psi_i(0) \} = \{ \bar{\psi}_i(\xi), \bar{\psi}_i(0) \} = 0 . \quad (6.92)$$

To evaluate the anticommutators in Eq. (6.91) we note, that the quark fields are given by [PS95] (we omit the index i for simplicity):

$$\psi(\xi) = \int \frac{d^3k}{(2\pi)^3 \sqrt{2k^0}} \sum_s \left(a_s(\vec{k}) u_s(\vec{k}) \exp(-ik \cdot \xi) + b_s^\dagger(\vec{k}) v_s(\vec{k}) \exp(ik \cdot \xi) \right), \quad (6.93)$$

$$\bar{\psi}(0) = \int \frac{d^3k'}{(2\pi)^3 \sqrt{2(k')^0}} \sum_{s'} \left(a_{s'}^\dagger(\vec{k}') \bar{u}_{s'}(\vec{k}') + b_{s'}(\vec{k}') \bar{v}_{s'}(\vec{k}') \right), \quad (6.94)$$

and all the annihilation and creation operators anticommute, except:

$$\left\{ a_s(\vec{k}), a_{s'}^\dagger(\vec{k}') \right\} = (2\pi)^3 \delta^{(3)}(\vec{k} - \vec{k}') \delta_{ss'}, \quad (6.95)$$

$$\left\{ b_s(\vec{k}), b_{s'}^\dagger(\vec{k}') \right\} = (2\pi)^3 \delta^{(3)}(\vec{k} - \vec{k}') \delta_{ss'}. \quad (6.96)$$

Then all that remains of the first anticommutator in Eq. (6.91) is:

$$\begin{aligned} \{\psi(\xi), \bar{\psi}(0)\} &= \int \frac{d^3k}{(2\pi)^3 \sqrt{2k^0}} \sum_s \int \frac{d^3k'}{(2\pi)^3 \sqrt{2(k')^0}} \sum_{s'} \\ &\quad \times \left(\left\{ a_s(\vec{k}), a_{s'}^\dagger(\vec{k}') \right\} u_s(\vec{k}) \bar{u}_{s'}(\vec{k}') \exp(-ik \cdot \xi) \right. \\ &\quad \left. + \left\{ b_s(\vec{k}), b_{s'}^\dagger(\vec{k}') \right\} v_s(\vec{k}) \bar{v}_{s'}(\vec{k}') \exp(ik \cdot \xi) \right) \\ &= \int \frac{d^3k}{(2\pi)^3 2k^0} \sum_s \left(u_s(\vec{k}) \bar{u}_s(\vec{k}) \exp(-ik \cdot \xi) + v_s(\vec{k}) \bar{v}_s(\vec{k}) \exp(ik \cdot \xi) \right) \\ &= \int \frac{d^3k}{(2\pi)^3 2k^0} \left((\not{k} + m) \exp(-ik \cdot \xi) + (\not{k} - m) \exp(ik \cdot \xi) \right) \\ &= (i\not{\partial}_\xi + m) \int \frac{d^3k}{(2\pi)^3 2k^0} \left(\exp(-ik \cdot \xi) - \exp(ik \cdot \xi) \right), \end{aligned} \quad (6.97)$$

where we have exploited the completeness relation for the quark spinors, cf. Appendix A.4.3. In the Bjorken limit the quark masses give only corrections to the massless case, and an expansion of the last integral around $m = 0$ yields [BD65, IZ80] (note a sign error in [Jaf85]):

$$\{\psi(\xi), \bar{\psi}(0)\} = \not{\partial}_\xi \left[\frac{1}{2\pi} \epsilon(\xi^0) \delta(\xi^2) \right] + O(m), \quad (6.98)$$

with $\epsilon(x) = \frac{x}{|x|}$. We note that:

$$\{\bar{\psi}(\xi), \psi(0)\} = \{\psi(\xi), \bar{\psi}(0)\}^\dagger = \not{\partial}_\xi \left[\frac{1}{2\pi} \epsilon(\xi^0) \delta(\xi^2) \right], \quad (6.99)$$

and so the current commutator of Eq. (6.91) has become:

$$[J_\mu(\xi), J_\nu(0)] = \sum_i e_i^2 [\bar{\psi}_i(\xi) \gamma_\mu \gamma_\rho \gamma_\nu \psi_i(0) - \bar{\psi}_i(0) \gamma_\nu \gamma_\rho \gamma_\mu \psi_i(\xi)] \partial_\xi^\rho \left[\frac{1}{2\pi} \epsilon(\xi^0) \delta(\xi^2) \right]. \quad (6.100)$$

The product of γ -matrices can be decomposed into a symmetric and an antisymmetric part:

$$\gamma_\mu \gamma_\rho \gamma_\nu = S_{\mu\rho\nu\sigma} \gamma^\sigma - i \epsilon_{\mu\rho\nu\sigma} \gamma^\sigma \gamma^5, \quad (6.101)$$

with the antisymmetric tensor ϵ and

$$S_{\mu\rho\nu\sigma} = g_{\mu\rho} g_{\nu\sigma} + g_{\mu\sigma} g_{\nu\rho} - g_{\mu\nu} g_{\rho\sigma}. \quad (6.102)$$

Since the leptonic tensor $L^{\mu\nu}$ is symmetric, we only have to retain the symmetric part and can replace in the current commutator:

$$\gamma_\mu \gamma_\rho \gamma_\nu \rightarrow S_{\mu\rho\nu\sigma} \gamma^\sigma, \quad (6.103)$$

$$\gamma_\nu \gamma_\rho \gamma_\mu \rightarrow S_{\nu\rho\mu\sigma} \gamma^\sigma = S_{\mu\rho\nu\sigma} \gamma^\sigma. \quad (6.104)$$

Thus, we so far have found for the hadronic tensor in the Bjorken limit:

$$\begin{aligned} \lim_{Q^2 \rightarrow \infty} W_{\mu\nu} &= \frac{S_{\mu\rho\nu\sigma}}{8\pi^2 M_p} \int d^4 \xi \exp(iq \cdot \xi) \\ &\times \sum_i e_i^2 \langle p | \bar{\psi}_i(\xi) \gamma^\sigma \psi_i(0) - \bar{\psi}_i(0) \gamma^\sigma \psi_i(\xi) | p \rangle \partial_\xi^\rho \left[\epsilon(\xi^0) \delta(\xi^2) \right] \end{aligned} \quad (6.105)$$

Before we go on, we shortly investigate the space-time region probed in deep inelastic scattering. We will work here in the proton rest frame and we align the negative z-axis along the momentum of the virtual photon. Then one finds:

$$q = \left(\nu, 0, 0, -\sqrt{\nu^2 + Q^2} \right), \quad (6.106)$$

which obviously fulfills $q^2 = -Q^2$. In the Bjorken limit we have $Q^2 \rightarrow \infty$ but we keep $x = \frac{Q^2}{2M_p \nu}$ fixed. In this limit the four momentum of the virtual photon becomes:

$$\begin{aligned} q &= \left(\nu, 0, 0, -\nu \sqrt{1 + \frac{Q^2}{\nu^2}} \right) \\ &= \left(\nu, 0, 0, -\nu \sqrt{1 + \frac{4M_p^2 x^2}{Q^2}} \right) \\ &\simeq \left(\nu, 0, 0, -\nu \left(1 + \frac{1}{2} \frac{4M_p^2 x^2}{Q^2} \right) \right) \\ &= \left(\nu, 0, 0, -\nu - M_p x \right). \end{aligned} \quad (6.107)$$

In light cone coordinates (cf. Appendix A.2) we find in the Bjorken limit, that only one component of q becomes infinite:

$$q^- = q^0 - q^3 \rightarrow \infty \quad (6.108)$$

$$q^+ = q^0 + q^3 = -M_p x = -\frac{Q^2}{2\nu} . \quad (6.109)$$

The space-time separation ξ of the currents is the conjugate variable of q in the Fourier transform in Eq. (6.86):

$$q \cdot \xi = \frac{1}{2} (q^+ \xi^- + q^- \xi^+) , \quad (6.110)$$

and in the limit $q^- \rightarrow \infty$, the theory of Fourier transforms shows, that the integrand is dominated by the region $\xi^+ \simeq 0$ [Jaf85]. As a consequence of $q^+ = -M_p x$ one also finds, that $|\xi^-| < \frac{2}{M_p x}$ [Jaf85, LS85]. Microcausality requires that the commutator $[J_\mu(\xi), J_\nu(0)]$ of the two observables vanishes for spacelike distances $\xi^2 < 0$. Therefore, contributions to the integral in (6.86) can only come from the region which satisfies $\xi^2 > 0$, since otherwise the space-time points where the two currents act were separated by a space-like distance. Then one obtains the condition:

$$\xi^2 = \xi^+ \xi^- - \vec{\xi}_\perp^2 \geq 0 , \quad (6.111)$$

and so $\xi^+ \simeq 0$ forces $\vec{\xi}_\perp \rightarrow 0$. Obviously only ξ^- stays finite in the Bjorken limit and the time and space distances probed in deep inelastic scattering become:

$$|\xi^0| = \frac{1}{2} |\xi^+ + \xi^-| < \frac{1}{M_p x} , \quad (6.112)$$

$$|\xi^3| = \frac{1}{2} |\xi^+ - \xi^-| < \frac{1}{M_p x} , \quad (6.113)$$

which shows that deep inelastic scattering in the Bjorken limit is a light-cone dominated process ($\xi^2 \rightarrow 0$). A general misconception is, that it probes short distances and time scales, which is evidently only true, if x does not become too small.

Now we come back to Eq. (6.105) and we note that we can get rid of the derivative of the δ -function, if we integrate by parts:

$$\begin{aligned} & \partial_\xi^\rho \left(\exp(iq \cdot \xi) \sum_i e_i^2 \langle p | \bar{\psi}_i(\xi) \gamma^\sigma \psi_i(0) - \bar{\psi}_i(0) \gamma^\sigma \psi_i(\xi) | p \rangle \right) \\ &= iq^\rho \left(\exp(iq \cdot \xi) \sum_i e_i^2 \langle p | \bar{\psi}_i(\xi) \gamma^\sigma \psi_i(0) - \bar{\psi}_i(0) \gamma^\sigma \psi_i(\xi) | p \rangle \right) + O(p^\rho) , \end{aligned} \quad (6.114)$$

where the terms with the proton momentum $O(p^\rho)$ come from the derivative of the matrix element (the quark fields) and can be neglected in the Bjorken limit. Then after partial integration the integral reads:

$$\begin{aligned} \lim_{Q^2 \rightarrow \infty} W_{\mu\nu} &= \lim_{q^- \rightarrow \infty} -\frac{S_{\mu\rho\nu\sigma}}{8\pi^2 M_p} i q^\rho \int d^4 \xi \exp(iq \cdot \xi) \\ &\times \sum_i e_i^2 \langle p | \bar{\psi}_i(\xi) \gamma^\sigma \psi_i(0) - \bar{\psi}_i(0) \gamma^\sigma \psi_i(\xi) | p \rangle \left[\epsilon(\xi^0) \delta(\xi^2) \right], \end{aligned} \quad (6.115)$$

In light-cone coordinates the integral becomes:

$$\begin{aligned} \lim_{Q^2 \rightarrow \infty} W_{\mu\nu} &= \lim_{q^- \rightarrow \infty} -\frac{S_{\mu\rho\nu\sigma}}{8\pi^2 M_p} i q^\rho \int \frac{1}{2} d\xi^+ d\xi^- d\vec{\xi}_\perp \exp\left(\frac{i}{2} q^+ \xi^- + \frac{i}{2} q^- \xi^+\right) \\ &\times \sum_i e_i^2 \langle p | \bar{\psi}_i(\xi) \gamma^\sigma \psi_i(0) - \bar{\psi}_i(0) \gamma^\sigma \psi_i(\xi) | p \rangle \\ &\times \left[\epsilon\left(\frac{1}{2}(\xi^+ + \xi^-)\right) \delta(\xi^+ \xi^- - \xi_\perp^2) \right]. \end{aligned} \quad (6.116)$$

Comparing the coefficient of $(-g_{\mu\nu})$ in Eqs. (6.60) and (6.116), one finds for the structure function $F_1 = M_p W_1$:

$$\begin{aligned} F_1 &= \lim_{q^- \rightarrow \infty} -\frac{g_{\rho\sigma}}{8\pi^2} i q^\rho \int \frac{1}{2} d\xi^+ d\xi^- d\vec{\xi}_\perp \exp\left(\frac{i}{2} q^+ \xi^- + \frac{i}{2} q^- \xi^+\right) \\ &\times \sum_i e_i^2 \langle p | \bar{\psi}_i(\xi) \gamma^\sigma \psi_i(0) - \bar{\psi}_i(0) \gamma^\sigma \psi_i(\xi) | p \rangle \\ &\times \left[\epsilon\left(\frac{1}{2}(\xi^+ + \xi^-)\right) \delta(\xi^+ \xi^- - \xi_\perp^2) \right]. \end{aligned} \quad (6.117)$$

We can use the δ -function to perform the ξ_\perp integration:

$$\int d\vec{\xi}_\perp \delta(\xi^+ \xi^- - \xi_\perp^2) = \int_0^{2\pi} d\phi \int_0^\infty d\xi_\perp \xi_\perp \delta(\xi^+ \xi^- - \xi_\perp^2) = \pi. \quad (6.118)$$

In the Bjorken limit $q^+ \ll q^-$ and thus:

$$\gamma_\sigma q^\sigma = \frac{1}{2} \gamma^+ q^-, \quad (6.119)$$

where the light-cone matrices are $\gamma^\pm = \gamma^0 \pm \gamma^3$. The structure function has become:

$$\begin{aligned} F_1 &= \lim_{q^- \rightarrow \infty} -\frac{1}{8\pi} i q^- \int \frac{1}{2} d\xi^+ d\xi^- \exp\left(\frac{i}{2} q^+ \xi^- + \frac{i}{2} q^- \xi^+\right) \\ &\times \sum_i e_i^2 \langle p | \bar{\psi}_i(\xi) \gamma^+ \psi_i(0) - \bar{\psi}_i(0) \gamma^+ \psi_i(\xi) | p \rangle \\ &\times [\Theta(\xi^+) \Theta(\xi^-) - \Theta(-\xi^+) \Theta(-\xi^-)], \end{aligned} \quad (6.120)$$

where the Θ -functions guarantee that $\xi_{\perp}^2 = \xi^+ \xi^- > 0$. We can perform the ξ^+ integration, if we integrate by parts:

$$\begin{aligned} & \partial_{\xi^+} \left(\exp \left(\frac{i}{2} q^+ \xi^- + \frac{i}{2} q^- \xi^+ \right) \sum_i e_i^2 \langle p | \bar{\psi}_i(\xi) \gamma^+ \psi_i(0) - \bar{\psi}_i(0) \gamma^+ \psi_i(\xi) | p \rangle \right) \\ &= \frac{i}{2} q^- \left(\exp \left(\frac{i}{2} q^+ \xi^- + \frac{i}{2} q^- \xi^+ \right) \sum_i e_i^2 \langle p | \bar{\psi}_i(\xi) \gamma^+ \psi_i(0) - \bar{\psi}_i(0) \gamma^+ \psi_i(\xi) | p \rangle \right) + O(p^-), \end{aligned} \quad (6.121)$$

and so F_1 reads (note a second sign error in [Jaf85]):

$$\begin{aligned} F_1 &= \lim_{q^- \rightarrow \infty} \frac{1}{8\pi} \int d\xi^+ d\xi^- \exp \left(\frac{i}{2} q^+ \xi^- + \frac{i}{2} q^- \xi^+ \right) \\ & \quad \times \sum_i e_i^2 \langle p | \bar{\psi}_i(\xi) \gamma^+ \psi_i(0) - \bar{\psi}_i(0) \gamma^+ \psi_i(\xi) | p \rangle \delta(\xi^+) \\ &= \lim_{q^- \rightarrow \infty} \frac{1}{8\pi} \int d\xi^- \exp \left(\frac{i}{2} q^+ \xi^- \right) \sum_i e_i^2 \langle p | \bar{\psi}_i(\xi) \gamma^+ \psi_i(0) - \bar{\psi}_i(0) \gamma^+ \psi_i(\xi) | p \rangle, \end{aligned} \quad (6.122)$$

with $\xi^+ = \xi_{\perp} = 0$. In the matrix element we find the following combination of γ -matrices:

$$\bar{\psi} \gamma^+ \psi = \psi^\dagger \gamma^0 (\gamma^0 + \gamma^3) \psi = \psi^\dagger (1 + \gamma^0 \gamma^3) \psi, \quad (6.123)$$

which is related to the operators defined by:

$$\begin{aligned} P^\pm &= \frac{1}{4} \gamma^\mp \gamma^\pm \\ &= \frac{1}{4} (\gamma^0 \mp \gamma^3) (\gamma^0 \pm \gamma^3) \\ &= \frac{1}{4} \left(1 \mp \gamma^3 \gamma^0 \pm \gamma^0 \gamma^3 - (\gamma^3)^2 \right) \\ &= \frac{1}{4} (2 \pm 2\gamma^0 \gamma^3) \\ &= \frac{1}{2} (1 \pm \gamma^0 \gamma^3), \end{aligned} \quad (6.124)$$

where we have used the definition of the γ -matrices $\{\gamma^\mu, \gamma^\nu\} = 2g^{\mu\nu}$. The properties

of the operators P^\pm are easily found:

$$P^+ + P^- = 1, \quad (6.125)$$

$$\begin{aligned} (P^\pm)^2 &= \frac{1}{4} \left(1 \pm 2\gamma^0\gamma^3 + \underbrace{\gamma^0\gamma^3\gamma^0\gamma^3}_{-\gamma^3} \right) \\ &= \frac{1}{2} (1 \pm \gamma^0\gamma^3) \\ &= P^\pm, \end{aligned} \quad (6.126)$$

$$\begin{aligned} P^\pm P^\mp &= \frac{1}{4} (1 \pm \gamma^0\gamma^3 \mp \gamma^0\gamma^3 - \gamma^0\gamma^3\gamma^0\gamma^3) \\ &= 0. \end{aligned} \quad (6.127)$$

The properties of P^\pm are exactly those of projection operators and so we can define "+"- and "-"-components of the quark fields as:

$$\psi_\pm = P^\pm \psi. \quad (6.128)$$

Then Eq. (6.123) becomes:

$$\bar{\psi}\gamma^+\psi = 2\psi^\dagger P^+\psi = 2\psi^\dagger (P^+)^2\psi = 2\psi_+^\dagger\psi_+, \quad (6.129)$$

since $(P^+)^\dagger = P^+$. The structure function simplifies to:

$$F_1 = \lim_{q^- \rightarrow \infty} \frac{1}{4\pi} \int d\xi^- \exp\left(\frac{i}{2}q^+\xi^-\right) \sum_i e_i^2 \langle p | \psi_{i+}^\dagger(\xi)\psi_{i+}(0) - \psi_{i+}^\dagger(0)\psi_{i+}(\xi) | p \rangle. \quad (6.130)$$

Before we go on, we note that only connected matrix elements contribute to the hadronic tensor $W_{\mu\nu}$ and, thus, to the structure function F_1 . This implies that we only have to consider the normal ordered product of the quark fields $\bar{\psi}$ and ψ . However, under the normal ordering operator all the annihilation and creation operators in Eqs. (6.93) and (6.94) anticommute and one finds:

$$\begin{aligned} \langle p | \psi_i^\dagger(0)\psi_i(\xi) | p \rangle \Big|_{\text{conn.}} &= \langle p | : \psi_i^\dagger(0)\psi_i(\xi) : | p \rangle \\ &= - \langle p | \psi_i(\xi)\psi_i^\dagger(0) | p \rangle \Big|_{\text{conn.}}. \end{aligned} \quad (6.131)$$

Therefore, we can switch the second term in the matrix element of Eq. (6.130) and recover:

$$F_1 = \lim_{q^- \rightarrow \infty} \frac{1}{4\pi} \int d\xi^- \exp\left(\frac{i}{2}q^+\xi^-\right) \sum_i e_i^2 \langle p | \psi_{i+}^\dagger(\xi)\psi_{i+}(0) + \psi_{i+}(\xi)\psi_{i+}^\dagger(0) | p \rangle. \quad (6.132)$$

One can now take away the ξ dependence from the quark fields, if one inserts a complete set of states $|n\rangle$ (again P is the momentum operator):

$$\begin{aligned}
 & \langle p | \psi_{i+}(\xi) \psi_{i+}(0) + \psi_{i+}(\xi) \psi_{i+}^\dagger(0) | p \rangle \\
 &= \sum_n \left(\langle p | \psi_{i+}^\dagger(\xi) | n \rangle \langle n | \psi_{i+}(0) | p \rangle + \langle p | \psi_{i+}(\xi) | n \rangle \langle n | \psi_{i+}^\dagger(0) | p \rangle \right) \\
 &= \sum_n \left(\langle p | \exp(iP\xi) \psi_{i+}^\dagger(0) \exp(-iP\xi) | n \rangle \langle n | \psi_{i+}(0) | p \rangle \right. \\
 &\quad \left. + \langle p | \exp(iP\xi) \psi_{i+}(0) \exp(-iP\xi) | n \rangle \langle n | \psi_{i+}^\dagger(0) | p \rangle \right) \\
 &= \sum_n \left(\langle p | \exp(ip \cdot \xi) \psi_{i+}^\dagger(0) \exp(-ip_n \cdot \xi) | n \rangle \langle n | \psi_{i+}(0) | p \rangle \right. \\
 &\quad \left. + \langle p | \exp(ip \cdot \xi) \psi_{i+}(0) \exp(-ip_n \cdot \xi) | n \rangle \langle n | \psi_{i+}^\dagger(0) | p \rangle \right) \\
 &= \sum_n \exp\left(\frac{i}{2}(p^+ - p_n^+) \cdot \xi^-\right) \left(|\langle n | \psi_{i+}(0) | p \rangle|^2 + \left| \langle n | \psi_{i+}^\dagger(0) | p \rangle \right|^2 \right), \quad (6.133)
 \end{aligned}$$

where we have used $\xi^+ = \xi_\perp = 0$. The ξ^- -integration is now easy to perform:

$$\begin{aligned}
 \int d\xi^- \exp\left(\frac{i}{2}(q^+ + p^+ - p_n^+)\xi^-\right) &= 2 \cdot 2\pi \cdot \delta(q^+ + p^+ - p_n^+) \\
 &= 4\pi \cdot \delta(p^+ - xp^+ - p_n^+), \quad (6.134)
 \end{aligned}$$

where we exploited, that in the proton rest frame $p^+ = M_p$ and so $q^+ = -M_p x = -xp^+$. Finally the structure function F_1 has become:

$$\begin{aligned}
 F_1 &= \sum_i e_i^2 \sum_n \delta(p^+ - xp^+ - p_n^+) \left(|\langle n | \psi_{i+}(0) | p \rangle|^2 + \left| \langle n | \psi_{i+}^\dagger(0) | p \rangle \right|^2 \right) \\
 &= \sum_i e_i^2 (f_i(x) + f_{\bar{i}}(x)), \quad (6.135)
 \end{aligned}$$

where we finally have found the parton distributions functions:

$$f_i(x) = \sum_n \delta(p^+ - xp^+ - p_n^+) |\langle n | \psi_{i+}(0) | p \rangle|^2, \quad (6.136)$$

$$f_{\bar{i}}(x) = \sum_n \delta(p^+ - xp^+ - p_n^+) \left| \langle n | \psi_{i+}^\dagger(0) | p \rangle \right|^2, \quad (6.137)$$

which are only functions of x . $f_i(x)$ can be understood as the probability to remove from the proton a quark of flavor i with momentum fraction x and leave behind a state with momentum $p_n^+ = (1-x)p^+$ [Jaf85].

At this point it is useful to remember the basic assumptions that entered into this result: first the parton model assumption, namely that the virtual photon interacts

with only one quasi-free quark or antiquark inside the proton and thus the hadronic currents can be replaced by free quark currents. And second the Bjorken limit, the rigorous exploitation of which led to the final form of the structure function F_1 . Thus, Eq. (6.135) finally justifies the ad-hoc introduction of the PDFs in Eqs. (6.78) and (6.79).

6.2.3 General properties of parton distribution functions

In the last section we have derived the PDFs of the proton and in this section we will explore some of their properties. The proton belongs to what is usually defined as matter (as opposed to antimatter) and in the simplest ansatz, it can be pictured as being composed of three constituent quarks (two up-quarks and one down-quark), which exactly make up the quantum numbers of the proton: the up-quarks carry spin $\frac{1}{2}$, isospin z -component $\frac{1}{2}$ and electric charge $\frac{2}{3}e$ and the down-quarks carry spin $\frac{1}{2}$, isospin z -component $-\frac{1}{2}$ and electric charge $-\frac{2}{3}e$ [Group10]. Thus, in the lowest possible state sit two up-quarks with opposite spin and one unpaired down-quark, which exactly form a state with spin $\frac{1}{2}$, isospin z -component $\frac{1}{2}$ and electric charge $+e$, the proton. Beside these *valence* quarks the proton contains antimatter particles, namely the antiquarks given by the distribution in Eq. (6.137). They originate in the interaction of the valence quarks, which is governed by QCD: the gluons exchanged by the valence quarks can decay into quark-antiquark pairs, which are called *sea* quarks. Thus, the virtual photon, which probes the proton in deep inelastic scattering, does not only see the valence quarks, but it can also scatter on a sea quark. Therefore, the up-quark and down-quark distributions inside the proton can be written as:

$$u(x) = u_v(x) + u_s(x) \quad (6.138)$$

$$\bar{u}(x) = \bar{u}_s(x) , \quad (6.139)$$

$$d(x) = d_v(x) + d_s(x) \quad (6.140)$$

$$\bar{d}(x) = \bar{d}_s(x) , \quad (6.141)$$

where the indices v and s stand for valence and sea, respectively. Since the proton does not carry any of the quantum numbers of the heavier quarks (strangeness, charm, ...), these quark flavors can only exist as sea quarks and so e.g. the strange-quark distributions read:

$$s(x) = s_s(x) \quad (6.142)$$

$$\bar{s}(x) = \bar{s}_s(x) . \quad (6.143)$$

Since the charm, top and bottom quark flavors are already much heavier than the proton itself, their distributions are heavily suppressed and we will neglect them from now on.

The quantum numbers of the proton can now be expressed in sum rules, which constrain the different distributions. For charge e , isospin z -component $\frac{1}{2}$ and strangeness

One finds [HM84]:

$$\int_0^1 dx (u(x) - \bar{u}(x)) = 2, \quad (6.144)$$

$$\int_0^1 dx (d(x) - \bar{d}(x)) = 1, \quad (6.145)$$

$$\int_0^1 dx (s(x) - \bar{s}(x)) = 0. \quad (6.146)$$

The total momentum of the proton must be carried by its constituents and therefore the momentum sum rule reads:

$$\int_0^1 dx x (u(x) + \bar{u}(x) + d(x) + \bar{d}(x) + s(x) + \bar{s}(x)) = 1 - x_g, \quad (6.147)$$

where x_g is the momentum fraction carried by the gluons inside the proton:

$$\int_0^1 dx g(x) = x_g. \quad (6.148)$$

The gluon distribution $g(x)$ is not directly accessible in deep inelastic scattering, since the gluons carry no electric charge.

The neutron is the isospin partner of the proton and if one assumes isospin symmetry (which is a reasonable assumption, since, for example, the masses of proton and neutron are almost equal) the quark distributions of the neutron are fixed by the proton distributions:

$$u^p(x) = d^n(x), \quad (6.149)$$

$$d^p(x) = u^n(x), \quad (6.150)$$

$$s^p(x) = s^n(x), \quad (6.151)$$

and analogously for the antiquarks. For the antiproton one finds simply by charge conjugation:

$$u^p(x) = \bar{u}^{\bar{p}}(x), \quad (6.152)$$

$$d^p(x) = \bar{d}^{\bar{p}}(x), \quad (6.153)$$

$$s^p(x) = \bar{s}^{\bar{p}}(x), \quad (6.154)$$

and vice versa for the antiquarks. We will exploit the relations (6.149- 6.154) when we consider DY processes in proton-nucleus (proton-neutron) or antiproton-proton reactions.

Note that the PDFs obviously carry information especially about the soft interactions of the quarks and gluons inside the proton, neutron, Their non-perturbative nature makes them so far inaccessible to calculational approaches. Thus, in practice they are fitted to the available experimental data from e.g. deep inelastic scattering and DY processes, taking into account basic principles as the sum rules shown above. An overview of properties and applications of PDFs can be found e.g. in [ESW96].

6.2.4 Scaling violations and the DGLAP equations

The discovery of Bjorken scaling, i.e. the dependence of the deep inelastic structure functions F_1 and F_2 on only one universal variable x , was an important step towards the parton model of the nucleon. However, there is experimental evidence, that Bjorken scaling is actually weakly broken and the structure functions do also depend on Q^2 . The quantitative explanation of these scaling violations is one of the successes of QCD which incorporates the parton model in its high-energy limit (asymptotic freedom), but goes beyond it for large, but finite Q^2 .

Analysing the data for F_2 over a wide range of Q^2 and for different values of x one finds (in contrast to Bjorken scaling as implied by Fig. 6.4 above) the situation depicted in Fig. 6.5. For very small and for large x there seems to be a logarithmic

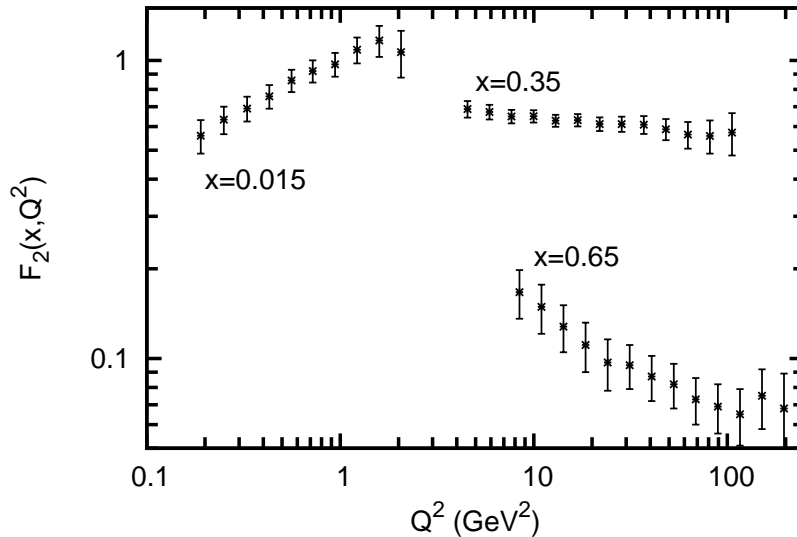


Figure 6.5: Inelastic structure function $F_2 = \nu W_2$ as a function of Q^2 for different x measured in $\nu\text{Fe} \rightarrow \nu X$. Data are from the CDHSW Collaboration [B⁺91].

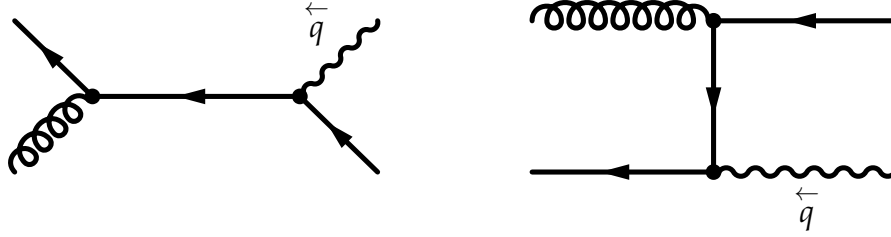


Figure 6.6: Virtual photon-quark interaction with gluon bremsstrahlung.

dependence of F_2 on Q^2 and only in the intermediate x -range Bjorken scaling seems to hold. The origin of these scaling violations can be traced back to two types of sources: bremsstrahlung type diagrams as depicted in Fig. 6.6 and virtual-photon gluon interactions as depicted in Fig. 6.7.

In the case of gluon bremsstrahlung the virtual photon can interact with a quark that has already lost some of its momentum fraction $p_1 = xP$ by the emission of gluon bremsstrahlung and only retains $p_2 = zxP$, where P is the proton momentum and $0 < z < 1$. For massless quarks these processes suffer from the same type of collinear (or mass) singularities as discussed in Chapter 5. One finds that the cross section for the process $\gamma^*q \rightarrow qg$ can be written as [HM84]:

$$\begin{aligned}
 \sigma_{\gamma^*q \rightarrow qg} &= \int_{\eta^2}^{\dots} dp_T^2 \frac{d\sigma_{\gamma^*q \rightarrow qg}}{dp_T^2} \\
 &\simeq \int_{\eta^2}^{\dots} dp_T^2 \frac{1}{p_T^2} \frac{\alpha_s}{2\pi} \hat{P}_{qq}(z) \\
 &\simeq \frac{\alpha_s}{2\pi} \hat{P}_{qq}(z) \log \left(\frac{Q^2}{\eta^2} \right), \quad (6.155)
 \end{aligned}$$

where again $Q^2 = -q^2$ and where a cut-off η^2 was introduced to regularise the otherwise divergent transverse momentum integral. The function $\hat{P}_{qq}(z)$ is called a splitting function and it gives the probability, that a quark, that originally carried a momentum fraction x , after emitting a gluon retains a momentum fraction $z \cdot x$.

In addition to the processes of Fig. 6.6 there exist virtual (loop) corrections to order α_s to the $\gamma^*q \rightarrow q$ process, which also have to be taken into account. Summing up all these contributions one finds that the splitting function P_{qq} to lowest order becomes [ESW96]:

$$P_{qq}(z) = \frac{4}{3} \left[\frac{1+z^2}{(1-z)_+} + \frac{3}{2} \delta(1-z) \right], \quad (6.156)$$

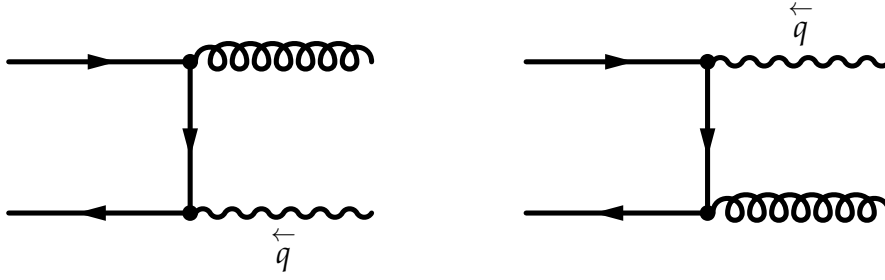


Figure 6.7: Virtual photon-gluon interaction with quark pair-production.

where $\frac{4}{3}$ is a color factor and the $+$ -prescription is given by:

$$\int_0^1 dx \frac{f(x)}{(1-x)_+} = \int_0^1 dx \frac{f(x) - f(1)}{1-x}, \quad (6.157)$$

for a smooth function $f(x)$ on the interval $[0, 1]$. In this picture the structure function F_2 of Eq. (6.78) is modified to [ESW96]:

$$F_2(x, Q^2) = x \sum_i e_i^2 \int_x^1 dy \frac{1}{y} f_i(y) \left[\delta \left(1 - \frac{x}{y} \right) + \frac{\alpha_s}{2\pi} P_{qq} \left(\frac{x}{y} \right) \log \left(\frac{Q^2}{\eta^2} \right) + C_q \left(\frac{x}{y} \right) \right], \quad (6.158)$$

where the second term takes into account the quarks which carry momentum fraction x (as seen by the virtual photon), but actually come from parent quarks that carried momentum fraction $y > x$. C_q is a finite function that takes into account possible non-divergent contributions to F_2 .

The second kind of process that can modify F_2 is gluon pair production. There a gluon carrying momentum fraction xP splits into a quark-antiquark pair and so the virtual photon actually interacts with a quark carrying momentum fraction zxP with $0 < z < 1$. In analogy to the gluon bremsstrahlung case above one finds for the cross section of this process [HM84]:

$$\sigma_{\gamma^* g \rightarrow q\bar{q}} \simeq \frac{\alpha_s}{2\pi} P_{qg}(z) \log \left(\frac{Q^2}{\eta^2} \right), \quad (6.159)$$

where the splitting function $P_{qg}(z)$ gives the probability, that a quark carrying momentum fraction $z \cdot x$ came originally from a gluon carrying momentum fraction x :

$$P_{qg}(z) = \frac{1}{2} \left(z^2 + (1-z)^2 \right), \quad (6.160)$$

where $\frac{1}{2}$ is a color factor. Thus, the structure function F_2 becomes:

$$F_2(x, Q^2) = x \sum_i e_i^2 \int_x^1 dy \frac{1}{y} \left\{ f_i(y) \left[\delta \left(1 - \frac{x}{y} \right) + \frac{\alpha_s}{2\pi} P_{qq} \left(\frac{x}{y} \right) \log \left(\frac{Q^2}{\eta^2} \right) + C_q \left(\frac{x}{y} \right) \right] \right. \\ \left. + g(y) \left[\frac{\alpha_s}{2\pi} P_{qg} \left(\frac{x}{y} \right) \log \left(\frac{Q^2}{\eta^2} \right) + C_g \left(\frac{x}{y} \right) \right] \right\}, \quad (6.161)$$

where g is the bare gluon PDF and C_g takes into account finite contributions from the gluon pair-production processes.

Note that we have found the $\log(Q^2)$ behavior of the structure function that we saw in the deep inelastic scattering data in Fig. 6.5. However, Eq. (6.161) cannot stand as it is, since it depends on the (arbitrary) regulator η^2 . On the other hand it also depends on the *bare* parton distributions $f_i(x)$ and $g(x)$ and since we cannot switch off the strong interaction when measuring e.g. F_2 , $f_i(x)$ and $g(x)$ are not measurable quantities. One can exploit this fact and define a renormalised quark distribution function in the following way [ESW96]:

$$f_i(x, \mu^2) = f_i(x) + \frac{\alpha_s}{2\pi} \int_x^1 dy \frac{1}{y} \left\{ f_i(y) \left[P_{qq} \left(\frac{x}{y} \right) \log \left(\frac{\mu^2}{\eta^2} \right) + \hat{C}_q \left(\frac{x}{y} \right) \right] \right. \\ \left. + g(y) \left[P_{qg} \left(\frac{x}{y} \right) \log \left(\frac{\mu^2}{\eta^2} \right) + \hat{C}_g \left(\frac{x}{y} \right) \right] \right\}, \quad (6.162)$$

where we have introduced the factorisation scale μ^2 . Note that the functions \hat{C}_q and \hat{C}_g do not have to be identical to the finite contributions C_q and C_g above. This arbitrariness in defining finite contributions into the PDFs is called factorisation scheme dependence and in principle one can choose any scheme one prefers. However, once chosen, the same scheme has to be applied in all further calculations involving these scheme dependent PDFs. In terms of the renormalised $f_i(x, \mu^2)$ the structure function is independent of the regulator η^2 , but now depends on the factorisation scale μ^2 :

$$F_2(x, Q^2) = x \sum_i e_i^2 \int_x^1 dy \frac{1}{y} \left\{ f_i(y, \mu^2) \left[\delta \left(1 - \frac{x}{y} \right) + \frac{\alpha_s}{2\pi} P_{qq} \left(\frac{x}{y} \right) \log \left(\frac{Q^2}{\mu^2} \right) \right. \right. \\ \left. \left. + \frac{\alpha_s}{2\pi} C_q^S \left(\frac{x}{y} \right) \right] \right. \\ \left. + g(y, \mu^2) \left[\frac{\alpha_s}{2\pi} P_{qg} \left(\frac{x}{y} \right) \log \left(\frac{Q^2}{\mu^2} \right) + \frac{\alpha_s}{2\pi} C_g^S \left(\frac{x}{y} \right) \right] \right\} \quad (6.163)$$

where the superscript S on the finite contributions indicates the scheme dependence. A particularly simple scheme is the *DIS* scheme, where one defines all finite contributions into the renormalised PDFs. Since the choice of the renormalisation scale μ^2 is arbitrary, one usually takes $\mu^2 = Q^2$ for simplicity and, thus, finds in the DIS scheme:

$$F_2^{\text{DIS}}(x, Q^2) = x \sum_i e_i^2 f_i^{\text{DIS}}(x, Q^2), \quad (6.164)$$

and so we can obtain the renormalised distribution functions $f_i^{\text{DIS}}(x, Q^2)$ by measuring F_2 as a function of x and Q^2 .

Obviously F_2 cannot depend on the arbitrary factorisation scale μ^2 and therefore the derivative of Eq. (6.163) with respect to μ^2 (or better $\log(\mu^2)$) must vanish:

$$\frac{\partial}{\partial \log(\mu^2)} f_i(x, \mu^2) = \frac{\alpha_s}{2\pi} \int_x^1 dy \frac{1}{y} \left[f_i(y, \mu^2) P_{qq} \left(\frac{x}{y} \right) + g(y, \mu^2) P_{qg} \left(\frac{x}{y} \right) \right]. \quad (6.165)$$

The last equation is called the Dokshitzer-Gribov-Lipatov-Altarelli-Parisi (DGLAP) equation [Dok77, GL72, Lip75, AP77] and it describes the evolution of the quark distributions with the factorisation scale μ^2 . Using (6.164) this translates to a prediction for the measurable Q^2 dependence of the structure function. The DGLAP equation is a basic ingredient of all PDF analyses and one of the basic equations of perturbative QCD. In our example the splitting functions were calculated only to order α_s , however in principle one can calculate the evolution to any desired order of the strong coupling. Note that also a similar equation for the evolution of the gluon distributions exist, which, however, will play no further role in this work.

In this subsection we have described the origin of the scaling violations and the DGLAP evolution equations for the PDFs. We will draw on our findings later on in Sec. 8.6, where we describe how to avoid double-counting of the NLO processes we explicitly consider (vertex corrections, gluon bremsstrahlung and gluon Compton scattering).

Part IV
Drell-Yan

7

The Drell-Yan process at leading order

In this chapter we will study the production of DY pairs at leading order (LO, $\alpha_s^0 = 1!$) in the strong coupling. We will start out with the standard parton model description of the DY process and point out its virtues and shortfalls. Afterwards we will introduce our extended model for this process and we will begin by calculating the partonic DY cross section for the general case of massive quarks. Our aim is to extend the parton model approach by parametrising the soft parton interactions through distributions for parton transverse momentum and quark masses. Therefore, we will investigate the kinematics of this process in detail and find, that special care is necessary, as to prevent unphysical kinematical solutions to spoil the result. After having fixed the correct kinematics, we will introduce our distributions for the initial transverse momenta and masses of the participating quarks and finally present the results of our extended LO approach.

Note that certain results of this chapter have been published in [ELM10].

7.1 Introduction - the Drell-Yan process in the parton model

The Drell-Yan process [DY70], depicted in Fig. 7.1, describes the production of lepton pairs with large invariant masses q^2 in collisions of two hadrons (usually nucleons). The idea is, that a quark from hadron 1 and an antiquark from hadron 2 annihilate and produce a virtual photon, that finally decays into a lepton pair. In experiments this pair is then measured in the detector, while the hadron remnants usually remain undetected. In the parton model the cross section for this particular process takes on a very simple form: it is given by the cross section of the partonic subprocess

$q\bar{q} \rightarrow \gamma^* \rightarrow l^+l^-$, which is given by QED, times the probabilities to actually find the two annihilating quarks inside the colliding hadrons. However, these probabilities are basically just the PDFs, that we found in Sec. 6.2 in deep inelastic scattering. So the hadronic cross section for this process reads (the hat denotes partonic quantities) [PS95, HM84]:

$$d\sigma = \sum_i \int_0^1 dx_1 dx_2 q_i^2 f_i(x_1, q^2) f_{\bar{i}}(x_2, q^2) \cdot d\hat{\sigma}(x_1, x_2, q^2), \quad (7.1)$$

where the q_i are the fractions of the quark charges. Since we do not know what kind of quarks formed the virtual photon, we have to sum over all flavors and ant flavors and integrate over all possible momentum fractions x_i of the quarks to obtain the full cross section. It is noteworthy, that, in contrast to deep inelastic scattering, one here probes correlations of valence- and sea-quark PDFs, which provides further input to constrain these distributions. The factorisation of the cross section into a hard part (subprocess) and a soft part (PDFs) is proven for the DY process for quarks moving collinearly with their parent nucleons, at least for leading twist (expansion in $\frac{1}{M}$) in [CSS88].

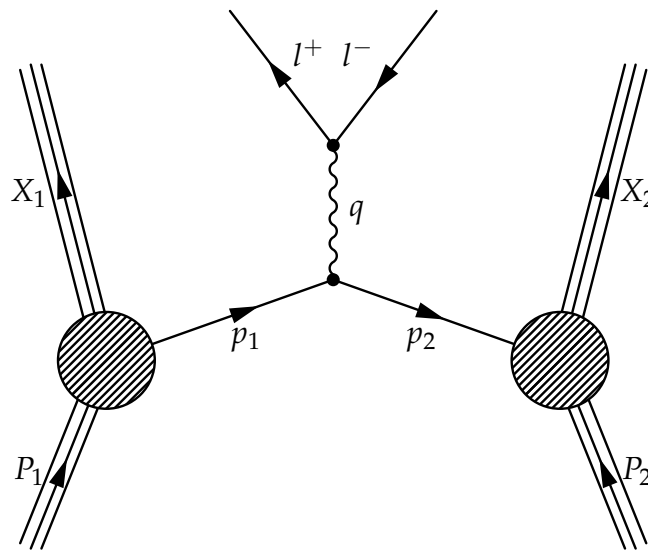


Figure 7.1: DY production in a nucleon-nucleon collision: a quark and an antiquark annihilate into a virtual photon, that eventually decays into a lepton pair; X_1 and X_2 denote the nucleon remnants. See main text for details.

Already at this point, one shortfall of the parton model approach becomes evident: we found in the derivation of Eqs. (6.136) and (6.137), that in the Bjorken limit the

quarks do not carry any transverse momentum (perpendicular to the momentum of the parent nucleon). Thus, in the parton model picture also the virtual photon (and so the DY pair) has vanishing transverse momentum by virtue of four momentum conservation. All DY pairs in the parton model approach are produced with transverse momentum $p_T = 0$, however, experimental evidence shows clearly, that DY pairs have a broad p_T -distribution. These distributions cannot be described in such a simple approach. Furthermore, one finds, that in the parton model one can describe the shape of measured DY pair invariant mass spectra, but that one always underestimates the cross section by a factor K . This K -factor depends on the kinematics (e.g. hadronic center-of-mass energy) of the conducted experiment and it is (in QCD) so far not a calculable quantity. We will illustrate the K -factor problem in Sec. 7.6. These two shortcomings where the main motivation to introduce the extended model which we will present in this work.

7.2 Observables, conventions and notation

In this section we present the relevant DY observables, conventions and notation used throughout the remainder of this work, unless where explicitly stated otherwise. It will turn out to be useful to write four-momenta using light-cone coordinates, cf. Appendix A. Leptons are treated as massless. We will exclusively study reactions involving nucleons and antiprotons, both carrying mass m_N . We define the target nucleon to carry the four momentum P_1 and the beam nucleon to carry the four momentum P_2 (cf. Fig. 7.1). In the hadron center-of-mass (c.m.) frame we choose the z -axis as the beam line and the beam (target) nucleon moves in the positive (negative) direction. Therefore, the nucleon four-momenta read:

$$P_1 = \left(\frac{\sqrt{S}}{2}, 0, 0, -\sqrt{\frac{S}{4} - m_N^2} \right), \quad (7.2)$$

$$P_2 = \left(\frac{\sqrt{S}}{2}, 0, 0, +\sqrt{\frac{S}{4} - m_N^2} \right), \quad (7.3)$$

which implies for the large momentum components of the nucleons:

$$P_1^- = P_2^+ = \frac{\sqrt{S}}{2} + \sqrt{\frac{S}{4} - m_N^2} \xrightarrow{m_N \rightarrow 0} \sqrt{S}, \quad (7.4)$$

with the hadronic c.m. energy \sqrt{S} . Note that in high energy experiments $\sqrt{S} \gg m_N$ and so the nucleon mass is usually neglected. However, we want to study our model also at comparatively low c.m. energies (e.g. $\sqrt{S} \sim 5.5$ GeV at $\bar{\text{P}}\text{ANDA}$ [TLP⁺09]). Therefore, in the present work we include the nucleon mass since its influence should

become significant at these energies. We denote the four momentum of the parton in nucleon 1 (2) as p_1 (p_2). The on-shell condition in light-cone coordinates then reads:

$$m_i^2 = p_i^2 = p_i^+ p_i^- - (\vec{p}_{i\perp})^2. \quad (7.5)$$

The observables accessible in experiment are the invariant mass $q^2 = M^2$ of the DY pair, its transverse momentum (with respect to the beam line) p_T and its momentum along the beam line q_z . However, instead of q_z often the Feynman variable x_F is used. Since there are different definitions of x_F around, we here will first clarify the situation in this work. For the virtual photon in Fig. 7.1 the maximal q_z is derived by requiring the invariant mass of the undetected remnants to vanish and the photon to move collinearly to the nucleons:

$$(P_1 + P_2 - q)^2 = X^2 \stackrel{!}{=} 0 \quad (7.6)$$

$$\Rightarrow S + q^2 - 2\sqrt{S}\sqrt{q^2 + (q_z)_{\max}^2} = 0 \quad (7.7)$$

$$\Rightarrow \frac{S - q^2}{2\sqrt{S}} = (q_z)_{\max}. \quad (7.8)$$

In the literature and in the data presented by many experimental groups the Feynman variable [Group10] is defined as:

$$x_F = \frac{2q_z}{\sqrt{S}} \simeq \frac{q_z}{(q_z)_{\max}} \\ \Rightarrow (q_z)_{\max} \simeq \frac{\sqrt{S}}{2}. \quad (7.9)$$

Note that this approximation for x_F is obviously only good for $q^2 \ll S$. Since we perform studies in the small S region, our definition of the Feynman variable x'_F is :

$$x'_F = \frac{q_z}{(q_z)_{\max}} = q_z \cdot \frac{2\sqrt{S}}{S - q^2}, \quad (7.10)$$

without any approximations. Depending on the experiment which we study we will use x_F or x'_F according to Eq. (7.9) and Eq. (7.10).

7.3 Partonic subprocess cross section at leading order

In this section we will first calculate the partonic cross section for the production of a virtual photon and then show that it is closely related to lepton pair production. The connection between the two cross sections will be helpful later on in the calculation of next-to-leading-order corrections in Chapter 8, since it considerably simplifies the phase space integrals. Although we introduce different masses for the annihilating quarks, we finally will show, that current conservation is not violated when actually considering the production of DY pairs.

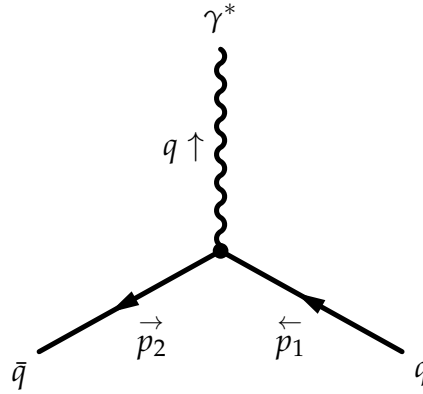


Figure 7.2: Quark-antiquark annihilation into a virtual photon.

7.3.1 Cross section for virtual photon production

Using the Feynman rules of Appendix B one finds for the amplitude of the process $q\bar{q} \rightarrow \gamma^*$ depicted in Fig. 7.2:

$$iM = \bar{v}_{s'}(p_2) (ie\gamma^\mu) u_s(p_1) \cdot \epsilon_\mu^*(q) \quad (7.11)$$

$$\Rightarrow |M|^2 = e^2 \bar{v}_{s'}(p_2) \gamma^\mu u_s(p_1) \bar{u}_s(p_1) \gamma^\nu v_{s'}(p_2) \cdot \epsilon_\mu^*(q) \epsilon_\nu(q) , \quad (7.12)$$

where we have omitted the fractional quark charges, since we will take them into account explicitly in the hadronic cross section later on. Averaging over initial spins and summing over the polarisations of the photon, one obtains:

$$|\bar{M}|^2 = \frac{e^2}{4} (-g_{\mu\nu}) \text{TR} [(\not{p}_2 - m_2) \gamma^\mu (\not{p}_1 + m_1) \gamma^\nu] , \quad (7.13)$$

where we have assigned masses according to $p_1^2 = m_1^2, p_2^2 = m_2^2$ to the quarks. Note, that the replacement $\sum_{\text{pol.}} \epsilon_\mu^*(q) \epsilon_\nu(q) \rightarrow -g_{\mu\nu}$ is actually only valid for real photons. However, in our calculations for DY pair production all we have to know is how to properly replace this factor, as we will see in Sec. 7.3.2. Therefore, we can keep this otherwise improper treatment of the photon polarisation sum without further consequences. The cross section for this process then becomes, cf. Appendix A:

$$\begin{aligned} d\hat{\sigma}_{q\bar{q} \rightarrow \gamma^*} &= \frac{1}{3} \frac{(2\pi)^4 \delta^{(4)}(p_1 + p_2 - q)}{4\sqrt{(p_1 \cdot p_2)^2 - m_1^2 m_2^2}} \frac{e^2}{4} (-g_{\mu\nu}) \text{TR} [(\not{p}_2 - m_2) \gamma^\mu (\not{p}_1 + m_1) \gamma^\nu] \frac{d^3 q}{(2\pi)^3 2E_q} , \\ & \quad (7.14) \end{aligned}$$

where $\frac{1}{3}$ is the color factor, cf. Appendix B.2.

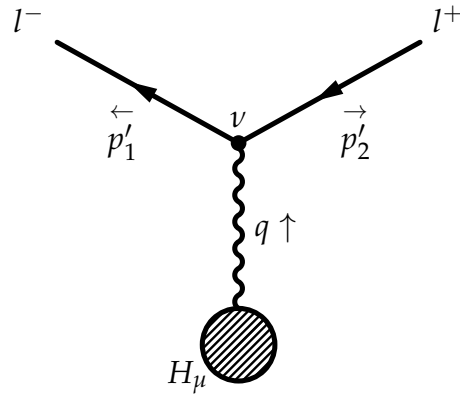


Figure 7.3: Virtual photon decay into a lepton pair.

7.3.2 Connection of virtual photon and DY pair production

Consider the process shown in Fig. 7.3: a virtual photon is emitted in a general type of scattering process and decays into a lepton pair. We denote the unknown part of this amplitude by H_μ and find:

$$iM = H_\mu \frac{-ig^{\mu\nu}}{q^2} \bar{u}_{s'}(p'_1) (-ie\gamma_\nu) v_s(p'_2) \quad (7.15)$$

$$\Rightarrow |M|^2 = H_\mu H_\nu^\dagger \frac{e^2}{q^4} \bar{u}_{s'}(p'_1) \gamma^\mu v_s(p'_2) \bar{v}_s(p'_2) \gamma^\nu u_{s'}(p'_1) . \quad (7.16)$$

Averaging over initial and summing over final spins, the squared amplitude becomes (remember that we treat the leptons as massless):

$$\begin{aligned} |M|^2 &= W_{\mu\nu} \frac{e^2}{q^4} \text{TR} [\not{p}'_1 \gamma^\mu \not{p}'_2 \gamma^\nu] \\ &= W_{\mu\nu} \frac{4e^2}{q^4} [(p'_1)^\mu (p'_2)^\nu + (p'_1)^\nu (p'_2)^\mu - g_{\mu\nu} p'_1 \cdot p'_2] \\ &= W_{\mu\nu} L^{\mu\nu} , \end{aligned} \quad (7.17)$$

where we have collected the spin-averaged unknown part in $W_{\mu\nu}$. The cross section for the entire process then can be factorised in the following way (we omit the phase space integrals of the unknown part $W_{\mu\nu}$, since they are of no consequence to the

following argumentation):

$$\begin{aligned}
 d\sigma &\sim W_{\mu\nu}(p_i, q)\delta^{(4)}\left(\sum_i p_i - p'_1 - p'_2\right) \cdot L^{\mu\nu}(p'_1, p'_2, q) \frac{d^3 p'_1}{(2\pi)^3 2E'_1} \frac{d^3 p'_2}{(2\pi)^3 2E'_2} \\
 &= W_{\mu\nu}(p_i, q)\delta^{(4)}\left(\sum_i p_i - q\right) \frac{d^4 q}{(2\pi)^3} \\
 &\quad \times \underbrace{\delta^{(4)}(q - p'_1 - p'_2) L^{\mu\nu}(p'_1, p'_2, q) \frac{d^3 p'_1}{(2\pi)^3 2E'_1} \frac{d^3 p'_2}{2E'_2}}_{J^{\mu\nu}(q)} \\
 &= W_{\mu\nu}(p_i, q)\delta^{(4)}\left(\sum_i p_i - q\right) \frac{d^4 q}{(2\pi)^3} \delta(q^2 - M^2) dM^2 \cdot J^{\mu\nu}(q), \tag{7.18}
 \end{aligned}$$

where the sum runs over all incoming and outgoing momenta of the unknown part. The function $J^{\mu\nu}$ can also be constructed out of the most general Lorentz form involving the metric tensor and the momentum q :

$$J^{\mu\nu} = f_1 g^{\mu\nu} + f_2 \frac{q^\mu q^\nu}{q^2}. \tag{7.19}$$

The electromagnetic current is conserved at the lepton-photon vertex, since one finds:

$$\begin{aligned}
 q_\mu L^{\mu\nu} &\sim [(p'_1)_\mu + (p'_2)_\mu] [(p'_1)^\mu (p'_2)^\nu + (p'_1)^\nu (p'_2)^\mu - g_{\mu\nu} p'_1 \cdot p'_2] \\
 &= [(p'_1 \cdot p'_2) (p'_2)^\nu + (p'_1 \cdot p'_2) (p'_1)^\nu - ((p'_1)^\nu + (p'_2)^\nu) (p'_1 \cdot p'_2)] \\
 &= 0. \tag{7.20}
 \end{aligned}$$

This implies:

$$q_\mu J^{\mu\nu} = q_\nu J^{\mu\nu} = 0 \tag{7.21}$$

$$\Rightarrow J^{\mu\nu} = f_1 \left(g^{\mu\nu} - \frac{q^\mu q^\nu}{q^2} \right). \tag{7.22}$$

The coefficient function f_1 is now easily found:

$$\begin{aligned}
 g_{\mu\nu}J^{\mu\nu} &= 3f_1 & (7.23) \\
 \Rightarrow f_1 &= \frac{1}{3}g_{\mu\nu}J^{\mu\nu} \\
 &= \frac{1}{3} \int \frac{d^3p'_1}{(2\pi)^3 2E'_1} \frac{d^3p'_2}{2E'_2} \delta^{(4)}(q - p'_1 - p'_2) g_{\mu\nu}L^{\mu\nu} \\
 &= \frac{4e^2}{3(2\pi)^3 q^4} \int \frac{d^3p'_1}{2E'_1} \delta((p'_2)^2) \Theta(E'_2) d^4p'_2 \delta^{(4)}(q - p'_1 - p'_2) [-2p'_1 \cdot p'_2] \\
 &= \frac{e^2}{3 \cdot 4\pi^3 q^4} \int \frac{d^3p'_1}{E'_1} \delta((q - p'_1)^2) \Theta(E_q - E'_1) [-q^2] \\
 &= \frac{-\alpha}{3\pi^2 q^2} \int_0^\infty |\vec{p}'_1| \Theta(E_q - |\vec{p}'_1|) d|\vec{p}'_1| \int d\Omega \delta(q^2 - 2|\vec{p}'_1|(E_q - |\vec{q}|\cos\theta)) \\
 &= \frac{-\alpha}{3\pi^2 q^2} 2\pi \int_{-\pi}^{\pi} \sin\theta d\theta \frac{q^2}{4(E_q - |\vec{q}|\cos\theta)^2} \\
 &= \frac{-2\alpha}{3\pi} \int_{-1}^1 d\cos\theta \frac{1}{4(E_q - |\vec{q}|\cos\theta)^2} \\
 &= \frac{-2\alpha}{3\pi} \frac{1}{|\vec{q}|} \left[\frac{1}{4(E_q - |\vec{q}|\cos\theta)} \right]_{-1}^1 \\
 &= \frac{-2\alpha}{3\pi} \frac{1}{|\vec{q}|} \left[\frac{1}{4(E_q - |\vec{q}|)} - \frac{1}{4(E_q + |\vec{q}|)} \right] \\
 &= \frac{-2\alpha}{3\pi} \frac{1}{2q^2} \\
 &= \frac{-\alpha}{3\pi q^2}, & (7.24)
 \end{aligned}$$

where we have introduced the electromagnetic fine-structure constant $\alpha = \frac{e^2}{4\pi} \simeq \frac{1}{137}$. Inserting Eqs. (7.19) and (7.24) into Eq. (7.18) one recovers:

$$\begin{aligned}
 d\sigma &\sim W_{\mu\nu}(p_i, q) \delta^{(4)} \left(\sum_i p_i - q \right) \frac{d^4q}{(2\pi)^3} \delta(q^2 - M^2) dM^2 \frac{\alpha}{3\pi q^2} \left(-g^{\mu\nu} + \frac{q^\mu q^\nu}{q^2} \right) \\
 &= W_{\mu\nu}(p_i, q) \delta^{(4)} \left(\sum_i p_i - q \right) \frac{d^3q}{(2\pi)^3 2E_q} \cdot \frac{\alpha}{3\pi q^2} \left(-g^{\mu\nu} + \frac{q^\mu q^\nu}{q^2} \right) dq^2, & (7.25)
 \end{aligned}$$

with $E_q^2 = q^2 + (\vec{q})^2$. Thus, the cross section for lepton pair production can always be found by calculating the cross section for virtual photon production and then

replacing:

$$-g^{\mu\nu} \rightarrow \frac{\alpha}{3\pi q^2} \left(-g^{\mu\nu} + \frac{q^\mu q^\nu}{q^2} \right) dq^2. \quad (7.26)$$

After this detour, we can finally calculate the partonic cross section for DY pair production by performing the replacement (7.26) in Eq. (7.14):

$$\begin{aligned} d\hat{\sigma}_{q\bar{q} \rightarrow l+l^-} &= \frac{1}{3} \frac{(2\pi)^4 \delta^{(4)}(p_1 + p_2 - q) e^2}{4\sqrt{(p_1 \cdot p_2)^2 - m_1^2 m_2^2}} \frac{1}{4} \text{TR} [(\not{p}_2 - m_2) \gamma^\mu (\not{p}_1 + m_1) \gamma^\nu] \\ &\cdot \frac{\alpha}{3\pi q^2} \left(-g^{\mu\nu} + \frac{q^\mu q^\nu}{q^2} \right) dq^2 \frac{d^3 q}{(2\pi)^3 2E_q} \\ &= \frac{4\pi\alpha^2}{9q^4} \frac{2q^4 - q^2 (m_1^2 - 6m_1 m_2 + m_2^2) - (m_1^2 - m_2^2)^2}{4\sqrt{(p_1 \cdot p_2)^2 - m_1^2 m_2^2}} \\ &\times \delta^{(4)}(p_1 + p_2 - q) dq^2 \frac{d^3 q}{2E_q}. \end{aligned} \quad (7.27)$$

Note, that if we put in the last equation all quark masses to zero and integrate over the phase space, we recover the textbook cross section [PS95], as it should be:

$$\begin{aligned} \hat{\sigma}_{q\bar{q} \rightarrow l+l^-} \Big|_{m_1=m_2=0} &= \int \frac{4\pi\alpha^2}{9q^4} \frac{2q^4}{4q^2} \delta^{(4)}(p_1 + p_2 - q) dq^2 \delta(q^2 - M^2) d^4 q \\ &= \frac{4\pi\alpha^2}{9M^2}. \end{aligned} \quad (7.28)$$

7.3.3 Current conservation

By assigning different masses m_1 and m_2 to the annihilating quark and antiquark in Fig. 7.2, current conservation is violated at the quark-photon vertex. One can easily see this by contracting the quark current with the photon momentum q_μ :

$$\begin{aligned} &\bar{v}(p_2, m_2) \gamma^\mu u(p_1, m_1) \cdot q_\mu \\ &= \bar{v}(p_2, m_2) \not{q} u(p_1, m_1) \\ &= \bar{v}(p_2, m_2) (\not{p}_1 + \not{p}_2) u(p_1, m_1) \\ &= \bar{v}(p_2, m_2) (m_1 - m_2) u(p_1, m_1) \neq 0. \end{aligned} \quad (7.29)$$

However, for DY pair production as depicted in Fig. 7.3 this is not an issue since the current is conserved at the lepton-photon vertex. To realise this one has to look at the gauge dependent part of the photon propagator. The propagator has the following

Lorentz structure, cf. Appendix B:

$$G_{\mu\nu}(q) \sim \left(g_{\mu\nu} - (1 - \xi) \frac{q_\mu q_\nu}{q^2} \right), \quad (7.30)$$

with gauge parameter ξ . Now we insert the gauge dependent part of Eq. (7.30) between the quark and lepton currents and exploit the Dirac equation, cf. Appendix A:

$$\begin{aligned} & \bar{v}(p_2, m_2) \gamma^\mu u(p_1, m_1) \cdot (q_\mu q_\nu) \cdot \bar{u}(k_1, m) \gamma^\nu v(k_2, m) \\ &= \bar{v}(p_2, m_2) \not{q} u(p_1, m_1) \cdot \bar{u}(k_1, m) \not{q} v(k_2, m) \\ &= \bar{v}(p_2, m_2) (\not{p}_1 + \not{p}_2) u(p_1, m_1) \cdot \bar{u}(k_1, m) (\not{k}_1 + \not{k}_2) v(k_2, m) \\ &= \bar{v}(p_2, m_2) (m_1 - m_2) u(p_1, m_1) \cdot \bar{u}(k_1, m) (m - m) v(k_2, m) \\ &= 0, \end{aligned} \quad (7.31)$$

and so the amplitude is current conserving as long as the produced leptons have equal masses (0 in our case).

7.4 Kinematics

In this section we will work out the kinematics of the LO DY process in different schemes. We begin by comparing the standard textbook parton model with a naive approach which uses the light-cone component definition of the parton momentum fractions. It will turn out that in the latter case unphysical solutions appear that must be removed to be consistent with the standard parton model. We will then apply the lessons learned from this comparison when we derive the kinematics for the case of quarks carrying initial transverse momentum and mass.

7.4.1 Standard collinear parton model

In the following we want to derive the standard textbook result for the differential LO DY cross section and, therefore, we treat the interacting partons as collinear with their parent nucleons and we here keep the nucleons and partons massless. The hadronic LO DY differential cross section in the standard parton model is given in Eq. (7.1). There x_1 and x_2 are the momentum fractions carried by the annihilating partons inside the colliding nucleons and in the standard parton model, cf. Eq. (6.74), they are connected to the nucleon momenta via:

$$p_1 = x_1 P_1, \quad (7.32)$$

$$p_2 = x_2 P_2. \quad (7.33)$$

Note that it becomes immediately clear from Eqs. (7.32) and (7.33) that the incoming partons move collinearly with the nucleons. According to Eq. (7.28) no transverse

momentum can be generated for the virtual photon (and thus for the DY pair) in the LO process:

$$\vec{p}_{1\perp} = \vec{p}_{2\perp} = 0 \quad (7.34)$$

$$\begin{aligned} \Rightarrow \delta^{(4)}(p_1 + p_2 - q) &= \delta((p_1 + p_2)^0 - q^0) \delta^{(2)}(\vec{q}_\perp) \\ &\times \delta((p_1 + p_2)^z - q^z) . \end{aligned} \quad (7.35)$$

The maximal information about the DY pair that can be gained from Eq. (7.1) is double differential and a common choice of variables is the squared invariant mass M^2 and Feynman's x_F (cf. Sec. 7.2) of the virtual photon:

$$\begin{aligned} \frac{d\hat{\sigma}}{dM^2 dx_F} &= \int d^4q \frac{4\pi\alpha^2}{9q^2} \delta(M^2 - q^2) \delta^{(4)}(p_1 + p_2 - q) \delta\left(x_F - \frac{q_z}{(q_z)_{\max}}\right) \\ &= \frac{4\pi\alpha^2}{9M^2} \delta\left(M^2 - (p_1 + p_2)^2\right) \delta\left(x_F - \frac{(p_1 + p_2)_z}{(q_z)_{\max}}\right) . \end{aligned} \quad (7.36)$$

The two δ -functions connect x_1 and x_2 with the chosen observables:

$$M^2 = 2p_1 p_2 = x_1 x_2 S , \quad (7.37)$$

$$x_F = + \frac{\sqrt{S} (x_2 - x_1)}{2(q_z)_{\max}} , \quad (7.38)$$

with $(q_z)_{\max} = \frac{\sqrt{S}}{2}$, cf. Eqs. (7.8) and (7.9). Solving for x_1 and x_2 yields:

$$\begin{aligned} x_{1\pm} &= \frac{-(q_z)_{\max} x_F \pm \sqrt{((q_z)_{\max} x_F)^2 + M^2}}{\sqrt{S}} \\ &= \frac{-(q_z)_{\max} x_F \pm E_{\text{coll}}}{\sqrt{S}} , \end{aligned} \quad (7.39)$$

$$\begin{aligned} x_{2\pm} &= \frac{(q_z)_{\max} x_F \pm \sqrt{((q_z)_{\max} x_F)^2 + M^2}}{\sqrt{S}} \\ &= \frac{(q_z)_{\max} x_F \pm E_{\text{coll}}}{\sqrt{S}} , \end{aligned} \quad (7.40)$$

with the energy of the collinear DY-pair:

$$E_{\text{coll}} = \sqrt{M^2 + ((q_z)_{\max} x_F)^2} . \quad (7.41)$$

However the solutions corresponding to the lower (negative) sign in Eqs. (7.39,7.40) are always negative. Only the upper solutions are in the integration range of Eq. (7.1)

and are physically meaningful. For the negative solutions the parton energies would be negative on account of Eqs. (7.32) and (7.33). The hadronic cross section then reads:

$$\begin{aligned}
 \frac{d\sigma}{dM^2 dx_F} &= \int_0^1 dx_1 \int_0^1 dx_2 \sum_i q_i^2 f_i(x_1, M^2) f_{\bar{i}}(x_2, M^2) \\
 &\quad \times \frac{4\pi\alpha^2}{9M^2} \delta\left(M^2 - (p_1 + p_2)^2\right) \delta\left(x_F - \frac{(p_1 + p_2)_z}{(q_z)_{\max}}\right) \\
 &= \int_0^1 dx_1 \int_0^1 dx_2 \sum_i q_i^2 f_i(x_1, M^2) f_{\bar{i}}(x_2, M^2) \\
 &\quad \times \frac{4\pi\alpha^2}{9M^2} \frac{(q_z)_{\max}}{S\sqrt{(q_z)_{\max}^2 x_F^2 + M^2}} \delta(x_1 - x_{1+}) \delta(x_2 - x_{2+}) \\
 &= \sum_i q_i^2 f_i(x_{1+}, M^2) f_{\bar{i}}(x_{2+}, M^2) \frac{4\pi\alpha^2}{9M^2} \frac{(q_z)_{\max}}{SE_{\text{coll}}} . \tag{7.42}
 \end{aligned}$$

The last equation is the standard parton model formula for the hadronic LO DY cross section.

7.4.2 Naive collinear parton model

In this section we work out the complete collinear kinematics using the definition of the parton momentum fraction as the ratio of light-cone components of the parton and the nucleon, cf. Eqs. (6.136) and Eqs. (6.137). We show that there exist other solutions for the parton momentum fractions x_i which are neglected in the standard parton model right from the start. These other solutions will turn out to be unphysical and are derived at this point only to provide insight into difficulties arising from a transverse-momentum dependent calculation as discussed in Secs. 7.4.3 and 7.4.4.

The partons inside the nucleons carry some fraction of their parent hadron's longitudinal momentum. Labeling the parton momentum inside nucleon i with p_i we can define these fractions as ratios of plus or minus components of the partons and the corresponding components of the nucleon momenta. In the DY scaling limit ($S \rightarrow \infty$ and M^2/S finite) $P_1^- = P_2^+ = \sqrt{S}$ become the large components while all other components vanish (again we keep the partons and nucleons massless in this section for

simplicity). We define the following momentum fractions:

$$x_1 = \frac{p_1^-}{P_1^-} = \frac{p_1^-}{\sqrt{S}}, \quad (7.43)$$

$$\tilde{x}_1 = \frac{p_1^+}{\sqrt{S}}, \quad (7.44)$$

$$x_2 = \frac{p_2^+}{P_2^+} = \frac{p_2^+}{\sqrt{S}}, \quad (7.45)$$

$$\tilde{x}_2 = \frac{p_2^-}{\sqrt{S}}. \quad (7.46)$$

Note that Eqs. (7.43) and (7.45) are the standard definitions for the light-cone momentum fractions, cf. Sec. 6.2.2. The tilde quantities in Eqs. (7.44) and (7.46) are introduced for later convenience. The kinematical constraints for these fractions are the onshell conditions:

$$p_1^2 = p_1^+ p_1^- = 0 \Rightarrow x_1 \tilde{x}_1 = 0, \quad (7.47)$$

$$p_2^2 = p_2^+ p_2^- = 0 \Rightarrow x_2 \tilde{x}_2 = 0, \quad (7.48)$$

together with the invariant mass condition:

$$\begin{aligned} M^2 &= (p_1 + p_2)^2 = 2p_1 p_2 = p_1^+ p_2^- + p_1^- p_2^+ \\ &= (\tilde{x}_1 \tilde{x}_2 + x_1 x_2) S, \end{aligned} \quad (7.49)$$

and the relation for Feynman x_F :

$$\begin{aligned} x_F &= \frac{(p_1 + p_2)_z}{(q_z)_{\max}} = \frac{1}{2(q_z)_{\max}} (p_1^+ - p_1^- + p_2^+ - p_2^-) \\ &= \frac{\sqrt{S}}{2(q_z)_{\max}} (\tilde{x}_1 - x_1 + x_2 - \tilde{x}_2). \end{aligned} \quad (7.50)$$

We will show now that the constraints in Eqs. (7.47-7.50) can be fulfilled by two different sets of momentum fractions x_i, \tilde{x}_i . Equation (7.47) implies $\tilde{x}_1 = 0$ or $x_1 = 0$. In the first case one finds:

$$\tilde{x}_1 = 0 \quad (7.51)$$

$$\text{Eq. (7.49)} \Rightarrow \frac{M^2}{S} = x_1 x_2 \quad (7.52)$$

$$\Rightarrow x_1 \neq 0 \neq x_2 \quad (7.53)$$

$$\text{Eq. (7.48)} \Rightarrow \tilde{x}_2 = 0 \quad (7.54)$$

$$\text{Eq. (7.50)} \Rightarrow x_F = (x_2 - x_1) \frac{\sqrt{S}}{2(q_z)_{\max}}. \quad (7.55)$$

This is just the standard parton model solution, Eqs. (7.37) and (7.38), as described in Sec. 7.4.1. However there exists another solution, namely for $x_1 = 0$:

$$x_1 = 0 \tag{7.56}$$

$$\text{Eq. (7.49)} \Rightarrow \frac{M^2}{S} = \tilde{x}_1 \tilde{x}_2 \tag{7.57}$$

$$\Rightarrow \tilde{x}_1 \neq 0 \neq \tilde{x}_2 \tag{7.58}$$

$$\text{Eq. (7.48)} \Rightarrow x_2 = 0 \tag{7.59}$$

$$\text{Eq. (7.50)} \Rightarrow x_F = (\tilde{x}_1 - \tilde{x}_2) \frac{\sqrt{S}}{2(q_z)_{\max}} . \tag{7.60}$$

Kinematically this second solution represents the (strange) case where each parton moves into the opposite direction of its respective parent nucleon (this solution corresponds to the lower (negative) sign solutions in Eqs. (7.39, 7.40)). One can see this in the following example, where we choose $x_F = 0$:

$$\tilde{x}_1 = \tilde{x}_2 = \frac{M}{\sqrt{S}} \tag{7.61}$$

$$\Rightarrow p_1^z = \frac{1}{2} (p_1^+ - p_1^-) = \frac{1}{2} \sqrt{S} \tilde{x}_1 = \frac{M}{2} , \tag{7.62}$$

and analogously one finds:

$$p_2^z = -\frac{M}{2} . \tag{7.63}$$

Since nucleon 1 (2) moves into negative (positive) z -direction, cf. Eqs. (7.2) and (7.3), the partons here move exactly *opposite*. The parton momentum fractions x_i (not \tilde{x}_i !) entering the PDFs, however, are those of partons that move into the *same* direction as their parent nucleon. The second solution is thus physically not meaningful and it is discarded right away in the standard parton model approach.

The essential difference between the standard and the naive parton model is the following: In the (collinear) standard parton model *all* components of p_i are fixed at once by $p_i = x_i P_i$. This automatically implies $\tilde{x}_i = 0$. Such a procedure is without problems if one sticks to the collinear dynamics. In Sec. 7.4.3 below, however, we include initial transverse momenta of the partons, i.e. we have to deviate from $p_i = x_i P_i$. The natural choice would be to define x_i via one nucleon momentum component (the large one). This is exactly what we have done here for the collinear case. However, in the naive parton model x_i and \tilde{x}_i , i.e. p_i^+ and p_i^- , are introduced as independent variables which are then constrained by the kinematical and onshell conditions (7.47)-(7.50). Therefore one falls into a trap by picking up the additional unphysical solutions for $\tilde{x}_i \neq 0$. The same happens for the more complicated case including initial transverse momenta in Secs. 7.4.3 and 7.4.4.

Including in addition initial transverse momenta for the partons one has to model the distributions of these momenta. However there is a constraint the chosen model has to obey: in the Bjorken limit one should come back to the standard parton model and not to the naive one since only the former emerges from QCD. In the following we will point out how to modify the naive parton model such that one ends up with the standard parton model. This procedure will then be generalised to the case where initial transverse momenta of the partons are included in Sec. 7.4.3. In the naive parton model the hadronic cross section reads:

$$\begin{aligned}
\frac{d\sigma_{\text{naive}}}{dM^2 dx_F} &= \int_0^1 dx_1 \int_0^1 dx_2 \sum_i q_i^2 f_i(x_1, M^2) f_{\bar{i}}(x_2, M^2) \\
&\quad \times \frac{4\pi\alpha^2}{9M^2} \delta\left(M^2 - (p_1 + p_2)^2\right) \delta\left(x_F - \frac{(p_1 + p_2)_z}{(q_z)_{\text{max}}}\right) \\
&= \int_0^1 dx_1 \int_0^1 dx_2 \sum_i q_i^2 f_i(x_1, M^2) f_{\bar{i}}(x_2, M^2) \\
&\quad \times \frac{4\pi\alpha^2}{9M^2} \frac{2(q_z)_{\text{max}} x_1 x_2 (\delta(x_1 - x_{1+}) \delta(x_2 - x_{2+}) + \delta(x_1) \delta(x_2))}{S^{3/2} |(x_1 x_2 - \tilde{x}_1 \tilde{x}_2)(x_1 + x_2 + \tilde{x}_1 + \tilde{x}_2)|}.
\end{aligned} \tag{7.64}$$

The unphysical second solution for the momentum fractions in the last expression is represented by:

$$\delta(x_1) \delta(x_2) x_1 f_i(x_1, M^2) x_2 f_{\bar{i}}(x_2, M^2). \tag{7.65}$$

Its contribution does not vanish since one obtains for large enough M^2 [GRV98]:

$$\lim_{x \rightarrow 0} (x f(x, M^2)) > 0. \tag{7.66}$$

We now introduce a notation which we will keep throughout the rest of this work. Whenever we explicitly disregard unphysical solutions of the type of Eqs. (7.56)-(7.60) under an integral we denote this integral by \hat{f} . Then for the naive model one finds:

$$\begin{aligned}
\frac{d\sigma_{\text{naive}}}{dM^2 dx_F} &= \int_0^1 dx_1 \int_0^1 dx_2 \frac{4\pi\alpha^2}{9M^2} \sum_i q_i^2 f_i(x_1, M^2) f_{\bar{i}}(x_2, M^2) \\
&\quad \times \frac{2(q_z)_{\text{max}} x_1 x_2 (\delta(x_1 - x_{1+}) \delta(x_2 - x_{2+}) + \delta(x_1) \delta(x_2))}{S^{3/2} |(x_1 x_2 - \tilde{x}_1 \tilde{x}_2)(x_1 + x_2 + \tilde{x}_1 + \tilde{x}_2)|},
\end{aligned} \tag{7.67}$$

whereas the correct model gives:

$$\begin{aligned}
 \frac{d\sigma}{dM^2 dx_F} &= \int_0^1 dx_1 \int_0^1 dx_2 \frac{4\pi\alpha^2}{9M^2} \sum_i q_i^2 f_i(x_1, M^2) f_{\bar{i}}(x_2, M^2) \\
 &\quad \times \frac{2(q_z)_{\max} x_1 x_2 (\delta(x_1 - x_{1+}) \delta(x_2 - x_{2+}) + \delta(x_1) \delta(x_2))}{S^{3/2} |(x_1 x_2 - \tilde{x}_1 \tilde{x}_2)(x_1 + x_2 + \tilde{x}_1 + \tilde{x}_2)|} \\
 &= \int_0^1 dx_1 \int_0^1 dx_2 \frac{4\pi\alpha^2}{9M^2} \sum_i q_i^2 f_i(x_1, M^2) f_{\bar{i}}(x_2, M^2) \\
 &\quad \times \frac{2(q_z)_{\max} (x_1 x_2) \delta(x_1 - x_{1+}) \delta(x_2 - x_{2+})}{S^{3/2} (x_1 x_2) (x_1 + x_2)} \\
 &= \sum_i q_i^2 f_i(x_{1+}, M^2) f_{\bar{i}}(x_{2+}, M^2) \frac{4\pi\alpha^2}{9M^2} \frac{2(q_z)_{\max}}{S^{3/2} (x_{1+} + x_{2+})} \\
 &= \sum_i q_i^2 f_i(x_{1+}, M^2) f_{\bar{i}}(x_{2+}, M^2) \frac{4\pi\alpha^2}{9M^2} \frac{(q_z)_{\max}}{SE_{\text{coll}}}. \tag{7.68}
 \end{aligned}$$

Note that in the last expression we have recovered the standard parton model result Eq. (7.42).

The main reason to present this naive approach in detail will become clear in the next section where we lift the simplification of a collinear movement of the partons with the nucleons.

7.4.3 Intrinsic transverse momentum

As already mentioned above, no DY pair transverse momentum (p_T) is generated in the simple collinear parton model approach. Nevertheless, measurements indicate a Gaussian form of the p_T spectra at not too large p_T . This has been studied in approaches including initial quark transverse momentum distributions, e.g. [DM04, A⁺06]. In the current work we also present an approach incorporating primordial quark transverse momentum to address this issue. However, we have to consider, that unphysical solutions for the momentum fractions x_i can appear, cf. Sec. 7.4.2, which have to be removed properly. In earlier studies [LLM05, LGLM06, LLM07, Lin06] this important constraint was not considered and, thus, wrong results obtained. Note that the correct solutions can always be identified by putting all transverse momenta and masses to zero and then by checking if the well known parton model solutions for the x_i as given in Eqs. (7.39) and (7.40) are recovered.

In our transverse momentum dependent approach the LO DY differential cross

section reads:

$$\begin{aligned} d\sigma_{\text{LO}} &= \int_0^1 dx_1 \int_0^1 dx_2 \int d\vec{p}_{1\perp} \int d\vec{p}_{2\perp} \\ &\times \sum_i q_i^2 \tilde{f}_i(x_1, \vec{p}_{1\perp}, q^2) \tilde{f}_{\bar{i}}(x_2, \vec{p}_{2\perp}, q^2) d\hat{\sigma}(x_1, \vec{p}_{1\perp}, x_2, \vec{p}_{2\perp}, q^2). \end{aligned} \quad (7.69)$$

The functions $\tilde{f}_i(x, \vec{p}_{\perp}, q^2)$ are now extensions of the standard longitudinal PDFs, since they also describe the distribution of quark transverse momentum. We will show our ansatz for these functions in Sec. 7.5.1. Note that we take into account the full kinematics in the partonic cross section, i.e. $d\hat{\sigma}_{\text{LO}} = d\hat{\sigma}_{\text{LO}}(x_1, \vec{p}_{1\perp}, x_2, \vec{p}_{2\perp}, q^2)$, however, the quark masses are neglected as in the last section. In this approach the transverse momentum ($p_T = |\vec{q}_{\perp}|$) of the DY pair is accessible, since the annihilating quark and antiquark can have finite initial transverse momenta. Then the partonic triple-differential cross section reads:

$$\begin{aligned} &\frac{d\hat{\sigma}}{dM^2 dx_F dp_T^2} \\ &= \int d^4q \frac{4\pi\alpha^2}{9q^2} \delta(M^2 - q^2) \delta^{(4)}(p_1 + p_2 - q) \delta\left(x_F - \frac{q_z}{(q_z)_{\text{max}}}\right) \delta\left(p_T^2 - (\vec{q}_{\perp})^2\right) \\ &= \frac{4\pi\alpha^2}{9M^2} \delta\left(M^2 - (p_1 + p_2)^2\right) \delta\left(x_F - \frac{(p_1 + p_2)_z}{(q_z)_{\text{max}}}\right) \delta\left(p_T^2 - (\vec{p}_{1\perp} + \vec{p}_{2\perp})^2\right). \end{aligned} \quad (7.70)$$

Inserting Eq. (7.70) in Eq. (7.69) yields a multiple integral for the triple-differential hadronic cross section:

$$\begin{aligned} \frac{d\sigma}{dM^2 dx_F dp_T^2} &= \int_0^1 dx_1 \int_0^1 dx_2 \int d\vec{p}_{1\perp} \int d\vec{p}_{2\perp} F(x_1, \vec{p}_{1\perp}, x_2, \vec{p}_{2\perp}, M^2) \\ &\times \delta\left(M^2 - (p_1 + p_2)^2\right) \delta\left(x_F - \frac{(p_1 + p_2)_z}{(q_z)_{\text{max}}}\right) \delta\left(p_T^2 - (\vec{p}_{1\perp} + \vec{p}_{2\perp})^2\right). \end{aligned} \quad (7.71)$$

The δ -functions in Eq. (7.71) must be worked out in a way that allows to discern physical and unphysical solutions for the momentum fractions x_i in order to perform the f -integrations. For this aim it is useful to rewrite the parton momenta in terms of different variables:

$$q = p_1 + p_2, \quad (7.72)$$

$$k = \frac{1}{2}(p_2 - p_1). \quad (7.73)$$

Inverting the last two equations, we can use the on-shell conditions for the partons to get:

$$0 = p_1^2 = \left(\frac{1}{2}q - k\right)^2 = \frac{1}{4}q^2 - k \cdot q + k^2, \quad (7.74)$$

$$0 = p_2^2 = \left(\frac{1}{2}q + k\right)^2 = \frac{1}{4}q^2 + k \cdot q + k^2. \quad (7.75)$$

Adding and subtracting Eqs. (7.74) and (7.75) yields:

$$k^2 = -\frac{1}{4}M^2, \quad (7.76)$$

$$k \cdot q = 0. \quad (7.77)$$

Solving Eq. (7.76) for k^+ yields:

$$k^+ = \frac{\vec{k}_\perp^2 - \frac{1}{4}M^2}{k^-}. \quad (7.78)$$

Inserting this result into Eq. (7.77) gives an equation quadratic in k^- :

$$\begin{aligned} 0 &= k^+ q^- + k^- q^+ - 2\vec{k}_\perp \cdot \vec{q}_\perp \\ &= \frac{\vec{k}_\perp^2 - \frac{1}{4}M^2}{k^-} q^- + k^- q^+ - 2\vec{k}_\perp \cdot \vec{q}_\perp \end{aligned} \quad (7.79)$$

$$\Rightarrow 0 = (k^-)^2 q^+ - 2\vec{k}_\perp \cdot \vec{q}_\perp k^- + \left(\vec{k}_\perp^2 - \frac{1}{4}M^2\right) q^-. \quad (7.80)$$

The solutions are:

$$(k^-)_\pm = \frac{\vec{k}_\perp \cdot \vec{q}_\perp}{q^+} \pm \sqrt{\left(\frac{\vec{k}_\perp \cdot \vec{q}_\perp}{q^+}\right)^2 + \frac{q^-}{q^+} \left(\frac{1}{4}M^2 - \vec{k}_\perp^2\right)}. \quad (7.81)$$

Inserting (7.81) into (7.79) gives the solutions for k^+ :

$$(k^+)_\mp = \frac{q^+}{q^-} \left(\frac{\vec{k}_\perp \cdot \vec{q}_\perp}{q^+} \mp \sqrt{\left(\frac{\vec{k}_\perp \cdot \vec{q}_\perp}{q^+}\right)^2 + \frac{q^-}{q^+} \left(\frac{1}{4}M^2 - \vec{k}_\perp^2\right)} \right). \quad (7.82)$$

Rewriting now Eqs. (7.39) and (7.40) in terms of q and k and taking into account the finite nucleon mass we obtain the solutions for the parton momentum fractions:

$$(x_1)_\pm = \frac{p_1^-}{P_1^-} = \frac{1}{P_1^-} \left(\frac{1}{2}q^- - (k^-)_\pm \right), \quad (7.83)$$

$$(x_2)_\mp = \frac{p_2^+}{P_2^+} = \frac{1}{P_1^+} \left(\frac{1}{2}q^+ + (k^+)_\mp \right). \quad (7.84)$$

Since there are two solutions for k^- and k^+ , respectively, we also get two solutions for x_1, x_2 . To determine which set of x_1, x_2 and thus k^+, k^- has to be chosen we take the limit of zero parton transverse momentum. In this way one can make the connection to the collinear case (then $q^2 \rightarrow q^+ q^- = M^2$):

$$(k^-)_\pm \rightarrow \pm \sqrt{\frac{q^-}{q^+} \frac{1}{4} M^2} = \pm \frac{q^-}{2}, \quad (7.85)$$

$$(k^+)_\mp \rightarrow \mp \sqrt{\frac{q^+}{q^-} \frac{1}{4} M^2} = \mp \frac{q^+}{2}. \quad (7.86)$$

Inserting expressions (7.85) and (7.86) into (7.83) and (7.84) yields two solutions for the momentum fractions, just as in the collinear case in Sec. 7.4.2:

$$(x_1)_\pm \rightarrow \frac{1}{P_1^-} \begin{cases} 0 \\ q^- \end{cases} \quad (7.87)$$

and

$$(x_2)_\mp \rightarrow \frac{1}{P_1^-} \begin{cases} 0 \\ q^+ \end{cases}. \quad (7.88)$$

The lower solutions correspond to the standard parton model Eqs. (7.39), (7.40), while the upper solutions then correspond to the unphysical case $x_1 = x_2 = 0$ and $\tilde{x}_1 \neq 0 \neq \tilde{x}_2$, see Eqs. (7.56)-(7.60).

This is the crucial point: to receive physically meaningful results from Eq. (7.71) one has to discard these upper solutions just as one does in the collinear case in Sec. 7.4.2. This requires that the integrals in Eq. (7.71) are evaluated in the correct order, otherwise one cannot disentangle the two different solutions for x_1 and x_2 . We will now present a calculation which respects this requirement and we begin by introducing several integrals over δ -functions in Eq. (7.71). In this way we will transform the integration variables to the above chosen q and \vec{k}_\perp :

$$\begin{aligned} & \frac{d\sigma}{dM^2 dx_F dp_T^2} \\ &= \int_0^1 dx_1 \int_0^1 dx_2 \int d\vec{p}_{1\perp} \int d\vec{p}_{2\perp} \int d\vec{q}_\perp \int d\vec{k}_\perp \int dq^+ \int dq^- F(x_1, \vec{p}_{1\perp}, x_2, \vec{p}_{2\perp}, M^2) \\ & \quad \times \delta(q^+ - (p_1^+ + p_2^+)) \delta(q^- - (p_1^- + p_2^-)) \\ & \quad \times \delta^{(2)}(\vec{q}_\perp - (\vec{p}_{1\perp} + \vec{p}_{2\perp})) \delta^{(2)}(\vec{k}_\perp - \frac{1}{2}(\vec{p}_{1\perp} - \vec{p}_{2\perp})) \\ & \quad \times \delta\left(M^2 - (p_1 + p_2)^2\right) \delta\left(x_F - \frac{(p_1 + p_2)_z}{(q_z)_{\max}}\right) \delta\left(p_T^2 - (\vec{p}_{1\perp} + \vec{p}_{2\perp})^2\right). \end{aligned} \quad (7.89)$$

Now we find:

$$\int d\vec{p}_{1\perp} \int d\vec{p}_{2\perp} \delta^{(2)}(\vec{q}_\perp - (\vec{p}_{1\perp} + \vec{p}_{2\perp})) \delta^{(2)}\left(\vec{k}_\perp - \frac{1}{2}(\vec{p}_{2\perp} - \vec{p}_{1\perp})\right) = 1. \quad (7.90)$$

Then we calculate the following integral:

$$\int_0^1 dx_1 \int_0^1 dx_2 \delta(q^+ - (p_1^+ + p_2^+)) \delta(q^- - (p_1^- + p_2^-)). \quad (7.91)$$

According to Eqs. (7.81)-(7.84) the δ -functions in the last expression have two possible solutions for each p_1^- and p_2^+ . However as explained above we now have to explicitly remove the unphysical solutions $(x_1)_+$ and $(x_2)_-$, which are the ones corresponding to the upper sign in Eqs. (7.81) and (7.82):

$$\begin{aligned} & \int_0^1 dx_1 \int_0^1 dx_2 \delta(q^+ - (p_1^+ + p_2^+)) \delta(q^- - (p_1^- + p_2^-)) \\ &= \int_0^1 dx_1 \int_0^1 dx_2 \delta\left(q^+ - \frac{\left(\frac{1}{2}\vec{q}_\perp - \vec{k}_\perp\right)^2}{x_1 P_1^-} - x_2 P_1^-\right) \\ & \quad \times \delta\left(q^- - x_1 P_1^- - \frac{\left(\frac{1}{2}\vec{q}_\perp + \vec{k}_\perp\right)^2}{x_2 P_1^-}\right) \\ &= \int_0^1 dx_1 \int_0^1 dx_2 \delta\left(q^+ - \frac{\left(\frac{1}{2}\vec{q}_\perp - \vec{k}_\perp\right)^2}{(x_1)_- P_1^-} - (x_2)_+ P_1^-\right) \\ & \quad \times \delta\left(q^- - (x_1)_- P_1^- - \frac{\left(\frac{1}{2}\vec{q}_\perp + \vec{k}_\perp\right)^2}{(x_2)_+ P_1^-}\right) \\ &= \left| (P_1^-)^2 - \frac{\left(\frac{1}{2}\vec{q}_\perp - \vec{k}_\perp\right)^2 \left(\frac{1}{2}\vec{q}_\perp + \vec{k}_\perp\right)^2}{(x_1)_-^2 (x_2)_+^2 (P_1^-)^2} \right|^{-1}. \end{aligned} \quad (7.92)$$

Using $dq^+ dq^- = 2dq_0 dq_z$ we can evaluate some of the remaining integrals of Eq.

(7.89) with the help of the δ -functions:

$$\begin{aligned}
& \int dq^+ dq^- d\vec{q}_\perp \delta(M^2 - q^2) \delta\left(x_F - \frac{q_z}{(q_z)_{\max}}\right) \delta(p_T^2 - (\vec{q}_\perp)^2) \\
&= 2 \int dq_0 d\vec{q}_\perp dq_z \delta(M^2 + (\vec{q}_\perp)^2 + q_z^2 - q_0^2) \delta\left(x_F - \frac{q_z}{(q_z)_{\max}}\right) \delta(p_T^2 - (\vec{q}_\perp)^2) \\
&= \frac{\pi (q_z)_{\max}}{E}, \tag{7.93}
\end{aligned}$$

with $E = \sqrt{M^2 + p_T^2 + x_F^2 (q_z)_{\max}^2}$. Collecting the pieces, what remains of Eq. (7.89) is

$$\begin{aligned}
& \frac{d\sigma}{dM^2 dx_F dp_T^2} \\
&= \int_{|\vec{k}_\perp|_{\max}} d\vec{k}_\perp \frac{\pi (q_z)_{\max}}{E} \left| (P_1^-)^2 - \frac{(\hat{p}_{1\perp})^2 (\hat{p}_{2\perp})^2}{(x_{1-})^2 (x_{2+})^2 (P_1^-)^2} \right|^{-1} F((x_{1-}), \hat{p}_{1\perp}, (x_{2+}), \hat{p}_{2\perp}, M^2). \tag{7.94}
\end{aligned}$$

$(x_{1-}), \hat{p}_{1\perp}, (x_{2+})$ and $\hat{p}_{2\perp}$ are now fixed:

$$(x_{1-}) = \frac{1}{P_1^-} \left(\frac{q^-}{2} - \frac{\vec{k}_\perp \cdot \vec{q}_\perp}{q^+} + \sqrt{\left(\frac{\vec{k}_\perp \cdot \vec{q}_\perp}{q^+}\right)^2 + \frac{q^-}{q^+} \left(\frac{1}{4}M^2 - \vec{k}_\perp^2\right)} \right), \tag{7.95}$$

$$(x_{2+}) = \frac{1}{P_1^-} \left(\frac{q^+}{2} + \frac{\vec{k}_\perp \cdot \vec{q}_\perp}{q^-} + \sqrt{\left(\frac{\vec{k}_\perp \cdot \vec{q}_\perp}{q^-}\right)^2 + \frac{q^+}{q^-} \left(\frac{1}{4}M^2 - \vec{k}_\perp^2\right)} \right), \tag{7.96}$$

$$\hat{p}_{1\perp} = \frac{1}{2} \vec{q}_\perp - \vec{k}_\perp, \tag{7.97}$$

$$\hat{p}_{2\perp} = \frac{1}{2} \vec{q}_\perp + \vec{k}_\perp, \tag{7.98}$$

with:

$$q^+ = E + x_F (q_z)_{\max}, \tag{7.99}$$

$$q^- = E - x_F (q_z)_{\max}, \tag{7.100}$$

$$|\vec{q}_\perp| = p_T, \tag{7.101}$$

$$\vec{k}_\perp \cdot \vec{q}_\perp = |\vec{k}_\perp| p_T \cos(\phi_\perp). \tag{7.102}$$

$|\vec{k}_\perp|_{\max}$ is fixed by the condition that (x_{1-}) and (x_{2+}) must be real numbers:

$$(\vec{k}_\perp)^2 < \frac{(M^2 + p_T^2) \frac{M^2}{4}}{M^2 + p_T^2 (1 - \cos^2(\phi_\perp))} = (\vec{k}_\perp)_{\max}^2. \tag{7.103}$$

We have convinced ourselves that this condition also guarantees that $0 < (x_1)_- < 1$ and $0 < (x_2)_+ < 1$. Finally we arrive at the following expression:

$$\begin{aligned} \frac{d\sigma}{dM^2 dx_F dp_T^2} &= \int_0^{2\pi} d\phi_\perp \int_0^{(\vec{k}_\perp)_{\max}^2} \frac{1}{2} d(\vec{k}_\perp)^2 \frac{\pi (q_z)_{\max}}{E} \\ &\times \left| (P_1^-)^2 - \frac{(\hat{p}_{1\perp})^2 (\hat{p}_{2\perp})^2}{(x_1)_-^2 (x_2)_+^2 (P_1^-)^2} \right|^{-1} F((x_1)_-, \hat{p}_{1\perp}, (x_2)_+, \hat{p}_{2\perp}, M^2), \end{aligned} \quad (7.104)$$

where the function F is given by:

$$F((x_1)_-, \hat{p}_{1\perp}, (x_2)_+, \hat{p}_{2\perp}, M^2) = \sum_i q_i^2 \tilde{f}_i((x_1)_-, \hat{p}_{1\perp}, M^2) \tilde{f}_{\bar{i}}((x_2)_+, \hat{p}_{2\perp}, M^2) \frac{4\pi\alpha^2}{9M^2}, \quad (7.105)$$

with our transverse momentum dependent parton distributions \tilde{f}_i .

7.4.4 Quark masses

In Sec. 7.4.3 we extended the standard collinear PDFs towards quark distributions which also include quark transverse momentum. However, we kept the masses of the quarks fixed at zero. Since in light cone coordinates the onshell condition reads $m^2 = p^2 = p^+ p^- - (\vec{p}_\perp)^2$, this is equivalent to varying only two of the three, in principle independent quark momentum components p^+ , p^- and p_\perp . A fully unintegrated parton distribution should depend on all three of these components. Therefore, we once more extend the parton distributions of Sec. 7.4.3:

$$\tilde{f}_i(x, \vec{p}_\perp, q^2) \rightarrow \hat{f}_i(x, \vec{p}_\perp, m^2, q^2) \quad (7.106)$$

We will present our ansatz for \hat{f} in Sec. 7.5.2. The differential hadronic cross section now becomes

$$\begin{aligned} d\sigma_{\text{LO}} &= \int_0^1 dx_1 \int_0^1 dx_2 \int d\vec{p}_{1\perp} \int d\vec{p}_{2\perp} \int dm_1^2 \int dm_2^2 \\ &\times \sum_i q_i^2 \hat{f}_i(x_1, \vec{p}_{1\perp}, m_1^2, q^2) \hat{f}_{\bar{i}}(x_2, \vec{p}_{2\perp}, m_2^2, q^2) \\ &\times d\hat{\sigma}(x_1, \vec{p}_{1\perp}, x_2, \vec{p}_{2\perp}, m_1^2, m_2^2, q^2). \end{aligned} \quad (7.107)$$

The partonic cross section is given by Eq. (7.27).

Now we have to perform the same procedure as described above to remove the unphysical solutions for the longitudinal momentum fractions x_i . In complete analogy we find (the details of this calculation can be found in Sec. 8.3.2, since it is just a special case of the kinematics of gluon bremsstrahlung):

$$\begin{aligned}
\frac{d\sigma_{\text{LO}}}{dM^2 dx_F dp_T^2} &= \int_0^{2\pi} d\phi_{\perp} \int_0^{(\vec{k}_{\perp})_{\text{max}}} \frac{1}{2} d(\vec{k}_{\perp})^2 \int_0^{(m_1)_{\text{max}}} dm_1^2 \int_0^{(m_2)_{\text{max}}} dm_2^2 \frac{\pi (q_z)_{\text{max}}}{E} \\
&\times \left| (P_1^-)^2 - \frac{\left[\left(\frac{1}{2} \vec{q}_{\perp} - \vec{k}_{\perp} \right)^2 + m_1^2 \right] \left[\left(\frac{1}{2} \vec{q}_{\perp} + \vec{k}_{\perp} \right)^2 + m_2^2 \right]}{(x_1)_- (x_2)_+ (P_1^-)^2} \right|^{-1} \\
&\times F_{\text{LO}}((x_1)_-, \hat{p}_{1\perp}, m_1^2, (x_2)_+, \hat{p}_{2\perp}, m_2^2, M^2) \\
&\times \Theta(1 - (x_1)_-) \Theta((x_1)_-) \Theta(1 - (x_2)_+) \Theta((x_2)_+) , \quad (7.108)
\end{aligned}$$

where the function F_{LO} is given by:

$$\begin{aligned}
&F_{\text{LO}}((x_1)_-, \hat{p}_{1\perp}, m_1^2, (x_2)_+, \hat{p}_{2\perp}, m_2^2, M^2) \\
&= \sum_i q_i^2 \hat{f}_i \left((x_1)_-, \hat{p}_{1\perp}, m_1^2, M^2 \right) \hat{f}_i \left((x_2)_+, \hat{p}_{2\perp}, m_2^2, M^2 \right) \\
&\times \frac{4\pi\alpha^2 2M^4 - M^2(m_1^2 - 6m_1m_2 + m_2^2) - (m_1^2 - m_2^2)^2}{9M^4 2\sqrt{(M^2 - m_1^2 - m_2^2)^2 - m_1^2m_2^2}} . \quad (7.109)
\end{aligned}$$

The momentum fractions read:

$$\begin{aligned}
(x_1)_- &= \frac{1}{P_1^-} \left(\frac{q^-}{2} - \frac{\vec{k}_{\perp} \cdot \vec{q}_{\perp}}{q^+} - \frac{m_2^2 - m_1^2}{2q^+} \right. \\
&\left. + \sqrt{\left(\frac{\vec{k}_{\perp} \cdot \vec{q}_{\perp}}{q^+} + \frac{m_2^2 - m_1^2}{2q^+} \right)^2 + \frac{q^-}{q^+} \left(\frac{1}{4}M^2 - \vec{k}_{\perp}^2 - \frac{m_1^2 + m_2^2}{2} \right)} \right) , \quad (7.110)
\end{aligned}$$

$$\begin{aligned}
(x_2)_+ &= \frac{1}{P_1^-} \left(\frac{q^+}{2} + \frac{\vec{k}_{\perp} \cdot \vec{q}_{\perp}}{q^-} + \frac{m_2^2 - m_1^2}{2q^-} \right. \\
&\left. + \sqrt{\left(\frac{\vec{k}_{\perp} \cdot \vec{q}_{\perp}}{q^-} + \frac{m_2^2 - m_1^2}{2q^-} \right)^2 + \frac{q^+}{q^-} \left(\frac{1}{4}M^2 - \vec{k}_{\perp}^2 - \frac{m_1^2 + m_2^2}{2} \right)} \right) , \quad (7.111)
\end{aligned}$$

with:

$$\hat{p}_{1\perp} = \frac{1}{2}\vec{q}_\perp - \vec{k}_\perp, \quad (7.112)$$

$$\hat{p}_{2\perp} = \frac{1}{2}\vec{q}_\perp + \vec{k}_\perp, \quad (7.113)$$

$$E = \sqrt{M^2 + p_T^2 + x_F^2(q_z)_{\max}^2} \quad (7.114)$$

$$q^+ = E + x_F(q_z)_{\max}, \quad (7.115)$$

$$q^- = E - x_F(q_z)_{\max}, \quad (7.116)$$

$$|\vec{q}_\perp| = p_T, \quad (7.117)$$

$$\vec{k}_\perp \cdot \vec{q}_\perp = |\vec{k}_\perp| p_T \cos(\phi_\perp), \quad (7.118)$$

$$(\vec{k}_\perp)_{\max}^2 = \frac{(M^2 + p_T^2) \frac{M^2}{4}}{M^2 + p_T^2(1 - \cos^2(\phi_\perp))}, \quad (7.119)$$

$$(m_1)_{\max}^2 = 2\vec{k}_\perp \cdot \vec{q}_\perp + q^+ q^- - \sqrt{4q^+ q^- \left(\vec{k}_\perp + \frac{1}{2}\vec{q}_\perp \right)^2}, \quad (7.120)$$

$$(m_2)_{\max}^2 = -2\vec{k}_\perp \cdot \vec{q}_\perp + m_1^2 + q^+ q^- - \sqrt{4q^+ q^- m_1^2 + 4q^+ q^- \left(\vec{k}_\perp - \frac{1}{2}\vec{q}_\perp \right)^2}. \quad (7.121)$$

In Sec. 7.6 we show the results of this calculation as well as of the approaches in Secs. 7.4.1 and 7.4.3.

7.5 Distributions

The Bjorken limit, in which the standard parton model is well defined and derived from LO pQCD, is an idealisation of real experiments. There the partons inside the nucleons will always interact before the collision and these interactions will generate momentum components, which are neglected in the (purely collinear) standard parton model, namely momentum components perpendicular to the beam line, $\vec{p}_{1\perp}, \vec{p}_{2\perp}$, as well as the small light-cone components p_1^+, p_2^- . The latter translate to non-vanishing quark masses.

Note that the factorisation into hard (subprocess) and soft (PDFs) physics is proven in the transverse case at least for partons with low transverse momentum in [JMY04]. For the case of mass distributions for the quarks we *assume* this factorisation.

7.5.1 Transverse momentum distributions

In Sec. 7.4.3 we introduced transverse momentum dependent parton distribution functions \tilde{f}_i . They are functions of the light-cone momentum fraction x_i , the transverse momentum $\vec{p}_{i\perp}$ and the hard scale of the subprocess q^2 . However, the general form of these functions is unknown. Known rather well are the longitudinal PDFs. Since data of DY pair production are compatible with a Gaussian form of the p_T spectrum up to a certain p_T [Web03, NuSea03], we assume factorisation of the longitudinal and the transverse part of \tilde{f}_i and make the following common ansatz [Wan00, RPN02, DM04]:

$$\tilde{f}_i(x, \vec{p}_{\perp}, q^2) = f_i(x, q^2) \cdot f_{\perp}(\vec{p}_{\perp}) . \quad (7.122)$$

Here f_i are the usual longitudinal PDFs and for f_{\perp} we choose a Gaussian form:

$$f_{\perp}(\vec{p}_{\perp}) = \frac{1}{4\pi D^2} \exp\left(-\frac{(\vec{p}_{\perp})^2}{4D^2}\right) . \quad (7.123)$$

The width parameter D is connected to the average squared transverse momentum:

$$\langle (\vec{p}_{\perp})^2 \rangle = \int d\vec{p}_{\perp} (\vec{p}_{\perp})^2 f_{\perp}(\vec{p}_{\perp}), = 4D^2 \quad (7.124)$$

and D has to be fitted to the available data.

7.5.2 Mass distributions

In Sec. 7.4.4 we extended our model by also distributing quark masses. This approach was motivated by studies of quark correlations and quark spectral functions, see for example [FLM03, FL07]. Note that in such a mass distribution approach one effectively parametrises higher twist effects, i.e. effects which are suppressed by inverse powers of the hard scale M . These higher twist contributions should become particularly important in the description of DY pair production in the region of small energies (and thus small M), which is one aim of our studies.

For the fully unintegrated parton distributions \hat{f}_i we make the following ansatz:

$$\hat{f}_i(x, \vec{p}_{\perp}, m^2, q^2) = f_i(x, q^2) \cdot f_{\perp}(\vec{p}_{\perp}) \cdot A(p) . \quad (7.125)$$

Again f_i are standard PDFs and f_{\perp} are the transverse momentum distributions of Sec. 7.5.1. Since the distribution of longitudinal parton momenta is determined by the argument of the PDFs $x \sim p^+$, we now allow for a distribution of the remaining degree of freedom, i.e. the small component p^- , by writing:

$$A(p) dp^- = \frac{1}{N} \frac{\hat{\Gamma}(m^2)}{\left(p^- - \frac{p_T^2}{p^+}\right)^2 + \hat{\Gamma}^2(m^2)} dp^- , \quad (7.126)$$

with $m^2 = p^2$. Rewriting in terms of m^2 yields:

$$A(p) dm^2 = \frac{1}{N} \frac{\hat{\Gamma}(m^2) p^+}{m^4 + (p^+)^2 \hat{\Gamma}^2(m^2)} dm^2 . \quad (7.127)$$

We choose a non-constant width such that the quark can never become heavier than its parent nucleon:

$$\hat{\Gamma}(m^2) = \frac{m_N^2 - m^2}{m_N^2} \Gamma , \quad (7.128)$$

for $0 < m^2 < m_N^2$ and $\hat{\Gamma}(m^2) = 0$ otherwise, where Γ is a free parameter. The factor $\frac{1}{N}$ normalises the spectral function such that

$$\int_0^\infty dm^2 A(p) = \int_0^{m_N^2} dm^2 A(p) = 1 . \quad (7.129)$$

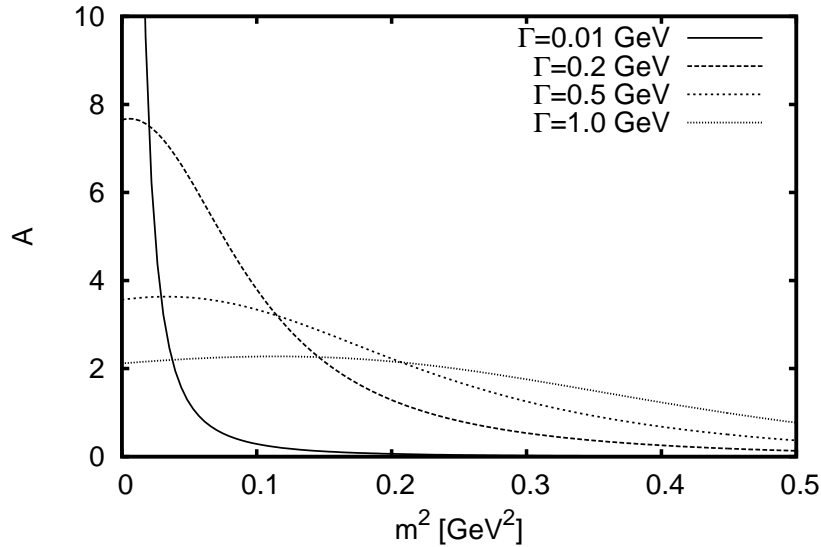


Figure 7.4: Spectral function A plotted for different values of the width Γ . Everywhere $p^+ = 0.5$ GeV.

In Fig. 7.4 we plot $A(p)$ as a function of m^2 for fixed $p^+ = 0.5$ GeV for different values of the width Γ . Note that for not too small Γ the region near $m^2 = 0$ is heavily suppressed as compared to, for example, $\Gamma = 0.01$ GeV.

7.6 Results of the leading order approach

In this section we present and compare our results for the different LO approaches of Secs. 7.4.1, 7.4.3 and 7.4.4. The data are from the NuSea Collaboration (E866) [Web03, NuSea03] and from FNAL-E439 [S⁺81]. For the collinear PDFs we used the *leading order* MSTW2008LO68cl parametrisation [MSTW09].

7.6.1 E866 - p_T spectra

Experiment E866 measured continuum dimuon production in pp collisions at $S \approx 1500 \text{ GeV}^2$. The triple-differential cross section as given by the E866 collaboration is:

$$E \frac{d\sigma}{d^3p} \equiv \frac{2E}{\pi\sqrt{S}} \frac{d\sigma}{dx_F dp_T^2}, \quad (7.130)$$

where an average over the azimuthal angle has been taken and where E is the energy of the DY pair, cf. Eq. (7.132). The data are given in several bins of M , x_F and p_T and for every datapoint the average values $\langle M \rangle$, $\langle x_F \rangle$ and $\langle p_T \rangle$ are given. Since our schemes provide Eqs. (7.104) and (7.108) we calculate the quantity of Eq. (7.130) for every datapoint using these averaged values and then perform a simple average in each M^2 bin:

$$\begin{aligned} \frac{2E}{\pi\sqrt{S}} \frac{d\sigma}{dx_F dp_T^2} &\rightarrow \frac{2E}{\pi\sqrt{S}} \int_{M^2\text{-bin}} \frac{d\sigma}{dM^2 dx_F dp_T^2} dM^2 \\ &\approx \frac{2E}{\pi\sqrt{S}} \Delta M^2 \frac{d\sigma}{dM^2 dx_F dp_T^2} (\langle M \rangle, \langle x_F \rangle, \langle p_T \rangle), \end{aligned} \quad (7.131)$$

where the energy of the DY pair is:

$$E = \sqrt{\langle M \rangle^2 + \langle p_T \rangle^2 + \langle x_F \rangle^2 \langle (q_z)_{\max} \rangle^2}. \quad (7.132)$$

$\Delta M^2 = M_{\max}^2 - M_{\min}^2$, where M_{\max} (M_{\min}) is the upper (lower) limit of the bin.

We plot the results for the two different approaches of Secs. 7.4.3 and 7.4.4 in Fig. 7.5. The different dashed lines represent the massless and the mass distribution approach for different values of Γ and they all agree within $\approx 20\%$. Note, however, that with increasing Γ the calculated cross section is slightly enhanced. Everywhere a value of $D = 0.5 \text{ GeV}$ for the transverse momentum dispersion was chosen. With this choice of the parameter D the shape of the spectra is described rather well. However, in both approaches the absolute size of the cross section is underestimated: we have to multiply the result of the mass distribution approach for $\Gamma = 0.5 \text{ GeV}$ by $K = 2$ to fit the data (solid line).

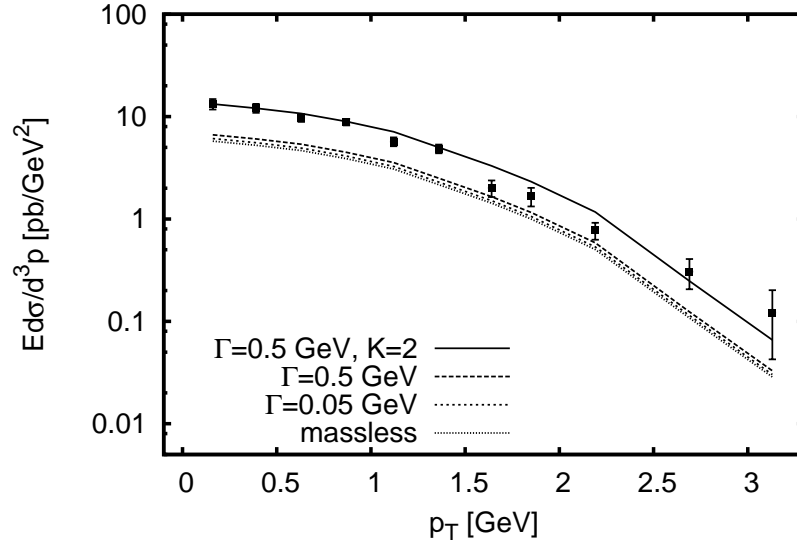


Figure 7.5: p_T spectrum obtained at LO from the massless and the mass distribution approach with different values of Γ . Everywhere $D = 0.5$ GeV. The solid line is the mass distribution approach for $\Gamma = 0.5$ GeV multiplied by a factor $K = 2$. Data are from E866 binned with $4.2 \text{ GeV} < M < 5.2 \text{ GeV}$, $-0.05 < x_F < 0.15$. Only statistical errors are shown.

Our value for the average intrinsic transverse momentum $\langle (\vec{p}_\perp)^2 \rangle = 4D^2 = 1 \text{ GeV}^2$ is in agreement with other LO approaches; for example in [DM04] a simplified model utilizing the collinear subprocess cross section together with Gaussian transverse momentum distributions for the (massless) quarks was developed. There a value of $\langle (\vec{p}_\perp)^2 \rangle \approx 0.95 \text{ GeV}^2$ was found for the energy range of E866. In addition in [DM04] a factor $K = 1.6$ was determined, which is considerably lower than the factor $K = 2$, which we found above. One should note, however, two things: first, in [DM04] the comparison of model and data was performed in invariant mass bins with $M > 7$ GeV in contrast to our calculation for $M < 5.2$ GeV. Second, the results in [DM04] for $K = 1.6$ change from slightly overshooting the data in higher mass bins ($M > 10$ GeV) to undershooting in lower mass bins ($M > 7$ GeV), cf. Fig. 4 in [DM04]. Extrapolating this behavior down to our values for M warrants a somewhat larger K factor for the model in [DM04], which would bring their value of K closer to ours. Thus, it is fair to say, that both their and our LO approaches are in reasonable agreement.

7.6.2 E439 - M spectrum

Experiment E439 measured dimuon production in proton-tungsten collisions at $S \approx 750 \text{ GeV}^2$. The double differential cross section

$$\frac{d\sigma}{dM dx'_F} \quad (7.133)$$

has been given at a fixed $x'_F = 0.1$.

As before we begin with Eqs. (7.104) and (7.108) and calculate the quantity Eq. (7.133) by integrating over p_T^2 and performing a simple transformation from x_F to x'_F :

$$\begin{aligned} \frac{d\sigma}{dM dx'_F} &= \int_0^{(p_T)_{\max}^2} dp_T^2 \frac{d\sigma}{dM dx'_F dp_T^2} \\ &= \int_0^{(p_T)_{\max}^2} dp_T^2 2M \left(1 - \frac{M^2}{S}\right) \\ &\quad \times \frac{d\sigma}{dM^2 dx_F dp_T^2} \left(M, x_F = x'_F \left(1 - \frac{M^2}{S}\right)\right). \end{aligned} \quad (7.134)$$

Since the experiment was done on tungsten we calculate the cross section for proton-proton and proton-neutron and average accordingly (74 protons and 110 neutrons). We compare the results in Fig. 7.6. Everywhere $D = 0.5 \text{ GeV}$ except for the simple parton model, which has no transverse momentum distribution. The lowest curve represents the indistinguishable results of the standard parton model (Sec. 7.4.1) and of the (massless) initial transverse momentum approach (Sec. 7.4.3). The result of the mass distribution approach (Sec. 7.4.4) for $\Gamma = 0.5 \text{ GeV}$ (long dashed) is somewhat larger but still underestimates the data: The solid line is the result of this mass distribution approach multiplied by a factor $K = 1.2$ and it fits the data very well.

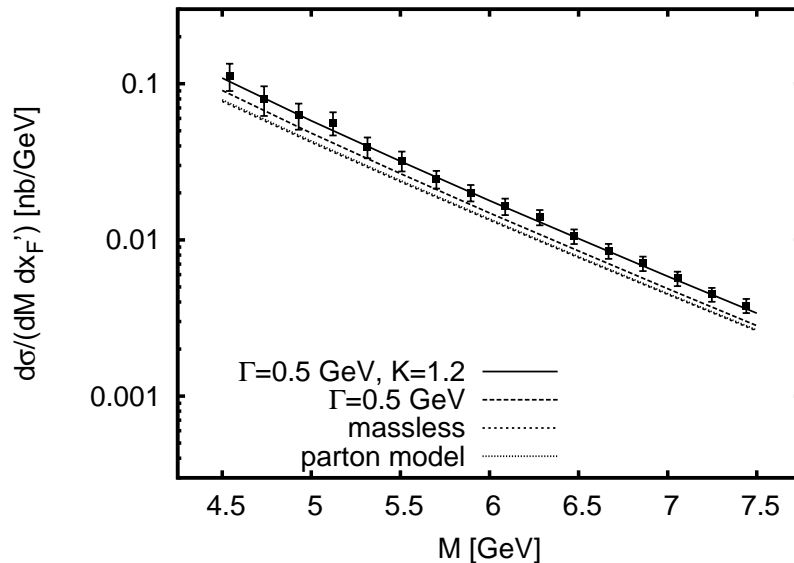


Figure 7.6: M spectrum obtained from the standard parton model, initial transverse momentum approach (massless) and mass distribution approach ($D = 0.5$ GeV for the latter two). The solid line is the result of the mass distribution approach multiplied by a factor $K = 1.2$. Data are from E439 with $x'_F = 0.1$. Only statistical errors are shown.

The K factor obtained in standard parton model calculations for the E439 regime is given as $K = 1.6 \pm 0.3$ [S⁺81, GPS86], which agrees well with the factor $K = 1.6$ found in the (massless) LO approach in [DM04]. The smaller factor $K = 1.2$, which we have obtained can therefore be attributed to the inclusion of the quark mass distributions and the full kinematics in the hard subprocess in our model. Note, that at E439 ($S = 750$ GeV²) our massive approach leads to a larger enhancement of the cross section than for example at E866 ($S = 1500$ GeV²), cf. Figs. 7.5 and 7.6. This is not totally unexpected, as at lower hadronic energies the calculated cross section should become more sensitive to the details of the soft physics encoded in our various distributions.

7.7 Conclusion for the LO calculation

In this chapter we have presented and compared three different approaches to DY pair production at LO in the partonic subprocess. The standard parton model approach describes invariant mass spectra only up to a K factor and it cannot describe transverse momentum (p_T) spectra. The latter issue was addressed in the initial transverse momentum approach. We found that with a suitable choice of an initial transverse momentum distribution the DY p_T spectra can be described very well, however, still only up to a K factor, in agreement with other LO approaches, see e.g. [DM04]. The mass distribution approach can improve the picture somewhat, but the enhancement

of the calculated cross sections is too small to describe the data. Still an a priori undetermined multiplicative factor K is needed to reproduce the measured cross sections. This finding triggered the NLO calculations, which will be presented in Chapter 8.

8

Next-to-leading order corrections to the Drell-Yan process

Building on the LO ($O(\alpha_s^0)$) calculations of Chapter 7 we will present in this chapter all relevant DY pair production processes to $O(\alpha_s)$ (NLO): loop corrections to the quark-photon vertex, gluon bremsstrahlung and gluon Compton scattering. As already mentioned in the introduction, the latter two processes produce divergent p_T spectra, if evaluated in the standard massless parton model approach. We will show, that we can soften the divergences of these NLO processes at low p_T by introducing initial parton transverse momentum k_T and quark mass distributions, just as we did for the LO case, cf. Sec. 7.5. Since the collinear divergences that produce the divergent p_T spectra are commonly absorbed into the PDFs, we will introduce a subtraction scheme to avoid double-counting of the NLO processes, that we explicitly consider. In the results in Part V we will then see, that in this approach we can describe p_T and M spectra without the need for an additional K factor.

8.1 Vertex correction

In this section we will treat the processes that modify the electromagnetic quark-photon vertex. They are depicted in Figs. 8.1 and 8.2. The vertex correction diagram (Fig. 8.1, right) alone does contribute only at order α_s^2 to the cross section. However, due to identical initial and final states it interferes with the LO process (Fig. 8.1, left) and the interference is of order α_s . The same is true for the wave function renormalisation processes of Fig. 8.2.

We will begin by calculating the modified vertex function Γ^μ , regulating the ultra-violet loop divergences in dimensional regularisation and the infrared divergences by introducing a finite (and fictitious) gluon mass λ . Inserting Γ^μ into the interference cross section, we will then obtain the relevant form factors of the quark-photon vertex. Since we assign different masses to the incoming quarks, we again have to make sure that current conservation is fulfilled and we will find, that this indeed the case. However, one unwanted effect of the different quark masses will become apparent, namely, that the electric charge at the quark-photon vertex is renormalised. Fortunately we will finally find, that this renormalisation does not affect our model. Note, that the quark-gluon vertex is unchanged, since by our construction the quark mass does not change at this vertex, cf. Sec. 8.1.5.

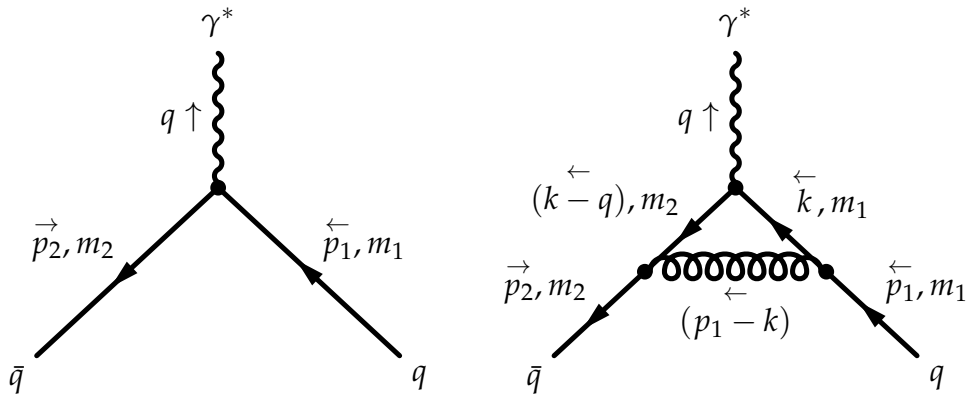


Figure 8.1: Leading order and vertex correction processes to DY production. Note that only the interference of the two processes contributes at NLO.

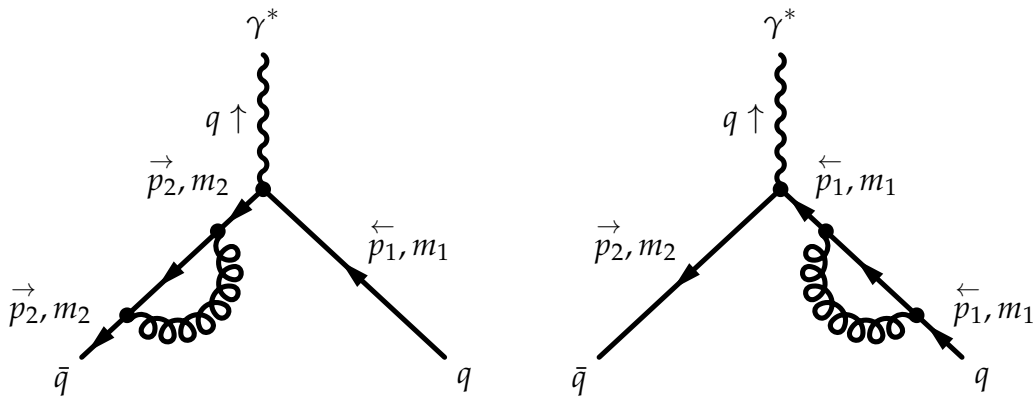


Figure 8.2: Wave function renormalisation processes for DY production at NLO.

8.1.1 Vertex function

We already found the amplitude for the LO process $q\bar{q} \rightarrow \gamma^*$ (Fig. 8.1 left) in Eq. (7.12):

$$iM_{\text{LO}} = \bar{v}_{s'}(p_2) (ie\gamma^\mu) u_s(p_1) \cdot \epsilon_\mu^*(q) . \quad (8.1)$$

We now have to calculate the amplitude including all the order α_s corrections induced by the loop diagrams in Figs. 8.1 right and 8.2. The two wave function renormalisation processes are taken into account by assigning a factor $\sqrt{Z_2}$ for each of the external quark legs, cf. Secs. 4.3 and 4.4. The vertex correction process modifies the bare quark-photon vertex:

$$\gamma^\mu \rightarrow \Gamma^\mu = \gamma^\mu + \delta\Gamma^\mu , \quad (8.2)$$

where $\delta\Gamma^\mu$ is of order α_s . Now one can expand the amplitude in powers of the strong coupling:

$$\begin{aligned} iM &= \sqrt{Z_2(p_2)} \bar{v}_{s'}(p_2) (ie\Gamma^\mu) \sqrt{Z_2(p_1)} u_s(p_1) \cdot \epsilon_\mu^*(q) \\ &= \left(1 + \frac{1}{2}\delta Z_2(p_2) + O(\alpha_s^2)\right) \bar{v}_{s'}(p_2) \\ &\quad \times [ie(\gamma^\mu + \delta\Gamma^\mu)] \\ &\quad \times \left(1 + \frac{1}{2}\delta Z_2(p_1) + O(\alpha_s^2)\right) u_s(p_1) \cdot \epsilon_\mu^*(q) \\ &= \bar{v}_{s'}(p_2) (ie\gamma^\mu) u_s(p_1) \cdot \epsilon_\mu^*(q) \\ &\quad + \bar{v}_{s'}(p_2) \left[ie\left(\frac{1}{2}\delta Z_2(p_2)\gamma^\mu + \frac{1}{2}\delta Z_2(p_1)\gamma^\mu + \delta\Gamma^\mu\right)\right] u_s(p_1) \cdot \epsilon_\mu^*(q) + O(\alpha_s^2) \\ &= iM_{\text{LO}} + iM_{\text{VC}} + O(\alpha_s^2) , \end{aligned} \quad (8.3)$$

where $M_{\text{VC}} \sim \alpha_s$. We already found the field strength corrections for the massive quark case in Eq. (4.90):

$$\delta Z_2(p_i) = \frac{\alpha_s}{4\pi} C_F \left[-4 - \frac{1}{\epsilon'} + \gamma - \ln\left(\frac{4\pi\mu^2}{m_i^2}\right) - 2\ln\left(\frac{\lambda^2}{m_i^2}\right) \right] . \quad (8.4)$$

Here λ is the fictitious gluon mass, which regulates the IR divergence and C_F is the color factor, cf. Appendix B. Left to do is the calculation of the correction $\delta\Gamma^\mu$. Using

the Feynman rules of Appendix B one finds for the loop in Fig. 8.1 right:

$$\begin{aligned}
 & \bar{v}_{s'}(p_2)\delta\Gamma^\mu u_s(p_1) \\
 &= C_F \bar{v}_{s'}(p_2) \int \frac{d^d k}{(2\pi)^d} (ig\gamma^\alpha) \frac{i(\not{k} - \not{q} + m_2)}{(k-q)^2 - m_2^2 + i\epsilon} \gamma^\mu \frac{i(\not{k} + m_1)}{k^2 - m_1^2 + i\epsilon} (ig\gamma^\beta) u_s(p_1) \\
 & \quad \times \frac{-ig_{\alpha\beta}}{(p_1 - k)^2 - \lambda^2 + i\epsilon} \\
 &= -ig^2 C_F \int \frac{d^d k}{(2\pi)^d} \frac{\bar{v}_{s'}(p_2)\gamma^\alpha(\not{k} - \not{q} + m_2)\gamma^\mu(\not{k} + m_1)\gamma_\alpha u_s(p_1)}{[k^2 - m_1^2 + i\epsilon] [(k-q)^2 - m_2^2 + i\epsilon] [(p_1 - k)^2 - \lambda^2 + i\epsilon]}, \quad (8.5)
 \end{aligned}$$

with λ and C_F as described above.

Feynman parameters

Following the results of Sec. 2.3 we introduce Feynman parameters to combine the propagator denominators:

$$\begin{aligned}
 & \frac{1}{[k^2 - m_1^2 + i\epsilon] [(k-q)^2 - m_2^2 + i\epsilon] [(p_1 - k)^2 - \lambda^2 + i\epsilon]} \\
 &= \int_0^1 dx dy dz \frac{2\delta(x+y+z-1)}{[xk^2 - xm_1^2 + y(k-q)^2 - ym_2^2 + z(p_1 - k)^2 - z\lambda^2 + i\epsilon]^3}. \quad (8.6)
 \end{aligned}$$

The denominator of the integrand can now be rewritten by completing the square in k (remember $x + y + z = 1!$):

$$\begin{aligned}
 & xk^2 - xm_1^2 + y(k-q)^2 - ym_2^2 + z(p_1 - k)^2 - z\lambda^2 + i\epsilon \\
 &= (x+y+z)k^2 + k(-2yq - 2zp_1) - xm_1^2 + yq^2 - ym_2^2 + zp_1^2 - z\lambda^2 + (x+y+z)i\epsilon \\
 &= l^2 - \Delta, \quad (8.7)
 \end{aligned}$$

with $l = k - yq - zp_1$ and:

$$\begin{aligned}
 \Delta &= (yq + zp_1)^2 + xm_1^2 - yq^2 + ym_2^2 - zp_1^2 + z\lambda^2 - i\epsilon \\
 &= -xyq^2 + m_1^2(1-z)^2 + (m_2^2 - m_1^2)y(1-z) + z\lambda^2 - i\epsilon, \quad (8.8)
 \end{aligned}$$

where we have used $q = p_1 + p_2$, $p_1^2 = m_1^2$ and $p_2^2 = m_2^2$. Shifting the momentum integration the correction then becomes:

$$\begin{aligned}
 \bar{v}_{s'}(p_2)\delta\Gamma^\mu u_s(p_1) &= -ig^2 C_F \int_0^1 dx dy dz \delta(x+y+z-1) \int \frac{d^d l}{(2\pi)^d} \\
 & \quad \times \frac{\bar{v}_{s'}(p_2)\gamma^\alpha(\not{k} - \not{q} + m_2)\gamma^\mu(\not{k} + m_1)\gamma_\alpha u_s(p_1)}{[l^2 - \Delta + i\epsilon]^3}, \quad (8.9)
 \end{aligned}$$

with $k = l + yq + zp_1$.

Dirac algebra

Before we go on and simplify the Dirac structure of the numerator, we note, that from general principles one can decompose the complete α_s correction into three parts:

$$\frac{1}{2}\delta Z_2(p_2)\gamma^\mu + \frac{1}{2}\delta Z_2(p_1)\gamma^\mu + \delta\Gamma^\mu = A \cdot \gamma^\mu + B \cdot (p_1 - p_2)^\mu + C \cdot (p_1 + p_2)^\mu, \quad (8.10)$$

where A , B and C are functions of q^2 , m_1 and m_2 . However, in DY pair-production the term $(p_1 + p_2)^\mu = q^\mu$ does not contribute, since at the quark-lepton vertex the current is conserved, cf. Sec. 7.3.3. Therefore, we will neglect this term in the calculation of $\delta\Gamma^\mu$.

Using the contraction identities for $d = 4 - 2\epsilon'$ dimensions, cf. Appendix A, and under symmetry considerations of the momentum integration, cf. Sec. 2.3.4, one finds:

$$\begin{aligned} & \bar{v}_{s'}(p_2)\gamma^\alpha(\not{k} - \not{q} + m_2)\gamma^\mu(\not{k} + m_1)\gamma_\alpha u_s(p_1) \\ \rightarrow & v_{s'}(p_2) \left\{ \gamma^\mu \left[\frac{(2 - 2\epsilon')^2}{d} l^2 - 2q^2(1-x)(1-y) \right. \right. \\ & \left. \left. + m_1^2 \left(2z^2 + 2yz \left(1 - \frac{m_2^2}{m_1^2} \right) + 2z \left(\frac{m_2}{m_1} + \frac{m_2^2}{m_1^2} \right) - 2\frac{m_2}{m_1} \right) \right] \right. \\ & \left. + (p_1^\mu - p_2^\mu) (2yz(m_2 - m_1) + 2m_1z(1-z)) \right\} u_s(p_1), \quad (8.11) \end{aligned}$$

where we have kept the terms involving ϵ' only in the divergent part $\sim l^2$.

Dimensional regularisation

The result (8.11) leaves us with a UV divergent and a UV finite momentum integral. Drawing on our findings in Sec. 2.3 we recover:

$$\begin{aligned} \frac{(2 - 2\epsilon')^2}{d} \int \frac{d^d l}{(2\pi)^d} \frac{2l^2}{[l^2 - \Delta]^3} &= 2 \frac{(2 - 2\epsilon')^2}{d} \frac{i}{(4\pi)^2} \frac{d}{2} \frac{\Gamma(\epsilon')}{2} \left(\frac{4\pi\mu^2}{\Delta} \right)^{\epsilon'} \\ &= \frac{i}{(4\pi)^2} 2(1 - \epsilon')^2 \Gamma(\epsilon') \left(\frac{4\pi\mu^2}{\Delta} \right)^{\epsilon'} \\ &= 2 \left[\frac{1}{\epsilon'} - \gamma - 2 + \log \left(\frac{4\pi\mu^2}{\Delta} \right) \right] + O(\epsilon'). \quad (8.12) \end{aligned}$$

The second integral converges for $d = 4$:

$$\int \frac{d^d l}{(2\pi)^d} \frac{2}{[l^2 - \Delta]^3} \stackrel{\epsilon' \rightarrow 0}{=} \frac{-i}{(4\pi)^2} \frac{1}{\Delta}. \quad (8.13)$$

Inserting Eqs. (8.11-8.13) into Eq. (8.9), we find for the vertex correction:

$$\begin{aligned}
 \delta\Gamma^\mu &= \frac{\alpha_s}{4\pi} C_F \int_0^1 dx dy dz \delta(x+y+z-1) \\
 &\quad \left\{ \gamma^\mu 2 \left[\frac{1}{\epsilon'} - \gamma - 2 + \log \left(\frac{4\pi\mu^2}{\Delta} \right) \right] \right. \\
 &\quad - \frac{\gamma^\mu}{\Delta} \left[-2q^2(1-x)(1-y) \right. \\
 &\quad \quad \left. + m_1^2 \left(2z^2 + 2yz \left(1 - \frac{m_2^2}{m_1^2} \right) + 2z \left(\frac{m_2}{m_1} + \frac{m_2^2}{m_1^2} \right) - 2\frac{m_2}{m_1} \right) \right] \\
 &\quad \left. - \frac{p_1^\mu - p_2^\mu}{\Delta} (2yz(m_2 - m_1) + 2m_1z(1-z)) \right\} \\
 &= \frac{\alpha_s}{4\pi} C_F \left[\frac{1}{\epsilon'} - \gamma - 2 + \log \left(\frac{4\pi\mu^2}{m_1^2} \right) \right] \\
 &\quad + \frac{\alpha_s}{4\pi} C_F \int_0^1 dx dy dz \delta(x+y+z-1) \\
 &\quad \left\{ \gamma^\mu 2 \log \left(\frac{m_1^2}{\Delta} \right) \right. \\
 &\quad - \frac{\gamma^\mu}{\Delta} \left[-2q^2(1-x)(1-y) \right. \\
 &\quad \quad \left. + m_1^2 \left(2z^2 + 2yz \left(1 - \frac{m_2^2}{m_1^2} \right) + 2z \left(\frac{m_2}{m_1} + \frac{m_2^2}{m_1^2} \right) - 2\frac{m_2}{m_1} \right) \right] \\
 &\quad \left. - \frac{p_1^\mu - p_2^\mu}{\Delta} (2yz(m_2 - m_1) + 2m_1z(1-z)) \right\}. \tag{8.14}
 \end{aligned}$$

Adding the corrections of the wave function renormalisation processes, Eq. (8.4), one obtains:

$$\begin{aligned}
 & \frac{1}{2}\delta Z_2(p_1)\gamma^\mu + \frac{1}{2}\delta Z_2(p_2)\gamma^\mu + \delta\Gamma^\mu \\
 &= \frac{1}{2}\frac{\alpha_s}{4\pi}C_F\gamma^\mu \left[-4 - \frac{1}{\epsilon'} + \gamma - \log\left(\frac{4\pi\mu^2}{m_1^2}\right) - 2\log\left(\frac{\lambda^2}{m_1^2}\right) \right] \\
 &+ \frac{1}{2}\frac{\alpha_s}{4\pi}C_F\gamma^\mu \left[-4 - \frac{1}{\epsilon'} + \gamma - \log\left(\frac{4\pi\mu^2}{m_2^2}\right) - 2\log\left(\frac{\lambda^2}{m_2^2}\right) \right] \\
 &+ \frac{\alpha_s}{4\pi}C_F\gamma^\mu \left[\frac{1}{\epsilon'} - \gamma - 2 + \log\left(\frac{4\pi\mu^2}{m_1^2}\right) \right] \\
 &+ \frac{\alpha_s}{4\pi}C_F \int_0^1 dx dy dz \delta(x+y+z-1) \\
 &\quad \left\{ \gamma^\mu 2\log\left(\frac{m_1^2}{\Delta}\right) \right. \\
 &\quad - \frac{\gamma^\mu}{\Delta} \left[-2q^2(1-x)(1-y) \right. \\
 &\quad \quad \left. + m_1^2 \left(2z^2 + 2yz \left(1 - \frac{m_2^2}{m_1^2} \right) + 2z \left(\frac{m_2}{m_1} + \frac{m_2^2}{m_1^2} \right) - 2\frac{m_2}{m_1} \right) \right] \\
 &\quad \left. - \frac{p_1^\mu - p_2^\mu}{\Delta} (2yz(m_2 - m_1) + 2m_1z(1-z)) \right\} \\
 &= \frac{\alpha_s}{4\pi}C_F\gamma^\mu \left[-6 - \frac{1}{2}\log\left(\frac{m_1^2}{m_2^2}\right) - \log\left(\frac{\lambda^2}{m_1^2}\right) - \log\left(\frac{\lambda^2}{m_2^2}\right) \right] \\
 &+ \frac{\alpha_s}{4\pi}C_F \int_0^1 dx dy dz \delta(x+y+z-1) \\
 &\quad \left\{ \gamma^\mu 2\log\left(\frac{m_1^2}{\Delta}\right) \right. \\
 &\quad - \frac{\gamma^\mu}{\Delta} \left[-2q^2(1-x)(1-y) \right. \\
 &\quad \quad \left. + m_1^2 \left(2z^2 + 2yz \left(1 - \frac{m_2^2}{m_1^2} \right) + 2z \left(\frac{m_2}{m_1} + \frac{m_2^2}{m_1^2} \right) - 2\frac{m_2}{m_1} \right) \right] \\
 &\quad \left. - \frac{p_1^\mu - p_2^\mu}{\Delta} (2yz(m_2 - m_1) + 2m_1z(1-z)) \right\} . \tag{8.15}
 \end{aligned}$$

The calculation of the remaining integrals in the last equation is lengthy and we show the details in Appendix C. We have finally found the functions A and B of Eq. (8.10). We will only need the real parts of A and B , see Eq. (8.33) below:

$$\begin{aligned} \text{Re}(A) = \frac{\alpha_s}{4\pi} C_F \cdot \text{Re} \left(-3 + \log(1 - v^2) - \frac{1}{2} \left(\log(1 - \alpha^2) + \log(1 - (\alpha + \phi)^2) \right) \right. \\ \left. - \frac{\alpha}{2} \left(\log \frac{\alpha + 1}{\alpha - 1} + \log \frac{\alpha + \phi + 1}{\alpha + \phi - 1} \right) - \frac{\phi}{2} \log \frac{\alpha + \phi + 1}{\alpha + \phi - 1} + I_1 \right), \end{aligned} \quad (8.16)$$

with:

$$\begin{aligned} I_1 = -1 + \frac{\phi}{2} \log \frac{1 - v^2}{1 - v^2 - 2\phi} - \frac{4v^2 + 3\phi + \tau + \frac{\phi^2}{2}}{2\alpha + \phi} \left(\log \frac{\alpha - 1}{\alpha + 1} + \log \frac{\alpha + \phi - 1}{\alpha + \phi + 1} \right) \\ + 2(1 + v^2 + \phi) \cdot I_3 - 2 \log(\kappa) + \frac{3}{2} \log \left(\frac{m_1^2}{m_2^2} \right), \end{aligned} \quad (8.17)$$

$$\begin{aligned} I_3 = \frac{1}{2r} \left[\log(\kappa) \log \frac{1 + r - \frac{\phi}{2}}{1 - r - \frac{\phi}{2}} + \log \frac{v^2 - 1}{2r} \log \frac{r + 1 - \frac{\phi}{2}}{r - 1 - \frac{\phi}{2}} \right. \\ \left. - \frac{1}{2} \log^2 \left(r + 1 - \frac{\phi}{2} \right) + \frac{1}{2} \log^2 \left(r - 1 - \frac{\phi}{2} \right) \right. \\ \left. + \text{Li}_2 \left(\frac{r + 1 - \frac{\phi}{2}}{2r} \right) - \text{Li}_2 \left(\frac{r - 1 - \frac{\phi}{2}}{2r} \right) \right. \\ \left. + \log^2 \left(\sqrt{\frac{1 - v^2}{1 - v^2 - 2\phi}} \right) + \log \left(\sqrt{\frac{1 - v^2}{1 - v^2 - 2\phi}} \right) \log(\kappa) \right], \end{aligned} \quad (8.18)$$

$$\begin{aligned} \text{Re}(B) = \\ \frac{\alpha_s}{4\pi} \frac{1}{m_1} \cdot \text{Re} \left[\frac{\frac{\tau}{4}(1 - \alpha) + \frac{v^2 - 1}{2}}{2\alpha + \phi} \left(\log \frac{\alpha - 1}{\alpha + 1} + \log \frac{\alpha + \phi - 1}{\alpha + \phi + 1} \right) - \frac{\tau}{4} \log \frac{\alpha + \phi + 1}{\alpha + \phi - 1} \right]. \end{aligned} \quad (8.19)$$

The auxiliary functions are given by:

$$v = \sqrt{1 - \frac{4m_1^2}{q^2}}, \quad (8.20)$$

$$\tau = (1 - v^2) \cdot \left(1 - \frac{m_2}{m_1} \right), \quad (8.21)$$

$$\phi = \frac{1}{2} \cdot \left(1 - \frac{m_2^2}{m_1^2} \right) \cdot (1 - v^2), \quad (8.22)$$

$$\alpha = -\frac{\phi}{2} + \sqrt{\phi + v^2 + \frac{\phi^2}{4}}, \quad (8.23)$$

$$r = \sqrt{\phi + v^2 + \frac{\phi^2}{4}}, \quad (8.24)$$

$$\kappa = \frac{\lambda^2}{m_1^2}. \quad (8.25)$$

Li_2 is the Dilogarithm of Sec. 3.1.2.

Form factors

The Gordon identity [PS95] for the case of different masses m_1 and m_2 reads:

$$\bar{v}(p_2, m_2) \gamma^\mu u(p_1, m_1) = \bar{v}(p_2, m_2) \left(\frac{(p_1 - p_2)^\mu}{m_1 + m_2} + \frac{i\sigma^{\mu\nu} q_\nu}{m_1 + m_2} \right) u(p_1, m_1), \quad (8.26)$$

and so we find:

$$\begin{aligned} M &= M_{\text{LO}} + M_{\text{VC}} \\ &= e \bar{v}_{s'}(p_2) \left[\gamma^\mu + \frac{1}{2} \delta Z_2(p_2) \gamma^\mu + \frac{1}{2} \delta Z_2(p_1) \gamma^\mu + \delta \Gamma^\mu \right] u_s(p_1) \cdot \epsilon_\mu^*(q) \\ &= e \bar{v}_{s'}(p_2) \left[\gamma^\mu (1 + A) + B (p_1 - p_2)^\mu \right] u_s(p_1) \cdot \epsilon_\mu^*(q) \\ &= e \bar{v}_{s'}(p_2) \left[\gamma^\mu \cdot (1 + A + (m_1 + m_2)B) + \frac{i\sigma^{\mu\nu} q_\nu}{m_1 + m_2} \cdot (-(m_1 + m_2)B) \right] u_s(p_1) \cdot \epsilon_\mu^*(q). \end{aligned} \quad (8.27)$$

We can now identify the well known form factors F_1 and F_2 [PS95]:

$$F_1 = 1 + A + (m_1 + m_2)B, \quad (8.28)$$

$$F_2 = -(m_1 + m_2)B. \quad (8.29)$$

We have checked and confirmed that in the limit of equal masses $m_2 \rightarrow m_1$ the well known formula for $F_1(q^2, m^2)$ [Mut98, BGG73] is recovered. We note that also for unequal masses the UV divergences of the loops, displayed in Figs. 8.1, 8.2, cancel, cf. Eq. (8.15). This is by virtue of the Ward-Takahashi identities, which are fulfilled at the quark-gluon vertices, since there by construction the mass of the quark does not change. However, for $m_1 \neq m_2$ one finds that current conservation is violated at the quark-photon vertex (the full amplitude conserves the current, see Sec. 7.3.3).

The gauge dependence of the quark-photon vertex results in a finite renormalisation of the charge, which cannot be canceled by gauge invariant counter terms. Therefore one finds:

$$\lim_{q^2 \rightarrow 0} F_1(q^2, m_1^2, m_2^2) \neq 1. \quad (8.30)$$

On the other hand, $q^2 = M^2$ sets the hard scale in DY pair production and thus our model should only be applied at reasonably large q^2 . A sensible lower limit would be $q^2 > 1 \text{ GeV}^2$. Thus, we probe F_1 far away from $q^2 = 0$ and we will show in Sec. 8.1.6 that for these physically interesting q^2 the influence of the renormalised charge is negligible.

8.1.2 Cross section

The squared, averaged and summed amplitude of Eq. (8.27) can be written as:

$$\begin{aligned} |\bar{M}|^2 &= |\bar{M}_{\text{LO}}|^2 + \overline{M_{\text{LO}} M_{\text{VC}}^*} + \overline{M_{\text{LO}}^* M_{\text{VC}}} + O(\alpha_s^2) \\ &= |\bar{M}_{\text{LO}}|^2 + 2\text{Re}(\overline{M_{\text{LO}} M_{\text{VC}}^*}) + O(\alpha_s^2) \\ &= \frac{e^2}{4} (-g_{\mu\nu}) \left\{ \text{TR} [(\not{p}_2 - m_2)\gamma^\mu(\not{p}_1 + m_1)\gamma^\nu] \right. \\ &\quad + 2\text{Re}(A)\text{TR} [(\not{p}_2 - m_2)\gamma^\mu(\not{p}_1 + m_1)\gamma^\nu] \\ &\quad \left. + 2\text{Re}(B)\text{TR} [(\not{p}_2 - m_2)\gamma^\mu(\not{p}_1 + m_1)(p_1 - p_2)^\nu] \right\} \end{aligned} \quad (8.31)$$

The first term in the curly brackets is just the matrix element of the LO process. The other terms contain all the order α_s interferences of the processes in Figs. 8.1 and 8.2. Using our results of Sec. 7.3.2 we can express the order α_s interference cross section for the process $q\bar{q} \rightarrow l^+l^-$ as:

$$d\hat{\sigma}_{\text{VC}} = \frac{4\pi\alpha^2}{9q^4} \frac{T_{\text{VC}}}{4\sqrt{(p_1 \cdot p_2)^2 - m_1^2 m_2^2}} \delta^{(4)}(p_1 + p_2 - q) \frac{d^3q}{2E_q}, \quad (8.32)$$

where we have used the LO cross section (7.27) and where:

$$\begin{aligned} T_{\text{VC}} &= \left(-g_{\mu\nu} + \frac{q_\mu q_\nu}{q^2} \right) \left(2\text{Re}(A) \cdot \text{Tr} [(\not{p}_2 - m_2)\gamma^\mu(\not{p}_1 + m_1)\gamma^\nu] \right. \\ &\quad \left. + 2\text{Re}(B) \cdot \text{Tr} [(\not{p}_2 - m_2)\gamma^\mu(\not{p}_1 + m_1)] \cdot (p_1 - p_2)^\nu \right). \end{aligned} \quad (8.33)$$

Note that $d\hat{\sigma}_{\text{VC}}$ depends on the gluon mass λ of Eq. (8.25) and so does the cross section for gluon bremsstrahlung, as we will see in Sec. 8.3.1. Only the sum of the two cross sections is a physically meaningful quantity, as we will show in the next subsection.

8.1.3 Soft gluon divergence

To obtain Eqs. (8.16-8.25) we have assigned to the gluon a mass λ which serves as an IR regulator in the loop integral. This is exactly the same mass we introduced in Sec. 5.2 to regulate the divergence of the bremsstrahlung processes in the soft gluon region. We will now show, that in the sum of the processes this fictitious gluon mass will exactly cancel.

From Eqs. (8.16- 8.25) we find, that only the real part of A depends on the mass λ . Therefore, we collect all λ -dependent parts of A :

$$\begin{aligned} & \text{Re}(A^\lambda) \\ &= \frac{\alpha_s}{4\pi} C_F \log\left(\frac{\lambda^2}{m_1^2}\right) \text{Re}\left[-2 + \frac{1+v^2+\phi}{r} \left(\log\frac{1+r-\frac{\phi}{2}}{1-r-\frac{\phi}{2}} + \log\left(\sqrt{\frac{1-v^2}{1-v^2-2\phi}}\right)\right)\right]. \end{aligned} \quad (8.34)$$

Now we note, that the real part of A simply multiplies the cross section of the LO process, cf. Eqs. (7.27, 8.32, 8.33) and so the λ -dependent part of the cross section reads:

$$d\hat{\sigma}_{\text{VC}}^\lambda = 2\text{Re}(A^\lambda) \cdot d\hat{\sigma}_{\text{LO}}. \quad (8.35)$$

Rewriting the terms in Eq. (8.34) piece by piece one obtains:

$$1 + v^2 + \phi = \frac{2}{q^2} (q^2 - m_1^2 - m_2^2), \quad (8.36)$$

$$r = \frac{\sqrt{(q^2 - m_1^2 - m_2^2)^2 - 4m_1^2 m_2^2}}{q^2}, \quad (8.37)$$

$$\begin{aligned} \frac{1+r-\frac{\phi}{2}}{1-r-\frac{\phi}{2}} &= \frac{q^2 - m_1^2 + m_2^2 + \sqrt{(q^2 - m_1^2 - m_2^2)^2 - 4m_1^2 m_2^2}}{q^2 + m_1^2 - m_2^2 - \sqrt{(q^2 - m_1^2 - m_2^2)^2 - 4m_1^2 m_2^2}} \\ &= \frac{q^2 - m_1^2 - m_2^2 + \sqrt{(q^2 - m_1^2 - m_2^2)^2 - 4m_1^2 m_2^2}}{2m_1^2} \\ &= \alpha_+, \end{aligned} \quad (8.38)$$

$$\sqrt{\frac{1-v^2}{1-v^2-2\phi}} = \sqrt{\frac{m_1^2}{m_2^2}} = \frac{m_1}{m_2}, \quad (8.39)$$

where we found α_+ already in Eq. (5.48). Thus, we recover:

$$\text{Re}(A^\lambda) = \frac{\alpha_s}{4\pi} C_F \log\left(\frac{\lambda^2}{m_1^2}\right) \text{Re}\left[-2 + \frac{2(q^2 - m_1^2 - m_2^2)}{\sqrt{(q^2 - m_1^2 - m_2^2)^2 - 4m_1^2 m_2^2}} \log\left(\alpha_+ \frac{m_1}{m_2}\right)\right]. \quad (8.40)$$

Since A^λ is a real number, the λ -dependent part of the cross section becomes:

$$\begin{aligned} & d\hat{\sigma}_{\text{VC}}^\lambda \\ &= d\hat{\sigma}_{\text{LO}} \frac{\alpha_s}{2\pi} C_F \log\left(\frac{\lambda^2}{m_1^2}\right) \left[-2 + \frac{2(q^2 - m_1^2 - m_2^2)}{\sqrt{(q^2 - m_1^2 - m_2^2)^2 - 4m_1^2 m_2^2}} \log\left(\alpha_+ \frac{m_1}{m_2}\right) \right]. \end{aligned} \quad (8.41)$$

In Sec. 5.2.2 we found for the bremsstrahlung cross section in the soft gluon region:

$$d\hat{\sigma}_{\text{B}}^\lambda = d\hat{\sigma}_{\text{LO}} \frac{\alpha_s}{2\pi} C_F \log\left(\frac{4\omega^2}{\lambda^2}\right) \left[-2 - \frac{\alpha_+(m_1^2 + m_2^2 - q^2)}{\alpha_+^2 m_1^2 - m_2^2} \log\left(\frac{\alpha_+^2 m_1^2}{m_2^2}\right) \right]. \quad (8.42)$$

We note the following relation:

$$\begin{aligned} & \frac{\alpha_+}{\alpha_+^2 m_1^2 - m_2^2} \\ &= 2 \frac{2m_1^2 \alpha_+}{\alpha_+^2 4m_1^4 - 4m_1^2 m_2^2} \\ &= \frac{q^2 - m_1^2 - m_2^2 + \sqrt{(q^2 - m_1^2 - m_2^2)^2 - 4m_1^2 m_2^2}}{(q^2 - m_1^2 - m_2^2)^2 - 4m_1^2 m_2^2 + (q^2 - m_1^2 - m_2^2) \sqrt{(q^2 - m_1^2 - m_2^2)^2 - 4m_1^2 m_2^2}} \\ &= \frac{1}{\sqrt{(q^2 - m_1^2 - m_2^2)^2 - 4m_1^2 m_2^2}} \end{aligned} \quad (8.43)$$

Thus, the bremsstrahlung cross section reads:

$$d\hat{\sigma}_{\text{B}}^\lambda = d\hat{\sigma}_{\text{LO}} \frac{\alpha_s}{2\pi} C_F \log\left(\frac{4\omega^2}{\lambda^2}\right) \left[-2 + 2 \frac{q^2 - m_1^2 - m_2^2}{\sqrt{(q^2 - m_1^2 - m_2^2)^2 - 4m_1^2 m_2^2}} \log\left(\frac{\alpha_+ m_1}{m_2}\right) \right], \quad (8.44)$$

and so the sum of the two cross sections is independent of the gluon mass λ :

$$\begin{aligned} & d\hat{\sigma}_{\text{VC}}^\lambda + d\hat{\sigma}_{\text{B}}^\lambda \\ &= \frac{\alpha_s}{2\pi} C_F \log\left(\frac{4\omega^2}{m_1^2}\right) \left[-2 + 2 \frac{q^2 - m_1^2 - m_2^2}{\sqrt{(q^2 - m_1^2 - m_2^2)^2 - 4m_1^2 m_2^2}} \log\left(\frac{\alpha_+ m_1}{m_2}\right) \right]. \end{aligned} \quad (8.45)$$

This is an explicit analytic verification of the theorems by Kinoshita-Poggio-Quinn [Kin62, KU76, PQ76, Ste76] and Kinoshita-Lee-Nauenberg [Kin62, LN64] for our model.

Based on this analysis we will also introduce the same gluon mass λ in our calculation of the full bremsstrahlung contribution (not just the soft gluon part) in Sec.

8.3 and we will show in our results in Part V, that the two divergences also actually cancel numerically, as they should. Note that this implies, that only the sum of the bremsstrahlung and vertex correction processes is a physically meaningful quantity and, thus, we will only plot the sum of the two in our results.

8.1.4 Kinematics

Since the vertex correction processes share initial and final states with the LO process, the hadronic cross section of the vertex correction is calculated exactly as described for the LO mass distribution case in Sec. 7.4.4.

8.1.5 Current conservation

As shown in Figs. 8.1 and 8.2 we always keep the quark masses fixed at any quark-gluon vertex. This ensures that all our calculations are also current conserving in the strong sector. The proof goes as follows: in Eq. (8.3) we already found the amplitude for the vertex correction processes. It reads:

$$iM_{\text{VC}} = ie\bar{v}_{s'}(p_2) \left[\frac{1}{2}\delta Z_2(p_2)\gamma^\mu + \frac{1}{2}\delta Z_2(p_1)\gamma^\mu + \delta\Gamma^\mu \right] u_s(p_1) \cdot \epsilon_\mu^*(q). \quad (8.46)$$

To prove current conservation we now have to calculate the gluon gauge dependent parts of $\delta\Gamma^\mu$ and δZ_2 , which we denote by the index g . We begin with $\delta\Gamma_g^\mu$. We denote the gluon momentum with k , insert only the gauge dependent part of the gluon propagator ($k^\alpha k^\beta$), cf. Appendix B, and exploit the Dirac equation, cf. Appendix

A:

$$\begin{aligned}
 & ie\bar{v}_{s'}(p_2) \delta\Gamma_g^\mu u_s(p_1) \\
 &= \int d^4k \bar{v}_{s'}(p_2) (ig\gamma_\alpha t^a) \frac{i(-\not{p}_2 - \not{k} + m_2)}{(p_2 + k)^2 - m_2^2} ie\gamma^\mu \frac{i(\not{p}_1 - \not{k} + m_1)}{(p_1 - k)^2 - m_1^2} (ig\gamma_\beta t^a) u_s(p_1) \\
 &\quad \times \frac{ik^\alpha k^\beta}{k^2} \frac{1}{k^2} \\
 &= -e4\pi\alpha_s(t^a t^a) \int d^4k \bar{v}_{s'}(p_2) \not{k} \frac{-\not{p}_2 - \not{k} + m_2}{(p_2 + k)^2 - m_2^2} \gamma^\mu \frac{\not{p}_1 - \not{k} + m_1}{(p_1 - k)^2 - m_1^2} \not{k} u_s(p_1) \cdot \frac{1}{k^4} \\
 &= -e4\pi\alpha_s(t^a t^a) \int d^4k \bar{v}_{s'}(p_2) ((-\not{p}_2 - m_2) - (-\not{p}_2 - \not{k} - m_2)) \\
 &\quad \times \frac{-\not{p}_2 - \not{k} + m_2}{(p_2 + k)^2 - m_2^2} \gamma^\mu \frac{\not{p}_1 - \not{k} + m_1}{(p_1 - k)^2 - m_1^2} \not{k} u_s(p_1) \cdot \frac{1}{k^4} \\
 &= -e4\pi\alpha_s(t^a t^a) \int d^4k \bar{v}_{s'}(p_2) (-1) \gamma^\mu \frac{\not{p}_1 - \not{k} + m_1}{(p_1 - k)^2 - m_1^2} \\
 &\quad \times ((-\not{p}_1 + \not{k} + m_1) - (-\not{p}_1 + m_1)) u_s(p_1) \cdot \frac{1}{k^4} \\
 &= -e4\pi\alpha_s(t^a t^a) \int d^4k \bar{v}_{s'}(p_2) (-1) \gamma^\mu (-1) u_s(p_1) \cdot \frac{1}{k^4} \\
 &= -e4\pi\alpha_s(t^a t^a) \int d^4k \bar{v}_{s'}(p_2) \frac{\gamma^\mu}{k^4} u_s(p_1) . \tag{8.47}
 \end{aligned}$$

The renormalisation factor $\delta Z_2^g(p)$ is connected to the QCD quark selfenergy, cf. Eq. (4.90):

$$\delta Z_2^g(p) = \left. \frac{\partial \Sigma^g(p)}{\partial \not{p}} \right|_{\not{p}=m} . \tag{8.48}$$

The gauge dependent part of the quark selfenergy is given by:

$$\begin{aligned}
 -i\Sigma^g(p) &= \int d^4k (ig\gamma_\alpha t^a) \frac{i(\not{p}_1 - \not{k} + m_1)}{(p_1 - k)^2 - m_1^2} (ig\gamma_\beta t^a) \cdot \frac{ik^\alpha k^\beta}{k^2} \frac{1}{k^2} \\
 \Rightarrow \Sigma^g(p) &= i4\pi\alpha_s(t^a t^a) \int d^4k \not{k} \frac{\not{p}_1 - \not{k} + m_1}{(p_1 - k)^2 - m_1^2} \not{k} \cdot \frac{1}{k^4} . \tag{8.49}
 \end{aligned}$$

Now we find for the renormalisation factor:

$$\begin{aligned}
\delta Z_2^g(p) &= i4\pi\alpha_s(t^a t^a) \int d^4k \, k \cdot \frac{\partial}{\partial p} \left(\frac{p - k + m}{(p - k)^2 - m^2} \right) \Big|_{p=m} \cdot k \cdot \frac{1}{k^4} \\
&= i4\pi\alpha_s(t^a t^a) \int d^4k \, k \cdot \left(\frac{1}{p^2 - pk - kp + k^2 - m^2} \right. \\
&\quad \left. + \frac{(p - k + m)(-2p + 2k)}{(p^2 - pk - kp + k^2 - m^2)^2} \right) \Big|_{p=m} \cdot k \cdot \frac{1}{k^4} \\
&= i4\pi\alpha_s(t^a t^a) \int d^4k \left(\frac{1}{-2mk + k^2} + \frac{(-k + 2m)(-2m + 2k)}{(-2mk + k^2)^2} \right) \cdot \frac{1}{k^2} \\
&= i4\pi\alpha_s(t^a t^a) \int d^4k \left(\frac{-2mk + k^2 + (-k + 2m)(-2m + 2k)}{k^2(4m^2 - 4mk + k^2)^2} \right) \cdot \frac{1}{k^2} \\
&= i4\pi\alpha_s(t^a t^a) \int d^4k \cdot \frac{-1}{k^4} . \tag{8.50}
\end{aligned}$$

Thus, the gauge dependent part of the amplitude becomes:

$$\begin{aligned}
&ie\bar{v}_{s'}(p_2) \left[\frac{1}{2}\delta Z_2^g(p_1) + \frac{1}{2}\delta Z_2^g(p_2) + \delta\Gamma_g^\mu \right] u_s(p_1) \\
&= ie\bar{v}_{s'}(p_2) \left[\gamma^\mu \left(i4\pi\alpha_s(t^a t^a) \int d^4k \cdot \frac{-1}{k^4} \right) + i4\pi\alpha_s(t^a t^a) \int d^4k \frac{\gamma^\mu}{k^4} \right] u_s(p_1) \\
&= 0 , \tag{8.51}
\end{aligned}$$

and so the amplitude in Eq. (8.46) indeed conserves the current.

8.1.6 Renormalised charge

As already mentioned in Sec. 8.1.1, we unintentionally renormalised the charge at the quark-photon vertex by assigning different masses m_1 and m_2 to the annihilating quark and antiquark, which violates current conservation, and, thus, gauge invariance, at the quark-photon vertex, see Sec. 7.3.3. Thus, we obtain:

$$\lim_{q^2 \rightarrow 0} F_1(q^2, m_1^2, m_2^2) \neq 1 , \tag{8.52}$$

which we illustrate in Fig. 8.3. There we plot the real part of the correction δF_1 to F_1 to order α_s for small $\sqrt{q^2}$. The correction is defined by:

$$F_1 = 1 + \frac{\alpha_s}{4\pi} \delta F_1 . \tag{8.53}$$

As one can see, δF_1 approaches zero for the case of equal quark masses $m_1 = m_2 = 0.1$ GeV, as it should according to the Ward-Takahashi identities. However, for different quark masses (in our example: $m_1 = 0.1$ GeV, $m_2 = 0.5$ GeV) this is clearly not the case.

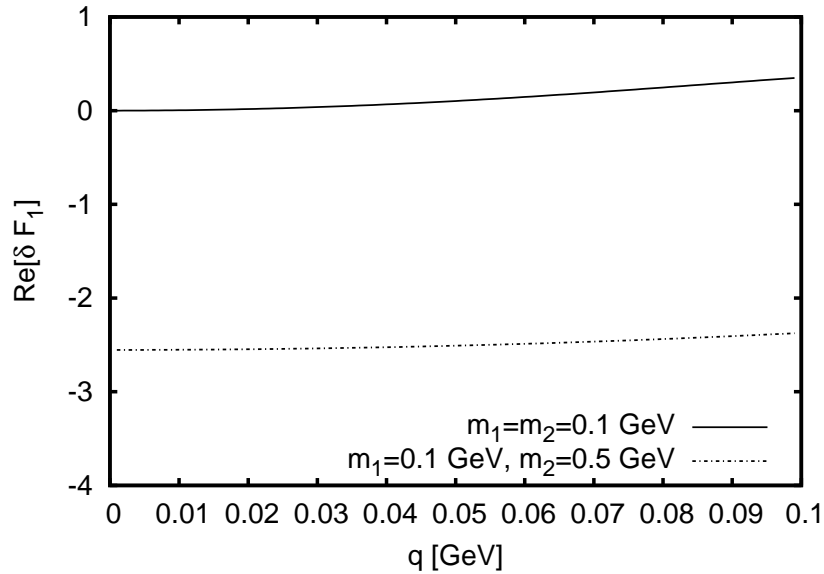


Figure 8.3: Correction to F_1 at order α_s for equal quark masses (solid) and different quark masses (dashed). See main text for details.

This behavior could potentially spoil our calculations. One should note, however, that we always stay far away from $q^2 = 0$, since $q^2 = M^2$ sets the hard scale for our calculations. Therefore, reasonable physical values of q^2 are larger than 1 GeV. To study the influence of different quark masses in the physically interesting range of q^2 we devise the following scheme: to calculate the hadronic cross section we weight the partonic subprocess cross sections by quark mass distributions (spectral functions), see Sec. 7.5.2. Thus also the form factor $F_1(q^2, m_1^2, m_2^2)$ is weighted by these distributions in our calculation. Therefore, it is worthwhile to compare the weighted form factors for different masses, $F_1(q^2, m_1^2, m_2^2)$, and for equal masses, $F_1(q^2, m^2, m^2)$, for physically interesting q^2 . Because of Eq. (8.53) it suffices to compare only the corrections δF_1 and so we define:

$$\delta \hat{F}_1(q^2) = \int_0^{m_N^2} dm^2 A(p) \delta F_1(q^2, m^2, m^2), \quad (8.54)$$

with the spectral function $A(p)$ defined in Eq. (7.127). Now we know that $\delta F_1(q^2, m^2, m^2)$

shows the correct low q^2 behavior:

$$\lim_{q^2 \rightarrow 0} \delta F_1(q^2, m^2, m^2) = 0, \quad (8.55)$$

and we know that the spectral function is normalised to 1, see Eq. (7.129). Therefore, also the weighted correction shows the right behavior for $q^2 \rightarrow 0$:

$$\lim_{q^2 \rightarrow 0} \delta \hat{F}_1(q^2) = \int_0^{m_N^2} dm^2 A(p) \cdot \lim_{q^2 \rightarrow 0} \delta F_1(q^2, m^2, m^2) = 1 \cdot 0 = 0. \quad (8.56)$$

Next we define the weighted correction for different masses:

$$\delta \tilde{F}_1(q^2) = \int_0^{m_N^2} dm_1^2 \int_0^{m_N^2} dm_2^2 A(p_1) A(p_2) \delta F_1(q^2, m_1^2, m_2^2). \quad (8.57)$$

In Fig. 8.4 we compare the real parts of $\delta \hat{F}_1(q^2)$ and $\delta \tilde{F}_1(q^2)$ for $\sqrt{q^2} = 1 \dots 20$ GeV. As one can see they agree very well over the entire range. Thus we conclude that the wrong behavior of $\delta F_1(q^2, m_1^2, m_2^2)$ near $q^2 = 0$ ultimately does not affect our calculations.

8.2 General kinematics of partonic NLO cross sections

In this section we shortly present the kinematic scheme, in which the remaining NLO calculations of this chapter are performed. Fig. 8.5 is a reference for our notation. For the initial particles we choose four-momenta p_1 and p_2 and masses m_1 and m_2 . For the final state we always choose q as the four momentum of the virtual photon, i.e., the DY pair, and $M = \sqrt{q^2}$ as its mass. We define the four momentum of the remaining final state particle as r and its mass as m_r (both 0 at LO). The differential partonic cross section then takes the following general form (the differential dM^2 is a remnant of the phase space integral of the lepton pair, cf. Sec. 7.3.2):

$$d\hat{\sigma} = F(p_1, p_2, q, r) \cdot \delta^{(4)}(p_1 + p_2 - q - r) dM^2 \frac{d^3q}{E_q} \frac{d^3r}{2E_r}, \quad (8.58)$$

where F contains squared matrix elements, the flux factor and constants and E_q (E_r) are the energies of the particles with momenta q (r). The Mandelstam variables read:

$$s = (p_1 + p_2)^2, \quad (8.59)$$

$$t = (p_2 - q)^2, \quad (8.60)$$

$$u = (p_1 - q)^2. \quad (8.61)$$

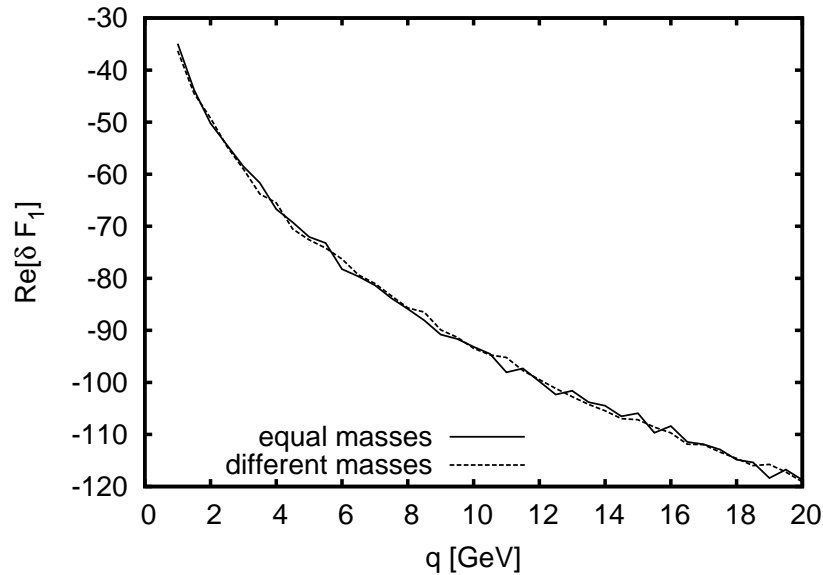


Figure 8.4: Comparison of the real parts of the weighted corrections to F_1 at order α_s for equal quark masses (solid) and different quark masses (dashed). For the spectral functions a width $\Gamma = 0.2$ GeV and a large quark momentum component $p^+ = \frac{q}{2}$ was chosen, cf. Eqs. (7.126-7.128). The gluon mass was set to $\lambda = 0.05$ GeV, cf. Eq. (8.25). Both curves agree well over the entire range.

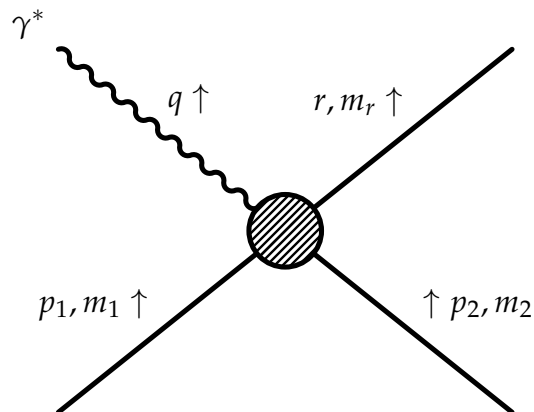


Figure 8.5: General kinematics of hard NLO subprocesses of DY production.

In DY measurements the common observables are the invariant mass M , the absolute transverse momentum p_T and the longitudinal momentum q_z of the lepton pair. Thus we can integrate Eq. (8.58) over the phase space of r :

$$\begin{aligned} d\hat{\sigma} &= F(s, t, M^2, m_1^2, m_2^2, m_r^2) \cdot \delta((p_1 + p_2 - q)^2 - m_r^2) dM^2 \frac{d^3q}{E_q} \\ &= F(s, t, M^2, m_1^2, m_2^2, m_r^2) \cdot \delta((p_1 + p_2 - q)^2 - m_r^2) dM^2 \frac{|\vec{q}|^2 d|\vec{q}| d\phi d\cos\theta}{E_q}. \end{aligned} \quad (8.62)$$

We note the following relations:

$$\frac{dE_q}{d|\vec{q}|} = \frac{|\vec{q}|}{E_q}, \quad (8.63)$$

$$\begin{aligned} t &= (p_2 - q)^2 = m_2^2 + M^2 - 2(E_2 E_q - |\vec{p}_2| |\vec{q}| \cos\theta) \\ &\Rightarrow \frac{dt}{d\cos\theta} = 2|\vec{p}_2| |\vec{q}|. \end{aligned} \quad (8.64)$$

In the partonic center-of-mass frame one finds $|\vec{p}_1| = |\vec{p}_2| = p_{\text{cm}}$, with the center-of-mass momentum of the incoming states [Group10]:

$$p_{\text{cm}} = \frac{\sqrt{(s - (m_1 + m_2)^2)(s - (m_1 - m_2)^2)}}{2\sqrt{s}}. \quad (8.65)$$

Then the partonic cross section can be written as:

$$\begin{aligned} \frac{d\hat{\sigma}}{dM^2 dt} &= F(s, t, M^2, m_1^2, m_2^2, m_r^2) \cdot \delta(s + M^2 - 2\sqrt{s}E_q - m_r^2) \frac{2\pi}{2p_{\text{cm}}} dE_q \\ &= F(s, t, M^2, m_1^2, m_2^2, m_r^2) \frac{2\pi}{2\sqrt{s}2p_{\text{cm}}} \\ &= \frac{\pi}{2\sqrt{s}p_{\text{cm}}} \cdot F(s, t, M^2, m_1^2, m_2^2, m_r^2). \end{aligned} \quad (8.66)$$

Now comparing Eqs. (8.58) and (8.66) one finds (cf. [HS78]):

$$\frac{E_q d\hat{\sigma}}{dM^2 d^3q} = \frac{2\sqrt{s}p_{\text{cm}}}{\pi} \cdot \frac{d\hat{\sigma}}{dM^2 dt} \cdot \delta\left((p_1 + p_2 - q)^2 - m_r^2\right). \quad (8.67)$$

Rewriting the photon momentum in terms of p_T and x_F and integrating over the angle in the \vec{p}_T -plane finally yields:

$$\frac{d\hat{\sigma}}{dM^2 dp_T^2 dx_F} = \frac{2\sqrt{s}p_{\text{cm}}(q_z)_{\text{max}}}{E_q} \cdot \frac{d\hat{\sigma}}{dM^2 dt} \cdot \delta\left((p_1 + p_2 - q)^2 - m_r^2\right). \quad (8.68)$$

Thus, for the NLO subprocesses in the following sections with two particles (virtual photon + quark/gluon) in the final state we actually only have to calculate $\frac{d\hat{\sigma}}{dM^2 dt}$ and can then use the relation (8.68) to obtain the partonic cross sections relevant for our model.

8.3 Gluon bremsstrahlung

DY pair production with gluon bremsstrahlung is depicted in Fig. 8.6. Here either the quark or the antiquark emits a real gluon before annihilating. Note that these processes share the initial state with the LO and vertex correction processes of Sec. 8.1. Note also, that we keep the quark masses at the quark-gluon vertices fixed, since otherwise current conservation would be violated. It poses no problem, that the quark mass changes at the quark-photon vertex, as we showed in detail in Sec. 7.3.3.

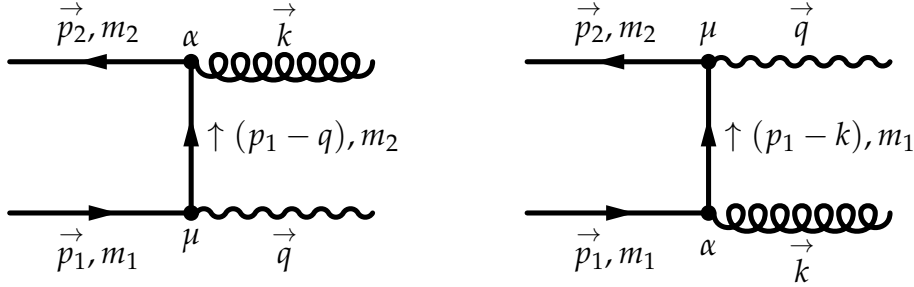


Figure 8.6: Gluon bremsstrahlung processes for DY production at NLO.

8.3.1 Cross section

We already found the cross section for the process $q\bar{q} \rightarrow \gamma^*g$ in Eqs. (5.21) and (5.22). Using the results of Sec. 7.3.2 we can immediately derive the partonic cross section for the process $q\bar{q} \rightarrow l^+l^-g$, which we consider here:

$$d\hat{\sigma}_B = \frac{(2\pi)^4 \delta^{(4)}(p_1 + p_2 - k - q)}{4\sqrt{(p_1 \cdot p_2)^2 - m_1^2 m_2^2}} |\overline{M}|^2 dM^2 \frac{d^3q}{(2\pi)^3 2E_q} \frac{d^3k}{(2\pi)^3 2E_k}, \quad (8.69)$$

where the spin averaged and squared amplitude reads:

$$|\overline{M}|^2 = \frac{4}{9} \frac{e^2 g^2}{4} \frac{\alpha}{3\pi M^2} \text{Tr} [(\not{p}_2 - m_2) S^{\alpha\mu} (\not{p}_1 + m_1) S^\nu_\alpha] \cdot \left(g_{\mu\nu} - \frac{q_\mu q_\nu}{q^2} \right), \quad (8.70)$$

with

$$S^{\alpha\beta} = \gamma^\alpha \frac{\not{p}_1 - \not{q} + m_2}{(p_1 - q)^2 - m_2^2} \gamma^\beta + \gamma^\beta \frac{\not{q} - \not{p}_2 + m_1}{(p_2 - q)^2 - m_1^2} \gamma^\alpha. \quad (8.71)$$

Here $\frac{4}{9}$ is the color factor (cf. Appendix B.2) and in the following we use:

$$T_B = \left(g_{\mu\nu} - \frac{q_\mu q_\nu}{q^2} \right) \cdot \text{Tr} [(\not{p}_2 - m_2) S^{\alpha\mu} (\not{p}_1 + m_1) S^\nu_\alpha]. \quad (8.72)$$

For completeness we give our result for T_B in Appendix C.2.1.

We assign the same fictitious mass λ to the gluon as for the vertex correction process in Sec. 8.1. This ensures the cancellation of the soft gluon divergences, as we have already shown in Sec. 8.1.3. Integrating over the phase space of the gluon the partonic cross section becomes:

$$\begin{aligned}
 d\hat{\sigma}_B &= \frac{4}{9} \frac{\alpha^2 \alpha_s}{3\pi M^2} \frac{T_B}{4\sqrt{(p_1 \cdot p_2)^2 - m_1^2 m_2^2}} \cdot \delta\left((p_1 + p_2 - q)^2 - \lambda^2\right) dM^2 \frac{d^3 q}{2E_q} \\
 &= \frac{4}{9} \frac{\alpha^2 \alpha_s}{3\pi M^2} \frac{T_B}{4\sqrt{s} p_{\text{cm}}} \cdot \delta\left(s + M^2 - 2\sqrt{s} E_q - \lambda^2\right) dM^2 \frac{|\vec{q}|^2 d|\vec{q}|^2 d\phi d\cos\theta}{2E_q} \\
 &= \frac{4}{9} \frac{\alpha^2 \alpha_s}{3\pi M^2} \frac{T_B}{4\sqrt{s} p_{\text{cm}}} \frac{\pi}{2\sqrt{s} 2p_{\text{cm}}} \Theta(E_g) dM^2 dt, \tag{8.73}
 \end{aligned}$$

with the energy of the gluon E_g . Thus the relevant partonic cross section reads ($E_g \geq \lambda$):

$$\frac{d\hat{\sigma}_B}{dM^2 dt} = \frac{4}{9} \frac{\alpha^2 \alpha_s}{48M^2} \cdot \frac{T_B}{s p_{\text{cm}}^2} \cdot \Theta(E_g). \tag{8.74}$$

The calculation of the hadronic cross section basically follows along the same lines as for the LO case in Sec. 7.4. Once again one has to remove unphysical solutions for the momentum fractions x_i , however, the calculation of the phase space is more subtle, as we will show in the next subsection.

8.3.2 Kinematics

The hadronic cross section for gluon bremsstrahlung can be written as, cf. Eqs. (8.68) and (7.107):

$$\begin{aligned}
 \frac{d\sigma_B}{dM^2 dp_T^2 dx_F} &= \int_0^1 dx_1 \int_0^1 dx_2 \int d\vec{p}_{1\perp} \int d\vec{p}_{2\perp} \int dm_1^2 \int dm_2^2 \\
 &\quad \times \sum_i q_i^2 \hat{f}_i(x_1, \vec{p}_{1\perp}, m_1^2, q^2) \hat{f}_{\bar{i}}(x_2, \vec{p}_{2\perp}, m_2^2, q^2) \cdot \frac{2\sqrt{s} p_{\text{cm}}(q_z)_{\text{max}}}{E_q} \\
 &\quad \times \frac{d\hat{\sigma}_B}{dM^2 dt} \delta\left((p_1 + p_2 - q)^2 - \lambda^2\right). \tag{8.75}
 \end{aligned}$$

Again, the \hat{f}_i are our unintegrated parton distributions, see Sec. 7.5.2, the partonic cross section $\frac{d\hat{\sigma}_B}{dM^2 dt}$ is given in Eq. (8.74) and λ is the fictitious gluon mass, introduced to regulate the soft divergence. Now we collect everything except δ - and Θ -functions

in F and rewrite the cross section as:

$$\begin{aligned} \frac{d\sigma_B}{dM^2 dx_F dp_T^2} &= \int_0^1 dx_1 \int_0^1 dx_2 \int d\vec{p}_{1\perp} \int d\vec{p}_{2\perp} \int dm_1^2 \int dm_2^2 \\ &\times F(x_1, \vec{p}_{1\perp}, m_1^2, x_2, \vec{p}_{2\perp}, m_2^2, M^2) \delta\left((p_1 + p_2 - q)^2 - \lambda^2\right) \Theta(E_g) . \end{aligned} \quad (8.76)$$

The δ -functions in Eq. (8.76) must be worked out in a way that allows to discern physical and unphysical solutions for the momentum fractions x_i in order to perform the f -integrations. For this aim it is useful to rewrite the parton momenta in terms of different variables:

$$\hat{q} = p_1 + p_2 , \quad (8.77)$$

$$k = \frac{1}{2}(p_2 - p_1) . \quad (8.78)$$

Inverting the last two equations, we can use the on-shell conditions for the partons and find:

$$m_1^2 = p_1^2 = \left(\frac{1}{2}\hat{q} - k\right)^2 = \frac{1}{4}\hat{q}^2 - k \cdot \hat{q} + k^2 , \quad (8.79)$$

$$m_2^2 = p_2^2 = \left(\frac{1}{2}\hat{q} + k\right)^2 = \frac{1}{4}\hat{q}^2 + k \cdot \hat{q} + k^2 . \quad (8.80)$$

Adding and subtracting Eqs. (8.79) and (8.80) yields:

$$k^2 = -\frac{1}{4}\hat{q}^2 + \frac{m_1^2 + m_2^2}{2} , \quad (8.81)$$

$$k \cdot q = \frac{m_2^2 - m_1^2}{2} . \quad (8.82)$$

Solving Eq. (8.81) for k^+ gives:

$$k^+ = \frac{\vec{k}_\perp^2 - \frac{1}{4}\hat{q}^2 + \frac{m_1^2 + m_2^2}{2}}{k^-} . \quad (8.83)$$

Inserting this result into Eq. (8.82) gives an equation quadratic in k^- :

$$\begin{aligned} m_2^2 - m_1^2 &= k^+ \hat{q}^- + k^- \hat{q}^+ - 2\vec{k}_\perp \cdot \overrightarrow{(\hat{q}_\perp)} \\ &= \frac{\vec{k}_\perp^2 - \frac{1}{4}\hat{q}^2 + \frac{m_1^2 + m_2^2}{2}}{k^-} \hat{q}^- + k^- \hat{q}^+ - 2\vec{k}_\perp \cdot \overrightarrow{(\hat{q}_\perp)} \end{aligned} \quad (8.84)$$

$$\begin{aligned} \Rightarrow 0 &= (k^-)^2 \hat{q}^+ + k^- (-2\vec{k}_\perp \cdot \overrightarrow{(\hat{q}_\perp)} - m_2^2 + m_1^2) \\ &+ \left(\vec{k}_\perp^2 - \frac{1}{4}\hat{q}^2 + \frac{m_1^2 + m_2^2}{2} \right) \hat{q}^- . \end{aligned} \quad (8.85)$$

The solutions are:

$$\begin{aligned} (k^-)_\pm &= \frac{\vec{k}_\perp \cdot \overrightarrow{(\hat{q}_\perp)}}{\hat{q}^+} + \frac{m_2^2 - m_1^2}{2\hat{q}^+} \\ &\pm \sqrt{\left(\frac{\vec{k}_\perp \cdot \overrightarrow{(\hat{q}_\perp)}}{\hat{q}^+} + \frac{m_2^2 - m_1^2}{2\hat{q}^+} \right)^2 + \frac{\hat{q}^-}{\hat{q}^+} \left(\frac{1}{4}\hat{q}^2 - \vec{k}_\perp^2 - \frac{m_1^2 + m_2^2}{2} \right)} . \end{aligned} \quad (8.86)$$

Inserting (8.86) into (8.84) gives the solutions for k^+ :

$$\begin{aligned} (k^+)_\mp &= \frac{\hat{q}^+}{\hat{q}^-} \left(\frac{\vec{k}_\perp \cdot \overrightarrow{(\hat{q}_\perp)}}{\hat{q}^+} + \frac{m_2^2 - m_1^2}{2\hat{q}^+} \right. \\ &\left. \mp \sqrt{\left(\frac{\vec{k}_\perp \cdot \overrightarrow{(\hat{q}_\perp)}}{\hat{q}^+} + \frac{m_2^2 - m_1^2}{2\hat{q}^+} \right)^2 + \frac{\hat{q}^-}{\hat{q}^+} \left(\frac{1}{4}\hat{q}^2 - \vec{k}_\perp^2 - \frac{m_1^2 + m_2^2}{2} \right)} \right) . \end{aligned} \quad (8.87)$$

Rewriting the parton momentum fractions x_i in terms of \hat{q} and k we obtain the solutions ($P_2^+ = P_1^-$):

$$(x_1)_\pm = \frac{1}{P_1^-} \left(\frac{1}{2}\hat{q}^- - (k^-)_\pm \right) \quad (8.88)$$

and

$$(x_2)_\mp = \frac{1}{P_1^-} \left(\frac{1}{2}\hat{q}^+ + (k^+)_\mp \right) . \quad (8.89)$$

Since there are two solutions for k^- and k^+ , respectively, we also get two solutions for x_1, x_2 . To determine which set of x_1, x_2 and thus k^+, k^- has to be chosen we take the limit of zero parton transverse momentum and vanishing masses:

$$(k^-)_\pm \rightarrow \pm \sqrt{\frac{\hat{q}^-}{\hat{q}^+} \frac{1}{4}\hat{q}^2} = \pm \frac{\hat{q}^-}{2} \quad (8.90)$$

$$(k^+)_\mp \rightarrow \mp \sqrt{\frac{\hat{q}^+}{\hat{q}^-} \frac{1}{4}\hat{q}^2} = \mp \frac{\hat{q}^+}{2} \quad (8.91)$$

Inserting expressions (8.90) and (8.91) into (8.88) and (8.89) yields two solutions for the momentum fractions:

$$(x_1)_\pm \rightarrow \frac{1}{P_1^-} \begin{cases} 0 \\ \hat{q}^- \end{cases} \quad (8.92)$$

and

$$(x_2)_\mp \rightarrow \frac{1}{P_1^-} \begin{cases} 0 \\ \hat{q}^+ \end{cases} . \quad (8.93)$$

The upper solutions correspond to the unphysical case $x_1 = x_2 = 0$. Thus, we only want to keep the lower solutions when evaluating the phase space integrals. This requires the integrals in Eq. (8.76) to be evaluated in the correct order, otherwise one cannot disentangle the two different solutions for x_1 and x_2 .

We begin by introducing several integrals over δ -functions in Eq. (8.76). In this way we will transform the integration variables to the above chosen \hat{q} and \vec{k}_\perp :

$$\begin{aligned} \frac{d\sigma_B}{dM^2 dx_F dp_T^2} &= \int_0^1 dx_1 \int_0^1 dx_2 \int d\vec{p}_{1\perp} \int d\vec{p}_{2\perp} \int d(\vec{\hat{q}}_\perp) \int d\vec{k}_\perp \int dm_1^2 \int dm_2^2 \\ &\int d\hat{q}^+ \int d\hat{q}^- F(x_1, \vec{p}_{1\perp}, m_1^2, x_2, \vec{p}_{2\perp}, m_2^2, M^2) \\ &\times \delta(\hat{q}^+ - (p_1^+ + p_2^+)) \delta(\hat{q}^- - (p_1^- + p_2^-)) \\ &\times \delta^{(2)}(\vec{\hat{q}}_\perp - (\vec{p}_{1\perp} + \vec{p}_{2\perp})) \delta^{(2)}\left(\vec{k}_\perp - \frac{1}{2}(\vec{p}_{1\perp} - \vec{p}_{2\perp})\right) \\ &\times \delta\left((p_1 + p_2 - q)^2 - \lambda^2\right) \Theta(E_g) . \end{aligned} \quad (8.94)$$

First we perform the initial transverse momentum integrals:

$$\int d\vec{p}_{1\perp} \int d\vec{p}_{2\perp} \delta^{(2)}(\vec{\hat{q}}_\perp - (\vec{p}_{1\perp} + \vec{p}_{2\perp})) \delta^{(2)}\left(\vec{k}_\perp - \frac{1}{2}(\vec{p}_{2\perp} - \vec{p}_{1\perp})\right) = 1 . \quad (8.95)$$

Now we have to calculate the integrals over the momentum fractions:

$$\int_0^1 dx_1 \int_0^1 dx_2 \delta(\hat{q}^+ - (p_1^+ + p_2^+)) \delta(\hat{q}^- - (p_1^- + p_2^-)) . \quad (8.96)$$

According to Eqs. (8.86)-(8.89) the δ -functions in the last expression have two possible solutions for each p_1^- and p_2^+ . However, as explained above, we now have to explicitly remove the unphysical solutions $(x_1)_+$ and $(x_2)_-$, which are the ones corresponding

to the upper sign in Eqs. (8.86) and (8.87):

$$\begin{aligned}
 & \int_0^1 dx_1 \int_0^1 dx_2 \delta(\hat{q}^+ - (p_1^+ + p_2^+)) \delta(\hat{q}^- - (p_1^- + p_2^-)) \\
 &= \int_0^1 dx_1 \int_0^1 dx_2 \delta \left(\hat{q}^+ - \frac{\left(\frac{1}{2}(\overrightarrow{\hat{q}}_{\perp}) - \vec{k}_{\perp}\right)^2 + m_1^2}{x_1 P_1^-} - x_2 P_1^- \right) \\
 & \quad \times \delta \left(\hat{q}^- - x_1 P_1^- - \frac{\left(\frac{1}{2}(\overrightarrow{\hat{q}}_{\perp}) + \vec{k}_{\perp}\right)^2 + m_2^2}{x_2 P_1^-} \right) \\
 &= \int_0^1 dx_1 \int_0^1 dx_2 \delta \left(\hat{q}^+ - \frac{\left(\frac{1}{2}(\overrightarrow{\hat{q}}_{\perp}) - \vec{k}_{\perp}\right)^2 + m_1^2}{(x_1)_- P_1^-} - (x_2)_+ P_1^- \right) \\
 & \quad \times \delta \left(\hat{q}^- - (x_1)_- P_1^- - \frac{\left(\frac{1}{2}(\overrightarrow{\hat{q}}_{\perp}) + \vec{k}_{\perp}\right)^2 + m_2^2}{(x_2)_+ P_1^-} \right) \\
 &= \left| (P_1^-)^2 - \frac{\left[\left(\frac{1}{2}(\overrightarrow{\hat{q}}_{\perp}) - \vec{k}_{\perp}\right)^2 + m_1^2\right] \left[\left(\frac{1}{2}(\overrightarrow{\hat{q}}_{\perp}) + \vec{k}_{\perp}\right)^2 + m_2^2\right]}{(x_1)_-^2 (x_2)_+^2 (P_1^-)^2} \right|^{-1} \\
 & \quad \times \Theta(1 - (x_1)_-) \Theta((x_1)_-) \Theta(1 - (x_2)_+) \Theta((x_2)_+) . \tag{8.97}
 \end{aligned}$$

Using $d\hat{q}^+ d\hat{q}^- = 2d\hat{q}_0 d\hat{q}_z$ we can evaluate one of the remaining integrals of Eq. (8.94) with the help of the δ -function:

$$2 \int d\hat{q}_0 \delta \left((p_1 + p_2 - q)^2 - \lambda^2 \right) = 2 \int d\hat{q}_0 \delta \left((\hat{q} - q)^2 - \lambda^2 \right) = \frac{1}{E_g} , \tag{8.98}$$

with $E_g = \sqrt{\left(\overrightarrow{\hat{q}} - \vec{q}\right)^2 + \lambda^2}$. Collecting the pieces, what remains of Eq. (8.94) is:

$$\begin{aligned} \frac{d\sigma_B}{dM^2 dx_F dp_T^2} &= \int_{(q_z)_{\min}}^{(q_z)_{\max}} d\hat{q}_z \int_0^{|\overrightarrow{\hat{q}_\perp}|_{\max}} d(\overrightarrow{\hat{q}_\perp}) \int_0^{|\vec{k}_\perp|_{\max}} d\vec{k}_\perp \int_0^{(m_1^2)_{\max}} dm_1^2 \int_0^{(m_2^2)_{\max}} dm_2^2 \\ &\times F((x_1)_-, \hat{p}_{1\perp}, m_1^2, (x_2)_+, \hat{p}_{2\perp}, m_2^2, M^2) \Theta(E_g) \frac{1}{E_g} \\ &\times \left| (P_1^-)^2 - \frac{\left[\left(\frac{1}{2}\overrightarrow{\hat{q}_\perp} - \vec{k}_\perp\right)^2 + m_1^2\right] \left[\left(\frac{1}{2}\overrightarrow{\hat{q}_\perp} + \vec{k}_\perp\right)^2 + m_2^2\right]}{(x_1)_-^2 (x_2)_+^2 (P_1^-)^2} \right|^{-1} \\ &\times \Theta(1 - (x_1)_-) \Theta((x_1)_-) \Theta(1 - (x_2)_+) \Theta((x_2)_+) . \end{aligned} \quad (8.99)$$

Now $(x_1)_-, \hat{p}_{1\perp}, (x_2)_+$ and $\hat{p}_{2\perp}$ are fixed:

$$\begin{aligned} (x_1)_- &= \frac{1}{P_1^-} \left(\frac{\hat{q}^-}{2} - \frac{\vec{k}_\perp \cdot \overrightarrow{\hat{q}_\perp}}{\hat{q}^+} - \frac{m_2^2 - m_1^2}{2\hat{q}^+} \right. \\ &\quad \left. + \sqrt{\left(\frac{\vec{k}_\perp \cdot \overrightarrow{\hat{q}_\perp}}{\hat{q}^+} + \frac{m_2^2 - m_1^2}{2\hat{q}^+}\right)^2 + \frac{\hat{q}^-}{\hat{q}^+} \left(\frac{1}{4}\hat{q}^2 - \vec{k}_\perp^2 - \frac{m_1^2 + m_2^2}{2}\right)} \right) , \end{aligned} \quad (8.100)$$

$$\begin{aligned} (x_2)_+ &= \frac{1}{P_1^-} \left(\frac{\hat{q}^+}{2} + \frac{\vec{k}_\perp \cdot \overrightarrow{\hat{q}_\perp}}{\hat{q}^-} + \frac{m_2^2 - m_1^2}{2\hat{q}^-} \right. \\ &\quad \left. + \sqrt{\left(\frac{\vec{k}_\perp \cdot \overrightarrow{\hat{q}_\perp}}{\hat{q}^-} + \frac{m_2^2 - m_1^2}{2\hat{q}^-}\right)^2 + \frac{\hat{q}^+}{\hat{q}^-} \left(\frac{1}{4}\hat{q}^2 - \vec{k}_\perp^2 - \frac{m_1^2 + m_2^2}{2}\right)} \right) , \end{aligned} \quad (8.101)$$

$$\hat{p}_{1\perp} = \frac{1}{2}\overrightarrow{\hat{q}_\perp} - \vec{k}_\perp , \quad (8.102)$$

$$\hat{p}_{2\perp} = \frac{1}{2}\overrightarrow{\hat{q}_\perp} + \vec{k}_\perp , \quad (8.103)$$

$$\vec{k}_\perp \cdot \overrightarrow{\hat{q}_\perp} = k_\perp \hat{q}_\perp \cos \phi_{k_\perp} , \quad (8.104)$$

with

$$\hat{q}^+ = E_q + E_g + \hat{q}_z, \quad (8.105)$$

$$\hat{q}^- = E_q + E_g - \hat{q}_z, \quad (8.106)$$

$$E_q = \sqrt{M^2 + p_T^2 + q_z^2}, \quad (8.107)$$

$$E_g = \sqrt{(\overrightarrow{\hat{q}}_\perp)^2 + \hat{q}_z^2 - 2\overrightarrow{\hat{q}}_\perp \cdot \vec{q}_\perp - 2\hat{q}_z \cdot q_z + p_T^2 + q_z^2 + \lambda^2}, \quad (8.108)$$

$$\overrightarrow{\hat{q}}_\perp \cdot \vec{q}_\perp = \hat{q}_\perp p_T \cos \phi_{\hat{q}_\perp}, \quad (8.109)$$

$$q_z = x_F (q_z)_{\max}. \quad (8.110)$$

The integration limits can now be found from general considerations. $(m_2^2)_{\max}$ is fixed by the condition that $(x_1)_-$ and $(x_2)_+$ must be real numbers:

$$(m_2^2)_{\max} = -2\vec{k}_\perp \cdot \overrightarrow{\hat{q}}_\perp + m_1^2 + \hat{q}^+ \hat{q}^- - \sqrt{4\hat{q}^+ \hat{q}^- m_1^2 + 4\hat{q}^+ \hat{q}^- \left(\frac{1}{2} \overrightarrow{\hat{q}}_\perp - \vec{k}_\perp \right)^2}. \quad (8.111)$$

From $(m_2^2)_{\max} \stackrel{!}{>} 0$ we find:

$$(m_1^2)_{\max} = 2\vec{k}_\perp \cdot \overrightarrow{\hat{q}}_\perp + \hat{q}^+ \hat{q}^- - 2\sqrt{\hat{q}^+ \hat{q}^- \left(\frac{1}{2} \overrightarrow{\hat{q}}_\perp + \vec{k}_\perp \right)^2}, \quad (8.112)$$

and from $(m_1^2)_{\max} \stackrel{!}{>} 0$ follows:

$$|\vec{k}_\perp|_{\max}^2 = \frac{\hat{q}^+ \hat{q}^- (\hat{q}^+ \hat{q}^- - \hat{q}_\perp^2)}{4 (\hat{q}^+ \hat{q}^- - \hat{q}_\perp^2 \cos^2(\phi_{k_\perp}))}. \quad (8.113)$$

The energy of the incoming partons must be less than the energy of the hadronic system, $\hat{q}_0 < \sqrt{S}$, and so:

$$|\overrightarrow{\hat{q}}_\perp|_{\max} = p_T \cos \phi_{\hat{q}} + \sqrt{p_T^2 (\cos^2 \phi_{\hat{q}} - 1) - (q_z - \hat{q}_z)^2 + (\sqrt{S} - E_q)^2 - \lambda^2}. \quad (8.114)$$

Finally, \hat{q}_\perp is a real number, thus:

$$(\hat{q}_z)_{\min}^{\max} = q_z \pm \sqrt{p_T^2 (\cos^2 \phi_{\hat{q}_\perp} - 1) + (\sqrt{S} - E_q)^2 - \lambda^2}. \quad (8.115)$$

A special case: kinematics of LO DY with massive quarks

The kinematics of the LO cross section is just a special case of the bremsstrahlung kinematics. Namely at LO the four momentum of the incoming partons is equal to the four momentum of the virtual photon: $\hat{q} = q$. From Eq. (7.108) we note for the partonic cross section:

$$\frac{d\hat{\sigma}_{\text{LO}}}{dM^2 dx_F dp_T^2} \sim \delta\left(M^2 - (p_1 + p_2)^2\right) \delta\left(p_T^2 - (\vec{p}_{1\perp} + \vec{p}_{2\perp})^2\right) \delta\left(x_F - \frac{(p_1)_z + (p_2)_z}{(q_z)_{\text{max}}}\right). \quad (8.116)$$

Now employing Eqs. (8.77-8.93) and Eqs. (8.95- 8.97) and everywhere replacing \hat{q} by q we find for the LO hadronic cross section:

$$\begin{aligned} \frac{d\sigma_{\text{LO}}}{dM^2 dx_F dp_T^2} &= \int 2dq_0 \int dq_z \int d\vec{q}_\perp \int d\vec{k}_\perp \int dm_1^2 \int dm_2^2 \\ &\quad \times F_{\text{LO}}((x_1)_-, \hat{p}_{1\perp}, m_1^2, (x_2)_+, \hat{p}_{2\perp}, m_2^2, M^2) \\ &\quad \times \left| (P_1^-)^2 - \frac{\left[\left(\frac{1}{2}\vec{q}_\perp - \vec{k}_\perp\right)^2 + m_1^2\right] \left[\left(\frac{1}{2}\vec{q}_\perp + \vec{k}_\perp\right)^2 + m_2^2\right]}{(x_1)_-^2 (x_2)_+^2 (P_1^-)^2} \right|^{-1} \\ &\quad \times \Theta(1 - (x_1)_-) \Theta((x_1)_-) \Theta(1 - (x_2)_+) \Theta((x_2)_+) \\ &\quad \times \delta\left(M^2 - q^2\right) \delta\left(p_T^2 - (\vec{q}_\perp)^2\right) \delta\left(x_F - \frac{q_z}{(q_z)_{\text{max}}}\right). \end{aligned} \quad (8.117)$$

With help of the three remaining δ -functions we can now easily perform the four integrations over the components of q :

$$\begin{aligned} \frac{d\sigma_{\text{LO}}}{dM^2 dx_F dp_T^2} &= \int_0^{2\pi} d\phi_\perp \int_0^{(\vec{k}_\perp)_{\text{max}}^2} \frac{1}{2} d(\vec{k}_\perp)^2 \int_0^{(m_1)_{\text{max}}^2} dm_1^2 \int_0^{(m_2)_{\text{max}}^2} dm_2^2 \frac{\pi (q_z)_{\text{max}}}{E_q} \\ &\quad \times \left| (P_1^-)^2 - \frac{\left[\left(\frac{1}{2}\vec{q}_\perp - \vec{k}_\perp\right)^2 + m_1^2\right] \left[\left(\frac{1}{2}\vec{q}_\perp + \vec{k}_\perp\right)^2 + m_2^2\right]}{(x_1)_-^2 (x_2)_+^2 (P_1^-)^2} \right|^{-1} \\ &\quad \times F_{\text{LO}}((x_1)_-, \hat{p}_{1\perp}, m_1^2, (x_2)_+, \hat{p}_{2\perp}, m_2^2, M^2) \\ &\quad \times \Theta(1 - (x_1)_-) \Theta((x_1)_-) \Theta(1 - (x_2)_+) \Theta((x_2)_+). \end{aligned} \quad (8.118)$$

The integration limits are now recovered from Eqs. (8.111-8.113), again by replacing \hat{q} with q .

8.4 Gluon Compton scattering

Gluon Compton scattering differs from all the other processes we consider, since here a gluon and a quark/antiquark fuse before or after emitting the virtual photon, see Fig. 8.7. In the case of gluon Compton scattering we keep the quark mass fixed at every vertex for the following reasons: In principle the final state quark is supposed to be "free" and thus one would assign to it a mass $m_1 = 0$. To preserve current conservation the quark mass at the gluon vertex must not change and thus the exchange quark in the right diagram in Fig. 8.7 would have to be also massless. This, however, immediately generates a collinear divergence, cf. Secs. 5.1 and 6.2.4. Therefore, we assign a mass m_1 to the entire quark line.

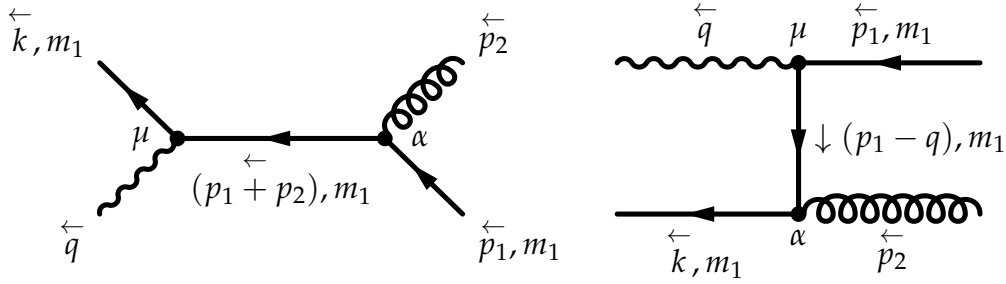


Figure 8.7: Gluon Compton scattering processes for DY production at NLO.

8.4.1 Cross section

We choose for the initial quark/antiquark to have four momentum p_1 and for the gluon to have four momentum p_2 , thus $m_2 = 0$ since the gluon is real. For the outgoing quark/antiquark we then have $m_r = m_1$. Using the Feynman rules of Appendix B one finds for the amplitude of the process $qg \rightarrow q\gamma^*$:

$$\begin{aligned}
 iM = & \bar{u}(k, m_1) (ie\gamma^\mu) \frac{i(\not{p}_1 + \not{p}_2 + m_1)}{(p_1 + p_2)^2 - m_1^2} (ig\gamma^\alpha t^a) u(p_1, m_1) \cdot \epsilon_\mu^*(q)\epsilon_\alpha(p_2) \\
 & + \bar{u}(k, m_1) (ie\gamma^\alpha) \frac{i(\not{p}_1 - \not{q} + m_1)}{(p_1 - q)^2 - m_1^2} (ig\gamma^\mu t^a) u(p_1, m_1) \cdot \epsilon_\mu^*(q)\epsilon_\alpha(p_2) . \quad (8.119)
 \end{aligned}$$

The squared matrix element, averaged and summed over spin, polarisations and color then reads:

$$|\bar{M}|^2 = \frac{1}{6} \frac{e^2 g^2}{4} T_C , \quad (8.120)$$

where $\frac{1}{6}$ is the color factor and T_C is given by:

$$T_C = \left(g_{\mu\nu} - \frac{q_\mu q_\nu}{q^2} \right) \cdot \text{Tr} [(\not{p}_1 + \not{p}_2 - \not{q} + m_1) S^{\mu\alpha} (\not{p}_1 + m_1) S_\alpha^\nu] \quad (8.121)$$

with:

$$S^{\alpha\beta} = \gamma^\alpha \frac{\not{p}_1 + \not{p}_2 + m_1}{(p_1 + p_2)^2 - m_1^2} \gamma^\beta + \gamma^\beta \frac{\not{p}_1 - \not{q} + m_1}{(p_1 - q)^2 - m_1^2} \gamma^\alpha. \quad (8.122)$$

For completeness we give our result for T_C in Appendix C.2.2. The partonic cross section for the process $qg \rightarrow l^+l^-q$ can then easily be found by using the results of Sec. 7.3.2:

$$d\hat{\sigma}_C = \frac{(2\pi)^4 \delta^{(4)}(p_1 + p_2 - k - q)}{4(p_1 \cdot p_2)} \frac{\alpha}{3\pi M^2} |\overline{M}|^2 dM^2 \frac{d^3q}{(2\pi)^3 2E_q} \frac{d^3k}{(2\pi)^3 2E_k}. \quad (8.123)$$

Inserting the squared matrix element and integrating over the phase space of the emitted quark the partonic cross section becomes:

$$\begin{aligned} d\hat{\sigma}_C &= \frac{1}{6} \frac{\alpha^2 \alpha_s}{3\pi M^2} \frac{T_C}{4(p_1 \cdot p_2)} \cdot \delta\left((p_1 + p_2 - q)^2 - m_1^2\right) dM^2 \frac{d^3q}{2E_q} \\ &= \frac{1}{6} \frac{\alpha^2 \alpha_s}{3\pi M^2} \frac{T_C}{2(s - m_1^2)} \cdot \delta\left(s + M^2 - 2\sqrt{s}E_q - m_1^2\right) dM^2 \frac{|\vec{q}|^2 d|\vec{q}|^2 d\phi d\cos\theta}{2E_q} \\ &= \frac{1}{6} \frac{\alpha^2 \alpha_s}{3\pi M^2} \frac{T_C}{2(s - m_1)^2} \frac{\pi}{2(s - m_1)^2} \Theta(E_r) dM^2 dt, \end{aligned} \quad (8.124)$$

with the energy of the emitted quark E_r . The relevant partonic cross section then reads ($E_r \geq m_r$):

$$\frac{d\hat{\sigma}_C}{dM^2 dt} = \frac{1}{6} \frac{\alpha^2 \alpha_s}{12M^2 (s - m_1^2)^2} \cdot T_C \cdot \Theta(E_r), \quad (8.125)$$

The calculation of the hadronic cross section is similar to the case of gluon bremsstrahlung. However, the inherent asymmetry of the initial state (massive quark hits massless gluon) requires additional care and we present the details in the next subsection.

8.4.2 Kinematics

At this point we want to stress the kinematical differences between bremsstrahlung and Compton scattering. For bremsstrahlung we have a quark from nucleon 1 annihilating with an antiquark from nucleon 2 or vice versa. However, we treat quarks and antiquarks on equal footing and distribute their masses with the same spectral function, cf. Sec. 7.5.2. Thus we can easily take care of both cases by simply summing over all quark- and antiquark-flavors in Eq. (8.75). Gluon Compton scattering is different since we keep the gluons massless and the simplification from above does not apply anymore. However, we can calculate one of the two cases, for example

quark/antiquark from nucleon 1 annihilates with gluon from nucleon 2, and then simply find the other case by symmetry considerations: nucleon 1 and 2 are defined by their direction of motion along the z -axis. Thus by changing z to $-z$ and so x_F to $-x_F$ we find that the second case corresponds to the first case with $x_F \rightarrow -x_F$. The hadronic cross section therefore reads, compare with Eq. (8.75):

$$\begin{aligned}
 \frac{d\sigma_C}{dM^2 dp_T^2 dx_F} &= \int_0^1 dx_1 \int_0^1 dx_2 \int d\vec{p}_{1\perp} \int d\vec{p}_{2\perp} \int dm_1^2 \\
 &\quad \times \sum_i q_i^2 (\hat{f}_i)_1(x_1, \vec{p}_{1\perp}, m_1^2, q^2) \tilde{g}_2(x_2, \vec{p}_{2\perp}, q^2) \cdot \frac{2\sqrt{s} p_{\text{cm}}(q_z)_{\text{max}}}{E_q} \\
 &\quad \times \frac{d\hat{\sigma}_C}{dM^2 dt} \delta\left((p_1 + p_2 - q)^2\right) \\
 &+ \int_0^1 dx_1 \int_0^1 dx_2 \int d\vec{p}_{1\perp} \int d\vec{p}_{2\perp} \int dm_1^2 \\
 &\quad \times \sum_i q_i^2 (\hat{f}_i)_2(x_1, \vec{p}_{1\perp}, m_1^2, q^2) \tilde{g}_1(x_2, \vec{p}_{2\perp}, q^2) \cdot \frac{2\sqrt{s} p_{\text{cm}}(q_z)_{\text{max}}}{E_q} \\
 &\quad \times \frac{d\hat{\sigma}_C}{dM^2 dt} \delta\left((p_1 + p_2 - q)^2\right) \Big|_{x_F \rightarrow -x_F} \\
 &= \frac{(d\sigma_C)_{12}}{dM^2 dp_T^2 dx_F} + \frac{(d\sigma_C)_{21}}{dM^2 dp_T^2 dx_F} \Big|_{x_F \rightarrow -x_F} .
 \end{aligned} \tag{8.126}$$

The indices 1 and 2 for the parton distributions denote the parent nucleons (p, n, \bar{p}) . \tilde{g} is the transverse momentum dependent gluon distribution function and we choose it in analogy with the transverse momentum dependent quark distribution function of Eq. (7.125):

$$\tilde{g}(x, \vec{p}_\perp, q^2) = g(x_i, q^2) \cdot f_\perp(\vec{p}_{i\perp}) , \tag{8.127}$$

with f_\perp defined in Eq. (7.123) and with the usual gluon PDF g . Now can we proceed similarly to Sec. 8.3.2:

$$\begin{aligned}
 \frac{(d\sigma_C)_{12}}{dM^2 dp_T^2 dx_F} &= \int_0^1 dx_1 \int_0^1 dx_2 \int d\vec{p}_{1\perp} \int d\vec{p}_{2\perp} \int d(\vec{\hat{q}}_\perp) \int d\vec{k}_\perp \int dm_1^2 \int d\hat{q}^+ \int d\hat{q}^- \\
 &\quad \times F(x_1, \vec{p}_{1\perp}, m_1^2, x_2, \vec{p}_{2\perp}, M^2) \\
 &\quad \times \delta(\hat{q}^+ - (p_1^+ + p_2^+)) \delta(\hat{q}^- - (p_1^- + p_2^-)) \\
 &\quad \times \delta^{(2)}\left(\vec{\hat{q}}_\perp - (\vec{p}_{1\perp} + \vec{p}_{2\perp})\right) \delta^{(2)}\left(\vec{k}_\perp - \frac{1}{2}(\vec{p}_{1\perp} - \vec{p}_{2\perp})\right) \\
 &\quad \times \delta\left((p_1 + p_2 - q)^2 - m_1^2\right) .
 \end{aligned} \tag{8.128}$$

Now we can make use of Eqs. (8.95) and (8.97) and:

$$\int dm_1^2 \delta\left((p_1 + p_2 - q)^2 - m_1^2\right) = 1. \quad (8.129)$$

We find:

$$\begin{aligned} \frac{(d\sigma_C)_{12}}{dM^2 dp_T^2 dx_F} &= \int_{(q_z)_{\min}}^{(q_z)_{\max}} d\hat{q}_z \int_0^{|\overrightarrow{\hat{q}_\perp}|_{\max}} d(\overrightarrow{\hat{q}_\perp}) \int_{(\hat{q}_0)_{\min}}^{(\hat{q}_0)_{\max}} 2d\hat{q}_0 \int_0^{|\vec{k}_\perp|_{\max}} d\vec{k}_\perp F(x_1, \vec{p}_{1\perp}, m_1^2, x_2, \vec{p}_{2\perp}, M^2) \\ &\times \left| (P_1^-)^2 - \frac{\left[\left(\frac{1}{2}\overrightarrow{\hat{q}_\perp} - \vec{k}_\perp\right)^2 + m_1^2\right] \left[\left(\frac{1}{2}\overrightarrow{\hat{q}_\perp} + \vec{k}_\perp\right)^2\right]}{(x_1)_-^2 (x_2)_+^2 (P_1^-)^2} \right|^{-1} \\ &\times \Theta(1 - (x_1)_-) \Theta((x_1)_-) \Theta(1 - (x_2)_+) \Theta((x_2)_+). \end{aligned} \quad (8.130)$$

Finally $(x_1)_-$, $\hat{p}_{1\perp}$, $(x_2)_+$ and $\hat{p}_{2\perp}$ are fixed:

$$\begin{aligned} (x_1)_- &= \frac{1}{P_1^-} \left(\frac{\hat{q}^-}{2} - \frac{\vec{k}_\perp \cdot \overrightarrow{\hat{q}_\perp}}{\hat{q}^+} + \frac{m_1^2}{2\hat{q}^+} \right. \\ &\quad \left. + \sqrt{\left(\frac{\vec{k}_\perp \cdot \overrightarrow{\hat{q}_\perp}}{\hat{q}^+} - \frac{m_1^2}{2\hat{q}^+}\right)^2 + \frac{\hat{q}^-}{\hat{q}^+} \left(\frac{1}{4}\hat{q}^2 - \vec{k}_\perp^2 - \frac{m_1^2}{2}\right)} \right), \end{aligned} \quad (8.131)$$

$$\begin{aligned} (x_2)_+ &= \frac{1}{P_1^-} \left(\frac{\hat{q}^+}{2} + \frac{\vec{k}_\perp \cdot \overrightarrow{\hat{q}_\perp}}{\hat{q}^-} - \frac{m_1^2}{2\hat{q}^-} \right. \\ &\quad \left. + \sqrt{\left(\frac{\vec{k}_\perp \cdot \overrightarrow{\hat{q}_\perp}}{\hat{q}^-} - \frac{m_1^2}{2\hat{q}^-}\right)^2 + \frac{\hat{q}^+}{\hat{q}^-} \left(\frac{1}{4}\hat{q}^2 - \vec{k}_\perp^2 - \frac{m_1^2}{2}\right)} \right), \end{aligned} \quad (8.132)$$

$$\hat{p}_{1\perp} = \frac{1}{2}\overrightarrow{\hat{q}_\perp} - \vec{k}_\perp, \quad (8.133)$$

$$\hat{p}_{2\perp} = \frac{1}{2}\overrightarrow{\hat{q}_\perp} + \vec{k}_\perp, \quad (8.134)$$

$$\vec{k}_\perp \cdot \overrightarrow{\hat{q}_\perp} = k_\perp \hat{q}_\perp \cos \phi_{k_\perp}, \quad (8.135)$$

$$m_1^2 = (\hat{q}_0 - E_q)^2 - \left(\overrightarrow{\hat{q}_\perp} - \vec{q}_\perp\right)^2 - (q_z - \hat{q}_z)^2 \quad (8.136)$$

with

$$\hat{q}^+ = \hat{q}_0 + \hat{q}_z, \quad (8.137)$$

$$\hat{q}^- = \hat{q}_0 - \hat{q}_z, \quad (8.138)$$

$$E_q = \sqrt{M^2 + p_T^2 + q_z^2}, \quad (8.139)$$

$$\overrightarrow{(\hat{q}_\perp)} \cdot \vec{q}_\perp = \hat{q}_\perp p_T \cos \phi_{\hat{q}_\perp}, \quad (8.140)$$

$$q_z = x_F(q_z)_{\max}. \quad (8.141)$$

The integration limits can be found from general considerations. $|\vec{k}_\perp|_{\max}$ is fixed by the condition that $(x_1)_-$ and $(x_2)_+$ must be real numbers:

$$\begin{aligned} |\vec{k}_\perp|_{\max} = & -\frac{|\overrightarrow{(\hat{q}_\perp)}| \cos \phi_{k_\perp} m_1^2}{2(\hat{q}^+ \hat{q}^- - \hat{q}_\perp^2 \cos^2 \phi_{k_\perp})} \\ & + \sqrt{\left(\frac{|\overrightarrow{(\hat{q}_\perp)}| \cos \phi_{k_\perp} m_1^2}{2(\hat{q}^+ \hat{q}^- - \hat{q}_\perp^2 \cos^2 \phi_{k_\perp})} \right)^2 + \left(\frac{-\frac{m_1^4}{4} - \frac{1}{4} \hat{q}^+ \hat{q}^- (\hat{q}^+ \hat{q}^- - \hat{q}_\perp^2) + \hat{q}^+ \hat{q}^- \frac{m_1^2}{2}}{\hat{q}_\perp^2 \cos^2 \phi_{k_\perp} - \hat{q}^+ \hat{q}^-} \right)^2}. \end{aligned} \quad (8.142)$$

From $0 < m_1^2 < m_N^2$ one gets:

$$(\hat{q}_0)_{\min} = E_q + \sqrt{(\overrightarrow{(\hat{q}_\perp)})^2 + \hat{q}_z^2 - 2\overrightarrow{(\hat{q}_\perp)} \cdot \vec{q}_\perp - 2\hat{q}_z \cdot q_z + p_T^2 + q_z^2}, \quad (8.143)$$

$$(\hat{q}_0)_{\max} = E_q + \sqrt{(\overrightarrow{(\hat{q}_\perp)})^2 + \hat{q}_z^2 - 2\overrightarrow{(\hat{q}_\perp)} \cdot \vec{q}_\perp - 2\hat{q}_z \cdot q_z + p_T^2 + q_z^2 + m_N^2}. \quad (8.144)$$

Since the energy of the incoming partons cannot be larger than the hadronic energy, we have $\hat{q}_0 < \sqrt{S}$, thus:

$$|\overrightarrow{(\hat{q}_\perp)}|_{\max} = p_T \cos \phi_{\hat{q}_\perp} + \sqrt{p_T^2 (\cos^2 \phi_{\hat{q}_\perp} - 1) - (q_z - \hat{q}_z)^2 - m_N^2 + (\sqrt{S} - E_q)^2}. \quad (8.145)$$

Finally, \hat{q}_\perp is a real number, which requires:

$$(\hat{q}_z)_{\min}^{\max} = q_z \pm \sqrt{p_T^2 (\cos^2 \phi_{\hat{q}_\perp} - 1) + (\sqrt{S} - E_q)^2 - m_N^2}. \quad (8.146)$$

8.5 Influence of quark mass distributions on DY p_T spectra

As already mentioned several times above, massless pQCD calculations of DY pair production at NLO produce divergent p_T spectra [G⁺95]. The origin of these IR

divergences are twofold: first there is soft gluon emission (bremsstrahlung). This type of soft divergence, however, is not problematic, since it exactly cancels against a divergence in the virtual processes (vertex correction), cf. Sec. 8.1.3. Second there is emission (bremsstrahlung) or capture (Compton scattering) of a gluon by a massless participant quark (also called mass or collinear singularity): the u-channel exchange quarks in Figs. 8.6 and 8.7 can become onshell at $p_T = 0$ and thus for $m_1 = m_2 = 0$ the propagators in Eqs. (8.71) and (8.122) produce a non-integrable (in p_T^2) singularity at $p_T = 0$. To address this problem was one reason for introducing mass distributions for the participating quarks. This procedure aims at smearing out the divergence and so making the p_T spectra integrable.

We will illustrate this procedure on the example of the gluon Compton scattering process. In Fig. 8.8 we compare p_T spectra produced by gluon Compton scattering in two different schemes: one calculation with massless quarks and a calculation which includes quark mass distributions. In both cases the quark's initial transverse momentum was set to zero. It is seen that now indeed transverse momentum of the dileptons is generated. One can also see clearly that the rise for $p_T \rightarrow 0$ of the calculation with mass distributions is slower than for the calculation with massless quarks. This is a consequence of the effective cut-off, which is introduced by distributing the quark masses. We find that the divergence in p_T is softened enough to make the p_T spectra integrable. Note, that the magnitude is still significantly underestimated, cf. also Sec. 8.7.

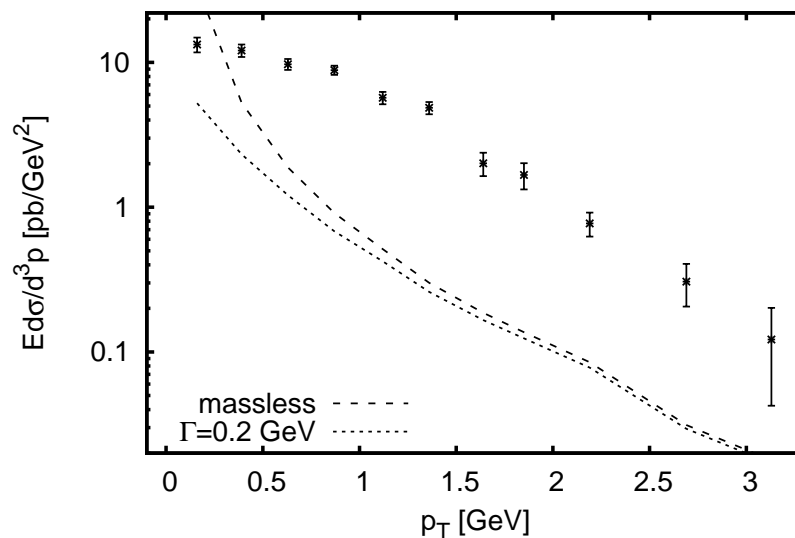


Figure 8.8: p_T spectrum of gluon Compton scattering obtained from massless and mass distribution approach with initially collinear quarks. The PDFs are the MSTW2008LO68cl set. Data are from E866 binned with $4.2 \text{ GeV} < M < 5.2 \text{ GeV}$, $-0.05 < x_F < 0.15$. Only statistical errors are shown.

8.6 Collinear (mass) singularities and parton distribution functions

As we have just shown, we have regularised the collinear singularities of the NLO processes by introducing quark mass distributions. However, for the calculation of our cross sections we would like to use PDFs as supplied in the literature. But exactly those collinear singularities, that we have just regularised, are commonly absorbed into the definition of the standard PDFs. Thus, to avoid double-counting, in this section we present a subtraction scheme, that leaves us with a consistent cross section to the order of the hard processes we are considering.

To set the stage we first review briefly the introduction of the renormalised PDFs into pQCD. For the DY process this concerns the calculation of M spectra, because the spectra differential in p_T are not accessible by pQCD. Since we are interested in the description of fully differential DY spectra by our model, we have to modify the way towards the standard renormalised PDFs. This is outlined in a second subsection.

8.6.1 Collinear singularities in pQCD

If Bjorken-scaling were not violated the PDFs found in deep inelastic scattering were functions of the momentum fraction x only. However, as we have discussed in Sec. 6.2.4, the interactions among the quarks and gluons induce scaling violations via processes like gluon bremsstrahlung and gluon quark-antiquark production. We found that the contributions of these processes to the longitudinal PDFs suffer from collinear (or mass) singularities, i.e. they are singular because the quarks are treated as massless. The divergences appear at the boundaries of the transverse momentum integrals (which is why they are called collinear divergences). Thus, we found that one can regulate these divergences by introducing a regulating cut-off η^2 in the transverse momentum integral. In this scheme one commonly defines renormalised longitudinal quark PDFs by absorbing the collinear singularities and the (non-measurable, scaling) bare quark and gluon PDFs, $f_i^0(x)$ and $g^0(x)$, into one function [ESW96]:

$$f_i(x, \mu^2) = f_i^0(x) + \frac{\alpha_s}{2\pi} \int_x^1 dy \frac{1}{y} \left\{ f_i^0(y) \left[P_{qq} \left(\frac{x}{y} \right) \log \left(\frac{\mu^2}{\eta^2} \right) + C_q^S \left(\frac{x}{y} \right) \right] + g^0(y) \left[P_{qg} \left(\frac{x}{y} \right) \log \left(\frac{\mu^2}{\eta^2} \right) + C_g^S \left(\frac{x}{y} \right) \right] \right\}, \quad (8.147)$$

with the hard scale μ^2 . The coefficient functions of the divergent logarithms are the splitting functions P_{qq} and P_{qg} , which were given in Eqs. (6.156) and (6.160). The functions C_q^S and C_g^S contain possible finite contributions of the scaling violating processes and the superscript S reminds us of the fact, that these finite contributions depend on

the chosen renormalisation scheme, since only the divergent contributions actually have to be absorbed into the renormalised PDFs.

Remarkably one finds the same splitting functions when calculating order α_s corrections to DY pair production [ESW96]: P_{qq} collects all the contributions from the processes with $q\bar{q}$ in the initial state, i.e. the vertex correction and gluon bremsstrahlung processes of Figs. 8.1, 8.2 and 8.6. P_{qg} contains the contributions from the gluon Compton scattering processes in Fig. 8.7. Then the partonic cross section for DY pair production to order α_s integrated over the transverse momentum of the DY pair can be written schematically as [ESW96]:

$$\frac{d\hat{\sigma}}{dM^2} = \frac{4\pi\alpha^2}{9M^4} e_i^2 z \left[\delta(1-z) + \frac{\alpha_s}{2\pi} (\mathcal{F}_{q\bar{q}}(z) + \mathcal{F}_{qg}(z)) \right], \quad (8.148)$$

for a quark of flavor i and with:

$$z = \frac{M^2}{\hat{s}} = \frac{M^2}{x_1 x_2 S} = \frac{\tau}{x_1 x_2}, \quad (8.149)$$

where $\sqrt{\hat{s}}$ (\sqrt{S}) is the partonic (hadronic) c.m. energy and x_1, x_2 the momentum fractions of the quarks. The δ -function in (8.148) gives just the leading-order contribution and the functions $\mathcal{F}_{q\bar{q}}$ and \mathcal{F}_{qg} give the contributions with initial states consisting of quark-antiquark (vertex correction and gluon bremsstrahlung) and quark-gluon (gluon Compton scattering), respectively:

$$\mathcal{F}_{q\bar{q}}(z) = 2P_{qq}(z) \log\left(\frac{M^2}{\eta^2}\right) + \hat{C}_q^S(z), \quad (8.150)$$

$$\mathcal{F}_{qg}(z) = P_{qg}(z) \log\left(\frac{M^2}{\eta^2}\right) + \hat{C}_g^S(z), \quad (8.151)$$

where again the cut-off η^2 was introduced to regulate the transverse momentum integration and where the functions \hat{C}_q^S and \hat{C}_g^S are again renormalisation scheme dependent, finite contributions. In principle one could obtain the hadronic cross section by folding the partonic cross section (8.148) with the bare parton distributions and summing over all quark flavors:

$$\begin{aligned} \frac{d\sigma}{dM^2} = & \frac{4\pi\alpha^2}{9M^4} \sum_i e_i^2 \int_0^1 dx_1 dx_2 \frac{\tau}{x_1 x_2} \Theta(x_1 x_2 - \tau) \\ & \times \left\{ \left(f_i^0(x_1) f_i^0(x_2) + (f_i^0 \leftrightarrow f_i^0) \right) \left[\delta(1-z) + \frac{\alpha_s}{2\pi} \mathcal{F}_{q\bar{q}}(z) \right] \right. \\ & \left. + \left(g^0(x_1) \left(f_i^0(x_2) + f_i^0(x_2) \right) + (g^0 \leftrightarrow f_i^0, f_i^0) \right) \frac{\alpha_s}{2\pi} \mathcal{F}_{qg}(z) \right\}. \end{aligned} \quad (8.152)$$

This cross section cannot be evaluated straightforwardly, since neither the bare parton distributions are available, nor are $\mathcal{F}_{q\bar{q}}$ and \mathcal{F}_{qg} well defined, since they depend on the arbitrary cut-off η^2 . However, we note the following relation for a general function P :

$$\begin{aligned}
 & \int_0^1 dx_1 dx_2 \frac{\tau}{x_1 x_2} \Theta(x_1 x_2 - \tau) f_i^0(x_1) f_{\bar{i}}^0(x_2) P\left(\frac{\tau}{x_1 x_2}\right) \\
 &= \tau \int_{\tau}^1 \frac{dx_1}{x_1} f_i^0(x_1) \int_{\frac{\tau}{x_1}}^1 \frac{dx_2}{x_2} P\left(\frac{\tau}{x_1 x_2}\right) f_{\bar{i}}^0(x_2) \\
 &= \tau \int_{\tau}^1 \frac{dx_1}{x_1} f_i^0(x_1) \int_{\tau}^1 dx_2 \delta\left(x_2 - \frac{\tau}{x_1}\right) \int_{x_2}^1 \frac{dy}{y} P\left(\frac{x_2}{y}\right) f_{\bar{i}}^0(y) \\
 &= \tau \int_0^1 dx_1 dx_2 dz \delta(1-z) \delta(x_1 x_2 z - \tau) f_i^0(x_1) \int_{x_2}^1 \frac{dy}{y} P\left(\frac{x_2}{y}\right) f_{\bar{i}}^0(y). \quad (8.153)
 \end{aligned}$$

In addition one finds for the product of two renormalised PDFs of the type of Eq. (8.147):

$$\begin{aligned}
 f_i(x_1, M^2) f_{\bar{i}}(x_2, M^2) &= f_i^0(x_1) f_{\bar{i}}^0(x_2) \\
 &+ f_i^0(x_1) \frac{\alpha_s}{2\pi} \int_{x_2}^1 dy \frac{1}{y} \left\{ f_{\bar{i}}^0(y) \left[P_{q\bar{q}}\left(\frac{x_2}{y}\right) \log\left(\frac{M^2}{\eta^2}\right) + C_q^S\left(\frac{x_2}{y}\right) \right] \right. \\
 &\quad \left. + g^0(y) \left[P_{qg}\left(\frac{x_2}{y}\right) \log\left(\frac{M^2}{\eta^2}\right) + C_g^S\left(\frac{x_2}{y}\right) \right] \right\} \\
 &+ f_{\bar{i}}^0(x_2) \frac{\alpha_s}{2\pi} \int_{x_1}^1 dy \frac{1}{y} \left\{ f_i^0(y) \left[P_{q\bar{q}}\left(\frac{x_1}{y}\right) \log\left(\frac{M^2}{\eta^2}\right) + C_q^S\left(\frac{x_1}{y}\right) \right] \right. \\
 &\quad \left. + g^0(y) \left[P_{qg}\left(\frac{x_1}{y}\right) \log\left(\frac{M^2}{\eta^2}\right) + C_g^S\left(\frac{x_1}{y}\right) \right] \right\} \\
 &+ O(\alpha_s^2). \quad (8.154)
 \end{aligned}$$

Comparing the last two equations, one finds, that one can express the hadronic cross

section (8.152) in terms of the renormalised PDFs (8.147). One obtains [ESW96]:

$$\begin{aligned} \frac{d\sigma}{dM^2} = & \frac{4\pi\alpha^2}{9M^4} \tau \sum_i e_i^2 \int_0^1 dx_1 dx_2 dz \delta(x_1 x_2 z - \tau) \\ & \times \left\{ \left(f_i(x_1, M^2) f_{\bar{i}}(x_2, M^2) + (f_i \leftrightarrow f_{\bar{i}}) \right) \left[\delta(1-z) + \frac{\alpha_s}{2\pi} \tilde{C}_q^S(z) \right] \right. \\ & + \left[g(x_1, M^2) \left(f_i(x_2, M^2) + f_{\bar{i}}(x_2, M^2) \right) \right. \\ & \left. \left. + (g \leftrightarrow f_i, f_{\bar{i}}) \right] \frac{\alpha_s}{2\pi} \tilde{C}_g^S(z) \right\} , \end{aligned} \quad (8.155)$$

which is correct to $O(\alpha_s)$. The collinear divergences and the bare PDFs have been absorbed into the renormalised PDFs. Again there remain finite contributions $\tilde{C}_q^S, \tilde{C}_g^S$, which can be calculated once the renormalisation scheme S has been fixed.

8.6.2 Collinear singularities in our model

In Sec. 6.2.4 we found, that the introduction of the renormalised PDFs gives rise to the famous DGLAP evolution equations which describe successfully the scaling violations [ESW96]. Clearly for our model we want to inherit this fundamental QCD property. Also from a pragmatic point of view we want to use the standard (renormalised) PDFs from the literature. On the other hand, in the pQCD approach to the DY process the reshuffling of the collinear singularities into the renormalised PDFs was only possible for the p_T integrated M spectrum. In our model we also want to describe the DY spectra differential in p_T . Therefore, we cannot follow the steps outlined in the previous subsection. However, we have an explicit regularisation of the collinear singularities. This allows to make contact between the bare and the renormalised PDFs by a kind of backward engineering, which we will describe next.

Since we explicitly take into account all $O(\alpha_s)$ processes, cf. Secs. 8.1-8.4, we now have to make sure that all the $O(\alpha_s)$ contributions to the cross section, that were absorbed into the renormalised PDFs are subtracted. Otherwise we would double-count the $O(\alpha_s)$ contributions. Schematically the hadronic cross section for DY pair production to next-to-leading order in α_s can be written as:

$$d\sigma = \int \sum_i e_i^2 \left[\underbrace{d\hat{\sigma}_{\text{LO}}}_{O(\alpha_s^0)=O(1)} f_i^0 \cdot f_{\bar{i}}^0 + \underbrace{d\hat{\sigma}_{\text{VC+B}}}_{O(\alpha_s)} f_i^0 \cdot f_{\bar{i}}^0 + \underbrace{d\hat{\sigma}_{\text{C}}}_{O(\alpha_s)} g^0 \cdot (f_i^0 + f_{\bar{i}}^0) \right] , \quad (8.156)$$

with the bare PDFs f_i^0, g^0 . We note that $f_i \cdot f_{\bar{i}} = f_i^0 f_{\bar{i}}^0 + O(\alpha_s)$ and $g \cdot (f_i + f_{\bar{i}}) = g^0 \cdot (f_i^0 + f_{\bar{i}}^0) + O(\alpha_s)$, and so to $O(\alpha_s)$ nothing changes if we replace the bare PDFs

multiplying the NLO partonic cross sections:

$$d\sigma = \int \sum_i e_i^2 \left[\underbrace{d\hat{\sigma}_{\text{LO}}}_{O(\alpha_s^0)=O(1)} f_i^0 \cdot f_{\bar{i}}^0 + \underbrace{d\hat{\sigma}_{\text{VC+B}}}_{O(\alpha_s)} f_i \cdot f_{\bar{i}} + \underbrace{d\hat{\sigma}_{\text{C}}}_{O(\alpha_s)} g \cdot (f_i + f_{\bar{i}}) \right] + O(\alpha_s^2). \quad (8.157)$$

However, if we were to do the same thing with the LO term, we would get additional $O(\alpha_s)$ contributions, cf. Eq. (8.154). How do we subtract these contributions? After all, we cannot calculate the integrals in Eq. (8.154), since we do not know η or the bare PDFs.

In our model we set out to calculate exactly those transverse momentum spectra that were integrated in the derivation of the renormalised PDFs in the pQCD case above. To accomplish this, we have introduced quark mass distributions to handle the collinear divergences that enter the quark PDF in Eq. (8.147). The important difference between the pQCD approach and our model is, therefore, the following: in pQCD the regulating cut-off η^2 is completely arbitrary and physical results can only be obtained by absorbing this arbitrariness into the renormalised PDFs. All the finite and scheme-dependent contributions can be calculated analytically. In our model we know the regulator η in (8.147), it is nothing but our quark mass m (or better m^2). However, we do not know the finite contributions $C_{q,g}^S$ in our model. To estimate them, we introduce two new parameters κ_q and κ_g , so that the functions $\mathcal{F}_{q\bar{q}}$ and \mathcal{F}_{qg} become:

$$\mathcal{F}_{q\bar{q}}^m(z) = 2P_{qq}(z) \log \left(\frac{M^2}{\kappa_q^2 m^2} \right), \quad (8.158)$$

$$\mathcal{F}_{qg}^m(z) = P_{qg}(z) \log \left(\frac{M^2}{\kappa_g^2 m^2} \right). \quad (8.159)$$

Since we expect that the finite contributions do not significantly change the log structure, we can assume that κ_q and κ_g are on the order of 1. Below we will vary κ_q, κ_g in a reasonable range and study the impact on the results of our calculation (cf. Secs. 9.1 and 10.6).

Now we can rewrite the renormalised PDFs in Eq. (8.154):

$$\begin{aligned}
 f_i(x_1, M^2) f_{\bar{i}}(x_2, M^2) &= f_i^0(x_1) f_{\bar{i}}^0(x_2) \\
 &+ f_i^0(x_1) \frac{\alpha_s}{2\pi} \int_{x_2}^1 dy \frac{1}{y} \left\{ f_{\bar{i}}^0(y) \left[P_{qq} \left(\frac{x_2}{y} \right) \log \left(\frac{M^2}{\kappa_q^2 m^2} \right) \right] \right. \\
 &\quad \left. + g^0(y) \left[P_{qg} \left(\frac{x_2}{y} \right) \log \left(\frac{M^2}{\kappa_g^2 m^2} \right) \right] \right\} \\
 &+ f_{\bar{i}}^0(x_2) \frac{\alpha_s}{2\pi} \int_{x_1}^1 dy \frac{1}{y} \left\{ f_i^0(y) \left[P_{qq} \left(\frac{x_1}{y} \right) \log \left(\frac{M^2}{\kappa_q^2 m^2} \right) \right] \right. \\
 &\quad \left. + g^0(y) \left[P_{qg} \left(\frac{x_1}{y} \right) \log \left(\frac{M^2}{\kappa_g^2 m^2} \right) \right] \right\} \\
 &+ O(\alpha_s^2) . \tag{8.160}
 \end{aligned}$$

Solving for the product of the bare PDFs gives:

$$\begin{aligned}
 f_i^0(x_1) f_{\bar{i}}^0(x_2) &= f_i(x_1, M^2) f_{\bar{i}}(x_2, M^2) \\
 &- f_i^0(x_1) \frac{\alpha_s}{2\pi} \int_{x_2}^1 dy \frac{1}{y} \left\{ f_{\bar{i}}^0(y) \left[P_{qq} \left(\frac{x_2}{y} \right) \log \left(\frac{M^2}{\kappa_q^2 m^2} \right) \right] \right. \\
 &\quad \left. + g^0(y) \left[P_{qg} \left(\frac{x_2}{y} \right) \log \left(\frac{M^2}{\kappa_g^2 m^2} \right) \right] \right\} \\
 &- f_{\bar{i}}^0(x_2) \frac{\alpha_s}{2\pi} \int_{x_1}^1 dy \frac{1}{y} \left\{ f_i^0(y) \left[P_{qq} \left(\frac{x_1}{y} \right) \log \left(\frac{M^2}{\kappa_q^2 m^2} \right) \right] \right. \\
 &\quad \left. + g^0(y) \left[P_{qg} \left(\frac{x_1}{y} \right) \log \left(\frac{M^2}{\kappa_g^2 m^2} \right) \right] \right\} \\
 &+ O(\alpha_s^2) . \tag{8.161}
 \end{aligned}$$

On the right hand side we can replace all the bare PDFs by their renormalised version,

since all additional corrections introduced by this procedure are $O(\alpha_s^2)$:

$$\begin{aligned}
 f_i^0(x_1)f_{\bar{i}}^0(x_2) &= f_i(x_1, M^2)f_{\bar{i}}(x_2, M^2) \\
 &- f_i(x_1, M^2)\frac{\alpha_s}{2\pi}\int_{x_2}^1 dy \frac{1}{y} \left\{ f_{\bar{i}}(y, M^2) \left[P_{qq} \left(\frac{x_2}{y} \right) \log \left(\frac{M^2}{\kappa_q^2 m^2} \right) \right] \right. \\
 &\quad \left. + g(y, M^2) \left[P_{qg} \left(\frac{x_2}{y} \right) \log \left(\frac{M^2}{\kappa_g^2 m^2} \right) \right] \right\} \\
 &- f_{\bar{i}}(x_2, M^2)\frac{\alpha_s}{2\pi}\int_{x_1}^1 dy \frac{1}{y} \left\{ f_i(y, M^2) \left[P_{qq} \left(\frac{x_1}{y} \right) \log \left(\frac{M^2}{\kappa_q^2 m^2} \right) \right] \right. \\
 &\quad \left. + g(y, M^2) \left[P_{qg} \left(\frac{x_1}{y} \right) \log \left(\frac{M^2}{\kappa_g^2 m^2} \right) \right] \right\} \\
 &+ O(\alpha_s^2) .
 \end{aligned} \tag{8.162}$$

We define:

$$\begin{aligned}
 f_i^{\text{sub}}(x, M^2) &= \frac{\alpha_s}{2\pi} \int_x^1 dy \frac{1}{y} f_i(y, M^2) P_{qq} \left(\frac{x}{y} \right) \log \left(\frac{M^2}{\kappa_q^2 m^2} \right) , \\
 g^{\text{sub}}(x, M^2) &= \frac{\alpha_s}{2\pi} \int_x^1 dy \frac{1}{y} g(y, M^2) P_{qg} \left(\frac{x}{y} \right) \log \left(\frac{M^2}{\kappa_g^2 m^2} \right) ,
 \end{aligned} \tag{8.163}$$

and so we find:

$$\begin{aligned}
 f_i^0(x_1)f_{\bar{i}}^0(x_2) &= f_i(x_1, M^2)f_{\bar{i}}(x_2, M^2) \\
 &- f_i(x_1, M^2)f_{\bar{i}}^{\text{sub}}(x_2, M^2) - f_i(x_1, M^2)g^{\text{sub}}(x_2, M^2) \\
 &- f_{\bar{i}}(x_2, M^2)f_i^{\text{sub}}(x_1, M^2) - f_{\bar{i}}(x_2, M^2)g^{\text{sub}}(x_1, M^2) \\
 &+ O(\alpha_s^2) .
 \end{aligned} \tag{8.164}$$

In this scheme the hadronic cross section (8.157) becomes:

$$\begin{aligned}
 d\sigma &= \int \sum_i e_i^2 [d\hat{\sigma}_{\text{LO}} f_i \cdot f_{\bar{i}} \\
 &\quad - d\hat{\sigma}_{\text{LO}} (f_i \cdot f_{\bar{i}}^{\text{sub}} + f_{\bar{i}}^{\text{sub}} \cdot f_i) + d\hat{\sigma}_{\text{VC+B}} f_i \cdot f_{\bar{i}} \\
 &\quad - d\hat{\sigma}_{\text{LO}} (f_i \cdot g^{\text{sub}} + f_{\bar{i}} \cdot g^{\text{sub}}) + d\hat{\sigma}_{\text{C}} g \cdot (f_i + f_{\bar{i}})] \\
 &+ O(\alpha_s^2) .
 \end{aligned} \tag{8.165}$$

From now on, we label the different contributions to the cross section as sketched in the following:

$$d\sigma_{\text{LO}} = \int \sum_i e_i^2 d\hat{\sigma}_{\text{LO}} f_i \cdot f_{\bar{i}}, \quad (8.166)$$

$$d\sigma_{q\bar{q}} = \int \sum_i e_i^2 \left[d\hat{\sigma}_{\text{VC+B}} f_i \cdot f_{\bar{i}} - d\hat{\sigma}_{\text{LO}} \left(f_i \cdot f_{\bar{i}}^{\text{sub}} + f_i^{\text{sub}} \cdot f_{\bar{i}} \right) \right], \quad (8.167)$$

$$d\sigma_{qg} = \int \sum_i e_i^2 \left[d\hat{\sigma}_{\text{C}} g \cdot (f_i + f_{\bar{i}}) - d\hat{\sigma}_{\text{LO}} \left(f_i \cdot g^{\text{sub}} + f_{\bar{i}} \cdot g^{\text{sub}} \right) \right]. \quad (8.168)$$

In Eqs. (8.167) and (8.168) we subtract now precisely those $O(\alpha_s)$ contributions which were absorbed before into the renormalised PDFs. Thus, by this procedure we have produced in our model a consistent cross section to $O(\alpha_s)$. Indeed, we have checked explicitly that the collinear divergences which appear in $d\sigma_{\text{VC+B}}$, if the quark masses are sent to zero, cancel the corresponding divergence of f_i^{sub} as given in Eq. (8.163). The same is true for $d\sigma_{\text{C}}$ and g^{sub} . Thus the expressions (8.167) and (8.168) remain finite for vanishing quark masses.

For the calculation of our results in Part V we will use Eqs. (8.166)-(8.168). The quantities which enter are, on the one hand, the standard PDFs which we can take from the literature, and, on the other hand, the parameters κ_q and κ_g which appear in Eq. (8.163). We recall that these parameters introduced in Eqs. (8.158) and (8.159) correspond to finite, i.e. infrared safe, contributions which appear, e.g., as $\hat{C}_{q,g}^S$ in Eqs. (8.150) and (8.151). We will vary the parameters κ_q and κ_g around natural values (i.e. around 1), to estimate these finite contributions.

8.7 Influence of initial transverse momentum distributions on DY p_T spectra

Even in the mass distribution approach at NLO we find that the p_T data are heavily underestimated, cf. Fig. 8.8. Therefore, we have also introduced parton initial transverse momentum distributions for the NLO processes, just as we did at LO in Sec. 7.4.3. Taking into account these distributions we obtain a good description of measured cross sections without K factors, as we will show in Part V.

Part V

Results and predictions

9

Drell-Yan in high energy proton-proton collisions - fixing parameters

In this chapter we present results of our full model. We will begin by fixing our model parameters on data from the E866 experiment [Web03, NuSea03]. We chose this experiment for two reasons: it measured the DY cross sections in pp collisions, instead of p-nucleus collisions, so there are no nuclear effects which have to be taken care of by experiment or theory. Second, the experiment measured at rather high energies ($S = 1500 \text{ GeV}^2$), where one assumes parton model like approaches to work reasonably well.

Before we go on, we want to stress, that the calculation in our full model reproduces measured DY p_T spectra without the need for a K factor, see for example Fig. 9.4. This is in contrast to the LO calculation of Sec. 7.6. In order to better understand the parameter dependence of our model, we explore the parameter space in the following. The details of how we obtain the presented cross sections were given in Sec. 7.6.1. First we show several plots, in which we vary only one parameter and keep the others fixed.

9.1 E866 - p_T spectrum

In Fig. 9.1 we plot the results of our full NLO model for different D . As one can see for D around 0.45 GeV, which corresponds to an average squared initial quark transverse momentum $\langle k_T^2 \rangle = (0.9)^2 \text{ GeV}^2$, the data are reproduced quite well. Obviously, D determines the shape of the p_T spectra.

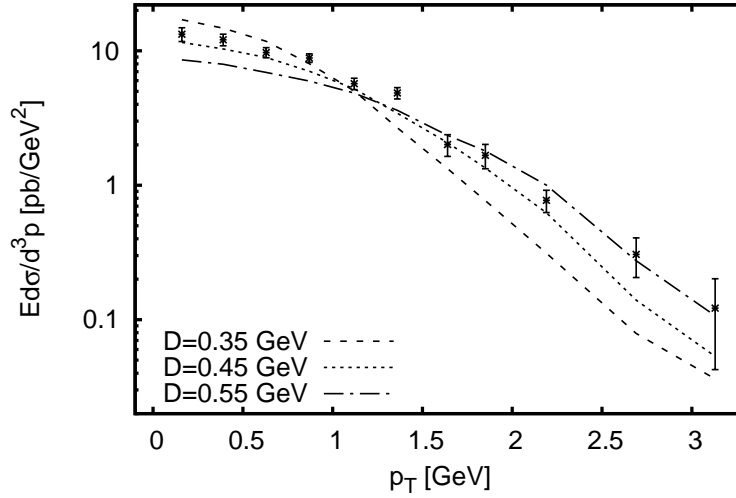


Figure 9.1: p_T spectrum obtained from our full model with different values of D . Everywhere $\Gamma = 0.2$ GeV, $\lambda = 5$ MeV, $\kappa_q = 1$ and $\kappa_g = 2$. The PDFs are the MSTW2008LO68cl set. Data are from E866 binned with $4.2 \text{ GeV} < M < 5.2 \text{ GeV}$, $-0.05 < x_F < 0.15$. Only statistical errors are shown.

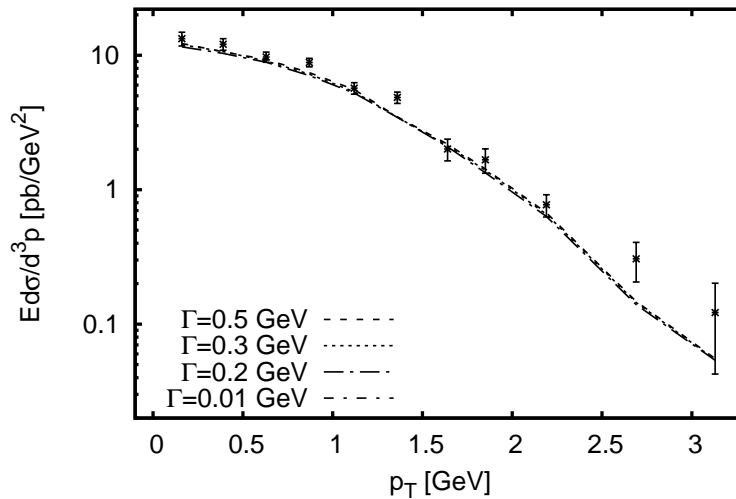


Figure 9.2: p_T spectrum obtained from our full model with different values of Γ . Everywhere $D = 0.45$ GeV, $\lambda = 5$ MeV, $\kappa_q = 1$ and $\kappa_g = 2$. The PDFs are the MSTW2008LO68cl set. Note that the curves for $\Gamma \geq 0.2$ GeV are on top of each other. The $\Gamma = 0.01$ GeV curve is slightly higher than the others. Data are from E866 binned with $4.2 \text{ GeV} < M < 5.2 \text{ GeV}$, $-0.05 < x_F < 0.15$. Only statistical errors are shown.

In Fig. 9.2 we show results for different Γ . The results for several values of Γ all agree very well with each other and at the same time reproduce the data quite well. Thus at E866 energies our model appears to be rather insensitive to changes of Γ over a wide range.

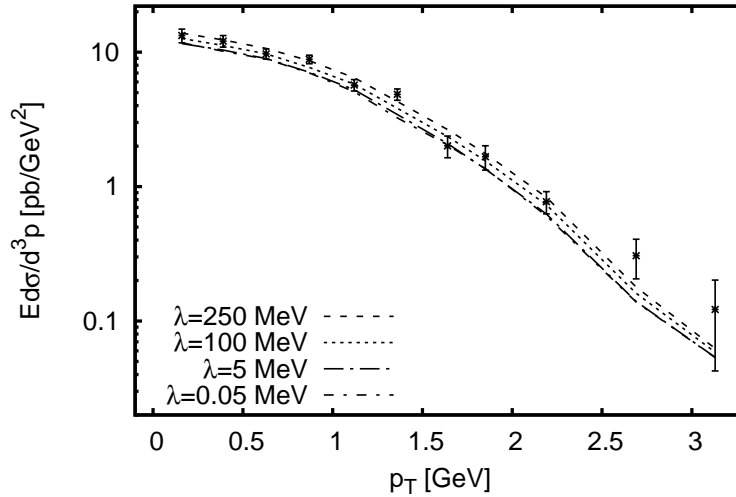


Figure 9.3: p_T spectrum obtained from our full model with different values of λ . Everywhere $D = 0.45$ GeV, $\Gamma = 0.2$ GeV, $\kappa_q = 1$ and $\kappa_g = 2$. The PDFs are the MSTW2008LO68cl set. Note that the curves for $\lambda \leq 5$ MeV are on top of each other. Data are from E866 binned with 4.2 GeV $< M < 5.2$ GeV, $-0.05 < x_F < 0.15$. Only statistical errors are shown.

Remember that the gluon mass λ was introduced to regulate divergences that occur when the gluons become very soft. In the limit of $\lambda \rightarrow 0$ these divergences of the bremsstrahlung and the vertex correction processes should exactly cancel. Therefore, it is sensible to choose λ as small as numerically feasible. Results for different choices of the gluon mass λ are shown in Fig. 9.3. While the results for $\lambda = 100, 250$ MeV are still visibly larger than the results for 5 and 0.5 MeV, the latter two agree very well with each other. Thus the calculated cross section appears to converge in the $\lambda \rightarrow 0$ limit. Therefore, we chose $\lambda = 5$ MeV for the calculation of all the following results.

We show an example of the influence of different parton distribution functions in Fig. 9.4. The results with the MSTW2008LO68cl [MSTW09] and GJR08lo [GJDR08] sets agree quite well with each other, with only small deviations. This is an illustration of the uncertainties induced by the different integrated (i.e. standard) parton distributions.

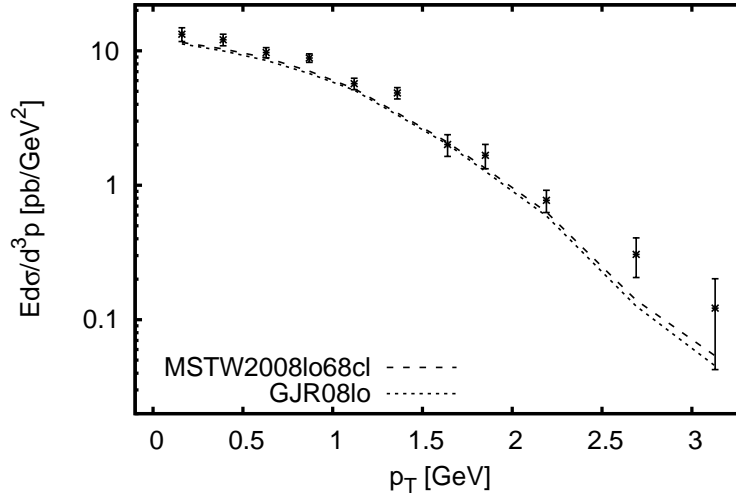


Figure 9.4: p_T spectrum obtained from our full model with different PDF sets. Everywhere $D = 0.45$ GeV, $\Gamma = 0.2$ GeV, $\lambda = 5$ MeV, $\kappa_q = 1$ and $\kappa_g = 2$. Data are from E866 binned with 4.2 GeV $< M < 5.2$ GeV, $-0.05 < x_F < 0.15$. Only statistical errors are shown.

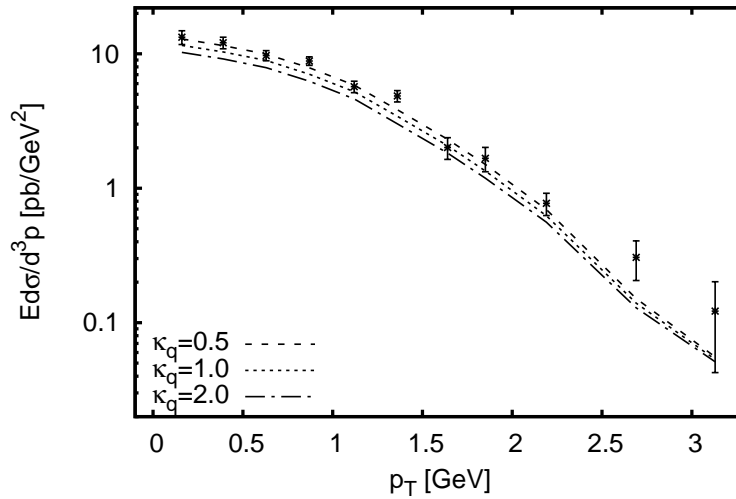


Figure 9.5: p_T spectrum obtained from our full model with different values of the subtraction parameter κ_q . Everywhere $D = 0.45$ GeV, $\Gamma = 0.2$ GeV, $\lambda = 5$ MeV and $\kappa_g = 2$. The PDFs are the MSTW2008LO68cl set. Data are from E866 binned with 4.2 GeV $< M < 5.2$ GeV, $-0.05 < x_F < 0.15$. Only statistical errors are shown.

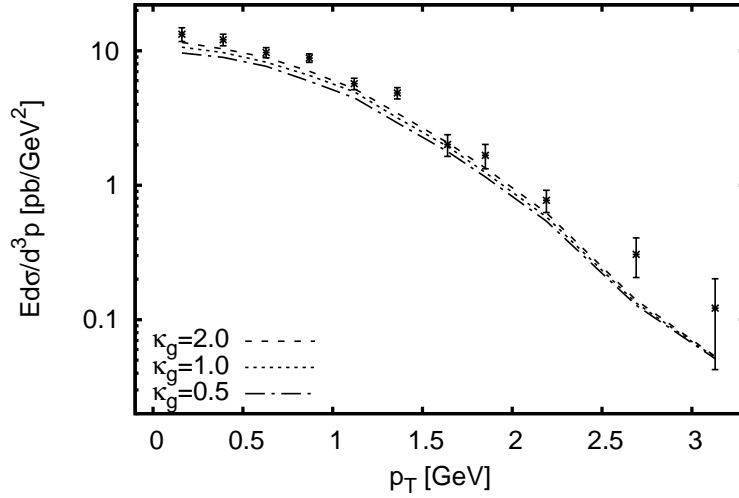


Figure 9.6: p_T spectrum obtained from our full model with different values of the subtraction parameter κ_g . Everywhere $D = 0.45$ GeV, $\Gamma = 0.2$ GeV, $\lambda = 5$ MeV and $\kappa_q = 1$. The PDFs are the MSTW2008LO68cl set. Data are from E866 binned with 4.2 GeV $< M < 5.2$ GeV, $-0.05 < x_F < 0.15$. Only statistical errors are shown.

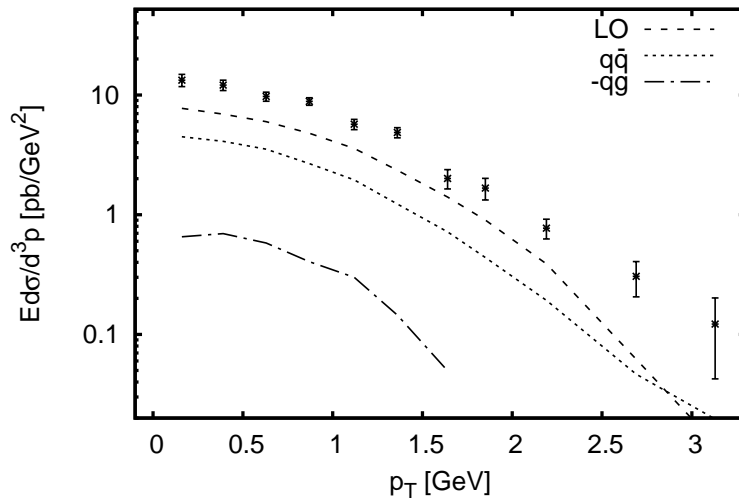


Figure 9.7: p_T spectrum obtained from our model decomposed into the different contributions as described at the end of Sec. 8.6. Note that we plot the *negative* quark-gluon contribution. Everywhere $D = 0.45$ GeV, $\Gamma = 0.2$ GeV, $\lambda = 5$ MeV, $\kappa_q = 1$ and $\kappa_g = 2$. The PDFs are the MSTW2008LO68cl set. Data are from E866 binned with 4.2 GeV $< M < 5.2$ GeV, $-0.05 < x_F < 0.15$. Only statistical errors are shown.

To determine the subtraction parameters κ_q and κ_g we explore the dependence of the cross section on these two parameters in Figs. 9.5 and 9.6. In the range of natural choices ($\kappa_q, \kappa_g = \frac{1}{2} \dots 2$) we find, that with $\kappa_q = 1$ and $\kappa_g = 2$ the data are described rather well. Although Fig. 9.5 would indicate a better fit for smaller κ_q , we stick to $\kappa_q = 1$, since for this value the slope of the M spectra fits also very well, as we will show for example in Sec. 10.2.

In Fig. 9.7 the cross sections of the different contributions to the full result are plotted individually. The definition of the LO, quark-antiquark ($q\bar{q}$) and quark-gluon (qg) contributions is given at the end of Sec. 8.6. Note that the sum of the LO contribution and the $q\bar{q}$ corrections make up most of the cross section. The contribution of the qg correction is relatively small and negative for not too large p_T .

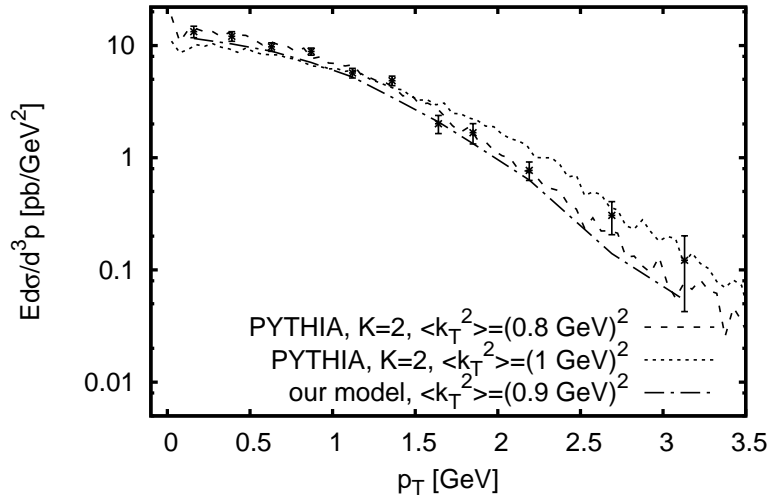


Figure 9.8: p_T spectrum comparison of PYTHIA results with our full model. For the PYTHIA calculations version 6.225 with CTEQ5L PDFs were used. The PYTHIA result is plotted for two different values of the average initial k_T^2 and multiplied by a factor $K = 2$. Our model was calculated with $D = 0.45$ GeV, $\Gamma = 0.2$ GeV, $\lambda = 5$ MeV, $\kappa_q = 1$, $\kappa_g = 2$ and MSTW2008LO68cl PDF set. Data are from E866 binned with 4.2 GeV $< M < 5.2$ GeV, $-0.05 < x_F < 0.15$. Only statistical errors are shown.

Fig. 9.8 shows a comparison of the results of our model with the results of a PYTHIA event generator calculation. For this specific plot PYTHIA version 6.225 [S⁺01] with CTEQ5L PDFs [Collaboration00] was used and the PYTHIA results were scaled up by a factor $K = 2$. The comparison with the experimental data suggests a good fit of the shape of the spectrum for a value of $\langle k_T^2 \rangle = (0.8 \text{ GeV})^2$ in PYTHIA (internal parameter PARP(91) = 0.8). For our value of D we get $\langle k_T^2 \rangle = (2D)^2 = (0.9 \text{ GeV})^2$. Although the PYTHIA parameter is obviously intended to have the same meaning as our definition for the average initial transverse momentum, the complex internal

treatment of the interaction in the PYTHIA code leads to some numerical mismatch with our implementation.

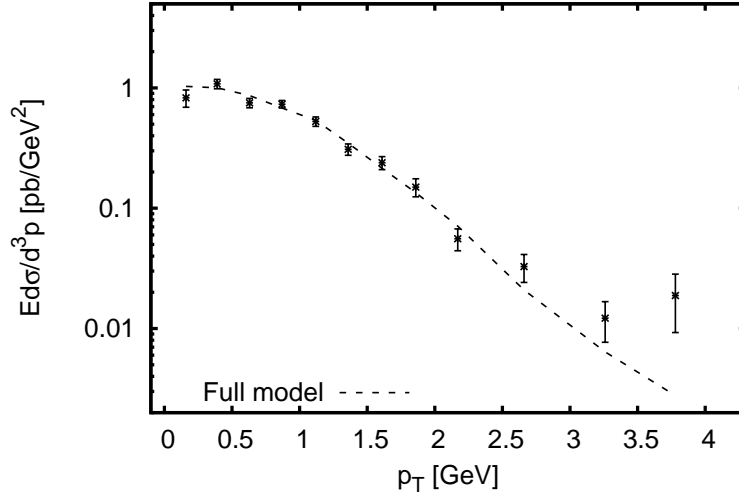


Figure 9.9: p_T spectrum obtained from our full model. Everywhere $D = 0.45$ GeV, $\Gamma = 0.2$ GeV, $\lambda = 5$ MeV, $\kappa_q = 1$ and $\kappa_g = 2$. The PDFs are the MSTW2008LO68cl set. Data are from E866 binned with 7.2 GeV $< M < 8.7$ GeV, $-0.05 < x_F < 0.15$. Only statistical errors are shown.

For comparison we show our results for a different M bin in Fig. 9.9. With the parameters determined above our full model reproduces the measured spectrum very well. In contrast to the LO approach of chapter 7 we do not need a K factor anymore to describe the absolute height of the spectrum. At the same time the width D of the intrinsic (non-perturbative) k_T distributions changes only little ($D = 0.5$ GeV vs. $D = 0.45$ GeV) when passing from the LO to the NLO calculation. Note, however, that Fig. 9.7 indicates, that at least the results for the $q\bar{q}$ corrections deviate from a Gaussian behavior at $p_T \geq 3$ GeV. Thus the contributions of some of the hard NLO processes are only significant in the high (perturbative) p_T region. Therefore, to describe the low p_T regime at NLO one still requires almost the same non-perturbative input for the intrinsic parton k_T , i.e., only little transverse momentum is generated dynamically and the width parameter D does not change considerably.

Note one more important point: in principle the divergence of the NLO processes near $p_T = 0$ can also be cured by choosing a finite and fixed quark mass. To illustrate this, we show in Fig. 9.10 the results from our full model, but calculated for a set of fixed quark masses. To be able to compare this result with our full model with broad mass distributions we estimate the average quark mass obtained there in the following scheme: our quark mass distribution $A(p)$ in Eq. (7.127) depends not only on m , but also on the large quark momentum component p^+ , which itself depends on the quark

transverse momenta, which are integrated over. However, in the E866 regime $x_F \approx 0$ and one can get a rough estimate by assuming simple collinear kinematics (i.e. putting all transverse momenta to zero). Then one finds simply $p^+ = M$ (cf. Eqs. (7.39-7.40)), which gives an upper limit for p^+ . For the M -bin under consideration here we choose a representative value of $M = 4.5$ GeV and so for a width $\Gamma = 0.2$ GeV one finds for the average squared quark mass:

$$\langle m^2 \rangle = \int_0^{m_N^2} dm^2 m^2 A(p) \approx 0.32 \text{ GeV}^2, \quad (9.1)$$

which corresponds to an average $m = \sqrt{\langle m^2 \rangle} \approx 0.57$ GeV. For fixed quark mass values around this number we again find good agreement of our calculation with the data.

A fixed quark mass scheme certainly has its virtues: none of the problems concerning the renormalised quark-photon vertex arise, since for fixed equal quark masses the Ward-Takahashi identities are at work, and the calculations are simplified, since fewer integrals have to be evaluated. Note, however, that it is much more natural to assume a broad mass distribution, since the nucleon is composed of strongly interacting partons. As we have already shown above and will also show in the next chapter, we can describe the experimental data quantitatively well assuming broad quark mass distributions.

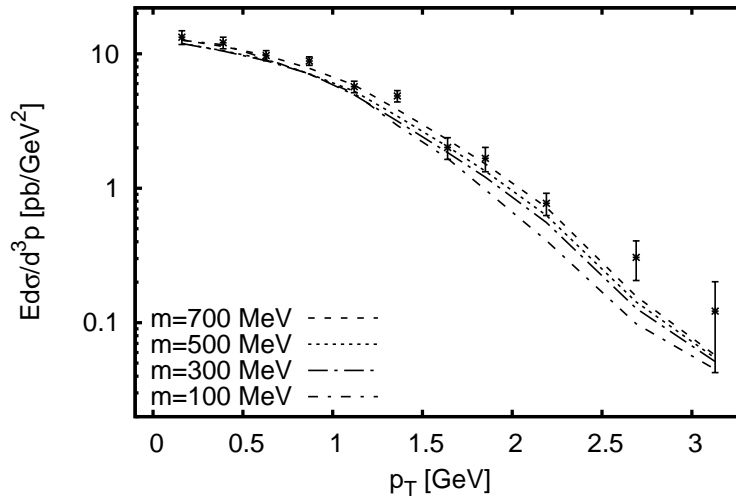


Figure 9.10: p_T spectrum obtained from our full model for different fixed quark masses m . Everywhere $D = 0.45$ GeV, $\lambda = 5$ MeV, $\kappa_q = 1$ and $\kappa_g = 2$. The PDFs are the MSTW2008LO68cl set. Data are from E866 binned with $4.2 \text{ GeV} < M < 5.2 \text{ GeV}$, $-0.05 < x_F < 0.15$. Only statistical errors are shown.

9.2 E866 - M spectrum

In this section we present our results for the measured M spectrum from E866, which are basically the p_T spectra integrated over p_T . The double-differential cross section is given by the E866 collaboration as:

$$M^3 \frac{d\sigma}{dM dx_F} . \quad (9.2)$$

Again the data are given in several bins of M and x_F and for every datapoint the average values $\langle M \rangle$ and $\langle x_F \rangle$ are provided. For the different contributions in our model we calculate the quantity of Eq. (9.2) by integrating over p_T^2 for every datapoint using these averaged values:

$$\begin{aligned} M^3 \frac{d\sigma}{dM dx_F} &\rightarrow \langle M \rangle^3 \int_0^{(p_T)_{\max}^2} dp_T^2 \frac{d\sigma}{dM dx_F dp_T^2} \\ &= \langle M \rangle^3 \int_0^{(p_T)_{\max}^2} dp_T^2 2 \langle M \rangle \frac{d\sigma}{dM^2 dx_F dp_T^2} (\langle M \rangle, \langle x_F \rangle) . \end{aligned} \quad (9.3)$$

The maximal possible p_T is determined by the kinematics:

$$P_1 + P_2 = q + X \quad (9.4)$$

$$\Rightarrow (P_1 + P_2 - q)^2 = X^2 = M_R^2 \quad (9.5)$$

$$\begin{aligned} \Rightarrow S + M^2 - M_R^2 &= 2 (P_1 + P_2) q \\ &= 2\sqrt{SE} \\ &= 2\sqrt{S} \sqrt{M^2 + (p_T)_{\max}^2 + x_F^2 (q_z)_{\max}^2} \end{aligned} \quad (9.6)$$

$$\Rightarrow E^2 = M^2 + (p_T)_{\max}^2 + x_F^2 (q_z)_{\max}^2 \quad (9.7)$$

$$= \frac{(S + M^2 - M_R^2)^2}{4S} \quad (9.8)$$

$$\Rightarrow (p_T)_{\max}^2 = \frac{(S + M^2 - M_R^2)^2}{4S} - M^2 - x_F^2 (q_z)_{\max}^2 . \quad (9.9)$$

M_R^2 is the minimal invariant mass of the undetected remnants. For pp and pn collisions we choose a value of $M_R = 2m_N$ and for $\bar{p}p$ a value of $M_R = 1.1$ GeV, which can be interpreted as two times a diquark mass. Note that at c.m. energies of $\sqrt{S} \approx 15.3$ GeV (E537), $\sqrt{S} \approx 27.4$ GeV (E288, E439) and $\sqrt{S} \approx 38.8$ GeV (E605, E772, E866) we are not really sensitive to these values if they stay at or below a few GeV.

In Fig. 9.11 we compare our result for the double differential cross section to the data from E866. The slope and absolute height of the curve agree with the data quite well. However, since here the experimental error bars are rather large, we will make comparisons to M spectra from other experiments in Secs. 10.2 and 10.4 to test our model further.

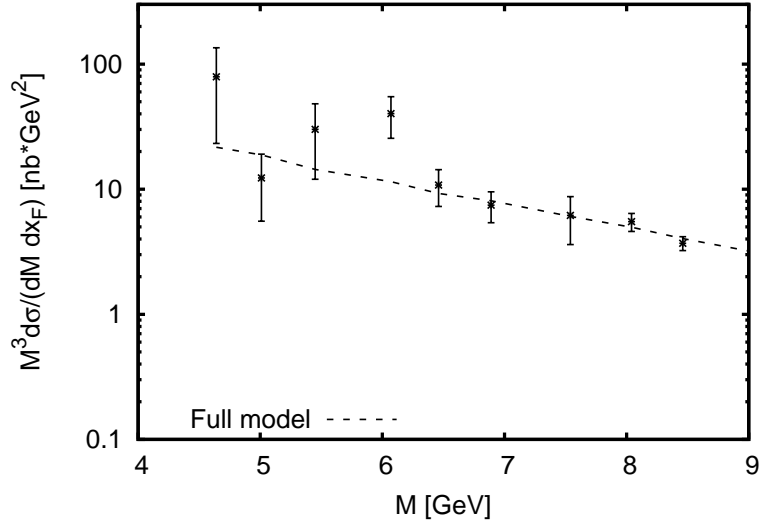


Figure 9.11: M spectrum obtained from our full model. Everywhere $D = 0.45$ GeV, $\Gamma = 0.2$ GeV, $\lambda = 5$ MeV, $\kappa_q = 1$ and $\kappa_g = 2$. The PDFs are the MSTW2008LO68cl set. Data are from E866 binned with $-0.05 < x_F < 0.05$. Only statistical errors shown.

10

Results and predictions for DY p_T and M spectra in proton and antiproton induced reactions

In the last chapter we explored in detail the dependence of our full model on the phenomenological parameters Γ (the width of the quark mass distributions), D (the width of the initial parton transverse momentum distributions) and κ_q, κ_g (the PDF subtraction parameters). Based on this analysis we fixed these parameters and in this chapter apply our full model to data taken in proton-nucleus and antiproton-proton reactions. We find that with our one set of parameters the different p_T and M spectra are reproduced well without any K factor. Based on these findings we finally present the predictions of our full model for fully differential DY pair production in the kinematics of the future $\overline{\text{P}}\text{ANDA}$ experiment.

10.1 E772 (pd)

Experiment E772 [E77294] measured dimuon production in pd collisions at $S \approx 1500$ GeV². For the calculation of the triple differential cross section we again use Eq. (7.131) and for the average values of M and x_F we use the center of the M and x_F bins. Since the experiment was done on deuterium we have calculated pp and pn cross sections and then averaged.

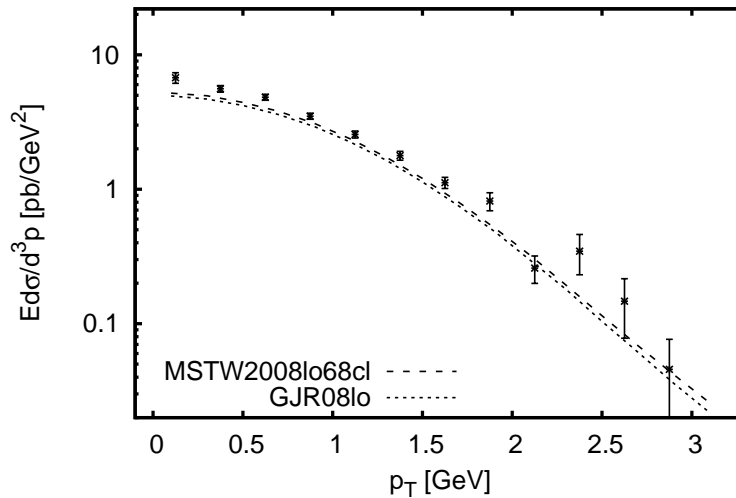


Figure 10.1: p_T spectrum obtained from our full model with different PDF sets. Everywhere $D = 0.45$ GeV, $\Gamma = 0.2$ GeV, $\lambda = 5$ MeV, $\kappa_q = 1$ and $\kappa_g = 2$. Data are from E772 binned with $5 \text{ GeV} < M < 6 \text{ GeV}$, $0.1 < x_F < 0.3$. Only statistical errors are shown.

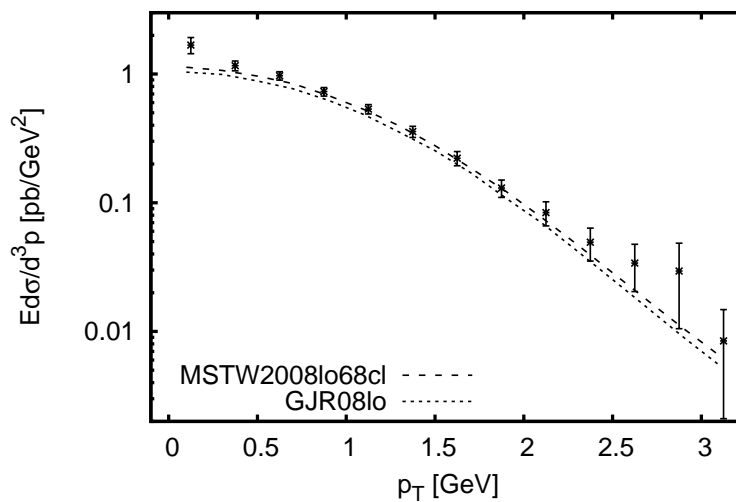


Figure 10.2: p_T spectrum obtained from our full model with different PDF sets. Everywhere $D = 0.45$ GeV, $\Gamma = 0.2$ GeV, $\lambda = 5$ MeV, $\kappa_q = 1$ and $\kappa_g = 2$. Data are from E772 binned with $7 \text{ GeV} < M < 8 \text{ GeV}$, $0.1 < x_F < 0.3$. Only statistical errors are shown.

In Figs. 10.1 and 10.2 we compare the results of our full model with different PDF

sets to triple differential data from E772 in different M bins. Agreement is again quite good, however, the shape of the spectrum seems to favor a slightly smaller value for D , which would enhance the spectrum near $p_T = 0$. Nevertheless, we have chosen $D = 0.45$ GeV, since this value allows us to describe the data from several different experiments with only minor deviations.

10.2 E605 (pCu)

Experiment E605 [M⁺91] measured dimuon production in pCu collisions at $S \approx 1500$ GeV². For the calculation of the triple differential cross section we again use Eq. (7.131) and for the average value of M we use the center of the M bin. For the p_T spectrum E605 gives $x_F = 0.1$. For the double differential cross section we use Eq. (9.2). Since the experiment was done on copper we have calculated pp and pn cross sections and then averaged (29 protons and 34 neutrons).

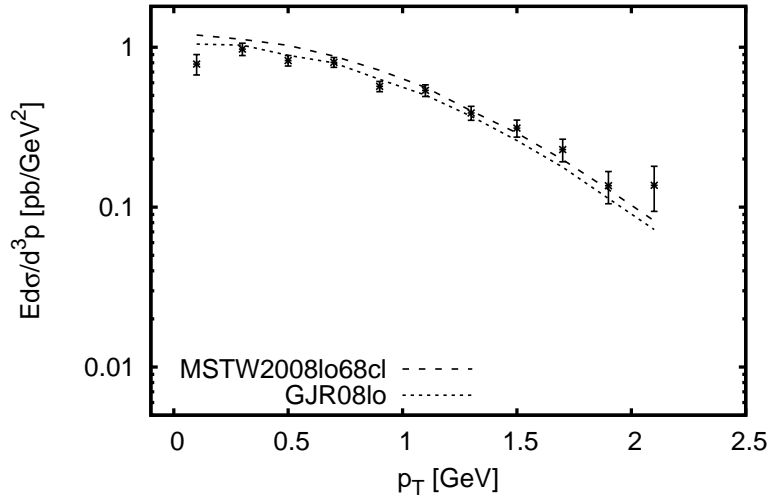


Figure 10.3: p_T spectrum obtained from our full model with different PDF sets. Everywhere $D = 0.45$ GeV, $\Gamma = 0.2$ GeV, $\lambda = 5$ MeV, $\kappa_q = 1$ and $\kappa_g = 2$. Data are from E605 binned with $7 \text{ GeV} < M < 8 \text{ GeV}$, $x_F = 0.1$. Only statistical errors are shown.

In Fig. 10.3 we compare the results of our full model with different PDF sets to triple differential data from E605. Here the shape of the spectrum confirms our chosen value for D and the overall agreement is good.

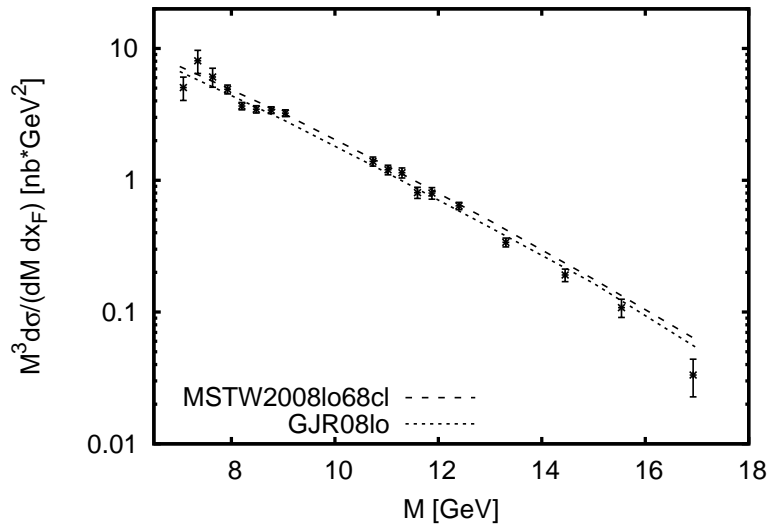


Figure 10.4: M spectrum obtained from our full model. Everywhere $D = 0.45$ GeV, $\Gamma = 0.2$ GeV, $\lambda = 5$ MeV, $\kappa_q = 1$ and $\kappa_g = 2$. Data are from E605 with $x_F = 0.125$. Only statistical errors shown.

In Fig. 10.4 we plot our result with different PDF sets for the double differential cross section together with the data from E605. Again agreement is quite good over the entire range of M .

10.3 E288 (pNucleus)

Experiment E288 [I⁺81] measured dimuon production in pA collisions at $S \approx 750$ GeV². For the calculation of the triple differential cross section we again use Eq. (7.131) and for the average value of M we use the center of the M bin. For the p_T spectrum E288 gives for the rapidity $y = 0.03$ and we thus chose $x_F = 0$ for our calculation. The experiment was done on different nuclei and only data averaged over the results from these nuclei have been presented. Therefore, we have calculated pp cross sections only.

In Fig. 10.5 we compare the results of our full model with different PDF sets to the triple differential data from E288. Again the agreement with the data is good and confirms our choice of parameters.

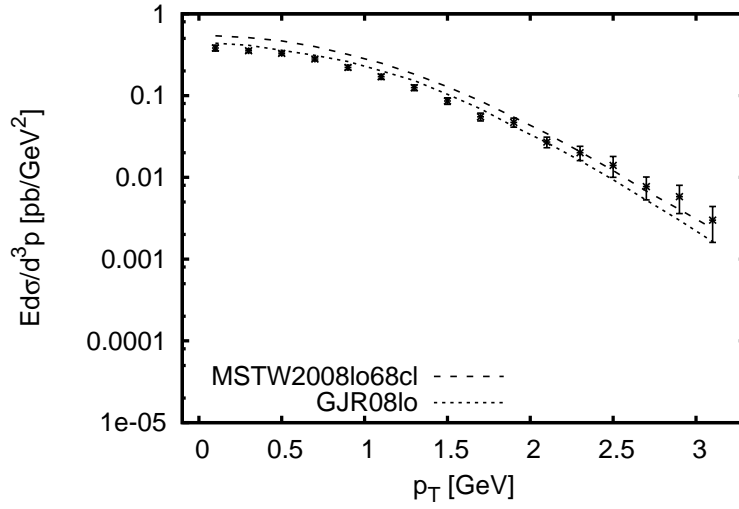


Figure 10.5: p_T spectrum obtained from our full model with different PDF sets. Everywhere $D = 0.45$ GeV, $\Gamma = 0.2$ GeV, $\lambda = 5$ MeV, $\kappa_q = 1$ and $\kappa_g = 2$. Data are from E288 binned with $7 \text{ GeV} < M < 8 \text{ GeV}$, $y = 0.03$, we have chosen $x_F = 0$ in our calculation. Only statistical errors are shown.

10.4 E439 (pW)

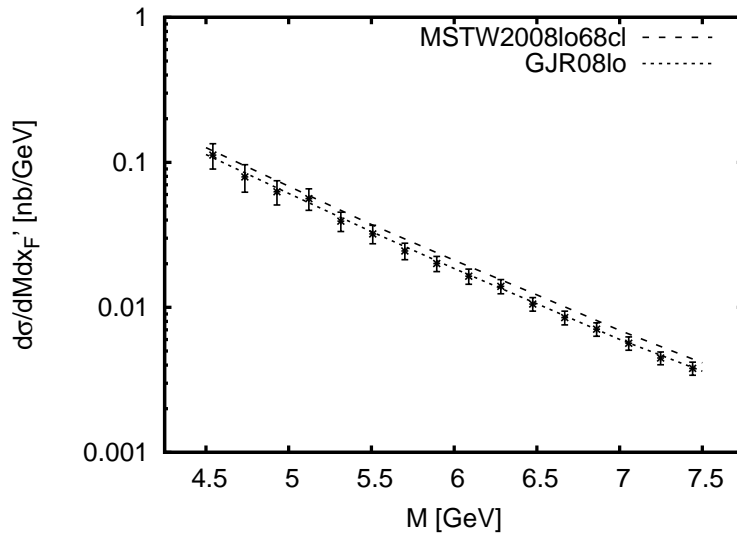


Figure 10.6: M spectrum obtained from our full model with different PDF sets. Everywhere $D = 0.45$ GeV, $\Gamma = 0.2$ GeV, $\lambda = 5$ MeV, $\kappa_q = 1$ and $\kappa_g = 2$. Data are from E439 with $x'_F = 0.1$. Only statistical errors are shown.

The details of experiment E439 and how we calculate the cross section are given in Sec. 7.6.2. In Fig. 10.6 we compare our results for the double differential cross section with the data from E439. For both PDF sets the absolute height and slope agrees with the data well.

10.5 E537 ($\bar{p}W$)

Experiment E537 [A⁺88] measured dimuon production in $\bar{p}W$ collisions at $S \approx 236$ GeV² in an invariant mass range of $4 < M < 9$ GeV. The obtained cross sections are double differential in two of the observables M , x_F and p_T^2 . To calculate the cross sections differential in p_T^2 with our model we use

$$\begin{aligned} \frac{d\sigma}{dx_F dp_T^2} &\rightarrow \int_{M^2\text{-bin}} \frac{d\sigma}{dM^2 dx_F dp_T^2} dM^2 \\ &\approx \sum_i \Delta M_i^2 \frac{d\sigma}{dM^2 dx_F dp_T^2} (\langle M_i \rangle, \langle x_F \rangle, \langle p_T \rangle) . \end{aligned} \quad (10.1)$$

The sum runs over several mass bins, which we choose as $M = 4..5, 5..6, 6..7, 7..8, 8..9$ GeV and in each bin we take the central value for $\langle M_i \rangle$. Since the experiment was done on tungsten we have calculated $\bar{p}p$ and $\bar{p}n$ cross sections and then averaged (74 protons and 110 neutrons).

We compare the calculated p_T spectrum with the data in Fig. 10.7. Our full model is on the lower side of the error bars of the data. However, one should note that the experimental error bars are rather large and thus the possibility to confirm or rule out our model is limited.

To calculate the M spectra we use

$$\begin{aligned} \frac{d\sigma}{dM dx_F} &= \int_0^{(p_T)_{\max}^2} dp_T^2 \frac{d\sigma}{dM dx_F dp_T^2} \\ &= \int_0^{(p_T)_{\max}^2} dp_T^2 2M \frac{d\sigma}{dM^2 dx_F dp_T^2} (M, x_F) , \end{aligned} \quad (10.2)$$

with $(p_T)_{\max}^2$ given in Eq. (9.9). We compare our calculated M spectrum with the data in Fig. 10.8. Agreement is better than for the p_T spectrum, however, the experimental error bars are again large compared to proton data.

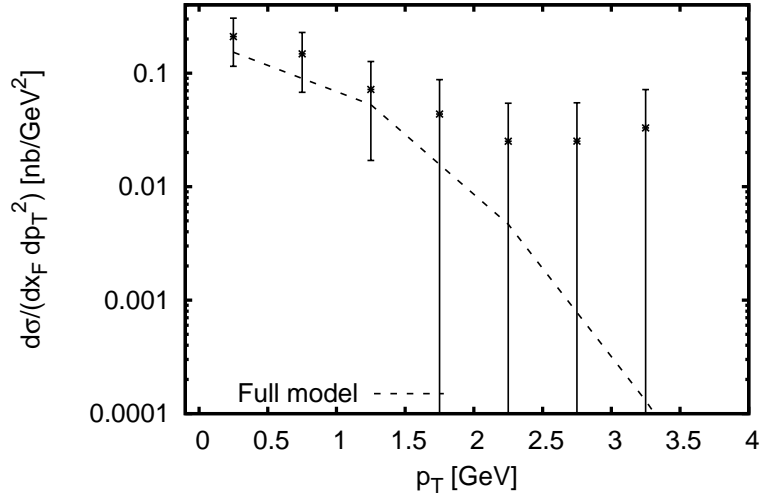


Figure 10.7: p_T spectrum obtained from our full model. Everywhere $D = 0.45$ GeV, $\Gamma = 0.2$ GeV, $\lambda = 5$ MeV, $\kappa_q = 1$ and $\kappa_g = 2$. The PDFs are the MSTW2008LO68cl set. Data are from E537 with $4 \text{ GeV} < M < 9 \text{ GeV}$, $0 < x_F < 0.1$. We have chosen $x_F = 0.05$ in our calculation. Only statistical errors are shown.

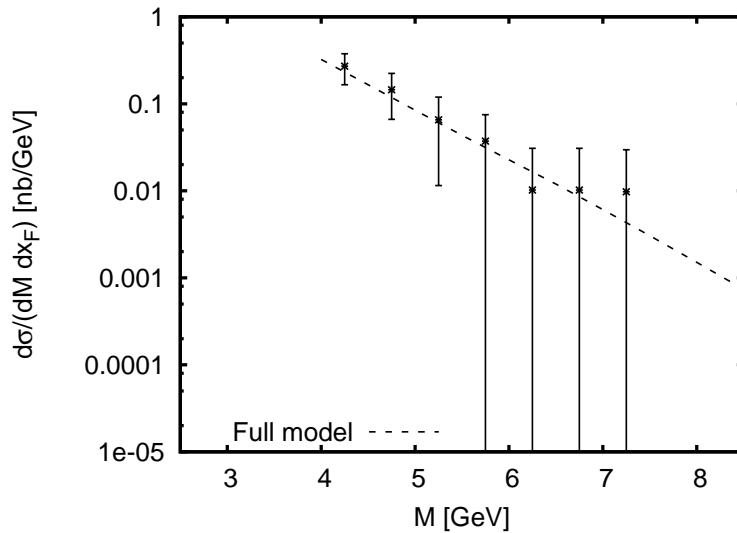


Figure 10.8: M spectrum obtained from our full model. Everywhere $D = 0.45$ GeV, $\Gamma = 0.2$ GeV, $\lambda = 5$ MeV, $\kappa_q = 1$ and $\kappa_g = 2$. The PDFs are the MSTW2008LO68cl set. Data are from E537 with $0 < x_F < 0.1$. We have chosen $x_F = 0.05$ in our calculation. Only statistical errors are shown.

10.6 Prediction for PANDA ($\bar{p}p$)

Based on the parameters which we have fixed on the available data above, we here present our predictions for DY pair production at $S = 30 \text{ GeV}^2$ in $\bar{p}p$ collisions, where, for example, PANDA [TLP⁺09] will measure.

For the calculation of the triple differential cross section we use a modified version of Eq. (7.131):

$$\begin{aligned}
 & \frac{2\sqrt{SE}}{\pi(S - M^2)} \frac{d\sigma}{dx'_F dp_T^2} \\
 & \rightarrow \frac{2\sqrt{SE}}{\pi(S - M^2)} \int_{M^2\text{-bin}} \frac{d\sigma}{dM^2 dx'_F dp_T^2} dM^2 \\
 & \approx \frac{2\sqrt{SE}}{\pi(S - \langle M \rangle^2)} \cdot \Delta M^2 \frac{d\sigma}{dM^2 dx'_F dp_T^2} (\langle M \rangle, x'_F, p_T) , \tag{10.3}
 \end{aligned}$$

where

$$E = \sqrt{\langle M \rangle^2 + p_T^2 + (x'_F)^2 \langle (q'_z)_{\max} \rangle^2} \tag{10.4}$$

and $\Delta M^2 = M_{\max}^2 - M_{\min}^2$ with M_{\max} (M_{\min}) the upper (lower) limit of the bin. For the average value of M we use the center of the M bin and we choose everywhere $x'_F = 0$. In Figs. 10.9-10.10 we show our predictions for different values of Γ in different M bins. Note that while at E866 energies we could not discriminate between different Γ over a wide range (cf. Fig. 9.2), the results here become more sensitive to this parameter. This is not totally unexpected, since at lower hadronic (S) and partonic (M^2) scales the model should become more sensitive to the soft physics introduced through the various distributions for mass and transverse momentum.

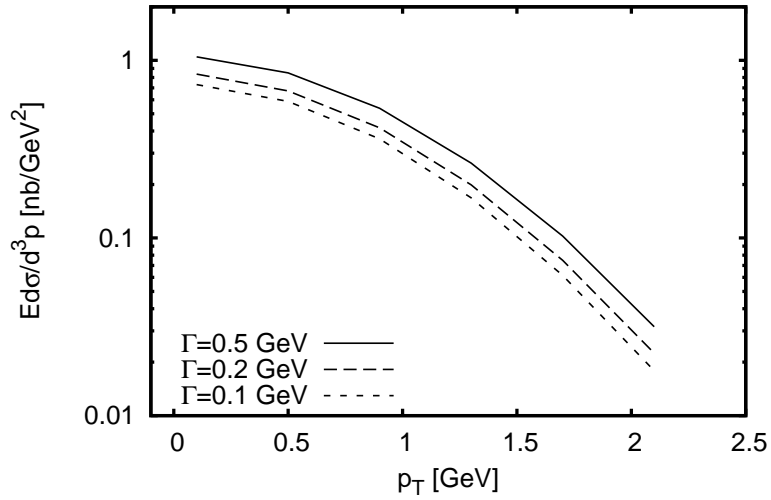


Figure 10.9: p_T spectrum obtained from our full model for different values of Γ . Everywhere $D = 0.45$ GeV, $\lambda = 5$ MeV, $\kappa_q = 1$ and $\kappa_g = 2$. The PDFs are the MSTW2008LO68cl set. $x'_F = 0$ and $1.5 \text{ GeV} < M < 2.5 \text{ GeV}$.

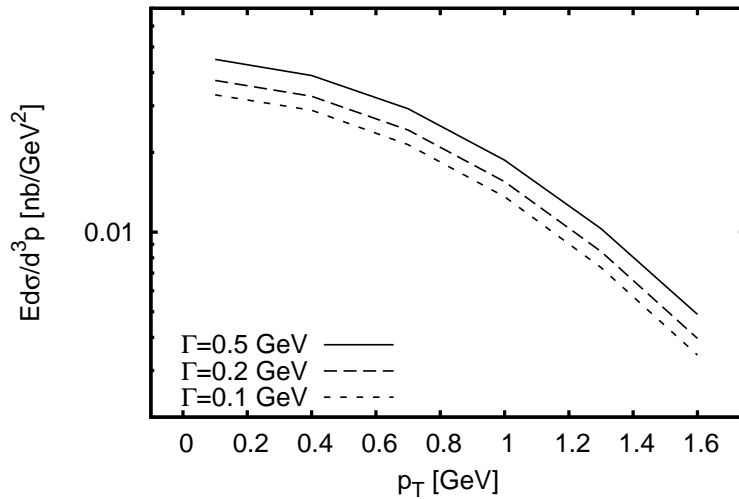


Figure 10.10: p_T spectrum obtained from our full model for different values of Γ . Everywhere $D = 0.45$ GeV, $\lambda = 5$ MeV, $\kappa_q = 1$ and $\kappa_g = 2$. The PDFs are the MSTW2008LO68cl set. $x'_F = 0$ and $2.5 \text{ GeV} < M < 3.5 \text{ GeV}$.

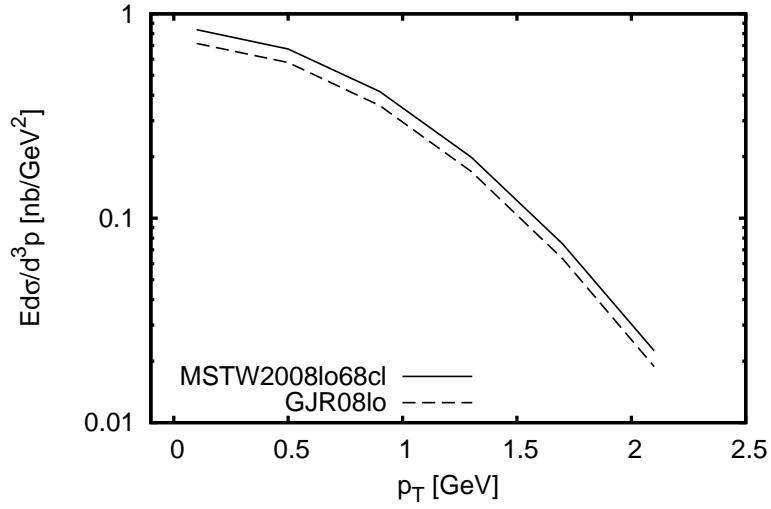


Figure 10.11: p_T spectrum obtained from our full model for different PDF sets. Everywhere $D = 0.45$ GeV, $\Gamma = 0.2$ GeV, $\lambda = 5$ MeV, $\kappa_q = 1$, $\kappa_g = 2$. $x'_F = 0$ and 1.5 GeV $< M < 2.5$ GeV.

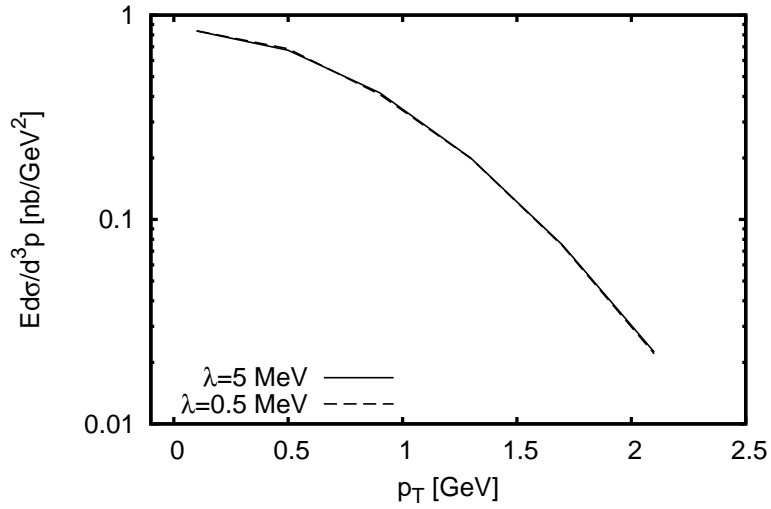


Figure 10.12: p_T spectrum obtained from our full model for different values of λ . Everywhere $D = 0.45$ GeV, $\Gamma = 0.2$ GeV, $\kappa_q = 1$ and $\kappa_g = 2$. The PDFs are the MSTW2008LO68cl set. $x'_F = 0$ and 1.5 GeV $< M < 2.5$ GeV. Note that both curves are basically on top of each other.

In Fig. 10.11 we compare results for different PDFs and the uncertainty induced by the choice of different PDFs is comparable to the uncertainties we found for high

energies (e.g. at E772). To make sure that at such low hadronic energies the fictitious gluon mass is still small enough, we studied our model at different values of λ , see Fig. 10.12. The results coincide, indicating that our standard choice of $\lambda = 5$ MeV is still applicable at these energies.

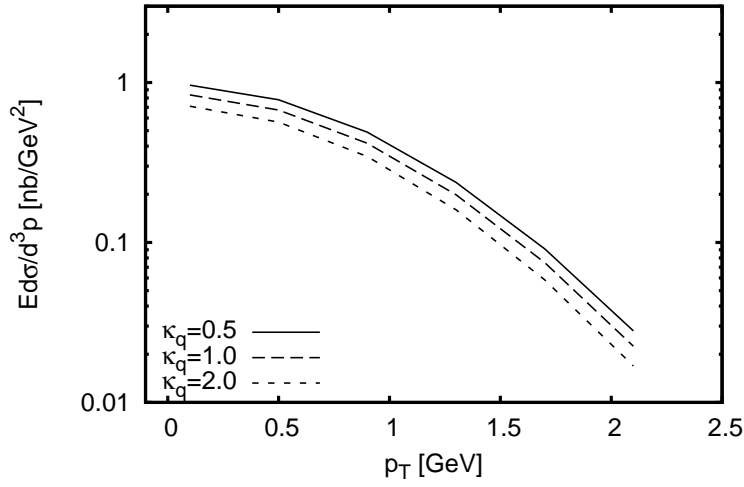


Figure 10.13: p_T spectrum obtained from our full model with different values of the subtraction parameter κ_q . Everywhere $D = 0.45$ GeV, $\Gamma = 0.2$ GeV, $\lambda = 5$ MeV and $\kappa_g = 2$. The PDFs are the MSTW2008LO68cl set. $x'_F = 0$ and 1.5 GeV $< M < 2.5$ GeV.

To check the dependence of our results on the choice of the subtraction parameters κ_q and κ_g (see Sec. 8.6 for details) at the low hadronic energies of the $\bar{P}ANDA$ kinematics, we again vary one of the two parameters and keep the other one fixed and show our results in Figs. 10.13 and 10.14. The results for different κ_q deviate by about 15%, which is comparable to the deviation at E866 energies. However the results are practically insensitive to variations in κ_g .

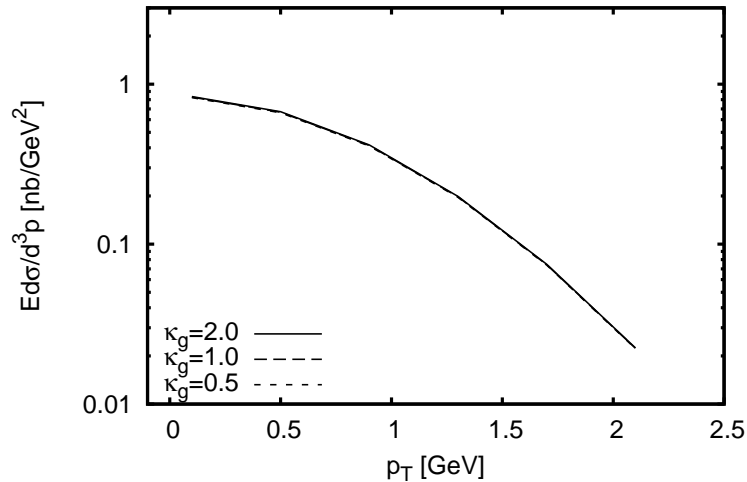


Figure 10.14: p_T spectrum obtained from our full model with different values of the subtraction parameter κ_g . Everywhere $D = 0.45$ GeV, $\Gamma = 0.2$ GeV, $\lambda = 5$ MeV and $\kappa_q = 1$. The PDFs are the MSTW2008LO68cl set. $x'_F = 0$ and 1.5 GeV $< M < 2.5$ GeV. Note that the curves are practically on top of each other.

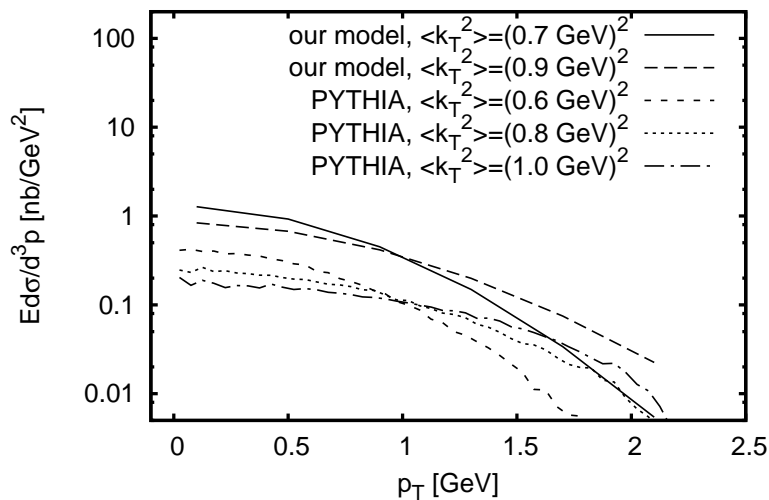


Figure 10.15: p_T spectrum obtained from our full model and from PYTHIA (see main text for details) for different values of the average initial k_T . The PYTHIA results shown are for $K = 1$. Our predictions were calculated with $\Gamma = 0.2$ GeV, $\lambda = 5$ MeV, $\kappa_q = 1$, $\kappa_g = 2$ and the MSTW2008LO68cl PDF set. $x'_F = 0$ and 1.5 GeV $< M < 2.5$ GeV.

Finally we compare in Fig. 10.15 our predictions with a PYTHIA calculation (PYTHIA

version 6.225, CTEQ5L PDFs), each for different values of the average initial k_T . As explained above, PYTHIA calculations for E866 conditions seem to prefer a somewhat smaller width for the initial k_T distribution, $\langle k_T^2 \rangle = (0.8 \text{ GeV})^2$ instead of $(0.9 \text{ GeV})^2$. Since various calculations ([Gal01],[GM09]) hint to some monotonic dependence of the initial k_T with the underlying \sqrt{S} , we would expect that at \bar{P} ANDA energies, a somewhat smaller $\langle k_T^2 \rangle$ should be used. Therefore, in Fig. 10.15, we also show calculations with $\langle k_T^2 \rangle = (0.6 \text{ GeV})^2$ for PYTHIA and $\langle k_T^2 \rangle = (0.7 \text{ GeV})^2$ ($D = 0.35 \text{ GeV}$) for our model. For PYTHIA, already with $\langle k_T^2 \rangle = (0.6 \text{ GeV})^2$, the difference in the functional behavior is rather large compared to the PYTHIA calculations with the higher parameter values. This may be taken as some hint for the theoretical uncertainties. On the other hand, the intrinsic k_T in PYTHIA is some effective parameter. It is not clear, whether this parameter should follow the same energy dependence in pp and in $p\bar{p}$ collisions, since multiple effects are encoded. Note, that the PYTHIA results shown in Fig. 10.15 were not multiplied by a K factor, i.e. $K = 1$.

Part VI
Conclusion

11

Summary and conclusion

In this thesis we have studied fully differential DY pair production in proton and antiproton induced reactions. For this purpose we have developed a model which incorporates phenomenological distributions for the intrinsic transverse momentum of partons and for the masses of the quarks, as well as standard longitudinal PDFs.

First, we have presented certain mathematical tools which are of importance for this work. Afterwards, the relevant physical background for our model has been presented, especially with a focus on studies of the nucleon structure. Following that, we have introduced the DY process and presented our LO model for the description of the DY observables. Taking into account parton transverse momentum and quark mass distributions we have shown, that our LO model cannot satisfactorily reproduce the absolute strength of the measured DY p_T and M spectra, i.e. a K factor is needed, just as in the standard parton model for the DY process. Therefore, we have subsequently extended our model by additionally taking into account all NLO processes of $O(\alpha_s)$. We have found, that with our quark mass distributions we can effectively overcome the problems of the standard $O(\alpha_s)$ pQCD calculation with massless quarks. Finally we have presented our results and shown, that a K factor free description of measured DY spectra is possible in our full model. Based on these results we have presented predictions for DY pair production at low hadronic energies, relevant for the future PANDA experiment.

11.1 Summary

After our introduction in Part I we have devoted Part II to the main mathematical tools, which are relevant for this work. In Chapter 2 we have explored the necessity

of regularisation methods in quantum field theories, taking the QCD quark selfenergy as an example. Several different methods of regularisation have been presented and their advantages and disadvantages discussed. Since the procedure of dimensional regularisation today is a common tool in gauge theories and in this work, we have presented this method in more mathematical detail, again on the example of the quark selfenergy. Since for our full model we need to calculate certain loop corrections, we have presented in Chapter 3 an explicit and detailed calculation of the type of loop integrals we encounter in this work, namely the three-point function.

Part III comprises the underlying physics for our model. Since at NLO we have to include quark field strength renormalisation factors when calculating amplitudes, we have presented in Chapter 4 first a short introduction to this topic. In the presented renormalisation framework we have then calculated the field strength renormalisation for the massive quark case, of which we make use later on in our model. The gluon bremsstrahlung and gluon Compton scattering processes we consider in our model suffer from infrared divergences, and so we have devoted Chapter 5 to the description of these divergences. One particular case is the divergence associated with the emission of soft gluons in bremsstrahlung. We have introduced a fictitious gluon mass to regulate the divergence and calculated the cross section of this process, which enables us to prove later on analytically, that this divergence actually cancels against a similar divergence in the loop corrections and, thus, the final result does not depend on the gluon mass. Since this work uses the DY process as a probe to study the structure of the nucleon, we have covered the latter topic in detail in Chapter 6. We have explored the standard tools to investigate the nucleon structure which are elastic and deep inelastic electron scattering. In the second part of this chapter we have discussed the parton model, which is the basis of most current nucleon structure studies. Especially the topics of Bjorken scaling and the collinear (or mass) singularities in DIS have been covered. The latter are the origin of the scaling violations of the PDFs and we have shown, how they can be systematically treated and absorbed into the PDFs through the important DGLAP equations of pQCD.

The DY process and its description by our model have been laid out in Part IV. In Chapter 7 we first have introduced the DY process and described the main shortfalls of the standard LO parton model description: since all the partons are assumed to move collinearly with the nucleon, p_T spectra are not accessible in such a simple approach. In addition the overall strength of the p_T and M spectra is underestimated by an a priori undetermined, but constant K factor. To remedy this situation, we have introduced parton intrinsic transverse momentum (width D) and quark mass distributions (width Γ) to parametrise the soft interactions among the partons which are neglected from the start in the standard parton model. Furthermore, we have calculated the LO hard subprocess taking into account the full kinematics in contrast to the collinear approximation assumed in the standard parton model. In evaluating the kinematics we have found that special care has to be taken, as to not include unphysical solutions for the longitudinal momentum fractions of the partons in the phase space integrals. We have

found, that the shape of the p_T spectra can be described well in such an approach, however, the absolute size of the cross section still cannot be accounted for without a multiplicative K factor. As a consequence, we have presented an extension to our LO model which includes all subprocesses to $O(\alpha_s)$ in Chapter 8. First, we have described the loop corrections to the electromagnetic quark-photon vertex: the calculation of the vertex form factors in the dimensional regularisation scheme has been given in full detail along with the relevant interference cross section of the loop corrections with the LO process. Since the loops also suffer from a soft gluon divergence, we again have given the gluon a finite mass to regulate the behavior of the cross section. Then we have shown explicitly, that the soft gluon divergent part of the cross section exactly cancels against the divergent part of the soft gluon bremsstrahlung mentioned above, and the resulting cross section is free of soft gluon problems and does not depend on the fictitious gluon mass. The introduction of quark mass distributions has warranted a close examination of current conservation and gauge invariance in our model, since invariably we have introduced quarks with different masses. However, since we have constructed our model such, that the quark masses only change at the quark-photon vertex, we have found, that the amplitudes we have calculated actually conserve the current in the electromagnetic as well as in the strong interaction sector. Furthermore, the introduction of different quark masses has another consequence: the electromagnetic charge is unintentionally renormalised. Fortunately, we have been able to show, that in the kinematic regions of DY pair production we are interested in, this charge renormalisation does not influence our results. Next we have presented the common subprocess kinematics of gluon bremsstrahlung and gluon Compton scattering in detail. Then we have shown the derivation of the partonic cross section for gluon bremsstrahlung and in special detail the evaluation of the phase space integrals of the hadronic cross section, where again unphysical solutions for parton momentum fractions have to be removed, just as in the LO case above. Gluon Compton scattering has been covered next and we have presented the partonic cross section and stressed the kinematical differences of the quark-gluon process in comparison to all the other contributing processes with quark-antiquark in the initial state. Since for massless quarks the $O(\alpha_s)$ processes suffer from the same kind of collinear/mass singularities as the DIS processes mentioned above, we then have demonstrated the regulating behavior of our quark mass distributions on the example of the p_T spectrum of gluon Compton scattering. We have found that we have effectively regulated the collinear singularities with our quark mass, however, as we had already shown above, exactly those singularities have already entered into the standard longitudinal PDFs. As our model relies on these PDFs, as given by the literature, we then have devised and explained in detail a subtraction scheme, that prevents double-counting of the $O(\alpha_s)$ processes which we consider explicitly. We have introduced two subtraction parameters κ_q and κ_g for the subtraction of the quark and gluon PDF, respectively. In this way, we have acquired a model which is consistent to $O(\alpha_s)$, in which we have regulated the collinear singularities by means of our quark mass distributions and which can

use the standard PDFs provided in the literature. As the p_T generated dynamically by the NLO processes cannot account for the measured p_T spectra, we have found that one still needs to include phenomenological intrinsic parton transverse momentum distributions to reproduce the measured hadronic cross sections.

In Part V we have presented the results of our full model including all contributions to $O(\alpha_s)$. First we have fixed our phenomenological parameters on data obtained in proton-proton collisions at high energies (Fermilab E866, $S = 1500 \text{ GeV}^2$). The results show that with our choice for the width of the initial parton transverse momentum distribution, $D \approx 0.45 \text{ GeV}$ ($\langle k_T^2 \rangle \approx (0.9)^2 \text{ GeV}^2$), the shape of the p_T spectra is reproduced very well. We note, however, that this width might be S dependent, which introduces additional uncertainties. At E866 energies we have found, that over a wide range the results depend only weakly on the width Γ of the mass distribution. We have been able to fix the subtraction parameters κ_q and κ_g and found that they are of natural magnitude ($O(1)$). Thus, within natural ranges for our parameters a K factor free description of DY p_T and invariant mass spectra is indeed possible in our full model. In Chapter 10 we have then applied our full model to data from several different other experiments, which measured DY spectra in proton-nucleus and antiproton-proton reactions. It has turned out, that a consistent description of all these data with our one set of fixed parameters is possible without any K factor. The general agreement of our results with the data from different experiments indicates that we effectively have parametrised the soft initial state interactions in the nucleon by fixing our parameters on the available data. Using this framework we have made predictions for DY pair production at the low hadronic energy regime, where the future experiment $\bar{\text{P}}\text{ANDA}$ is aiming at. We have found that our predictions become more sensitive to the mass distribution width Γ , which we could not reliably fix at higher energies. In addition we found some sensitivity on the subtraction parameter κ_q , which is comparable to the finding at high energies (E866). Nevertheless, in this thesis we have found that our model provides a narrow band of estimates for the fully differential DY pair production cross section at low energies.

11.2 Outlook

Possible improvements to our model include testing the influence of different kinds of quark mass distributions on the hadronic cross sections, and judging the possibility of using NLO PDFs by devising a modified subtraction scheme for the collinear divergences. In addition predictions for the exclusive process of DY pair production with an associated jet might prove interesting, since so far there is no data available for this reaction. Once $\bar{\text{P}}\text{ANDA}$ data become available, they might be used to further constrain the parameters of our model. Since several DY experiments aim at measuring spin-dependent observables, a possible extension of our model towards the description of DY pair production with polarised beams and targets might prove

useful.

Appendices



Conventions and notation

A.1 Units

This work is presented in natural units:

$$\hbar = c = 1 . \tag{A.1}$$

For conversion between units we use [Group10]:

$$\hbar c = 0.197327 \text{ GeV fm} . \tag{A.2}$$

A.2 Light-cone coordinates

We employ the following convention for general four-vectors a and b :

$$a^+ = a^0 + a^3 , \tag{A.3}$$

$$a^- = a^0 - a^3 , \tag{A.4}$$

$$\vec{a}_\perp = (a^1, a^2) , \tag{A.5}$$

$$\Rightarrow a^2 = a^+ a^- - (\vec{a}_\perp)^2 , \tag{A.6}$$

$$\Rightarrow a \cdot b = \frac{1}{2} (a^+ b^- + a^- b^+ - 2 \vec{a}_\perp \cdot \vec{b}_\perp) . \tag{A.7}$$

The 4-dimensional Minkowski volume element then reads:

$$\begin{aligned}
 d^4a &= da^0 d\vec{a}_\perp da^3 \\
 &= \frac{\partial(a^0, a^3)}{\partial(a^+, a^-)} da^+ da^- d\vec{a}_\perp \\
 &= \frac{1}{2} da^+ da^- d\vec{a}_\perp .
 \end{aligned} \tag{A.8}$$

A.3 Complex logarithm

Let $z \in \mathcal{C}$. We define the complex logarithm as the inverse function of the complex exponential function:

$$\ln(\exp(z)) = z , \tag{A.9}$$

where $\ln(x)$ has a branch cut along the negative real axis and where $\Im[\ln|x|] = 0$.

A.4 Metric, Dirac algebra and completeness relations

A.4.1 Metric tensor

In four dimensions we use the following metric tensor:

$$g_{\mu\nu}^{(4)} = \begin{pmatrix} 1 & 0 & 0 & 0 \\ 0 & -1 & 0 & 0 \\ 0 & 0 & -1 & 0 \\ 0 & 0 & 0 & -1 \end{pmatrix} , \tag{A.10}$$

and in general for d dimensions we use:

$$g_{\mu\nu} = \begin{cases} 1, & \mu = \nu = 0 \\ -1, & d \geq \mu = \nu \geq 1 \\ 0, & \mu \neq \nu \end{cases} . \tag{A.11}$$

A.4.2 Dirac algebra

Here we present the relevant Dirac algebra for this work, for the general case of d dimensions [Mut98, PS95]. The Dirac matrices obey the following anticommutation relation:

$$\{\gamma^\mu, \gamma^\nu\} = 2g^{\mu\nu} , \tag{A.12}$$

with the d -dimensional metric tensor, which obeys the following contraction identity:

$$g^{\mu\nu} g_{\mu\nu} = d . \tag{A.13}$$

Contraction identities

The contraction identities for the Dirac matrices follow immediately from the last two equations:

$$\gamma^\mu \gamma_\mu = d , \quad (\text{A.14})$$

$$\gamma^\mu \gamma^\alpha \gamma_\mu = (2 - d) \gamma^\alpha , \quad (\text{A.15})$$

$$\gamma^\mu \gamma^\alpha \gamma^\beta \gamma_\mu = 4g^{\alpha\beta} + (d - 4) \gamma^\alpha \gamma^\beta , \quad (\text{A.16})$$

$$\gamma^\mu \gamma^\alpha \gamma^\beta \gamma^\rho \gamma_\mu = -2\gamma^\rho \gamma^\beta \gamma^\alpha + (4 - d) \gamma^\alpha \gamma^\beta \gamma^\rho . \quad (\text{A.17})$$

Trace relations

In general the trace relations are modified in d dimensions, but we are always only interested in results for $d \rightarrow 4$. Therefore we can stick to the trace relations in four dimensions [Mut98]. Important traces over products of Dirac matrices are:

$$\text{Tr}(\mathbb{1}) = 4 , \quad (\text{A.18})$$

$$\text{Tr}(\gamma^\mu \gamma^\nu) = 4g^{\mu\nu} , \quad (\text{A.19})$$

$$\text{Tr}(\gamma^\mu \gamma^\nu \gamma^\alpha \gamma^\beta) = 4(g^{\mu\nu} g^{\alpha\beta} - g^{\mu\alpha} g^{\nu\beta} + g^{\mu\beta} g^{\nu\alpha}) , \quad (\text{A.20})$$

and all traces of an odd number of Dirac matrices vanish.

A.4.3 Dirac spinors and polarisation vectors

Dirac equation

The Dirac spinors for fermions and antifermions obey the Dirac equation:

$$(\not{p} - m) u^s(p) = \bar{u}^s(p) (\not{p} - m) = 0 \quad (\text{A.21})$$

$$(\not{p} + m) v^s(p) = \bar{v}^s(p) (\not{p} + m) = 0 . \quad (\text{A.22})$$

Gauge bosons

Gauge bosons (e.g. photons and gluons) are polarised in the transverse plane. Thus, for a gauge boson with polarisation vector $\epsilon^\mu = (0, \vec{\epsilon})$ and four momentum $p = (p^0, \vec{p})$ the polarisation condition reads:

$$\vec{\epsilon} \cdot \vec{p} = 0 . \quad (\text{A.23})$$

Completeness relations

When summing over their different spin states, one obtains the completeness relations for the fermions and antifermions:

$$\sum_s u^s(p) \bar{u}^s(p) = \not{p} + m, \quad (\text{A.24})$$

$$\sum_s v^s(p) \bar{v}^s(p) = \not{p} - m. \quad (\text{A.25})$$

Analogously, when summing over the polarisations of the photon, one can make the following replacement (considering the Ward identity [PS95]):

$$\sum_{\text{pol.}} \epsilon_\mu^* \epsilon_\nu \rightarrow -g_{\mu\nu}. \quad (\text{A.26})$$

A.5 SU(3) color algebra

The SU(3) color matrices t^a form a representation r of a Lie Algebra and they obey the following commutator relation [PS95]:

$$[t^a, t^b] = i f^{abc} t^c, \quad (\text{A.27})$$

where f^{abc} are totally antisymmetric structure constants. In the fundamental representation one finds for the contraction of two color matrices ($N_C = 3$ colors):

$$t^a t^a = C_2 \cdot \mathbb{1} = \frac{N_C^2 - 1}{2N_C} \cdot \mathbb{1} = \frac{4}{3} \cdot \mathbb{1}, \quad (\text{A.28})$$

where $\mathbb{1}$ is the identity in the SU(3) color space with:

$$\text{Tr}(\mathbb{1}) = N_C = 3. \quad (\text{A.29})$$

A.6 Cross sections

The differential cross section for $2 \rightarrow n$ particle scattering is given by [Group10]:

$$d\sigma = \frac{(2\pi)^4 \delta^{(4)}(p_1 + p_2 - \sum_{i=1}^n k_i)}{4\sqrt{(p_1 \cdot p_2)^2 - m_1^2 m_2^2}} \overline{|M|^2} \prod_{i=1}^n \frac{d^3 k_i}{(2\pi)^3 2E_i}, \quad (\text{A.30})$$

where p_1, p_2 and m_1, m_2 are the momenta and masses of the incoming particles, k_i and E_i are the momenta and energies of the outgoing particles and $\overline{|M|^2}$ is the transition matrix element.

B

Feynman rules and color factors

B.1 Feynman rules

In this appendix we present the Feynman rules, that were employed throughout this work. Using these rules one can obtain transition amplitudes iM and selfenergies $-i\Sigma$. Note that time runs from right to left.

External particles

Assign factors for external particles according to the following rules:

- initial fermion (particle)

$$\bullet \xrightarrow{\overleftarrow{p}, m} = u_s(p) \quad (\text{B.1})$$

- final fermion (particle)

$$\xrightarrow{\overleftarrow{p}, m} \bullet = \bar{u}_s(p) \quad (\text{B.2})$$

- initial antifermion (antiparticle)

$$\bullet \xrightarrow{\leftarrow p, m} = \bar{v}_s(p) \quad (\text{B.3})$$

- final antifermion (antiparticle)

$$\xrightarrow{\leftarrow p, m} \bullet = v_s(p) \quad (\text{B.4})$$

- initial photon

$$\bullet \xrightarrow{\leftarrow p} = \epsilon_\mu(p) \quad (\text{B.5})$$

- final photon

$$\xrightarrow{\leftarrow p} \bullet = \epsilon_\mu^*(p) \quad (\text{B.6})$$

- initial gluon

$$\bullet \xrightarrow{\leftarrow p} = \epsilon_\mu(p) \quad (\text{B.7})$$

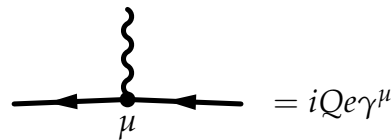
- final gluon

$$\xrightarrow{\leftarrow p} \bullet = \epsilon_\mu^*(p) \quad (\text{B.8})$$

Vertices

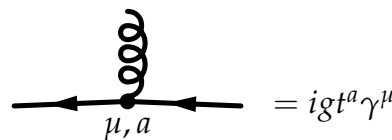
Assign factors for vertices according to the following rules:

- fermion-photon vertex (fermion electric charge $Q \cdot e$)



$$= iQe\gamma^\mu \quad (\text{B.9})$$

- quark-gluon vertex

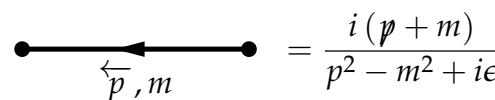


$$= igt^a \gamma^\mu \quad (\text{B.10})$$

Propagators and loops

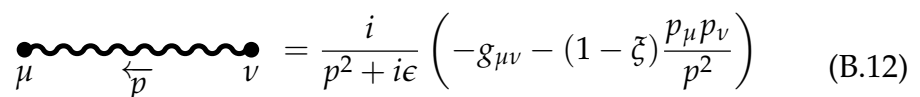
For every closed loop assign an integral over the undetermined loop momentum via $\int \frac{d^4k}{(2\pi)^4}$. Assign factors for propagators according to the following rules:

- free fermion propagator



$$= \frac{i(\not{p} + m)}{p^2 - m^2 + i\epsilon} \quad (\text{B.11})$$

- free photon propagator



$$= \frac{i}{p^2 + i\epsilon} \left(-g_{\mu\nu} - (1 - \xi) \frac{p_\mu p_\nu}{p^2} \right) \quad (\text{B.12})$$

where we have used the results of Appendix A.5.

Gluon bremsstrahlung

For both incoming quarks assign a factor of $\frac{1}{N_C}$. For the quark-gluon vertex assign a color matrix t^a , cf. Eq. (B.10), and then square the amplitude and sum over the internal color indices, which gives a trace over the contraction of the two color matrices just as for the vertex correction above:

$$\begin{aligned}
 C_F^B &= \frac{1}{N_C^2} \text{Tr}(t^a t^a) \\
 &= \frac{1}{N_C^2} \frac{N_C^2 - 1}{2N_C} \text{Tr}(\mathbb{1}) \\
 &= \frac{1}{N_C^2} \frac{N_C^2 - 1}{2N_C} N_C \\
 &= \frac{4}{9}.
 \end{aligned} \tag{B.16}$$

The identical color factors of the vertex correction and bremsstrahlung processes are another consequence of the Kinoshita-Poggio-Quinn [Kin62, KU76, PQ76, Ste76] and Kinoshita-Lee-Nauenberg [Kin62, LN64] theorems, since otherwise the soft gluon divergences of these processes would not cancel out.

Gluon Compton scattering

For the incoming quark assign a factor of $\frac{1}{N_C}$ and for the incoming gluon assign a factor of $\frac{1}{N_C^2 - 1}$ to average over the 8 possible non-singlet color states of the gluon. For the quark-gluon vertex assign a color matrix t^a , cf. Eq. (B.10), and then square the amplitude and sum over the internal color indices, which gives a trace over the contraction of the two color matrices just as above:

$$\begin{aligned}
 C_F^B &= \frac{1}{N_C} \frac{1}{N_C^2 - 1} \text{Tr}(t^a t^a) \\
 &= \frac{1}{N_C} \frac{1}{N_C^2 - 1} \frac{N_C^2 - 1}{2N_C} \text{Tr}(\mathbb{1}) \\
 &= \frac{1}{N_C} \frac{1}{2N_C} N_C \\
 &= \frac{1}{6}.
 \end{aligned} \tag{B.17}$$

C

Formulas

C.1 Vertex function integrals

During the evaluation of the vertex function in Sec. 8.1.1 we encountered a lengthy integral over Feynman parameters and there we only gave the result. In this Appendix we will outline the evaluation of this integral. The object of interest reads, cf. Eq. (8.15):

$$\begin{aligned} I = & \int_0^1 dx dy dz \delta(x + y + z - 1) \\ & \times \left\{ \gamma^\mu 2 \log \left(\frac{m_1^2}{\Delta} \right) \right. \\ & - \frac{\gamma^\mu}{\Delta} \left[-2q^2(1-x)(1-y) \right. \\ & \quad \left. + m_1^2 \left(2z^2 + 2yz \left(1 - \frac{m_2^2}{m_1^2} \right) + 2z \left(\frac{m_2}{m_1} + \frac{m_2^2}{m_1^2} \right) - 2 \frac{m_2}{m_1} \right) \right] \\ & \left. - \frac{p_1^\mu - p_2^\mu}{\Delta} (2yz(m_2 - m_1) + 2m_1z(1-z)) \right\} . \end{aligned} \quad (\text{C.1})$$

First we transform the integration variables:

$$a = x + y = 1 - z , \quad (\text{C.2})$$

$$b = x - y , \quad (\text{C.3})$$

$$\Rightarrow \int_0^1 dx dy dz \delta(x + y + z - 1) = \int_0^1 dx \int_0^{1-x} dy = \frac{1}{2} \int_0^1 da \int_{-a}^a db . \quad (\text{C.4})$$

In terms of these new variables the function Δ becomes:

$$\begin{aligned} \Delta &= -xyq^2 + m_1^2(1-z)^2 + (m_2^2 - m_1^2)y(1-z) + z\lambda^2 - i\epsilon \\ &= \frac{q^2}{4} \left[b^2 + a^2(-v^2 - \phi) + ab\phi + (1-a)\kappa(1-v^2) - i\epsilon \right] , \end{aligned} \quad (\text{C.5})$$

with the help functions:

$$v = \sqrt{1 - \frac{4m_1^2}{q^2}} , \quad (\text{C.6})$$

$$\phi = \frac{1}{2} \cdot \left(1 - \frac{m_2^2}{m_1^2} \right) \cdot (1 - v^2) , \quad (\text{C.7})$$

$$\kappa = \frac{\lambda^2}{m_1^2} - i\epsilon . \quad (\text{C.8})$$

Note that we have absorbed the $i\epsilon$ term into κ since we will only need it for the evaluation of the IR divergent part of the integrals. Now we split up the integral I and evaluate the parts individually. First we define:

$$\begin{aligned} I_1 &= \int_0^1 dx dy dz \delta(x + y + z - 1) 2 \log \left(\frac{m_1^2}{\Delta} \right) \\ &= \int_0^1 da \int_{-a}^a db \left[\log \left(\frac{4m_1^2}{q^2} \right) - \log \left(b^2 + a^2(-v^2 - \phi) + ab\phi + (1-a)\kappa(1-v^2) \right) \right] . \end{aligned} \quad (\text{C.9})$$

Note that we introduced the gluon mass λ to regulate possible IR divergences. However, I_1 is finite in the soft gluon limit and so we can put λ and, thus, κ to zero:

$$\begin{aligned} I_1 &= \int_0^1 da \int_{-a}^a db \left[\log \left(\frac{4m_1^2}{q^2} \right) - \log \left(b^2 + a^2(-v^2 - \phi) + ab\phi \right) \right] \\ &= \log \left(\frac{4m_1^2}{q^2} \right) - \int_0^1 da \int_{-a}^a db \log \left(b^2 + a^2(-v^2 - \phi) + ab\phi \right) \\ &= \log \left(\frac{4m_1^2}{q^2} \right) - I_2 . \end{aligned} \quad (\text{C.10})$$

To solve the integral I_2 one can make use of the methods we presented in detail in Sec. 3.1.3: we substitute $b' = b - \alpha a$ and choose α such, that the a^2 term in the logarithm vanishes. Then, after changing the order of the integrations, the integral over a becomes trivial:

$$I_2 = \left(\int_0^{1-\alpha} db' \int_{\frac{b'}{1-\alpha}}^1 da - \int_0^{-(1-\alpha)} db' \int_{\frac{-b'}{1-\alpha}}^1 da \right) \log \left(b'^2 + ab'(2\alpha + \phi) \right), \quad (\text{C.11})$$

with:

$$\alpha = -\frac{\phi}{2} + \sqrt{\phi + v^2 + \frac{\phi^2}{4}}. \quad (\text{C.12})$$

The remaining integrals in I_2 are standard and after some algebra one finds:

$$\begin{aligned} I_2 = & -3 + \frac{1}{2} \log(\alpha^2 - 1) + \frac{\alpha}{2} \log\left(\frac{\alpha + 1}{\alpha - 1}\right) \\ & + \frac{1}{2} \log((\alpha + \phi)^2 - 1) + \frac{\alpha + \phi}{2} \log\left(\frac{\alpha + \phi + 1}{\alpha + \phi - 1}\right). \end{aligned} \quad (\text{C.13})$$

The next integral to solve is:

$$\begin{aligned} I_3 = & \int_0^1 dx dy dz \delta(x + y + z - 1) \\ & \times \frac{1}{\Delta} \left[-2q^2(1-x)(1-y) \right. \\ & \left. + m_1^2 \left(2z^2 + 2yz \left(1 - \frac{m_2^2}{m_1^2} \right) + 2z \left(\frac{m_2}{m_1} + \frac{m_2^2}{m_1^2} \right) - 2\frac{m_2}{m_1} \right) \right]. \end{aligned} \quad (\text{C.14})$$

Rewriting in the new variables a and b yields:

$$I_3 = \int_0^1 da \int_{-a}^a db \frac{b^2 + ab\phi + a^2(-v^2 - \phi) - b\phi + a(4v^2 + 3\phi + \tau) - 2(1 + v^2) - 2\phi}{b^2 + a^2(-v^2 - \phi) + ab\phi + (1-a)\kappa(1-v^2)}, \quad (\text{C.15})$$

with:

$$\tau = (1 - v^2) \cdot \left(1 - \frac{m_2}{m_1} \right). \quad (\text{C.16})$$

One can get rid of the b^2 and ab terms in the numerator by adding zero:

$$I_3 = 1 + \int_0^1 da \int_{-a}^a db \frac{-b\phi + a(4v^2 + 3\phi + \tau) - 2(1 + v^2) - 2\phi + (1 - a)\kappa(1 - v^2)}{b^2 + a^2(-v^2 - \phi) + ab\phi - (1 - a)\kappa(1 - v^2)} \quad (\text{C.17})$$

We note the following relation:

$$\begin{aligned} & \frac{d}{db} \log \left(b^2 + a^2(-v^2 - \phi) + ab\phi + (1 - a)\kappa(1 - v^2) \right) \\ &= \frac{2b + a\phi}{b^2 + a^2(-v^2 - \phi) + ab\phi + (1 - a)\kappa(1 - v^2)} \end{aligned} \quad (\text{C.18})$$

and so I_3 can be written as:

$$\begin{aligned} I_3 &= 1 + \int_0^1 da \int_{-a}^a db \left(-\frac{\phi}{2} \right) \frac{d}{db} \log \left(b^2 + a^2(-v^2 - \phi) + ab\phi + (1 - a)\kappa(1 - v^2) \right) \\ &+ \int_0^1 da \int_{-a}^a db \frac{a(4v^2 + 3\phi + \tau + \frac{\phi^2}{2}) - 2(1 + v^2) - 2\phi - (1 - a)\kappa(1 - v^2)}{b^2 + a^2(-v^2 - \phi) + ab\phi + (1 - a)\kappa(1 - v^2)} \\ &= 1 + I_4 + I_5. \end{aligned} \quad (\text{C.19})$$

The first integral is again convergent for $\kappa \rightarrow 0$ and the integration is then straightforward:

$$\begin{aligned} I_4 &= \int_0^1 da \int_{-a}^a db \left(-\frac{\phi}{2} \right) \frac{d}{db} \log \left(b^2 + a^2(-v^2 - \phi) + ab\phi \right) \\ &= -\frac{\phi}{2} \log \left(\frac{1 - v^2}{1 - v^2 - 2\phi} \right). \end{aligned} \quad (\text{C.20})$$

In the case of I_5 we note that we can drop the κ term in the numerator, since the integral over the denominator is at most divergent like $\log(\kappa)$ and in the end we are

only interested in terms that do not vanish for $\kappa \rightarrow 0$. Then I_5 becomes:

$$\begin{aligned}
 I_5 &= \int_0^1 da \int_{-a}^a db \frac{a(4v^2 + 3\phi + \tau + \frac{\phi^2}{2}) - 2(1 + v^2) - 2\phi}{b^2 + a^2(-v^2 - \phi) + ab\phi + (1-a)\kappa(1-v^2)} \\
 &= \int_0^1 da \int_{-a}^a db \frac{a(4v^2 + 3\phi + \tau + \frac{\phi^2}{2})}{b^2 + a^2(-v^2 - \phi) + ab\phi + (1-a)\kappa(1-v^2)} \\
 &\quad + \int_0^1 da \int_{-a}^a db \frac{-2(1 + v^2) - 2\phi}{b^2 + a^2(-v^2 - \phi) + ab\phi + (1-a)\kappa(1-v^2)} \\
 &= (4v^2 + 3\phi + \tau + \frac{\phi^2}{2}) \cdot I_6 + (-2(1 + v^2) - 2\phi) \cdot I_7. \tag{C.21}
 \end{aligned}$$

Again I_6 is convergent for $\kappa \rightarrow 0$ and with the same substitution $b' = b - \alpha a$ as above one finds:

$$\begin{aligned}
 I_6 &= \int_0^1 da \int_{-a}^a db \frac{a}{b^2 + a^2(-v^2 - \phi) + ab\phi} \\
 &= \int_0^1 da \int_{-a(1-\alpha)}^{a(1-\alpha)} db' \frac{a}{b'^2 + ab'(2\alpha + \phi)} \\
 &= \frac{1}{(2\alpha + \phi)} \int_0^1 da \int_{-a(1+\alpha)}^{a(1-\alpha)} db' \left[\frac{1}{b'} - \frac{1}{b' + a(2\alpha + \phi)} \right] \\
 &= \frac{1}{(2\alpha + \phi)} \left[\log \left(\frac{\alpha - 1}{\alpha + 1} \right) + \log \left(\frac{\alpha - 1 + \phi}{\alpha + 1 + \phi} \right) \right]. \tag{C.22}
 \end{aligned}$$

The integral I_7 is the only one, that is actually divergent for $\kappa \rightarrow 0$. With the substitution $b' = \frac{b+a}{2}$ it becomes:

$$\begin{aligned}
 I_7 &= \int_0^1 da \int_{-a}^a db \frac{1}{b^2 + a^2(-v^2 - \phi) + ab\phi + (1-a)\kappa(1-v^2)} \\
 &= 2 \int_0^1 da \int_0^a db' \frac{1}{4b'^2 + a^2(1-v^2-2\phi) + ab'(2\phi-4) + (1-a)\kappa(1-v^2)}. \tag{C.23}
 \end{aligned}$$

Fortunately we already solved this integral in Sec. 3.1 and extracted its behavior for $\kappa \rightarrow 0$ in Sec. 3.2, so there is nothing more to do at this point.

Finally only one integral in Eq. (C.1) remains to be calculated:

$$I_8 = \int_0^1 dx dy dz \delta(x + y + z - 1) \frac{1}{\Delta} (2yz(m_2 - m_1) + 2m_1z(1 - z)) . \quad (\text{C.24})$$

This integral is also IR convergent and so we can again neglect the gluon mass and express it in terms of the variables a and b as:

$$\begin{aligned} I_8 &= \frac{-1}{m_1} \int_0^1 da \int_{-a}^a db \frac{a^2 (1 - v^2 - \frac{\tau}{2}) + a (-1 + v^2 + \frac{\tau}{2}) - b \frac{\tau}{2} + ab \frac{\tau}{2}}{b^2 + a^2 (-v^2 - \phi) + ab\phi} \\ &= \frac{-1}{m_1} \left[\left(1 - v^2 - \frac{\tau}{2}\right) \cdot I_9 + \left(-1 + v^2 + \frac{\tau}{2}\right) \cdot I_6 - \frac{\tau}{2} \cdot I_{10} + \frac{\tau}{2} \cdot I_{11} \right] , \end{aligned} \quad (\text{C.25})$$

where we already solved the integral I_6 in Eq. (C.22). The remaining three integrals are again easily solved by the usual substitution $b' = b - \alpha a$:

$$\begin{aligned} I_9 &= \int_0^1 da \int_{-a}^a db \frac{a^2}{b^2 + a^2 (-v^2 - \phi) + ab\phi} \\ &= \int_0^1 da \int_{-a(1+\alpha)}^{a(1-\alpha)} db' \frac{a^2}{b'^2 + ab'(2\alpha + \phi)} \\ &= \frac{1}{2\alpha + \phi} \int_0^1 da \int_{-a(1+\alpha)}^{a(1-\alpha)} db' \left(\frac{a}{b'} - \frac{a}{b' + a(2\alpha + \phi)} \right) \\ &= \frac{1}{2} \frac{1}{2\alpha + \phi} \left[\log \left(\frac{\alpha - 1}{\alpha + 1} \right) + \log \left(\frac{\alpha - 1 + \phi}{\alpha + 1 + \phi} \right) \right] . \end{aligned} \quad (\text{C.26})$$

$$\begin{aligned} I_{10} &= \int_0^1 da \int_{-a}^a db \frac{b}{b^2 + a^2 (-v^2 - \phi) + ab\phi} \\ &= \int_0^1 da \int_{-a(1+\alpha)}^{a(1-\alpha)} db' \frac{b' + \alpha a}{b'^2 + ab'(2\alpha + \phi)} \\ &= \int_0^1 da \int_{-a(1+\alpha)}^{a(1-\alpha)} db' \left(\frac{1}{b' + a(2\alpha + \phi)} + \frac{\alpha a}{b'^2 + ab'(2\alpha + \phi)} \right) \\ &= \log \left(\frac{\alpha + 1 + \phi}{\alpha - 1 + \phi} \right) + \frac{\alpha}{2\alpha + \phi} \left[\log \left(\frac{\alpha - 1}{\alpha + 1} \right) + \log \left(\frac{\alpha - 1 + \phi}{\alpha + 1 + \phi} \right) \right] , \end{aligned} \quad (\text{C.27})$$

where we have used the result for I_6 .

$$\begin{aligned}
 I_{11} &= \int_0^1 da \int_{-a}^a db \frac{ab}{b^2 + a^2(-v^2 - \phi) + ab\phi} \\
 &= \int_0^1 da \int_{-a(1+\alpha)}^{a(1-\alpha)} db' \frac{a(b' + \alpha a)}{b'^2 + ab'(2\alpha + \phi)} \\
 &= \int_0^1 da \int_{-a(1+\alpha)}^{a(1-\alpha)} db' \left(\frac{a}{b' + a(2\alpha + \phi)} + \frac{\alpha a^2}{b'^2 + ab'(2\alpha + \phi)} \right) \\
 &= \frac{1}{2} \log \left(\frac{\alpha + 1 + \phi}{\alpha - 1 + \phi} \right) + \frac{\alpha}{2(2\alpha + \phi)} \left[\log \left(\frac{\alpha - 1}{\alpha + 1} \right) + \log \left(\frac{\alpha - 1 + \phi}{\alpha + 1 + \phi} \right) \right], \quad (\text{C.28})
 \end{aligned}$$

where we have used the results for I_6 and I_9 .

C.2 Dirac traces

In Secs. 8.3.1 and 8.4.1 we encountered two lengthy expressions involving traces over Dirac matrices. We evaluated those expressions with the help of the FeynCalc package [Fey] for Wolfram Mathematica [Wol08].

C.2.1 Gluon bremsstrahlung

For gluon bremsstrahlung the Dirac trace in Eq. (8.72) becomes:

$$\begin{aligned}
 T_B &= \left(g_{\mu\nu} - \frac{q_\mu q_\nu}{q^2} \right) \cdot \text{Tr} [(\not{p}_2 - m_2) S^{\alpha\mu} (\not{p}_1 + m_1) S^\nu_\alpha] \\
 &= -16 + \frac{4}{M^2} \left(\frac{u (2M^2 (t - m_1^2) - 2m_1^4 + m_1^2 (3m_2^2 - t) + t (t - m_2^2))}{(m_1^2 - t)^2} \right. \\
 &\quad + \frac{2m_1^2 (-2M^4 + 2M^2 m_1 (m_1 - 3m_2) + (m_1 - m_2)(m_1 + m_2) (m_1^2 - s))}{(m_1^2 - t)^2} \\
 &\quad + \frac{M^4 + 2M^2 (m_2^2 - s) - 2m_1^4 + m_1^2 m_2^2 + 2m_2^4 - 4m_2^2 s + s^2}{t - m_1^2} \\
 &\quad + \frac{M^4 (-5m_1^2 - 2m_1 m_2 - 4m_2^2 + 4s + t)}{(m_1^2 - t) (m_2^2 - u)} \\
 &\quad + \frac{2M^2 (-6m_1^3 m_2 + 2m_1^2 m_2^2 - 6m_1 m_2^3 + 8m_1 m_2 s + m_2^4 - m_2^2 s - st + t^2)}{(m_1^2 - t) (m_2^2 - u)} \\
 &\quad + \frac{m_1^4 (-3m_2^2 + 2s + 3t) - m_1^2 s (-4m_2^2 + s + 4t) - 2m_1 m_2 s^2 + 2m_2^6}{(m_1^2 - t) (m_2^2 - u)} \\
 &\quad + \frac{-2m_2^4 s - 2m_2^4 t + m_2^2 t^2 + s^2 t - t^3}{(m_1^2 - t) (m_2^2 - u)} \\
 &\quad + \frac{2m_2^2 (-2M^4 + 2M^2 m_2 (m_2 - 3m_1) - (m_1 - m_2)(m_1 + m_2) (m_2^2 - s - t))}{(m_2^2 - u)^2} \\
 &\quad \left. + \frac{u^2}{m_1^2 - t} - 3m_1^2 - 3m_2^2 + 4s + t \right). \tag{C.29}
 \end{aligned}$$

C.2.2 Gluon Compton scattering

For gluon Compton scattering the Dirac trace in Eq. (8.121) becomes:

$$\begin{aligned}
T_C &= \left(g_{\mu\nu} - \frac{q_\mu q_\nu}{q^2} \right) \cdot \text{Tr} [(\not{p}_1 + \not{p}_2 - \not{q} + m_1) S^{\mu\alpha} (\not{p}_1 + m_1) S_\alpha^\nu] \\
&= \frac{8}{(m_1^2 - s)^2 (m_1^2 - u)^2} \left(-2M^4 (m_1^2 - s) (m_1^2 - u) \right. \\
&\quad \left. + 2M^2 (m_1^4 (s + u) - 4m_1^2 su + su(s + u)) \right. \\
&\quad \left. + 6m_1^8 - m_1^4 (3s^2 + 14su + 3u^2) + m_1^2 (s + u) (s^2 + 6su + u^2) - su (s^2 + u^2) \right) .
\end{aligned} \tag{C.30}$$

D

Numerics

D.1 Parton distribution functions

To calculate the cross sections for this work, we utilised several different sets of parton distribution functions. These were made available through the Les Houches Accord PDF Interface (LHAPDF) library, version 5.8.4 [WBG05].

D.2 Numerical integration

For the numerical evaluation of the multi-dimensional cross section integrals a C++ code was developed. The numerical integration routines were provided by the CUBA library, version 1.6 [Hah05]. Specifically we used the CUHRE and VEGAS routines with the desired accuracy set to 1%. Depending on the data set computational time was between a few minutes for transverse momentum spectra and a few hours for invariant mass spectra.

D.3 Special functions

Numerical routines for the evaluation of certain special mathematical functions (e.g. complex dilogarithm) were provided by the GNU Scientific Library (GSL), version 1.14 [GDT⁺10], available from <http://www.gnu.org/s/gsl/>.

Bibliography

- [A⁺88] E. Anassontzis et al., *High mass dimuon production in $\bar{p}n$ and π^-n interactions at 125-GeV/c*, Phys. Rev. D **38**, 1377 (1988).
- [A⁺05] V. V. Abramov et al., *Spin physics program in the U70 polarized proton beam*, (2005), arXiv:hep-ex/0511046.
- [A⁺06] M. Anselmino et al., *The general partonic structure for hadronic spin asymmetries*, Phys. Rev. D **73**, 014020 (2006), arXiv:hep-ph/0509035.
- [ABC⁺05] A. V. Afanasev, S. J. Brodsky, C. E. Carlson, Y.-C. Chen and M. Vanderhaeghen, *The Two-photon exchange contribution to elastic electron-nucleon scattering at large momentum transfer*, Phys. Rev. D **72**, 013008 (2005), arXiv:hep-ph/0502013.
- [AMP06] S. Alekhin, K. Melnikov and F. Petriello, *Fixed target Drell-Yan data and NNLO QCD fits of parton distribution functions*, Phys. Rev. D **74**, 054033 (2006), arXiv:hep-ph/0606237.
- [AMT07] J. Arrington, W. Melnitchouk and J. Tjon, *Global analysis of proton elastic form factor data with two-photon exchange corrections*, Phys. Rev. C **76**, 035205 (2007), arXiv:0707.1861.
- [AP77] G. Altarelli and G. Parisi, *Asymptotic Freedom in Parton Language*, Nucl. Phys. B **126**, 298 (1977).
- [AS64] M. Abramowitz and I. A. Stegun, *Handbook of Mathematical Functions with Formulas, Graphs, and Mathematical Tables*, Dover, New York, ninth dover printing, tenth gpo printing edition, 1964.
- [B⁺91] J. Berge et al., *A Measurement of Differential Cross-Sections and Nucleon Structure Functions in Charged Current Neutrino Interactions on Iron*, Z. Phys. C **49**, 187–224 (1991).
- [B⁺08] G. Bunce et al., *Plans for the RHIC Spin Physics Program*, (2008), http://spin.riken.bnl.gov/rsc/report/spinplan_2008/spinplan08.pdf.

- [BD65] J. D. Bjorken and S. D. Drell, *Relativistic quantum fields*, McGraw-Hill Book Company, New York, 1965.
- [BGG73] F. A. Berends, K. J. F. Gaemer and R. Gastmans, *Hard photon corrections for the process $e^+ e^- \rightarrow \mu^+ \mu^-$* , Nucl. Phys. B **57**, 381–400 (1973).
- [BMT05] P. Blunden, W. Melnitchouk and J. Tjon, *Two-photon exchange in elastic electron-nucleon scattering*, Phys. Rev. C **72**, 034612 (2005), arXiv:nucl-th/0506039.
- [BSSV00] G. Bunce, N. Saito, J. Soffer and W. Vogelsang, *Prospects for spin physics at RHIC*, Ann. Rev. Nucl. Part. Sci. **50**, 525–575 (2000), arXiv:hep-ph/0007218.
- [CCOR79] A. L. S. Angelis et al. (CCOR Collaboration), *A Measurement of the Production of Massive $e^+ e^-$ Pairs in Proton Proton Collisions at $s^{*1/2} = 62.4$ -GeV*, Phys. Lett. B **87**, 398 (1979).
- [Cha32] J. Chadwick, *Possible Existence of a Neutron*, Nature **129**, 312 (1932).
- [Col84] J. C. Collins, *Renormalization*, Cambridge University Press, Cambridge, 1984.
- [Collaboration85] J. Aubert et al. (European Muon Collaboration Collaboration), *A Detailed Study of the Proton Structure Functions in Deep Inelastic Muon - Proton Scattering*, Nucl. Phys. B **259**, 189 (1985).
- [Collaboration00] H. Lai et al. (CTEQ Collaboration Collaboration), *Global QCD analysis of parton structure of the nucleon: CTEQ5 parton distributions*, Eur. Phys. J. C **12**, 375–392 (2000), arXiv:hep-ph/9903282.
- [COMPASS96] G. Baum et al. (COMPASS Collaboration), *COMPASS: A Proposal for a Common Muon and Proton Apparatus for Structure and Spectroscopy*, (1996), CERN-SPSLC-96-14.
- [COMPASS97] F. Bradamante (COMPASS Collaboration), *The COMPASS experiment at CERN*, Nucl. Phys. A **622**, 50c–65c (1997).
- [Cre83] M. Creutz, *Quarks, gluons and lattices*, Cambridge University Press, Cambridge, UK, 1983.
- [CSS85] J. C. Collins, D. E. Soper and G. Sterman, *Transverse Momentum Distribution in Drell-Yan Pair and W and Z Boson Production*, Nucl. Phys. B **250**, 199 (1985).

-
- [CSS88] J. C. Collins, D. E. Soper and G. Sterman, *Factorization of Hard Processes in QCD*, Adv. Ser. Direct. High Energy Phys. **5**, 1–91 (1988), arXiv:hep-ph/0409313.
- [DM04] U. D’Alesio and F. Murgia, *Parton intrinsic motion in inclusive particle production: Unpolarized cross sections, single spin asymmetries and the Sivers effect*, Phys. Rev. D **70**, 074009 (2004), arXiv:hep-ph/0408092.
- [DMDS90] D. B. Day, J. S. McCarthy, T. W. Donnelly and I. Sick, *Scaling in inclusive electron - nucleus scattering*, Ann. Rev. Nucl. Part. Sci. **40**, 357–410 (1990).
- [Dok77] Y. L. Dokshitzer, *Calculation of the Structure Functions for Deep Inelastic Scattering and e^+e^- Annihilation by Perturbation Theory in Quantum Chromodynamics.*, Sov. Phys. JETP **46**, 641–653 (1977).
- [DWS85] C. T. H. Davies, B. R. Webber and W. J. Stirling, *Drell-Yan Cross-Sections at Small Transverse Momentum*, Nucl. Phys. B **256**, 413 (1985).
- [DY70] S. D. Drell and T.-M. Yan, *Massive Lepton Pair Production in Hadron-Hadron Collisions at High-Energies*, Phys. Rev. Lett. **25**, 316–320 (1970).
- [E77294] P. L. McGaughey et al. (E772 Collaboration), *Cross-sections for the production of high mass muon pairs from 800-GeV proton bombardment of H-2*, Phys. Rev. D **50**, 3038–3045 (1994).
- [ELM10] F. Eichstaedt, S. Leupold and U. Mosel, *Phenomenological model for the Drell-Yan process: Reexamined*, Phys. Rev. D **81**, 034002 (2010), arXiv:0909.4159.
- [ESW96] R. Ellis, W. Stirling and B. Webber, *QCD and collider physics*, Camb. Monogr. Part. Phys. Nucl. Phys. Cosmol. **8**, 1–435 (1996).
- [Fey] <http://www.feyncalc.org>.
- [Fey69] R. Feynman, *The Behavior of Hadron Collisions at Extreme Energies*, Proceedings, Conference on High Energy Collisions, Stony Brook (1969).
- [FL07] F. Froemel and S. Leupold, *Short-range correlations in quark matter*, Phys. Rev. C **76**, 035207 (2007), arXiv:nucl-th/0702017.

- [FLM03] F. Froemel, S. Leupold and U. Mosel, *Spectral function of quarks in quark matter*, Phys. Rev. C **67**, 015206 (2003), arXiv:nucl-th/0111004.
- [FQZ03] G. I. Fai, J.-w. Qiu and X.-f. Zhang, *Full transverse-momentum spectra of low-mass Drell-Yan pairs at LHC energies*, Phys. Lett. B **567**, 243–250 (2003), arXiv:hep-ph/0303021.
- [G⁺95] S. Gavin et al., *Production of the Drell-Yan pairs in high-energy nucleon-nucleon collisions*, Int. J. Mod. Phys. A **10**, 2961–2998 (1995), arXiv:hep-ph/9502372.
- [G⁺07] Y. Goto et al., *Proposal - Polarized Proton Acceleration at J-PARC*, (2007), http://j-parc.jp/NuclPart/pac_0801/pdf/Goto.pdf.
- [Gal01] K. Gallmeister, *Dileptonen und Photonen in relativistischen Schwerionenstößen*, Diss., Techn. Univ. Dresden, 2001.
- [GDT⁺10] M. Galassi, J. Davies, J. Theiler, B. Gough, G. Jungman, P. Alken, M. Booth and F. Rossi, *GNU Scientific Library Reference Manual*, Network Theory Ltd, 2010.
- [GJDR08] M. Glück, P. Jimenez-Delgado and E. Reya, *Dynamical parton distributions of the nucleon and very small- x physics*, Eur. Phys. J. C **53**, 355–366 (2008), arXiv:0709.0614.
- [GL72] V. Gribov and L. Lipatov, *Deep inelastic $e p$ scattering in perturbation theory*, Sov. J. Nucl. Phys. **15**, 438–450 (1972).
- [GM64] M. Gell-Mann, *A Schematic Model of Baryons and Mesons*, Phys. Lett. **8**, 214–215 (1964).
- [GM09] K. Gallmeister and U. Mosel, *Production of charged pions off nuclei with 3...30 GeV incident protons and pions*, Nucl. Phys. A **826**, 151–160 (2009), arXiv:0901.1770.
- [GPS86] C. Grosso-Pilcher and M. Shochet, *High mass dilepton production in hadron collisions*, Ann.Rev.Nucl.Part.Sci. **36**, 1–28 (1986).
- [Group10] K. Nakamura et al. (Particle Data Group Collaboration), *Review of particle physics*, J. Phys. G **37**, 075021 (2010).
- [GRV98] M. Glück, E. Reya and A. Vogt, *Dynamical parton distributions revisited*, Eur. Phys. J. C **5**, 461–470 (1998), arXiv:hep-ph/9806404.
- [GW73] D. Gross and F. Wilczek, *Ultraviolet Behavior of Nonabelian Gauge Theories*, Phys. Rev. Lett. **30**, 1343–1346 (1973).

-
- [Hah05] T. Hahn, *CUBA: A library for multidimensional numerical integration*, *Comput. Phys. Commun.* **168**, 78–95 (2005), arXiv:hep-ph/0404043.
- [HM84] F. Halzen and A. D. Martin, *Quarks and Leptons: An Introductory Course In Modern Particle Physics*, John Wiley & Sons, New York, 1984.
- [HS78] F. Halzen and D. M. Scott, *Testing QCD in the Hadroproduction of Real and Virtual Photons*, *Phys. Rev. Lett.* **40**, 1117 (1978).
- [I⁺81] A. S. Ito et al., *Measurement of the continuum of dimuons produced in high-energy proton - nucleus collisions*, *Phys. Rev. D* **23**, 604 (1981).
- [IZ80] C. Itzykson and J. Zuber, *Quantum field theory*, McGraw-Hill, New York, USA, 1980.
- [Jaf85] R. L. Jaffe, *Deep Inelastic Scattering With Application To Nuclear Targets*, (CTP-1261. MIT-CTP-1261) (Jul 1985), Lectures presented at the Los Alamos School on Quark Nuclear Physics, Los Alamos, N.Mex., Jun 10-14, 1985, MIT-CTP-1261.
- [JBD⁺11] N. Jarosik, C. Bennett, J. Dunkley, B. Gold, M. Greason et al., *Seven-Year Wilkinson Microwave Anisotropy Probe (WMAP) Observations: Sky Maps, Systematic Errors, and Basic Results*, *Astrophys. J. Suppl.* **192**, 14 (2011), arXiv:1001.4744.
- [JMY04] X.-d. Ji, J.-P. Ma and F. Yuan, *QCD factorization for spin-dependent cross sections in DIS and Drell-Yan processes at low transverse momentum*, *Phys. Lett. B* **597**, 299–308 (2004), arXiv:hep-ph/0405085.
- [JR76] J. M. Jauch and F. Rohrlich, *The Theory of Photons and Electrons*, Springer, Berlin, 1976.
- [Kin62] T. Kinoshita, *Mass singularities of Feynman amplitudes*, *J. Math. Phys.* **3**, 650–677 (1962).
- [KU76] T. Kinoshita and A. Ukawa, *New Approach to the Singularities of Feynman Amplitudes in the Zero Mass Limit*, *Phys. Rev. D* **13**, 1573 (1976).
- [Kum08] S. Kumano, *High-energy hadron physics at J-PARC*, *AIP Conf. Proc.* **1056**, 444–451 (2008), arXiv:0807.4207.
- [Lei75] G. Leibbrandt, *Introduction to the technique of dimensional regularization*, *Rev. Mod. Phys.* **47**, 849–876 (1975).

- [Lew81] L. Lewin, *Polylogarithms and Associated Functions*, Elsevier North Holland, New York, 1981.
- [LGLM06] O. Linnyk, K. Gallmeister, S. Leupold and U. Mosel, *Prediction for the transverse momentum distribution of Drell-Yan dileptons at PANDA*, Phys. Rev. D **73**, 037502 (2006), arXiv:hep-ph/0506134.
- [Lid09] A. Liddle, *An introduction to modern cosmology*, Wiley-VCH, Weinheim, Germany, 2009.
- [Lin06] O. Linnyk, *Quark off-shellness effect on parton distributions*, Diss., Univ. Gießen, 2006.
- [Lip75] L. Lipatov, *The parton model and perturbation theory*, Sov. J. Nucl. Phys. **20**, 94–102 (1975).
- [LLM05] O. Linnyk, S. Leupold and U. Mosel, *Quark Initial State Interaction in Deep Inelastic Scattering and the Drell-Yan process*, Phys. Rev. D **71**, 034009 (2005), arXiv:hep-ph/0412138.
- [LLM07] O. Linnyk, S. Leupold and U. Mosel, *Next-to-leading order vs. quark off-shellness and intrinsic $k(T)$ in the Drell-Yan process*, Phys. Rev. D **75**, 014016 (2007), arXiv:hep-ph/0607305.
- [LN64] T. D. Lee and M. Nauenberg, *Degenerate Systems and Mass Singularities*, Phys. Rev. **133**, B1549–B1562 (1964).
- [LS85] C. Llewellyn Smith, *Nuclear Effects in Deep Inelastic Lepton Scattering*, Nucl. Phys. A **434**, 35C–56C (1985).
- [M⁺91] G. Moreno et al., *Dimuon production in proton - copper collisions at $\sqrt{s} = 38.8$ -GeV*, Phys. Rev. D **43**, 2815–2836 (1991).
- [MH56] R. McCallister and R. Hofstadter, *Elastic Scattering of 188-MeV Electrons from the Proton and the Alpha Particle*, Phys. Rev. **102**, 851–856 (1956).
- [MSTW09] A. D. Martin, W. J. Stirling, R. S. Thorne and G. Watt, *Parton distributions for the LHC*, Eur. Phys. J. C **63**, 189–285 (2009), arXiv:0901.0002.
- [Mut98] T. Muta, *Foundations of quantum chromodynamics. Second edition*, World Sci. Lect. Notes Phys. **57**, 1–409 (1998).
- [NuSea03] J. C. Webb et al. (NuSea Collaboration), *Absolute Drell-Yan dimuon cross sections in 800-GeV/c $p p$ and $p d$ collisions*, (2003), arXiv:hep-ex/0302019.

- [P⁺05] V. Punjabi et al., *Proton elastic form-factor ratios to $Q^{*2} = 3.5\text{-GeV}^{*2}$ by polarization transfer*, Phys. Rev. C **71**, 055202 (2005), arXiv:nucl-ex/0501018.
- [P⁺06] J. Peng et al., *Proposal - Measurement of High-Mass Dimuon Production at the 50-GeV Proton Synchrotron*, (2006), http://j-parc.jp/NuclPart/pac_0606/pdf/p04-Peng.pdf.
- [PAX05] V. Barone et al. (PAX Collaboration), *Antiproton proton scattering experiments with polarization*, (2005), arXiv:hep-ex/0505054.
- [Pol73] H. Politzer, *Reliable Perturbative Results for Strong Interactions?*, Phys. Rev. Lett. **30**, 1346–1349 (1973).
- [PQ76] E. C. Poggio and H. R. Quinn, *The Infrared Behavior of Zero-Mass Green's Functions and the Absence of Quark Confinement in Perturbation Theory*, Phys. Rev. D **14**, 578 (1976).
- [PS95] M. E. Peskin and D. V. Schroeder, *An Introduction to quantum field theory*, Addison-Wesley, Reading, USA, 1995.
- [PV49] W. Pauli and F. Villars, *On the Invariant regularization in relativistic quantum theory*, Rev. Mod. Phys. **21**, 434–444 (1949).
- [Q⁺05] I. Qattan et al., *Precision Rosenbluth measurement of the proton elastic form-factors*, Phys. Rev. Lett. **94**, 142301 (2005), arXiv:nucl-ex/0410010.
- [Rei07] P. E. Reimer, *Exploring the partonic structure of hadrons through the Drell-Yan process*, J. Phys. G **34**, S107–S126 (2007), arXiv:0704.3621.
- [RPN02] J. Raufeisen, J.-C. Peng and G. C. Nayak, *Parton model versus color dipole formulation of the Drell-Yan process*, Phys. Rev. D **66**, 034024 (2002), arXiv:hep-ph/0204095.
- [Rut11] E. Rutherford, *The scattering of alpha and beta particles by matter and the structure of the atom*, Phil. Mag. **21**, 669–688 (1911).
- [S⁺81] S. R. Smith et al., *Experimental Test of the Drell-Yan Model in $p W \rightarrow \mu^+ \mu^- X$* , Phys. Rev. Lett. **46**, 1607 (1981).
- [S⁺01] T. Sjostrand et al., *High-energy physics event generation with PYTHIA 6.1*, Comput. Phys. Commun. **135**, 238–259 (2001), arXiv:hep-ph/0010017.

- [SSNI09] A. Sissakian, O. Shevchenko, A. Nagaytsev and O. Ivanov, *Transversity, Boer-Mulders and Sivers distributions from Drell-Yan processes with pp , pD and DD collisions*, Eur. Phys. J. C **59**, 659–673 (2009), arXiv:0807.2480.
- [Ste76] G. F. Sterman, *Kinoshita's Theorem in Yang-Mills Theories*, Phys. Rev. D **14**, 2123–2125 (1976).
- [tH71] G. 't Hooft, *Renormalization of massless Yang-Mills fields*, Nucl. Phys. B **33**(1), 173 – 199 (1971).
- [tHV72] G. 't Hooft and M. J. G. Veltman, *Regularization and Renormalization of Gauge Fields*, Nucl. Phys. B **44**, 189–213 (1972).
- [tHV79] G. 't Hooft and M. J. G. Veltman, *Scalar One Loop Integrals*, Nucl. Phys. B **153**, 365–401 (1979).
- [TLP⁺09] The PANDA collaboration, M. F. M. Lutz, B. Pire, O. Scholten and R. Timmermans, *Physics Performance Report for PANDA: Strong Interaction Studies with Antiprotons*, (2009), arXiv:0903.3905.
- [UA292] J. Alitti et al. (UA2 Collaboration), *Study of electron pair production below the Z mass at the CERN anti-p p collider*, Phys. Lett. B **275**, 202–208 (1992).
- [Wan00] X.-N. Wang, *Systematic study of high p_T hadron spectra in pp , pA and AA collisions from SPS to RHIC energies*, Phys. Rev. C **61**, 064910 (2000), arXiv:nucl-th/9812021.
- [WBG05] M. R. Whalley, D. Bourilkov and R. C. Group, *The Les Houches Accord PDFs (LHAPDF) and Lhaglu*, (2005), arXiv:hep-ph/0508110.
- [Web03] J. C. Webb, *Measurement of continuum dimuon production in 800-GeV/c proton nucleon collisions*, (2003), arXiv:hep-ex/0301031.
- [Wol08] Wolfram Research Inc., *Mathematica Edition: Version 7.0*, Wolfram Research Inc., Champaign, Illinois, 2008.
- [Zwi33] F. Zwicky, *Die Rotverschiebung von extragalaktischen Nebeln*, Helvetica Physica Acta **6**, 110–127 (1933).